

Analysis of Urban Green Space in Chongqing and Nanjing
using Multi-resolution Segmentation, Object-oriented
Classification Approach and Landscape Ecology Metrics

SO Lek Hang Lake

A Thesis Submitted in Partial Fulfillment
of the Requirements for the Degree of
Master of Philosophy

in

Geography and Resource Management

© The Chinese University of Hong Kong

August 2005

The Chinese University of Hong Kong holds the copyright of this thesis. Any person(s) intending to use a part or while of the materials in the thesis in a proposed publication must seek copyright release from the Dean of the Graduate School.



A Thesis entitled:

Analysis of Urban Green Space in Chongqing and Nanjing using Multi-resolution Segmentation, Object-oriented Classification Approach and Landscape Ecology Metrics

Submitted by: SO, Lek Hang Lake

For the degree of: **Master of Philosophy in Geography and Resource Management**
at **The Chinese University of Hong Kong**

Abstract

Awareness of environmental problems induced by rapid urbanization began to emerge in many cities, especially those in China, in the last 5 years. There has been increasing volume of literature concerning the interaction between the structure of urban green space and urbanization in different Chinese cities. This research aims at comparing two Chinese cities, Chongqing and Nanjing, which have high disparities in locations, urbanization and industrialization levels, in respect of their landscape structure of green space within and surrounding the city proper. Landscape metrics are utilized to anatomize the different aspects of landscape structure of urban areas.

Thematic information, such as different land covers, can be extracted from remotely sensed data using various image classification algorithms. Conventional classification methods tend to use only spectral reflectance to decide on class assignments. The main problem of these classifiers is that such spectral classification methods fail to utilize textural and shape information from the image, which are crucial for characterization of some land uses, especially woodland and urban areas. Besides, Most of them are "hard classifiers" in the sense that they classify each pixel of the image to the class to which the

pixel has the highest membership values, while the possibilities of these pixels to other classes are largely discredited.

Object-oriented classification concept has emerged in recent years which are able to extract textural, shape and other contextual information from remotely sensed images and utilize them to constitute object features of different land covers, which may be contributive to more accurate image classification. Object-oriented system is equipped with Multiresolution segmentation, which allows the generation of image objects at user-specified segmentation scales. Segmented objects of different scales are linked up under object hierarchy. Numerous spectral, textural and shape features of each object can be extracted, which can be selected to formulate classifying rules for each land cover class. Classification procedure is operated in the form of decision tree under class hierarchy, through which class assignment is based on comparison of segmented objects with classifying rules at each node of the decision tree. In this research, object-oriented classification of ASTER images of Chongqing and Nanjing are compared with other conventional spectral classifiers.

Results of the research show that when spectral-shape ratio is decreased during segmentation, image objects generated are larger in average size at each segmentation level. Besides, low spectral-shape ratio seriously distorts the images. On the other hand, too high spectral-shape ratio may create image objects which are too fractal. Observation of the variation of various spectral, textural and shape features along segmentation levels reveals that for most of the land cover objects, object features obviously show break points at segmentation level 5, indicating that level 5 is suitable to be selected as one of the object levels. Break points are less discernible at other segmentation levels. Above all,

the research found that transferability of classifying rules between Chongqing and Nanjing is possible for many classes. Water body in both cities has particularly low values in GLCM Contrast and Standard Deviation of VNIR channels at high object level. At the lowest object level, "low density urban" in both cities has particularly high GLCM Contrast of VNIR 1 and 2. These findings confirm the earlier literature that textural and shape information, if utilized, is contributive to classification of some land covers which are not satisfactorily classified by solely spectral classifiers.

Object-oriented classification of images in both cities are compared with maximum likelihood classification, linear spectral unmixing and supervised fuzzy classification utilizing additional shortwave infrared (SWIR) channels. Results of this research show that classification using linear spectral unmixing attained the lowest accuracy, followed by that using supervised fuzzy classification. Accuracies attained by Object-oriented classification and maximum likelihood classifier are not significantly different. Serious class mixing negatively affect the performance of these two classifiers.

Patch- and class-metrics are used to analyze the 4 aspects of landscape structure urban green space: landscape composition, fragmentation pattern, contagion and patch shape complexity. Buffer rings and circles surrounding city centers of the two cities are applied to study the change of landscape structure of green space along distances from city centers. Results found that both cities have low proportion of green occupation and highly fragmented green space configuration, with low contagion, within 2 km buffer. Beyond 4 to 5 km buffer, both green coverage and aggregation begins to increase. However, green space in both cities are disaggregated in nature and simple in shape.

重慶及南京市城市綠地的研究—利用物體主導的遙感分類技術、ASTER 衛星圖像及景觀生態學

論文摘要

中國城市於最近五年城市發展非常迅速，引來很多惹人關注的環境問題。大量有關中國城市化與環境問題之間的互動關係的文獻在近年出現，當中有不少研究城市化對城市綠地結構的影響。本文主要討論兩個中國城市—重慶及南京—市內綠地景觀結構的差異。本文將會從景觀生態學的角度對這兩城市內綠地的狀況進行分別。

利用遙感分類技術可從遙感圖像析出很多主題資訊，如土地利用分佈。一般的遙感分類法多倚重圖像的光譜反射資訊來決定土地利用分類，它們的缺點是忽略了圖像內的有關組織及形狀的資訊對某些土地利用，如林地和城市，的辨認的重要性。另外，一般的遙感分類法假設了每一個像元只有一種土地利用分類，否定了「混亂像元」的可能性。因此很多研究需要更靈活的分類技術。

物體主導的遙感分類技術在近年出現。除了光譜反射資訊，它更可從遙感圖像析取組織及形狀的資訊以改善遙感分類的準確度。它能利用 Multiresolution Segmentation 技術把圖像分割，從而製造不同空間比例的「圖像物體」。從而製造不同空間比例的「圖像物體」由 Object hierarchy 連繫。大量的組織及形狀的資訊更可從物體析出。這些資訊可作成不同土地類別的特質。物體主導的遙感分類技術利用每一土地類別的特質建構 Decision tree，把各「圖像物體」分類 (Definiens-

Imaging, 2003)。這研究利用此遙感分類技術把重慶和南京市的 ASTER 衛星圖像分類。

此研究的結果顯示當「光譜—形狀比率」下降，分割所產生的「圖像物體」的平均面積便會變大；而且，「光譜—形狀比率」過低會扭曲圖像。過高的「光譜—形狀比率」則會使「圖像物體」的形狀過於複雜。大部分的土地類別的物體的特徵會在「第五分割層」出現改變。這顯示「第五分割層」適合作為其中一層 Object level。土地類別的物體特徵在其他的「分割層」出現的改變較難辨識。此研究的結果亦顯示很多土地類別的分類法則在重慶及南京十分相近。如：水體在兩城均顯示很低的 GLCM Contrast 和 VNIR Standard Deviation；在最底「物體層」，兩城的低密度城區在綠色及紅色波段均顯示很高的 GLCM Contrast。這些發現肯定了組織及形狀的資訊在遙感分類技術上應更充分利用。

此研究亦把物體主導的遙感分類技術跟另外三種分類技術—包括最大可能性分類法 (MLC)、線性光譜反混合分類法 (Linear spectral unmixing) 及模糊分類法 (Supervised fuzzy classification)—進行比較。結果顯示線性光譜反混合分類及模糊分類法準確度最低，而物體主導的遙感分類及最大可能性分類法準確度相若。土地類別間的模糊性對這兩分類法產生負面影響。

「塊狀景觀測量」及「類別景觀測量」被利用分析兩城城內綠地四方面的結構，包括景觀成分、景觀分裂狀態、景觀連接度及景觀塊狀的形狀複雜度。這研究從兩城中心劃出多個緩衝以分析城內綠地與市中心的距離是否影響城內綠地的景觀結

構。結果顯示兩城的綠地的某些景觀特質十分相似，包括：距離市中心兩公里之內城市的綠地覆蓋率低、綠地分裂度高、景觀連接度低。距離市中心四至五公里外的綠地覆蓋率及連接度開始上升。但總括而言，兩城的綠地都是連接度偏低及形狀簡單。

Acknowledgement

It is really hard to say thanks to all people who have ever given me hands on my road to completion of this thesis, because there are too many to remember.

Professor Fung Tung, my supervisor, actually deserves much more than just a few words in this acknowledgement. Under his heartedly and patient guidance, I have broadened my horizon in many disciplines such as remote sensing, landscape ecology, etc. He continually pointed me a new road, which I have never thought of, when I was frustrated at different stages of the research. By looking at him I find a classical model of how a quality researcher looks like. His earnestness in every aspect of research will always be rooted in my mind in the rest of my life.

Thanks should also be granted to Mr. Honda Lee and Mr. Kai-hang Choi, who are technicians of computers and remote sensing data in Department of Geography and Resource Management. Without their help in maintenance of the quality of both computer and data, by no means can I finish this research and thesis.

Also, I have to say thanks to my colleagues and seniors, Frankie and Larry, and other colleagues, who have given me courage and support which are badly required for a two-year Master program.

Ling have stood on my side every time I found disheartened during my pursuit of my career. I owe her more than my life. Thanks are deserved by all the brothers and

sisters in my church who have prayed for my accomplishment of this two-year study;
Michael, who helped me type the proposal; and other friends who support me.

Table of Content

Abstract.....	i
Acknowledgement.....	vii
Table of Content.....	ix
List of Figures.....	xiii
List of Tables.....	xvi
CHAPTER 1. Introduction.....	1
1.1 Problem Statement.....	1
1.2 Research Objectives.....	5
1.3 Research Significance.....	6
1.4 Organization of the thesis.....	7
1.5 Definition of Urban Green Space.....	9
CHAPTER 2. Literature Review.....	10
2.1 Introduction.....	10
2.2 Urban Green Space.....	10
2.2.1 Classification of Urban Green Space.....	11
2.2.2 Configuration of Urban Green Space System.....	12
2.2.3 Different Approaches to Urban Green Space Study.....	14
2.3 Urban Green Space in China.....	15
2.3.1 General Problems.....	16
2.3.2 Increasing Awareness of Environment.....	16
2.3.3 Chinese Definition of Urban Green Space.....	18
2.4 Remote Sensing Techniques.....	21
2.4.1 Review of Image Classification Techniques.....	21
2.4.1.1 Conventional Classification Methods.....	22
2.4.1.2 Mixed Pixels Problem.....	23
2.4.1.3 Mixed Pixels' Effects on Conventional Classifiers.....	25
2.4.1.4 Alternative Solutions to Mixed Pixels Problems (Fuzzy Sets).....	26
2.4.1.5 Problems Fuzzy Classifications are unable to solve.....	28
2.4.2 Object-oriented Classification Concept.....	30
2.4.2.1 Multiresolution Segmentation.....	30
2.4.2.2 Fuzzy Classification Procedure.....	31
2.4.2.3 Object-oriented Approach to Image Processing.....	32
2.4.2.4 Ecognition.....	33
2.4.2.5 Research about ecognition.....	34
2.5 Landscape Ecology.....	35
2.5.1 Basic Principles.....	35
2.5.2 Landscape Metrics.....	36
2.5.3 Application of Landscape Ecology in Landscape Analysis.....	38
2.6 Conclusion.....	39
CHAPTER 3. Study Sites and Methodology.....	41
3.1 Introduction.....	41
3.2 Study Area.....	41
3.2.1 Chongqing.....	41
3.2.1.1 Geography and geomorphology.....	42
3.2.1.2 Administration and governance.....	42
3.2.1.3 Environmental Quality.....	43
3.2.1.4 Government Attempt to Improvement.....	43
3.2.2 Nanjing.....	46
3.2.2.1 Geography and Geomorphology.....	46
3.2.2.2 Administration and Governance.....	46
3.2.2.3 Landscape Planning of Nanjing.....	47

3.2.3	Comparison between Chongqing and Nanjing	47
3.2.3.1	<i>Geographical setting</i>	49
3.2.3.2	<i>Population</i>	49
3.2.3.3	<i>Urbanization and Industrialization Levels</i>	51
3.2.3.4	<i>Variation in Landscape Quantity</i>	51
3.2.3.5	<i>Comparison from Satellite Images</i>	52
3.3	Working procedures	56
3.3.1	Data	56
3.3.1.1	<i>VNIR channels</i>	58
3.3.1.2	<i>SWIR channels</i>	59
3.3.1.3	<i>Data Fusion</i>	59
3.3.2	Designing Hierarchical Classification System	60
3.3.2.1	<i>Chongqing</i>	60
3.3.2.2	<i>Nanjing</i>	61
3.3.3	Object-oriented Classification	62
3.3.3.1	<i>Introduction</i>	63
3.3.3.2	<i>Procedure of Object-oriented Classification</i>	65
3.3.3.2.1	<i>Analysis of Image Objects</i>	65
3.3.3.2.2	<i>Image Segmentation</i>	67
3.3.3.2.3	<i>Selection of Features and Data Conversion</i>	67
3.3.3.2.4	<i>Class-based Objects Sampling</i>	68
3.3.3.2.5	<i>Class-based Objects Analysis</i>	68
3.3.3.2.6	<i>Designing Object Level Hierarchy</i>	69
3.3.3.2.7	<i>Designing Class Hierarchy</i>	69
3.3.3.2.8	<i>Decision Tree Classification Structure</i>	69
3.3.4	Comparison with other classification algorithms	70
3.4	Landscape Analyses	71
3.4.1	Selection of Landscape Metrics	72
3.4.2	Landscape Analysis for entire cities	74
3.4.3	Buffer Analysis	74
3.5	Conclusion	77
CHAPTER 4.	Results and Discussion I Variations of Image Object Signatures	
for Sampled Land Covers		78
4.1	Introduction	78
4.2	Chongqing	79
4.2.1	Spectral-shape ratio	79
4.2.1.1	<i>Selection Criteria</i>	80
4.2.1.2	<i>Observations</i>	80
4.2.2	Segmentation levels	85
4.2.2.1	<i>Selection Criteria</i>	85
4.2.2.2	<i>Observations</i>	86
4.2.3	Classifying Rules	93
4.2.3.1	<i>Selection Criteria</i>	93
4.2.3.2	<i>Level 9</i>	94
4.2.3.3	<i>Level 5</i>	101
4.2.3.4	<i>Level 1</i>	103
4.3	Nanjing	104
4.3.1	Spectral-shape ratio	104
4.3.1.1	<i>Selection Criteria</i>	105
4.3.1.2	<i>Observations</i>	105
4.3.2	Segmentation Levels	111
4.3.2.1	<i>Selection Criteria</i>	111
4.3.2.2	<i>Observations</i>	111
4.3.3	Classifying Rules	119
4.3.3.1	<i>Selection Criteria</i>	119

4.3.3.2	Level 8.....	119
4.3.3.3	Level 4.....	126
4.3.3.4	Level 1.....	129
4.4	Discussion.....	131
CHAPTER 5.	Results and Discussion II Image Classification.....	134
5.1	Introduction.....	134
5.2	Chongqing.....	135
5.2.1	Class hierarchy.....	135
5.2.2	Description of the site.....	136
5.2.3	Classification of “lake”.....	138
5.2.4	Classification of “crops and grassland”.....	139
5.2.5	Classification of “low density urban”.....	140
6.3.3	Classification Result.....	142
5.2.7	Error matrix.....	144
5.2.8	Class Proportion.....	144
5.2.9	Post-classification Aggregation.....	147
5.3	Nanjing.....	149
5.3.1	Class Hierarchy.....	149
5.3.2	Description of the site.....	151
5.3.3	Classification of lake.....	151
5.3.4	Classification of “crops and grassland II”.....	153
5.3.5	Classification of “low density urban”.....	154
5.3.6	Classification Result.....	155
5.3.7	Error Matrix.....	156
5.3.8	Class Proportion.....	161
5.3.9	Post-classification Aggregation.....	161
5.4	Discussion.....	163
5.4.1	Problems of object-oriented classification.....	163
5.4.2	Strengths of object-oriented classification.....	165
5.4.3	Transferability of classifying rules.....	166
CHAPTER 6.	Results and Discussion III Landscape Structure of “Urban Green Space”, Chongqing and Nanjing.....	167
6.1	Introduction.....	167
6.2	Chongqing.....	167
6.2.1	Landscape composition.....	167
6.2.2	Fragmentation.....	169
6.2.3	Contagion.....	171
6.2.4	Patch Shape Complexity.....	171
6.3	Nanjing.....	173
6.3.1	Landscape composition.....	173
6.3.2	Fragmentation.....	175
6.3.3	Contagion.....	177
6.3.4	Patch Shape Complexity.....	178
6.4	Discussion.....	179
6.4.1	Similarities.....	179
6.4.2	Differences.....	182
CHAPTER 7.	Conclusion.....	186
7.1	Summary on findings.....	186
7.1.1	Summary on image object analyses.....	186
7.1.2	Summary on object-oriented classification.....	187
7.1.3	Summary on landscape studies of “urban green space”.....	189

7.2	Limitations of the research	190
7.2.1	Data preparation	190
7.2.2	Image classification	191
7.2.3	Landscape Analysis	193
7.3	Suggestions for further research	194
Bibliography		196
Appendix 1—Equations of object features		204
Appendix 2—Equations for Landscape Metrics		208
Appendix 3—Variations of Object Features along Segmentation Levels in Chongqing		216
Appendix 4—Variations of Object Features along Segmentation Levels in Nanjing		244
Appendix 5—Classifying Rules		277
Appendix 6—Variations in Landscape Metrics along Buffers from City Center in Chongqing		282
Appendix 7—Variations in Landscape Metrics along Buffers from City Center in Nanjing		290

List of Figures

Figure 1.1 Semantic net based on prior knowledge and image interpretation.....	4
Figure 3.1 Chongqing (City proper) Urban Master Plan, 1996-2010.....	44
Figure 3.2 Nanjing (City Proper) Urban Master Plan, 1991-2010	48
Figure 3.3 Satellite Image of Chongqing.....	54
Figure 3.4 Satellite Image of Nanjing.....	55
Figure 3.5 Schematic diagram of working flow	57
Figure 3.6 Comparison between original SWIR data and SFIM SWIR data. (a) is raw SWIR channel 4. Edge details of lakes, roads and buildings are blurred. After SFIM, edges are sharpened, very much like a normal 15 m VNIR image, which is shown in (b).....	60
Figure 3.7 City centers of Chongqing (a) and Nanjing (b) are highlighted by stars.....	75
Figure 3.8 Buffer analysis on ArcMap interface	77
Figure 4.1 Number of image objects generated along segmentation levels in Chongqing	82
Figure 4.2 Variability of Standard Deviation (VNIR 3) of image objects along segmentation gradient for land cover classes: "Woodland" (a), "Lake" (b) and "Low density urban" (c). Case in Chongqing	83
Figure 4.3 Segmented images at the lowest segmentation level (left) and highest segmentation level (right). Top figures are segmented at spectral-shape ratio of 1:9 (a); the bottom ones are segmented at 10:0 (c); the middle at 5:5 (b). Notice that as spectral-shape ratio goes down, the images become more distorted from reality, esp. at high segmentation levels.	84
Figure 4.4 Variability of Standard Deviation (on the left) and Angular Second Moment (on the right) of VNIR 3 for the classes: "lake", "grassland" and "high density urban". Case in Chongqing.....	87
Figure 4.5 Variability of HOM (VNIR 3) for "grassland" in Chongqing	88
Figure 4.6 Variability of Standard deviation (VNIR 2) for "high density urban in Chongqing.....	89
Figure 4.7 Variability of HOM (VNIR 2) for "grassland" in Chongqing	90
Figure 4.8 Standard Deviation of VNIR 2 (left) and VNIR 3 (right) for "lake", "grassland", "woodland" and "low density urban" in Chongqing.....	91
Figure 4.9 Image segmented at scale parameter 2 (Upper) and without segmentation (Lower) in Chongqing.....	93
Figure 4.10 Image objects of "river" (a), "lake" (b) and "industrial"(c) and their visualization	100
Figure 4.11 Comparisons of Area: between Lake and River (Left) and between Industrial and High density urban (Right) in Chongqing.....	101
Figure 4.12 Visualization of contrast between "vegetation" and "non-vegetation" at segmentation level 5 using VNIR 3/VNIR 2 ratio (a); and between "low density urban" and other non-vegetation classes using GLCM contrast VNIR 2 (b). Case in Chongqing.....	102
Figure 4.13 Comparison between the original image (a), visualization of spectral mean VNIR 2 (b) and visualization of spectral mean VNIR 3 (c) for "woodland"- "grassland" contrast (Upper) and "high density urban"- "bareland" contrast (Lower). Notice the low contrast for VNIR 3.	104
Figure 4.14 Object number generated by varying spectral-shape ratio across segmentation gradient. Case in Nanjing.....	106

Figure 4.15 Variability of Standard deviation (VNIR 3) of land covers "Pond" (a), "Agricultural crop I" (b) and "Bareland" (c). Case in Nanjing.....	108
Figure 4.16 Segmented images of Nanjing at segmentation level 1 (left) and 12 (right). They are generated at spectral-shape of 10:0 (a), 9:1 (b), 7:3 (c) and 1:9 (d). Notice: First the regular shapes of objects at 1:9; second the similarity of image quality at level 1 for 10:0, 9:1 and 7:3 and third the fractal objects at both 10:0 and 9:1.	110
Figure 4.17 Variability of Contrast (VNIR 3) (Left) and Angular Second Moment (VNIR 3) (Right) for lake (a) and agricultural crop II (b) in Nanjing	113
Figure 4.18 Image of "agricultural crop II" from pixel image (a) to segmentation level 4 (b) to level 5 (c) in Nanjing. Notice the gradual loss in details	113
Figure 4.19 Variability of CON (VNIR 2) for "agricultural crop II" in Nanjing	114
Figure 4.20 Variability of CON (VNIR 2) for "lake" in Nanjing	115
Figure 4.21 Variation of Standard Deviation of VNIR 2 (Left) and VNIR 3 (Right) for "lake" (a), "agricultural crops II" (b) and "low density urban" (c) in Nanjing.....	116
Figure 4.22 Comparison between pixel image of Nanjing (a), segmented image at segmentation level 1 at spectral-shape ratio of 7:3 (b), and segmented image at segmentation level 1 at spectral-shape ratio of 9:1 (c). Difference is hardly found even at large scale	118
Figure 4.23 Image of Nanjing showing "river", "lake" and "high density urban" and their values in terms of spectral mean VNIR 3	126
Figure 4.24 Image showing small river channels and lakes; and how they are divided from each other by length-width ratio	126
Figure 4.25 Three super-categories of vegetation and visualization of their varying magnitude in CON (VNIR 3)	128
Figure 4.26 Image showing "low density urban" and "high density urban". Notice the relative brightness of "low density urban" in the visualization of CON VNIR 1	129
Figure 4.27 Discrimination of land covers using spectral mean at level 1: "wetland" vs. "agri crop II" with VNIR 3 (a); "woodland" vs "grassland" with VNIR 2 and "bareland" vs "fallowed land" with VNIR 1 (b); and "high density urban" vs "bareland" with VNIR 3 (c).....	130
Figure 5.1 Class hierarchy for classification of Chongqing	135
Figure 5.2 Conceptual Decision Tree for Classification of Chongqing.....	137
Figure 5.3 Appearance of "lake" (a), "grassland" (b) and "low density urban" (c) in Chongqing.....	138
Figure 5.4 Classified images of Chongqing using different approaches: Object-oriented classification (a), maximum-likelihood classification (b), supervised fuzzy classification (c) and linear spectral unmixing (d).....	143
Figure 5.5 Classified Image of Chongqing after class aggregation	148
Figure 5.6 Class hierarchy for Classification of Nanjing	149
Figure 5.7 Conceptual decision tree for classification of Nanjing.....	150
Figure 5.8 Appearance of "lake" (a), "agricultural crop II" (b) and "low density urban" (c) in Nanjing.....	151
Figure 5.9 Classified images of Nanjing using different approaches: Object-oriented classification (a), maximum-likelihood classification (b), supervised fuzzy classification (c) and linear spectral unmixing (d)	158
Figure 5.10 Classified Image of Nanjing after class aggregation	162
Figure 6.1 Total class area of "urban green space" along distance to city center for <i>circle</i> (a) and <i>ring</i> (b) buffers. Chongqing as a case	168

Figure 6.2 Proportion of landscape occupied by "urban green space" along distance to city center for <i>circle</i> (a) and <i>ring</i> (b) buffers. Chongqing as a case	168
Figure 6.3 Number of Patch (a), Patch Density (b), Area-weighted mean (c) and Coefficient of Variation (d) (<i>ring</i>) for the class "urban green space". Chongqing as a case	169
Figure 6.4 6 km (a) and 9 km (b) buffer rings of Chongqing	170
Figure 6.5 Clumpiness Index and Landscape Division Index (<i>ring</i>) of "urban green space" in Chongqing	172
Figure 6.6 Area-weighted mean of Fractal Dimension Index (<i>circle</i>) (a) and Area-weighted mean of Perimeter-Area Ratio (<i>circle</i>) (b) of "urban green space" in Chongqing	173
Figure 6.7 Total class area of "urban green space" along distance to city center for <i>circle</i> (a) and <i>ring</i> (b) buffers. Case in Nanjing	174
Figure 6.8 Proportion of Landscape occupied by "urban green space" along distance to city center for <i>circle</i> (a) and <i>ring</i> (b) buffers. Case in Nanjing	174
Figure 6.9 3 km (a) and 9 km (b) buffer rings of Nanjing	174
Figure 6.10 Number of patches (a) and patch density (b) of "urban green space" along buffer rings in Nanjing. Notice the coincidence between leveling of NP and falling of PD.	175
Figure 6.11 Area-weighted mean (a) and Coefficient of variation (b) of patch area for the class "urban green space" in ring buffers in Nanjing	176
Figure 6.12 Landscape Division Index (a) and Clumpiness Index (b) of "urban green space" for ring buffers in Nanjing	177
Figure 6.13 Periphery of Nanjing city. 9-km buffer ring is outlined in yellow	178
Figure 6.14 Area-weighted mean Fractal Dimension Index (a) and Perimeter-Area Ratio (b) of "urban green space" for buffer circles in Nanjing	179
Figure 6.15 Frequency distribution of area of "urban green space" in Chongqing	181
Figure 6.16 Frequency distribution of area of "urban green space" in Nanjing	181

List of Tables

Table 3.1 Green Space Availability of the Municipalities	45
Table 3.2 Comparison of Population between Nanjing and Chongqing	50
Table 3.3 Industrialization and Urbanization Levels of Nanjing and Chongqing	50
Table 3.4 Comparison between Nanjing and Chongqing in urban green coverage.....	52
Table 3.5 Basic information of VNIR and SWIR channels.....	58
Table 3.6 Three-tiered classification scheme for object-oriented classification in Chongqing (a) and Nanjing (b)	62
Table 3.7 Features calculated for image object analyses	67
Table 3.8 Landscape metrics calculated in the research	73
Table 4.1 Values of Spectral (a), Shape (b) and Textural (c) indicators for different land cover classes at segmentation level 9 in Chongqing.....	95
Table 4.2 Values of Spectral (a), Shape (b) and Textural (c) indicators for different land cover classes at segmentation level 5 in Chongqing.....	97
Table 4.3 Values of Spectral (a) and Shape (b) and indicators for different land cover classes at segmentation level 1 in Chongqing.....	99
Table 4.4 Object variables and the classes which have break points at segmentation level 5 in Nanjing.....	112
Table 4.5 Values of Spectral (a), Shape (b) and Textural (c) indicators for different land cover classes at segmentation level 8 in Nanjing.....	121
Table 4.6 Values of Spectral (a), Shape (b) and Textural (c) indicators for different land cover classes at segmentation level 4 in Nanjing.....	123
Table 4.7 Values of Spectral (a) and Shape (b) indicators for different land cover classes at segmentation level 1 in Nanjing.....	125
Table 5.1 Comparison of classification accuracy between different classification algorithms. Case in Chongqing.....	142
Table 5.2 Error matrix (upper) and accuracy statistics (lower) for MLC. Case in Chongqing	145
Table 5.3 Error matrix (upper) and accuracy statistics (lower) for Object oriented classification. Chongqing as a case.....	146
Table 5.4 Class proportion (by Object-oriented approach). Case in Chongqing	147
Table 5.5 Accuracy Statistics for Object-oriented Classification after Aggregation. Case in Chongqing	147
Table 5.6 Comparison of classification accuracy between different classification algorithms. Case in Nanjing.....	156
Table 5.7 Error matrix (upper) and accuracy statistics (lower) for Object-oriented classification. Case in Nanjing.....	159
Table 5.8 Error matrix (upper) and accuracy statistics (lower) for Maximum-likelihood Classification. Case in Nanjing.....	160
Table 5.9 Class proportion (by Object-oriented approach). Case in Nanjing.....	161
Table 5.10 Accuracy Statistics for Object-oriented Classification after Aggregation. Case in Nanjing.....	163
Table 6.1 Class-level landscape metrics for “urban green space” in the 10 km buffer circles of Chongqing and Nanjing	183

CHAPTER 1. Introduction

1.1 Problem Statement

Urbanization and its impacts on the environment is now one of the most urgent concerns of both policy makers and scholars in the world. Global urban population grows much faster than does the total world population (Sui & Zeng, 2000), in which rate of urbanization in the developing countries has long surpassed that in the developed world. Far more important, however, is not the speed of urbanization; but rather the “environmental stress” brought about by it, which manifests itself as urban sprawl, traffic congestion and various types of pollution (De Ridder, 2003). Urban green space is highly potential in mitigating the adverse effects of urbanization and enhancing people’s sense of quality of life, therefore making cities livable and sustainable human settlements (De Ridder, 2003). Careful investigation and planning of green areas in urban areas, especially in respect of their compositional condition and spatial relationships with urban concrete fabrics, are substantiated.

Awareness of environmental problems induced by rapid urbanization and the importance of urban greening began to emerge in the five years, which is evidently shown by surge in volume of literature concerning urban green space in Chinese cities. Most of the relevant literature pointed out directions on how to improve vegetation coverage in urban areas of China. However, amount of researches falls short of enough when it comes to analyses of existing condition of vegetation within and bounding cities. This finding provides aspiration for this research project. Particularly, we are concerned about the differences between cities in the eastern seaboard, which are more developed

and urbanized; and those in inner China, which are backward and less urbanized. Question as to whether disparity in the state of urban growth brings forth different conditions of urban green space in China is by and large unknown. It constitutes one of the two goals of this research.

Landscape ecology provides an established theoretical framework under which our research concerning with the condition of urban green space in China can be undertaken. It is a relatively new branch of ecology specifically focusing on the interaction between structure of landscape element and ecological processes operating within the landscape element; plus patterns of changes of the interaction over time (Forman & Godron, 1986). One of the basic premises of landscape ecology is that it perceives a landscape as patches (basic homogeneous units of landscape) of different types/classes embedded within a background matrix. Different states of a landscape can be indicated by the changes in configuration of patches of a particular type (Turner et al., 2001). Based on this reason, landscape ecologists have been striving to work out methods to describe spatial structure of landscape patches, the most common of which being landscape metrics. Landscape metrics is a variety of quantitative measures of spatial pattern of landscape mosaic (Frohn, 1998; Farina, 1998; Lěitao & Ahern, 2002; McGarigal, 2001). The development of landscape metrics has been very rapid. Hundred of metrics have been developed to quantify different aspects of landscape structure. Chiefly, four types of spatial patterns can be revealed: landscape composition, contagion/aggregation of a particular patch type, fragmentation, and patch shape complexity (Frohn, 1998). Using metrics of these four types, insight is expected to be shed on the disparities of landscape structure in different Chinese cities.

Analysis of any urban phenomenon relies upon remotely sensed data and geographic information. A classification map derived from remotely sensed imagery describing accurately the spatial distribution of different land covers is a prerequisite for landscape study at the later stage. Conventional classification methodologies, especially those using spectral features as sole data input for classification, has been increasingly found inadequate in many classification tasks. Their operations are usually so simple that Gaussian probability distribution of spectral variables for each class is assumed. Such simplicity is often criticized as too unrealistic to apply in real case (e.g. Frizzelle & Moody, 2001; Foody, 1996; Gopal & Woodcock, 1994; Low et al., 1999). Besides, many of them assume within-pixel homogeneity, regardless of spatial resolutions of sensors and sizes of real-world features under investigation (Fisher, 1997). Such rigidity is also too inflexible to deal with real case in which mixture of land covers within a pixel is a norm (Atkinson et al., 1997; Frizzelle & Moody, 2001). Moreover, conventional classifiers tend to neglect the importance of contextual and textural features to accurate classification. For instance, size, shape, and texture of a spatial object can be helpful in identifying which class a local region belongs to. Failure of recognizing meaningful spatial entities, and their inter-linkages, to derive image semantics from an image deems conventional classifiers inhuman (Blaschke et al., 2000; Definiens-Imaging, 2003).

Object-oriented classification concept allowing segmentation of image at whatever scale of image abstraction is suitable to represent a particular spatial feature. A diversity of attributes about an image segment, including configuration and texture, is automatically obtained and used as features for classification at a later stage (Definiens-Imaging, 2003). Segmented image objects of different scales are linked by hierarchical network. Fuzzy rules can be generated to define a class based on spectral, spatial and

semantic information about image objects, by which membership values to each potential class is derived and ordered. By making use of the knowledge extracted from the segmented image, a decision tree can be created which is similar to Figure 1.1 (Lawrence & Wright, 2001; Borak & Strahler, 1999).

In this research, object-oriented classification concept will be tested on the interface of ecognition™ whether classification accuracy can be significantly increased by this approach compared to conventional classifiers. In light of multitudes of possibilities for operating segmentation in terms of size, spectral and shape heterogeneities; and numerous statistics to formulate features for each class, we are especially interested in how different possibilities of segmentation affect the representation of different land covers; and which object statistics are suitable to identify a particular land cover. Accompanying by these knowledge, we expect to find the best series of segmentation levels and classifying rules for our multi-level object-based classification.

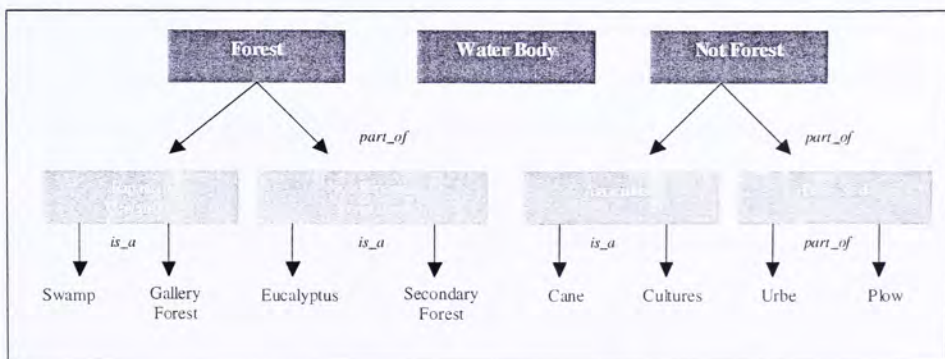


Figure 1.1 Semantic net based on prior knowledge and image interpretation.

Source: Antunes et al., (2003)

1.2 Research Objectives

The goal of this research is twofold: In the field of image classification techniques, this research aims at understanding whether object-oriented classification concept is capable of improving the defects of conventional classification methods, by which classification accuracy can be lifted. In the aspect of urban landscaping in China, it applies the measurements derived from landscape ecology in order to identify landscape structure of urban green space in Chinese cities, and compare the urban green landscape between coastal and inland cities.

Specifically, the research is expected to attain the following tasks:

In the field of object-oriented classification:

- I. Identifying spectral, shape and textural features of image objects generated by multiresolution segmentation, which constitute “class signatures” for expected land cover classes; and tracking their variability for each class along different scales of segmentation, thus extracting classifying rules for classification.
- II. Detecting the variability of class mixing within segmented objects at different scales and spectral-shape ratios, in an attempt to optimize the segmentation operation, with which multi-level object-based classification can be optimized.
- III. Comparing both segmentation specifications and “class signatures” of expected class between different Chinese cities to investigate into the transferability of object classification knowledge in different locations.
- IV. Operating multi-level classification with segmentation at optimized scales and spectral-shape ratio and pre-designed Decision Tree structure, which is of higher accuracy compared to other conventional pixel-based classification methods.

In the field of urban landscaping in China:

- I. Analyzing structure of urban green space in two Chinese cities, Nanjing in the eastern seaboard and Chongqing in inland China, and its changes from city center to periphery with class-based landscape metrics, focusing on landscape composition, fragmentation pattern, class contagion and patch shape complexity.
- II. Explaining the similarities and disparities of structure of urban green space in the two cities with respect to their patterns of urban development.

1.3 Research Significance

Increasing awareness of the importance of green space to the environment of urban China is revealed by the surge in volume of literature concerning with the issue in the last five years. Also, much of the relevant literature advocates the application of landscape ecological concepts in improving urban parks and other green areas in urban China. Nevertheless, researches which focus on anatomizing specific problems of urban green space in different cities are found insufficient. Accompanying with remotely sensed data and spatial metrics derived from landscape ecology, this research is able to detail the structure of green areas of Chinese cities at macro-scale. Structure of urban green space of a city will be indicated with respect to composition, fragmentation, contagion and complexity of the shape of green "patches". Collectively, these indicators help identify the anthropogenic impacts on urban green space.

The research adopts a buffer approach to investigating the change in landscape structure of green space from city center to urban periphery, which is expected contributive to understanding of the interaction between urban green space and urban development in China. Above all, disparities of both socio-economic conditions and

urbanization levels between eastern cities and cities in inner China have been widely documented (e.g. China Urban Statistical Yearbook, 2003; Luo & Chen, 1999; etc.). Whether these discrepancies lead to obvious differences in patterns of urban development and thus green landscaping is, however, generally untouched. This research is expected to shed insight on such uncertainties.

Segmentation is actually not a new remote sensing technique. Much literature has critiques of its strengths and weaknesses (e.g. Raucoles & Thompson, 1999; Ivtis et al., 2002). However, less literature point out that segmentation is actually a process grouping heterogeneous pixels as one homogenous segment, which intrinsically induces within-segment heterogeneity. Therefore, it is by and large unknown as to how the within-segment heterogeneity extends with increasing scale of segmentation, and how such heterogeneity extension in turn influences the quality of object-oriented classification. Besides, most of the researches testing object-oriented classification focus on one study site at a time (e.g. Herold et al., 2002; Gomes & Marçal, 2003; etc.); while this research also investigate into the transferability of the classification knowledge (mainly classifying rules derived from “class signatures”) in different sites.

1.4 Organization of the thesis

This thesis is organized as follows:

The first chapter is introduction, briefly explaining the rationale of this research. It is followed by Chapter 2, in which literature concerning major concepts in this research is reviewed. It includes the definitions and various classification methods of urban green space and different approaches to studying it; development of image classification

methods, specifically pinpointing weaknesses of conventional classification methodology and uniqueness of object-oriented classification concept; and basic principles and application of landscape ecology on recent landscape studies.

Study sites and methodology of the research are outlined in Chapter 3. Two study sites, Chongqing and Nanjing, will be preliminarily described and compared regarding their geographical settings, political and governance statuses, and quality of environment and landscaping. ASTER data, which is the main data source of this research, will be introduced next, concerning chiefly its spectral and spatial resolution and pre-processing. The workflow of the object-based classification will then be elaborated step-by-step. Landscape analyses with focuses set on buffer analysis approach and metrics applied in the research are discussed to finish the chapter.

Presentation and interpretation of results of the research go through the thesis from Chapter 4 to Chapter 6. In Chapter 4, variations in spectral, shape and textural features of segmented image objects along the segmentation gradient will be interpreted, which has two aims: Firstly, detecting the extension of within-object heterogeneity, thus class mixing, with increasing scales and spectral-shape ratio of segmentation; by which segmentation process is optimized, generating three object levels for classification. Secondly, the distinctiveness of each land cover class in terms of “object features” is revealed, which is a means of extracting classifying rules for the object-oriented classification.

Chapter 5 details the design of Decision Tree, or Class Hierarchy (Definiens-Imaging, 2003), for object-oriented classification in both Chongqing and Nanjing, with

classifying rules of some special land cover classes enumerated as case studies. After that, comparison of object-oriented classification with other conventional classification methods in terms of classification accuracy and proportion of land cover in the study site will follow. Comments on the defects of classification rules and the transferability of classifying rules based on our classification experience will conclude this chapter.

Results of landscape ecological analyses of urban green space in Chongqing and Nanjing are summarized in Chapter 6. Structure of urban green space in each city, in aspects of landscape composition, fragmentation, class aggregation and patch shape complexity, and its change from city center to city periphery, will be discussed with the aid of class-based metrics. Comparison of the structure of urban green space in total landscape between two cities will be followed in order to interpret their similarities and disparities. Precautions about the explanation power of landscape metrics and limitations of buffer analyses will also be added.

Chapter 7 is a conclusion chapter. Summary of research results are briefed, followed by discussion of limitations and constraints of the research. It will also shed light on the future of further research in this field.

1.5 Definition of Urban Green Space

Operational definition of urban green space in this research includes all vegetation in the city proper areas, which is the 10-km buffer from city centers. It includes natural woodland and grassland, wetland vegetation in riparian areas, plantation in urban parks, residential, commercial and other land uses and agricultural crops.

CHAPTER 2. Literature Review

2.1 Introduction

In this chapter, major relevant concepts related to this thesis are reviewed. It will begin with urban green space, the sole target of the research. Following it is a brief discussion of crises and futures of contemporaneous urban landscaping in major Chinese cities. After that, remote sensing techniques, especially image classification methodology, will be evaluated, with particular focus put on object-oriented image classification techniques, which will be assessed in this research. Finally, concepts and applied metrics of landscape ecology will be canvassed in an attempt to generate a conceptual frame under which this thesis proceeds.

2.2 Urban Green Space

Value of urban greenery in terms of facilitating effective functioning of a city is well documented. Fabos's (1995) review paper helped generalize the importance of urban green space to urban centers. Its benefits are threefold. Green open space enhances a healthy environment, in which a range of recreation needs, either active or passive, are satisfied. Besides, some green space contains and thus helps preserve historical and cultural heritage. Most of all, urban green space is often the only landscape element in urban centers which possesses the ability to maintain and enhance biodiversity. This is especially the case in many Asian cities characterized by high pace and density of urban development (Jim, 1989; Jim, 1989a; Jim, 1998; Jim & Liu, 2001).

Therefore, a proper arrangement of urban green space is an essential element with which urban planning is concerned. Before any green space plan of a city is to be blueprinted, systematic investigation of existing condition and spatial distribution of the city's urban green space system is necessary.

2.2.1 Classification of Urban Green Space

Researchers classify urban green space in different ways depending upon their own research objectives and perspectives into urban green space. Jim (2002) used the ideology of town planning in Hong Kong to classify "Plantable Spaces (PSs)", that is potential urban green space, in terms of their locations and land ownership. Such kind of classification approach is seldom adopted in landscape ecological studies which focus more on functions, distribution patterns, habitats and scales of green space. For instance, Tyrvainen and Vaananen (1998) divided urban forests based on their functions into three categories: forested parks, wooded recreational areas and protection forest belts separating housing.

On the other hand, some researchers use their classification schemes to indicate different relationships between urban green space and urban settlements at varying scales. Gobster (2001) categorized urban open space according to four scales: Interspaces (i.e. small planters and lawns along pavements, parking lots and so forth) within neighborhood at the lowest scale; public park shared by different neighborhoods; regional greenways that spans across counties or even states; and metropolitan bioserve at the highest scales.

2.2.2 Configuration of Urban Green Space System

The classification described above is chiefly based on different roles urban green space play in the urban context. There are also classification schemes which differentiate urban green space with the criterion of green space's configuration. Configuration of urban green space is a representation of size and shape of green canopy in urban area (Jim, 1989). According to Yu (1998), configuration of urban green space system can be analyzed at different scales. Each scale indicates a particular level of spatial details and carries different meanings: 1) Macro-scale—a regional planning issue which conceptualizes an open space system as a manifestation of relationship between green space system and urban concrete built-up; 2) Meso-scale—a more detailed analysis of layout of open space system components, with special attention being paid to the planning of urban center open space; and 3) Micro-scale—every green space unit is anatomized for design, protection and management.

Not all scales of green space are able or needed to be considered in landscape ecological studies (Turner et al., 2001). It depends largely on research objectives concerned and research tools that are used. For studying urban green system as a whole with remote sensing tools, as in the case of Jim (1989 & 1989a), a classification of urban green space spatial structures at meso-scale or higher is apparently more practical.

Yu (1998) generalized four classical models of spatial arrangement of green space system at macro-scale after analyzing green space system development overseas:

1. Concentric Ring Pattern—a pattern in which open space acts as a concentric barrier cordoning off urban sprawl. The whole urban region is

encircled by 4 concentric green rings including: inner-city ring, suburban ring, green belt and rural ring. The most notable example is the Greater London.

2. Embedment Pattern—open spaces and urban settlements exist alternatively resulting in ribbons, rings, polygons and especially wedges extending from suburbs. Green spaces often exist between growth axes such as highways and railways. The Greater Copenhagen is one of those typical examples.
3. Nuclei Pattern—individual settlements (nuclei) develop around a “green heart” at the center well protected by greenbelts separating them apart. It is not very common because of intense urban growth. But we can still find a close example in the Amsterdam-Rotterdam-Hague metro region.
4. Ribbon Pattern—usually evolved in metropolis with linear growth. (Linear) green space runs along the sides of linear metropolis so as to prevent against excessive urban sprawl. The linear green space tends to go along river channels or highways parallel to urban region. The Greater Paris grows following such pattern.

In short, green spaces are most commonly classified with respect to their functions, forms and shapes. However, the best classification method should be tailor-made in different cases, fully considering research objectives, research methodology and local condition. In the next section, different approaches to urban green space study are

presented. Their implications on data and tools used, and henceforth classification schemes applied, are discussed.

2.2.3 Different Approaches to Urban Green Space Study

There are mainly two approaches to the analysis of urban green spaces. The first approach is small-scale investigation of individual trees or small tree patches such as local parks by ground survey. This approach merits itself by its comprehensiveness and high precision in terms of both targeted population and variables. For example, Jim and Liu (2001) survey urban trees in five zones of Guangzhou and acquire a comprehensive record of individual tree patches, which includes species composition, location, frequency, dimensions, growth forms and amenity characteristics, at 100 percent sampling intensity. However, the coverage of ground survey is often insufficient to reveal a distribution pattern of green space of a whole city; or it is very expensive if anyone wants to conduct a comprehensive survey at such a high precision level (O'Neill et. al., 1997).

Another approach is synoptic identification and subsequent investigation of urban green space in a large area from remotely sensed imagery. This approach studies a large region (e.g. a city) as a landscape, into which green space is investigated. It is the reason why it is sometimes called "landscape approach" (O'Neill et. al., 1997). Research using landscape approach commonly resort to remotely sensed images as main data source, from which different classes of green space and other land uses are extracted through automatic classification or visual interpretation, with respect to their spectral signatures, configuration and distribution patterns (Jim & Liu, 2001). For example, Bin et al. (2003) extract green space and other urban land uses of Pudong of Shanghai from Landsat TM

imageries and analyze their multi-temporal variations. Landscape approach to urban green space study has many limitations, For example, scale and image classification accuracy may influence the interpretation of landscape pattern (Chuvieco, 1999; O'Neill et. al., 1999). Its limitations will be discussed in detail in later sections on landscape ecology. Notwithstanding its weaknesses, landscape approach is less expensive and more practical than ground surveys when labor and budget is constrained while research is to focus on spatial distribution of green space in a city, rather than detailed variables about individual trees or tree patches (O'Neill et. al., 1997).

Implication from this section is that in case of green space study in which detailed in-situ investigation is difficult to carry out (like this research), remotely sensed imagery is the dominant data source, from which spectral reflectance and configuration are key variables for identifying green spaces. Henceforth, sizes and forms of, and spatial relationships between green space will be quintessential to research (Jim, 1989).

2.3 Urban Green Space in China

Needs of green space are soaring in China where an increasing proportion of people will live in cities (Jim, 1989; Jim, 1989a; Jim, 1998; Jim & Liu, 2001). There is a lot of literature about urban green space published in China in the last 5 years (Zhang, 1999; Cao, 2001; Wang, 1999; Fang et al., 2001; Feng et al., 2003; Qin, 2001; Zhou & Tao, 2003; Zang & Feng, 2003). A rising awareness of the need of urban green space in China is palpable. A summarized description of the general problems and potential development of landscaping in major Chinese cities is provided in the following sections.

2.3.1 General Problems

Urban green spaces in Chinese cities are mainly threatened by 3 problems. First of all, unrestrained urban development and chaotic land use allotment have seriously contaminated, or even outrageously destroyed, urban green space and other natural habitats within and around cities. Second, urban green spaces in many cities are unevenly distributed. A few very large scale public parks take a predominant share of the total urban green coverage, with insufficient number of medium or small green spaces which can serve local residential neighborhoods. Third, patches of green spaces in urban districts seldom have connections with one another or to natural environment outside city proper. Lack of green corridors paralyzes some critical ecological functions of urban green spaces such as species migration and genetic exchange.

2.3.2 Increasing Awareness of Environment

Scientists and government decision makers are increasingly aware of the environmental impacts of rapid urbanization of urban cities. Sui and Zeng (2000) argue their paper that promotion of the development of middle-level and intermediate cities by many policy makers in China will impose harmful impacts on the environment by seriously fragmenting forested and agricultural land neighboring cities. The Tenth Five-Year Plan for Social and Economic Development in Chongqing (2001) revealed government's attention on the functions of urban greening: controlling soil erosion and river pollution. Volume of literature concerning improvement of city landscapes has been multiplying in the last few years. Some of them are about ecological analyses of vegetation within and bounding big cities in China. Guan et al. (1999) compared landscape structures between old urban areas and new urban areas in Guangzhou using landscape metrics and pointed out the merits of high landscape heterogeneity of

vegetation on urban environmental quality. Zhang et al. (2004) used both class-level and landscape-level metrics to analyze the spatial pattern of urbanization in the Shanghai metropolitan area and its impact on fragmentation of surrounding rural landscape. Zhao et al. (2003) also analyzed urban landscape of Shanghai focusing on landscape heterogeneity and stability of Pudong, city center of Shanghai.

Most of the research articles about Chinese landscaping, however, punctuated directions to improve the existing green space system, which are rather similar to one another. They are more or less inspired by two critical concepts. The first one is landscape ecology, which is a subject trying to explore the interaction between landscape pattern and ecological processes, and their changes over time. (Forman & Godron, 1986) Chinese landscape experts are increasingly inclined to adopt models and measuring methodology derived from landscape ecology to analyze urban green spaces and synthesize landscape plans to ameliorate persistent environmental problems. Elaborated discussion of landscape ecology, its concepts, models and metrics, will be left to later section.

The second one is the so called Greenway Movement, which aims at creating "green corridor" along urban linear features such as river channels to connect existing isolated patchy green spaces within and around the city region, an attempt to enhance green space connectivity and diversified functions (Little, 1990; Fabos, 1995; Walmsley, 1995). Much literature about Chinese landscaping set up plans to utilize "urban lines" to provide connecting green corridors interweaving both inside and surrounding cities (Jim & Chen, 2003; Yan & Wang, 1999; Yang, 2003).

2.3.3 Chinese Definition of Urban Green Space

Urban development in many Chinese cities is different from western countries because they are the results of blending of planned economy (before 1980) with market economy, especially after 1990s (Zhou, 1998; He et al., 2002). This fact seems to deviate from western green space spacing model when it comes to analyzing green space configuration in China. For this reason, Zheng (1999) grouped urban green space in Chinese cities into 4 types:

1. Patchy pattern—usually found in old cities like Shanghai and Tianjin in which large public green parks spread regularly in the city proper. Such pattern is criticized mainly of its lack of green connection, which can enhance green spaces' capacity of supporting flora and fauna (which in turn enhancing its amenity values), and shading and absorbing pollutants (esp. greenhouse gases), which help improving the atmospheric environment of urban areas (Jim & Chen, 2003).
2. Ribbon pattern—green space develops along waterway systems, road networks and ancient city walls and other linear features, forming greenways or even green web of capricious patterns such as rectangular, radiated and ring. Its strength in terms of beautifying cityscape is eminent. Examples include Nanjing and Harbin.
3. Wedge pattern—green space at the outskirts of city infiltrates into city proper with decreasing width, forming wedge shape. For example, Hefei is surrounded by wedges. Generally, designers utilize river channels,

natural landforms and radiated highways to create greenways which then connect to agro-forests or windbreak woodlands in suburbs.

4. Combined pattern—that is to say, a composite of the layouts mentioned above. Its merit is an integration of the strength of all the three patterns. The resulting arrangement is likely to be a composite of urban green “points, lines and polygons”.

After taking balance between green space classification scheme of Chinese government and the ability of Landsat TM and SPOT to identify green features, Che and Song (2001) classified urban green space in Shanghai into 5 types: public green space, resident green space, auxiliary green space, agro-forest space and remnant natural green space. This classification scheme is similar to that generated by Zhou and Tao (2003) in Ningbo, who created an extra class “roadside green space” while deleting the classes “agro-forest” and “remnant natural green space”. Advantages of imposing such kind of classification schemes are twofold: green space categories under such classification systems have clear definitions offered by landscaping and gardening authorities in China (Cheng & Lo, 1999). Besides, the green space categories are readily recognizable on remote sensing imagery. For example, roadside green spaces are often recognizable by their linear forms; whereas public green spaces are easily distinguished from residential and auxiliary green spaces by their much larger sizes and more compact patch shapes.

A brief review of literature about urban planning and specifically landscape planning in China reveals that definition of green space adopted in urban planning, which mainly includes vegetation in designated plantable spaces, may not be suitable for

landscape ecological studies. In fact, woodland and grassland in other land uses, such as those planted beside residential areas, parking lots, etc., contribute as much to improvement of urban environment as designated green spaces do. Besides, agro-vegetation within the urban boundary is common in many Chinese cities and hardly found different from other urban vegetation from the perception of both urban inhabitants and landscape ecologists (Che & Song, 2001).

Furthermore, both academia and governments tend to decompose urban green space system into points, lines and polygons (Guan et al., 1999; Zhen, 1999; He et al., 2002; Zhou & Tao, 2003; Zhang, 1999). Such decomposition looks simple and coarse, but it may be very convenient for green space identification, investigation and planning in Chinese cities. It is easy to associate green space categories under Chinese classification system with these three spatial features, especially when remote sensing technique is applied in landscape study. For instance, public green spaces are usually large scale public parks and thus exhibit polygonal shapes in satellite image; linear features in satellite image logically represent roadside green space or other types of green corridors; scattered residential pockets may reveal themselves as green pixels. It is thus possible to first identify green "points, lines and polygons" on satellite image and then associate them spatially, which may help illustrate the urban green space system structure. Landscaping problems in a city investigated may henceforth be discerning after comparison between observed green space pattern and Chinese cities' green space models mentioned above.

2.4 Remote Sensing Techniques

Analysis of any urban phenomenon and urban green space in particular, relies upon remotely sensed data and geographic information, which can provide a synoptic view of an urban landscape (Turner et al., 2001). An accurate recognition and subsequent classification of spatial layouts of different land cover types from these kinds of data is a prerequisite. In this section, focus is on evolution of image classification to 10 years. A short review of image classification techniques is reported in the first sub-section, which includes description of some conventional classification methods, discussion of mixed pixel problems—a common deadlock in the field of remote sensing—and their impacts on conventional classifier. Because of basic deficiencies of conventional classifications, alternatives have been developed in the last 5 years. Their advantages, defects and implications will be reviewed next. A new image analysis software, e-Cognition, emerged 2 years ago and is expected to solve problems still plaguing alternative classifiers. Its multiple functions and merits will be presented at the last portion of this section.

2.4.1 Review of Image Classification Techniques

According to Jensen (1996), one of the most commonly used methods, by which thematic information (such as land use/land cover) can be extracted out of a remote sensing image, is image classification. It is a procedure of categorizing image units (usually pixels) into land cover classes useful to a particular study based on available information (usually multi-spectral digital values) from each image unit. As Lillesand, et al. (2004) stated, there is a large variety of image classification procedures, which can dichotomously into: supervised procedures in which statistical descriptors of the various land cover classes are pre-specified to classification system by representative “training”

samples of known classes; and unsupervised procedures which aggregate pixels into spectral “clusters” whose corresponding land cover classes in real world are determined by analysts afterwards. In the following section, only supervised procedures will be discussed because they are more commonly used during image classification and easier to be handled.

2.4.1.1 Conventional Classification Methods

Conventional classification methods (classifiers) can be termed as spectral classifiers because they tend to use only information provided from multivariate spectral reflectance to decide on which one of pre-defined classes is most probable to be assigned to a pixel (Atkinson et al., 1997). Atkinson and Tatnall (1997) pointed out that the most significant similarity shared by most of the traditional classifiers is their parametric nature, that is, they assume a multi-spectral Gaussian distributed feature space for each class.

Much literature has accounted for characteristics and drawbacks of conventional classifiers (Frizzelle & Moody, 2001; Foody, 1996; Gopal & Woodcock, 1994; Low et al., 1999). Summing them up, conventional spectral classifiers, particularly those applying Gaussian distribution assumption (such as discriminant analysis classifier), have two major characteristics: the first is that they are per-pixel classifications, in which each pixel in an image is treated individually during class assignment, while spatial relationships between pixels within a close neighborhood are ignored. It implies that classification of image can only rely on spectral reflectance of pixels, while many researches have pinpointed that such spectral classification methods cannot generate satisfying classification results, because textural and shape information are crucial for

characterization of some land uses, especially woodland and urban areas (Zhang, 2001; Fung & Chan, 1994). The second is that they are “hard” classification because every pixel in an image is assigned to only one class. Conventional classifiers assume land cover homogeneity within an entire area represented by a pixel and class labeling is thus based on multi-dimensional digital values of training sample pixels for each land cover class. They then assign each pixel to the class to which the pixel has the highest probability of membership, while the remaining classes of lower membership values are totally disregarded.

From the above descriptions about conventional classifiers, it is obvious that their limitations to image classification are rooted into their two fundamental assumptions: purity of pixel and membership dichotomy. These two weaknesses of traditional classification methods will be elaborated in the next sub-section on mixed pixel problem. Besides, these classification methods have the third weakness: unrealistic assumption about parametric probability distribution of spectral variables for each class. In real situation, the spectral values for defining feature space of a class do not always follow this parametric model. In short, conventional classification methods are constraints-ridden, even though they are widely used because of their ease of operation and automatic classification nature.

2.4.1.2 Mixed Pixels Problem

In remote sensing analysis, it is commonly agreed that pixels (the basic mapping units of an image) are “pure” in the sense that each of them represents an area assumed to be homogeneous, regardless of spatial resolutions of different sensors and sizes of real-

world features under investigation (Fisher, 1997). Actually, it is this assumption about pixel from which various conventional classification methods are derived.

Nevertheless, there are both intrinsic and extrinsic properties which render this basic assumption about pixel unrealistic and thus inappropriate. Intrinsically, Cracknell (1998) confirmed the non-uniform response within Geometrical Instantaneous Field of View (GIFOV) of a sensor corresponding to the pixel in image. That is, the sensitivity of sensor to a source of reflectance in terms of digital values (DVs) is variable within the GIFOV, rather than spatially homogeneous as commonly assumed, because of constant motion of spacecraft and continuous rotation of scanning mirror. Extrinsic problem which hampers basic concept of pixel is incurred by ground objects themselves. If a ground object is to be fully represented by a pixel, it has to fulfill three conditions: first, it is of the same size as that of the IFOV or its multiples; second, its edges run parallel or perpendicular to, or exactly overlapping pixel edges; and third, it should be such aligned that its center overlaps that of the pixel. However, few objects can satisfy even one of the above conditions. It is therefore reasonable that many pixels in an image cannot represent ground features purely. While intrinsic problems of pixel can be improved by sensor calibration and resampling, extrinsic pixel representation problems cannot be reversed unless some mutations of traditional image analysis methods arise (Fisher, 1997).

Because of the problems of pixel representation described above, especially the extrinsic pixel representation problems, a mismatch between scale of detection and that of details of spatial variation in land cover occur frequently, which results in a mixture of land cover classes within a pixel (Atkinson et al., 1997; Frizzelle & Moody, 2001). This phenomenon is termed as mixed pixel (such as Gulinck et al., 1993), sub-pixel mixing

(Atkinson et al., 1997) or “mixels” (Zhang & Foody, 1998). Mixed pixels can be discovered in almost all remotely sensed data. But they are particularly serious in urban environment, which is chaotically conglomerated by different land cover types with contrasting configurations and spectral signatures (Lein, 2003), as well as along boundaries of ground objects (Fisher, 1996). Fisher (1997) pinpointed four major forms of mixed pixel problems whenever a study attempts to extract information which is smaller than pixel size:

1. Boundaries between two or more land cover classes within a pixel;
2. Intergrade between land cover classes, i.e. ecotones;
3. Linear sub-pixel objects, e.g. rivers; and
4. small sub-pixel objects

2.4.1.3 Mixed Pixels’ Effects on Conventional Classifiers

As mentioned above, conventional classification techniques are characterized by their two assumptions—pixel purity and “hard” membership. The fact that these two characteristics impose great limitation on their abilities to deal with mixed pixel problems is widely discussed in literature (Blaschke et al., 2000; Cracknell, 1998; Fisher, 1996; Foody, 1996; Foody & Boyd, 1999; Zhang & Foody, 1998; Leung, 1988). They mainly spot two major weaknesses of conventional classifiers in terms of mixed pixels handling: first, per-pixel classification assumes sub-pixel homogeneity, which is an oversimplification of real world situation in which several features of interest can be found in an area represented by one pixel however high the spatial resolution. Second, the relative strengths of membership to all possible classes are shredded during production of “hard”

classification result, overlooking much classification information such as uncertainty of classification and class definition and inter-class similarity.

In short, conventional classification techniques are inadequate, or even erroneous, image analysis methods when an image is occupied by mixed pixels (a rather normal situation). Alternative methodologies may be needed to enhance the representation of actual land cover distribution.

2.4.1.4 Alternative Solutions to Mixed Pixels Problems (Fuzzy Sets)

Leung (1988) gave a clear definition of a fuzzy set, which is shown in equation 2.1. Let X be a universe of discourse (i.e. all objects of interest) with a generic element of X being denoted by x . Then a fuzzy set A in X is a set of ordered pairs:

$$[x, \mu_A(x)] : x \in X, \quad (\text{equation 2.1})$$

where $\mu_A(x) : X \rightarrow M$ is a membership function which maps $x \in X$ into $\mu_A(x)$ in an ordered set M which is called the membership set. $\mu_A(x)$ indicates the grade of membership of x in the fuzzy set A . Unlike conventional "two-valued logic approach", The membership set M can be any real number within a closed interval $[0,1]$, in which $0 < \mu_A(x) < 1$ implies that x belongs to A to a certain degree.

Implication of this definition is that a transition from membership to non-membership of a certain concept is gradual rather than abrupt. This concept has potential to be utilized in classification of real world objects because, according to Gopal and Woodcock (1994), categories in the real world are usually easily differentiable in their central states, while they are getting less separable with decreasing distances from

dividing lines between the categories. Trees and grassland often form an ecotone in which separation between these two classes is getting more difficult near the middle region of transitional area (Foody & Boyd, 1999).

Because of its distinctive ability to handle uncertainty and concept imprecision, fuzzy sets techniques, if adopted in image classification, may provide a feasible way to solve mixed pixel problems, informing image analysts of sub-pixel class proportion, which in turn delivering them with knowledge of classification uncertainty (Gopal & Woodcock, 1994; Foody, 1996). From the definition of fuzzy sets given above, it is understood that the most distinguishing feature of fuzzy representation is the subtle variation in membership values of object to different classes. It can then be inferred that fuzziness of classification can be modeled by assigning (or deriving) each pixel real membership values (within the range between 0.0 and 1.0) to all candidate classes. As a result, output of classification will be a set of membership values of a pixel to all possible classes, instead of a definitive judgment about the classification of any pixel. Such a classification approach is called soft classification approach (Lein, 2003; Frizzelle & Moody, 2001).

There are 2 main ways of deriving fuzzy membership values to land cover classes for pixels: the first method is to “soften” the output of conventional classification procedures by deriving a measurement of fuzziness of membership. For example, discriminant analysis classifier such as Maximum-Likelihood Classifier contains *a posteriori* probability of class membership to each class for each pixel, which can be utilized to surrogate pixels’ membership values to the corresponding class. In the case of Artificial Neural Network (ANN) classification, the strength of class membership can be

converted from the activation level of network output unit for a particular class (Foody, 1996; Zhang & Foody, 1998). The second method is using Fuzzy classifier directly, which calculates the membership values to each class based on the measurement of the distances between value points (usually spectral values) of a pixel and mean value points of each class in class-defining feature space. The most widely used fuzzy classifier is Fuzzy C-means Clustering Algorithm (FCM) (Atkinson et al., 1997).

A “fuzzified” or soft classification method does not always mean sub-pixel classification. It is only the case if fuzzy membership values of a pixel in various land cover classes derived from soft classification can help estimate the proportions of pixel area occupied by the corresponding land cover classes consistently. Fortunately, much literature found that the proportions of each land cover classes in a pixel are highly and positively correlated to their corresponding class membership values, no matter which types of soft classification procedures (direct or indirect fuzzy) are used (Foody, 1996; Zhang & Foody, 1998; Atkinson et al., 1998), which is a fact that makes the problems of mixed pixels solvable.

2.4.1.5 Problems Fuzzy Classifications are unable to solve

It is undoubted that soft classification techniques can highly improve the accuracy of classification, especially in terms of mixed pixels handling. Nevertheless, there are many problems inherent in classification yet to be solved. One of the most significant problems is still incurred from pixel representation. Fung and Chan (1994) and Blaschke et al. (2000) argued that mixed pixel problems is only one side of the mismatch between scale of sensor detection and scale of variations in landscape a particular research is interested in investigating. While mixed pixels can be satisfactorily solved by fuzzified

classification methods, another side of the scale problem (i.e. spatial resolution is too fine relative to some more generalized features such as urban land) is not the same case. Tools may be needed to group relatively homogeneous neighboring pixels in its stead. More generally, a universal scale of observation for different spatial features in an image does not exist. Image analysis system should be flexible enough to engender multiresolution perspectives into spatial features of different sizes (Blaschke et al., 2000).

Related to the first problem is the second one: pixel-based image representation is fundamentally limited and not intuitive to human beings. Human beings do not interpret remote sensing image like that. Rather, they rely on their recognition of some meaningful spatial entities, or objects, and their inter-linkages, i.e. image semantics (Blaschke et al., 2000). For instance, image interpreter will not perceive a highway as a string of pixels, but recognize it by its shape (long), its size compared to other roads nearby (bigger), complexity of linkages with other roads and volumes of vehicles within it. All of these attributes of a highway cannot be recognized until pixels can be regrouped into more meaningful items. It implies that only by acquiring knowledge at object level is it possible to attain a better image classification result (Sester, 2000). Various methods of modeling compact objects out of pixels have been developed. Filtering techniques with floating windows to generate similar textural units were widely adopted due to ease of their operations (Kiema, 2000; Teng & Fairbairn, 2002; Low et al., 1999; Franklin et al., 2001). However, such techniques induce loss of details provided by an image (Fung & Chan, 1995; Blaschke et al., 2000). Another main method of object extraction is segmentation or grouping of similar pixels. Although many segmentation algorithms have been developed, few of them lead to convincing results (such as Raucoles & Thompson, 1999). One reason is that segmentation involves many parameters and thus

enormous possibilities, some of which are unexpected (Ivitis et al., 2002). In other words, an image can be segmented into different numbers of image objects of varying sizes, which are then up to analysts to interpret. Besides, image objects created by segmentation may still be meaningless. A real object-based image analysis will be needed to explicitly express and handle a network of objects at multiple scales.

Summing up, a better image analysis and classification system will have the following requirements: 1) it may adopt soft classification approach to solve sub-pixel problems; 2) it may be sufficiently flexible to allow multi-scale perspectives into spatial features on an image—from pixel level to “region” level; and 3) it may evolve into a real object-based analysis, thereby image objects are not only extracted out of pixels, but also inherit a set of semantics relationships with objects of different scales. Such a system will rely on analysts to define object features, which implies a more integrated and interactive collaboration between computer system and human knowledge (Definiens-Imaging, 2003).

2.4.2 Object-oriented Classification Concept

Object-oriented classification concept has three characteristics with respect to image classification and analysis compared to other conventional software: multiresolution segmentation, fuzzy classification and object-based image processing environment (Definiens-Imaging, 2003).

2.4.2.1 Multiresolution Segmentation

Multiresolution segmentation is a function allowing extraction of image “object primitives” (i.e. image objects without semantics information) at different scales without

much prior knowledge about the site of interest. Pixels are grouped into spatially compact and spectrally similar regions. Different scales of image objects are linked together by object level hierarchy (Definiens-Imaging, 2003).

Unlike conventional pixel-based image classification methods, segmentation is an operation aggregating raw image pixels into regions which are spectrally and texturally intact. As Ivits et al. (2002) stated, hierarchical object-based image analysis has two major advantages: first, different segmentation levels enable perception of landscape objects at different scales; second, objects of different levels are such linked up that each object has its own set of relationships with its neighboring objects, “sub-objects” and “super-objects” which are interchangeable with human lexicon such as “containing”, “part of” and so on (Definiens-Imaging, 2003). Besides, a diversity of attributes about an object segment, including configuration, reflectance, texture and spatial relationship, is automatically calculated and will be used in later classification process.

2.4.2.2 Fuzzy Classification Procedure

Unlike conventional classifiers, fuzzy logic features during class assignment process is offered, allowing us to consider uncertainties of all kinds. In fuzzy logic space, an object has a variable membership value, term “*z-scores*”, to each and every class, depending on its degree of similarity to those classes (Definiens-Imaging, 2003; Foody, 1996; Foody & Boyd, 1999; Leung, 1988; Zhang & Foody, 1998).

Two fuzzy tools are provided: manual fuzzy rule and automatic nearest neighbor classifier. Manual Fuzzy rule allows us to create our own fuzzy “if-then” rules to define a class, based on the spectral, morphological, and hierarchical statistics pre-calculated for

segmented objects (Definiens-Imaging, 2003). For example, a class “vegetation” can be defined as “NDVI higher than 0.2”. Fuzzy membership function can be edited to refine class definition. Nearest Neighbor Classifier, on the other hand, is an automatic classification operation. The principle behind is simple: selecting representative samples for each class. Based on the samples, multivariate class rules for a class is automatically defined, using same statistics mentioned above. The algorithm will then search for the closest sample object of each class in the multivariate feature space for each object. “Z-scores” of an object to a class is converted from the distance between the location of the object in the feature space and that of the closest sample of that particular class (Definiens-Imaging, 2003).

It is meaningless if the classification only displays the class assignment with the highest membership value, ignoring other class assignments with lower membership values, which is the way conventional classification evaluation approaches (Foody, 1996; Ricotta & Avena, 1999; Zhang & Foody, 1998). So, classification evaluation is available by which the class assignments with the highest, the second highest and the third highest membership values are shown.

2.4.2.3 Object-oriented Approach to Image Processing

Object-oriented Approach is originally a new concept of database modeling in which class and objects, rather than relational tables, are basic units for representing real world features (Laurini, 2001). In object-oriented database, each entity is considered as an object which has a set of variables that describe the object, a set of messages that the object can use to communicate with other objects, and a set of methods which hold the codes to implement messages. Objects which share common properties are grouped into

an object class, while object classes are grouped into class hierarchy. Properties of a class would automatically “pass” to its sub-classes by *inheritance*, while the sub-classes can have its own specific properties (Han & Kamber, 2001; Leung, 1999).

A similar concept is adopted in this research. A class hierarchy is formulated by users to define a set of classes and relationships between the classes according to their classification scheme. However, it is different from the original concept of object-oriented approach in that a class does not automatically have a set of objects and attributes to define its objects. Rather, a class is merely a split between membership and non-membership which is determined by a set of rules (manual fuzzy rules or nearest neighbor rules described in earlier section) defined by users, or what are called “class properties” (Definiens-Imaging, 2003). Image objects are assigned membership to a particular class if their values of attributes satisfy properties of the class. It is important to know that knowledge for determining a rule is usually based on analysis of spectral, shape, spatial signatures, or all of them, which is already measured by the image analysis system. Therefore, knowledge base is inherent in the image system itself, rather than the user-defined class hierarchy.

2.4.2.4 Ecognition

In our research, ecognition™ is used to apply object-oriented image classification concept. The image analysis system will be used due to the following features. Image objects of different scales can be generated by multiresolution segmentation; object semantics are formulated from object level hierarchy and a diversity of measurements describing image objects are automated. Fuzzy classification procedures allow explicit expression of classification uncertainty. Above all, Fuzzy rules can be generated to define

a class based on spectral and spatial information about image objects obtained from the system. By making full use of the above functions, a decision tree can be created with specified fuzzy rules forming a series of dichotomous splits. Image objects will in turn use these rules to derive membership values in each class (Lawrence & Wright, 2001; Borak & Strahler, 1999). Classification result may be optimized by a more interactive cooperation between computer and human expertise and experience in a fuzzified semi-automated image analysis interface (Definiens-Imaging, 2003).

2.4.2.5 Research about ecognition

Several researches have been done to solve different landscape problems using ecognition™. Herold et al. (2002) applied multiresolution segmentation techniques to operate multi-level classification of IKONOS data, aiming to differentiate urban functions of Santa Barbara urban area and prepare the data for further landscape studies. Ivits et al. (2002) also applied the multiresolution segmentation and object-based classification concept through ecognition™ to classify forested landscape from Landsat-ETM+ and aerial photography, with which landscape connectivity is then calculated. Compared with visual interpretation, researchers found that object-based classification leads to more accurate detection of forested patches. Antunes et al. (2003) utilized the spatial, textural and semantic information provided by the object-based image processing technique to improve the classification of riparian environment, to which only spectral information is not enough, and attained positive classification accuracy.

Multiresolution segmentation can be operated at a numerous compositions of color and shape and a variety of scale parameter/size value. Infinite possibilities will thus occur when image objects are to be generated while which one among them is the best in representing a particular landscape element and for classification is yet to be known. Gomes and Marçal (2003) also pointed out that the “best” parameters for image segmentation is difficult to be identified. It implies that a systematic investigation of multiresolution segmentation to identify a set of parameters: color-shape ratio, average object size, object features, etc., suitable for separating land covers is reasonably needed.

2.5 Landscape Ecology

Landscape ecology is a new branch of ecology which specifically focuses on spatial dimension of ecological processes. Its concepts and derived metrics provide a linkage between a variety of disciplines such as biology, planning, geography, etc., which help academics and practitioners concerned realize sustainability (Leitão & Ahern, 2002).

2.5.1 Basic Principles

Landscape ecology, according to Forman and Godron (1986), is a subject which specifically focuses on the three characteristics of landscape: 1) structure, the spatial patterns of landscape elements and such ecological components as animals, biomass, energy and so forth; 2) function, or the interactions of objects between landscape elements, which are fundamentally assumed to be highly related to landscape structure; and 3) change, alterations in the landscape structure and function through time. From this definition, it can be inferred that landscape ecology attempts mainly to understand the interactions between spatial pattern and ecological processes of a landscape (Zhang et al.,

2004). In fact, many natural phenomena about natural landscapes seem to show that reciprocal relationship between ecological processes and patterns exist. That is to say process creates, modifies, and maintains a landscape pattern whereas pattern constrains, promotes, or neutralizes a process (Li & Wu, 2004).

Another remarkable concept of landscape ecology is that all landscapes can be perceived as essentially composites of patches, corridors and a background matrix. Variations in sizes, numbers, shapes, compositions and configurations of these three components are compelling indicators to differentiate one landscape from others. This so called “patch-corridor-matrix” landscape model have been widely adopted in many different landscape researches, especially urban landscape planning and architecture projects (Jim & Chen, 2003; Ivitis et al., 2002).

2.5.2 Landscape Metrics

Landscape metrics can be defined as a variety of quantitative measures of spatial pattern of landscape mosaic (Frohn, 1998; Farina, 1998; Leitao & Ahern, 2002; McGarigal, 2001). As pinpointed by Turner et al. (2001), a method of quantifying and describing spatial pattern of landscape components is necessary for the establishment of understanding of structure-process relationships in landscape ecology. Knowledge of landscape pattern is contributive to at least four practical aspects: 1) confirmation of the occurrence and nature of landscape change; 2) comparison between two or more landscapes in terms of the degree of similarity; 3) a quantitative yardstick for evaluation of land management or development alternatives; and 4) an objective tool for description of spatial patterns, which in turn can implicate ecological processes e.g. movement

patterns of organisms. These four tangible functions of landscape metrics render it fruitful in addressing the spatial issues of landscape planning (Leitao & Ahern, 2002).

The development of landscape metrics has been very rapid. However, utilization of landscape metrics should be cautious. Neel et al. (2004) tested 55 commonly used class-level landscape metrics using both modeled and real landscape at gradients of class area proportion and class autocorrelation levels. The test reveals many significant findings about behavior of these class-level metrics. Several metrics purported to measure certain landscape attributes, such as class autocorrelation do not show high correlation to them during the test. A number of those whose correlation values are high fail to output non-linear responses to what they are supposed to measure. For instance, class area proportion metrics may behave asymmetrically at low versus high level of spatial autocorrelation. In addition, some metrics which are the most commonly used even exhibit erratic behavior at very high or low level of class area proportion. Unstable behavior of metrics deems interpretation of them very difficult or even misleading. Above all, the test also find that some metrics which are claimed to measure conceptually different attributes of landscape pattern actually show similar response to same attribute. It implies that some metrics are highly correlated to each other and thus redundant, which is a point criticized frequently in literature (Turner et al., 2001; Cifaldi et al., 2004). These major limitations, together with others such as vulnerability to scale of observation and accuracy of classification map (Li & Wu, 2001; O'Neill et al., 1997), are needed to be considered before we choose any metrics for describing landscape pattern.

Roughly, landscape metrics tend to indicate the following 5 types of spatial patterns of landscape (Frohn, 1998):

- Diversity: Total number of landscape types
- Dominance: Degree of dominance of a landscape by a few patch types
- Contagion: The tendency of a land cover type to cluster into a few large patches
- Fragmentation: The tendency of a land cover type to break into small patches
- Patch shape complexity: The relationship between the perimeter of a patch and the area of that patch.

2.5.3 Application of Landscape Ecology in Landscape Analysis

Applications of landscape ecological concepts and metrics in research and policy address applying landscape ecological concepts and landscape metrics are enormous, especially in study of rural landscape. Weiers, et al. (2004) chose 3 principal metrics (mean patch size, patch density and mean shape index) to evaluate the effects of European agricultural policy on improvement of ecological structure in Germany. Selinger-Looten et al. (1999) quantitatively analyzed the spatial patterns of meadows to establish the relationships between landscape pattern of meadows, ecological processes and effects of human activities in the flood plains in north-east France. Because landscape metrics are sensitive to class area proportion and class aggregation, (Neel et al. 2004), they are widely used in studying trends of forest or habitat fragmentation (Bélandger & Grenier, 2002; Schumaker, 1996) and other similar themes (Gulink et al., 1993; Chuvieco, 1999).

However, application of landscape ecology should go beyond the scope of rural or natural landscape. Zhang et al. (2004), Guan et al. (1999) and Wu and David (2002)

argued that landscape ecology is in fact able to provide new perspectives into study of spatial pattern and dynamics of urban system, henceforth facilitating our understanding of urban settlements, major habitats for human beings. Actually, research on urban landscape with landscape pattern indices is numerous. Fung and Siu (2001) analyzed temporal change in magnitude and variability of NDVI and their spatial patterns using entropy of NDVI. Guan et al. (1999) Guan et al. (1999) studied urban vegetation in Guangzhou classified in species, districts and patch sizes using a suit of heterogeneity indices. In metropolitan centers of China like Shanghai and Beijing, some research attempt to quantify urbanization processes with class-based landscape metrics (Bin et al., 2003; Zhang et al., 2004; Qi et al., 2004).

Among urban landscape research, most of those operate analyses on pixel-based classification data. Whether result would be different if object-approach classification data is used is by and large unknown. Object-based classification produces more natural pattern of landscape than pixel-based classification does, thus potentially improve quality of environmental monitoring (Blaschke et al., 2000; Ivtis et al., 2002). Herold et al. (2002) used object-based classification to map and analyze land cover/land use in urban area. Their research reaches similar conclusion that object approach improve separation of some otherwise confusing urban land covers. It implies that urban landscape analysis with landscape metrics may be different using object-oriented classification map from that using pixel-based mapping.

2.6 Conclusion

Summing up, urban green space is a landscape element which maintains/enhance the biodiversity and livability of every city and thus deserves much more attention paid

by academics and planners than it has ever been. It is especially so in Chinese metropolitan areas which are often plagued with dense and chaotic urban development at the expense of urban green space.

There are two ways of studying urban green space, each of which has particular characteristics and merits. However, studying urban green space using remote sensing and image classification data is preferred for research in which detailed field investigation is hardly feasible. Besides, image classification method concerned should be able to take into consideration the spatial relationship between patches of urban green space from an image. In this respect, multi-scale image segmentation and object-oriented approach to classification may outperform other conventional pixel-based classification methods in study of urban green space.

Landscape ecology is a branch of ecology which explicitly expresses the importance of spatial dimension in analyzing the interaction between ecological pattern and processes. Some of its core concepts, such as patch-corridor-matrix model, and derived landscape metrics may be useful in interpretation of landscape problems of a city if they are used with precaution.

CHAPTER 3. Study Sites and Methodology

3.1 Introduction

After the review of all the concepts and researches relevant to this research in the previous chapter, study sites and methodology of this research will be detailed in this chapter. The two cities under investigation, Chongqing and Nanjing, will be introduced in terms of their geography, administration characteristics and environmental problems. The differences between them in urban layout are briefed by interpretation of their images. Next, the whole working procedure of this research will be discussed. First, ASTER data and its pre-processing will be introduced; Second, hierarchical classification systems of the two cities and their disparities will be presented; Third, the process of object-oriented classification will be explained, which includes image objects analyses, creation of object hierarchy, design of class hierarchy and classification accuracy after the classification is accomplished. After that, organization of landscape analyses of urban green space will be discussed, which is followed by conclusion of this chapter.

3.2 Study Area

3.2.1 Chongqing

Chongqing is a very special place with respect to its geographical, geomorphologic, political and ecological situations. Its city proper region deserves special focus because it is one of the most vivid economic centers in western China (Zhao, 2000).

3.2.1.1 Geography and geomorphology

Chongqing is situated at the joint of Changjiang River and Jialing River (Zhongguo Chengshi Dituji Bianji Weiyuan Hui, 1995a). It extends from 105°17' to 107°04'E in longitudes and 28°22' to 30°26'N in latitudes (Liu, 1989; Zhao, 2000), occupying an area of over 82,000 km². By classification of mountainous cities innovated by He et al. (2003), Chongqing is composed of very distinctive landforms: high mountain ranges in eastern and southern parts while low hills and valleys in the middle. The city proper is located at the middle low-hill region, which is further divided by Changjiang and Jialing River into 3 regions. The 3 regions are in aggregate about 600 km². Low hills and rivers arrange themselves alternatively across the city proper.

3.2.1.2 Administration and governance

Chongqing Municipality (直轄市) was set up during the 8th National People's Congress in March 1997 because of its two strategic characteristics: First, Chongqing is located at the upper course of Changjiang and thus can act as another growth pole of the "Changjiang Fazhan Janliue" besides Shanghai at the lower course. Second, Chongqing can act as the main city supporting the "Xianshia Kuqu Fazhan Janliue" (Luo & Chen, 1999). Chongqing city proper includes Yu zhong district, Nan an district, Jiu long bo district, Jiang bei district, Yu bei district and Sa ping ba district. Yu zhong district is the city center, attracting the highest population and most of the governmental, commercial and cultural functions ("Zhang ling yang zi zhu lu xing shou ce" bian xie zu, 2002). Master Plan of Chongqing City Proper (Chongqing Gueihua Sheji Yanjiouyuan, 1995) is shown in Figure 3.1. For nearly seven years after the establishment of the Municipality, Chongqing developed rapidly in urban size, population and economic strength.

Considering the landscape situation of Chongqing and the ambition of its government, it is reasonable to deepen investigation into the landscape pattern, problems and opportunities of Chongqing.

3.2.1.3 Environmental Quality

In spite of its rapid development, Chongqing is still backward compared with the other three Municipalities in terms of environmental quality. As shown from Table 3.1, green coverage in built-up area (21.8%) ranks second lowest among the four municipalities, only higher than Shanghai. Its per-capita green space coverage is the lowest among the four cities. Besides, like other major cities in China, green space of Chongqing is often highly patchy, without sufficient connections provided by green corridors (He et al., 2003).

3.2.1.4 Government Attempt to Improvement

In order to tackle the problems faced with Chongqing, municipal government resorted to the re-planning of main urban centers. Chongqing Municipal General Committee passed the "Chongqing Municipal Area Landscape Planning 2001-2020" in 2002, aiming at re-forestation across the whole city and integrating trees into the hill slopes and meandering rivers in the city proper. Moreover, new zone development was initiated north of the original old urban centers in an attempt to focus all the main financial and transportation functions in the north. The target is to increase forest coverage by 30% and decrease water silting by 45% (Luo & Chen, 1995; Chongqing Zhenfu Gongzhong Xinxiwang, 2003; Duan, 2002; Yang, 2003).



Figure 3.1 Chongqing (City proper) Urban Master Plan, 1996-2010

Source: Chongqing Guohua Sheji Yanjiuyuan, 1995

Table 3.1 Green Space Availability of the Municipalities

Cities	Urban non-agricultural population (10,000 person)	Built-up area (sq. km)	Green coverage in built up area (%)	Per capita green space occupation (sq. m ² person)
Beijing	726.88	488	42.3	27.39
Tianjin	499.01	386	25	11.07
Shanghai	938.21	550	20.9	9.58
Chongqing	381.66	262	21.8	9.45

Source: Urban Statistical Yearbook of China, 2001

3.2.2 Nanjing

Nanjing was the capital of many dynasties of ancient China and has long been the political, economic and cultural centre of Jiangsu province (Nanjing Urban Planning Bureau, 2003). Its geographical, demographic and political characteristics render Nanjing one of the most suitable urban centers to be compared with Chongqing, which will be further elaborated later.

3.2.2.1 Geography and Geomorphology

Nanjing is situated in the hilly region at the lower course of Changjiang. Its geographical location is 33°31' N latitude and 118°47' E longitude, occupying an area of 6597 km² (Nanjing Urban Planning Bureau, 2003). Mountains, river channels and low land interweave one another within the political boundary of Nanjing (Jiangsu Almanac, 2003). Two major lakes (Xuanwu and Muochou) are located in the northeast and west of major urban area bounded by the ancient city walls. Two rivers (Qinhuai and Jinchuang) running through the city from south to north, together with Changjiang on the west, constitute water system of Nanjing. Most of the mountains distribute in the east-west direction, such as Zi Jing Shan, Wu Tai Shan, etc. Gupin and Shizi mountains, on the other hand, run from south to north (Nanjing Urban Planning Bureau, 2003; Jim & Chen, 2003; Jim & Chen, 2003a).

3.2.2.2 Administration and Governance

Nanjing is the provincial capital of Jiangsu province. Unlike Chongqing Municipality, Nanjing is not ranked the highest in terms of city hierarchy level of China. It governs fewer regions than Chongqing does. 13 Districts and Counties, 69 Street Affairs Offices, 58 towns, 797 Residential Committees and 997 Village Committees are

under the governance of Nanjing municipal government. Major urban districts include: Yuanmu (northeast), Qinhuai (southeast), Jianye (southwest), Guliu (north west), Xiaguan (northwest), Yuhuatai (southwest suburb), Jianning (southwest), Liuhe (north suburb), and Pukou (northwest) (Nanjing Urban Planning Bureau, 2003; Jiangsu Almanac, 2003).

3.2.2.3 Landscape Planning of Nanjing

According to Nanjing Master Plan 1981-2000 (Nanjing Urban Planning Bureau, 2003), landscape and urban structure of Nanjing municipal area has a clear concentric ring pattern. Nanjing is divided into 3 ring zones. The first ring zone is the city proper zone: an ellipse nucleus of 2 km radius bounded by Xinmuofanmalu (north), Neiqiao (south), Longpan Road (east), and Fujou Road (west). This zone is planned to be political center, university and science research center, commercial center and high quality residential area. The second zone surrounds the first ring zone at 3 to 4 km radius. It mainly serves as mechanics and textile industrial agglomeration. The third zone is termed the Boundary zone, which defines the boundary of municipal Nanjing. Logistics infrastructure occupies the northern and southern edge, while natural landscape spots and vegetables production bound from east and west. From the master plan shown in Figure 3.2, it can be inferred that Nanjing seems to have a distinct gradient of urban density from urban center (city wall zone) outwards in all directions. Landscape distribution may be planned based on this urban density gradient.

3.2.3 Comparison between Chongqing and Nanjing

After separate description of the two cities under investigation, they are compared in various aspects in the following sections. Their similarities or discrepancies are used later in the interpretation of the results of landscape studies in these two cities.

南京市城市总体规划(1991-2010)

— 南京主城

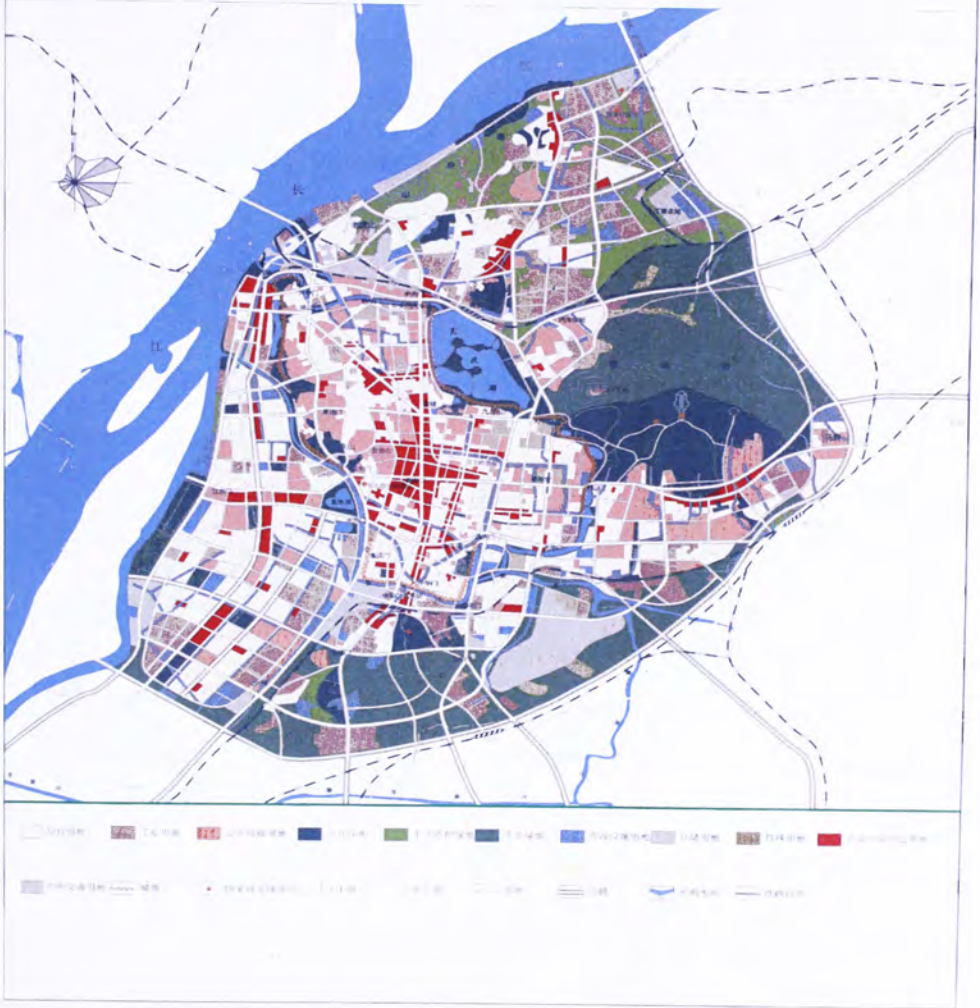


Figure 3.2 Nanjing (City Proper) Urban Master Plan, 1991-2010

3.2.3.1 Geographical setting

Both cities are located in similar latitudinal setting: northern end of the sub-tropical region ranging from 28° N to 30° N. Additionally, both of them are major cities along the Yangtze development region. The paramount difference between Chongqing and Nanjing is their distance from the coast. Nanjing is much nearer to coast, which is the reason of its sub-tropical monsoon climate, vis-à-vis Chongqing which is an inland city and experiences continental climate (Nanjing Urban Planning Bureau, 2003; Liu, 1989; Zhao, 2000). Whether such locational and climatic differences are able to explain their differences in green space quality is unknown.

3.2.3.2 Population

Comparisons of Nanjing and Chongqing are shown in Table 3.2. Chongqing was upgraded into Municipality in 1997 and occupies larger area and thus population (Luo & Chen, 1999). Non-agricultural population in the municipal area of Chongqing is more than that of Nanjing by 1 million. Another fact which deserves our attention is the rapid growth of population in Chongqing compared to Nanjing, which is evidenced by over 2.5% natural growth rate in Chongqing municipal area. Based on this fact, it is logical to state that Chongqing is growing at a faster pace in terms of both total population and urban non-agricultural population as compared to Nanjing.

Table 3.2 Comparison of Population between Nanjing and Chongqing

	Nanjing	Chongqing
Non-agricultural (Municipal)	3.23 million (8)	4.24 million (6)
Total population (Municipal)	4.80 million (9)	9.99 million (3)
Natural growth rate (Municipal)	0.74%	2.53%

Note: Number in the blanket is the city's national ranking in that variable

Source: China Urban Statistical Yearbook 2003

Table 3.3 Industrialization and Urbanization Levels of Nanjing and Chongqing

	Nanjing	Chongqing
Industrial output	197 billion (Yuan)	123 billion (Yuan)
Proportion of employment in the 2 nd industry	45.06%	51.91%
Percentage of Urban population*	67%	42%
Urban population density	1016 p/km ² (98)	613 p/km ² (173)
Urban builtup area	439 km ² (5)	438 km ² (6)

Note: Number in the blanket is the city's national ranking in that variable

* It is the non-agricultural population divided by total population in the urban area

Source: China Urban Statistical Yearbook 2003

3.2.3.3 Urbanization and Industrialization Levels

Industrialization level of the two cities is hard to be compared based on the indicators in Table 3.3. While Nanjing has a higher industrial output than Chongqing does, higher proportion of labor force is in industrial activities in Chongqing. On the other hand, Nanjing ranks on top of Chongqing in various indicators of urbanization levels, including percentage of non-agricultural/urban population in municipal area and urban population density. It may imply that Nanjing is a comparatively more urbanized area. From the images shown in Figure 3.3 and 3.4 it is observed that Nanjing built-up area are spreading and nuclei towns are developing in the close neighborhood. On the other hand, built-up area of Chongqing is more compact, with its spread confined by Gele Shan and Nan Shan on the east and west. New urban development is only found on the northern and southern borders of original city proper. Whether different development pattern of built-up areas influences the structure of green space can thus be revealed by selecting these two cities as study sites.

3.2.3.4 Variation in Landscape Quantity

Huge difference can be noticed from Table 3.4 which illustrates urban landscape quantities of the two cities. While both per-capita urban green area and built-up area green coverage of Nanjing rank among the top at national level, Chongqing barely reaches the national ranking of 200 in both indicators. Taking into account the rapid urban development and population growth of Chongqing, further reduction in quantity of green space coverage seems to be imminent. However, from national data, we can at best determine the difference in quantity of urban green space between the two cities, while their difference in aspects of landscape structure is largely ignored. In the research,

remote sensing is a tool to analyze urban green space of the two cities, Nanjing and Chongqing, in both composition and spatial configuration.

Table 3.4 Comparison between Nanjing and Chongqing in urban green coverage

	Nanjing	Chongqing
Built-up area (km²)	439 (5)	438 (6)
Per-capita green acreage (m²)	138.19 (4)	10.82 (200)
Proportion of green coverage in built-up area (%)	42.87 (15)	17.40 (233)

Note: Numbers in the blanket are national ranks of the cities with respect to the variables.

Source: China Urban Statistical Yearbook, 2003

3.2.3.5 Comparison from Satellite Images

Differences between Chongqing and Nanjing can be compared using the satellite images (Figure 3.3 and 3.4). Chongqing city area is identified on the image as being dissected by two big river channels, Changjiang running north-south and Jialing River west-east. Bright urban regions are located on the northern and southern ends while the dark urban area concentrating at the center. Besides, numerous lakes of irregular shapes scatter in the boundary area. Major woodland (of dark red) runs north and south in Gele Shan and Nan Shan, while patchy woodland are also found scattering in the suburban area. Special species of vegetation cannot be distinguished.

From Figure 3.4, city centers of Nanjing are more compacted, which are located at the center of the satellite image. Agricultural and natural landscapes, compared to Chongqing, produce clear-cut contrast with urban landscapes. Unlike in Chongqing, different species of agricultural crops and wetland vegetation are easily distinguished

from woodland and grassland. Moreover, patches of fallow agricultural land are noticeable mainly in the bottom and bottom-right, which are highly contrasted with the construction sites at the top of the image. Lakes and flooded paddy fields of larger size and more regular shape are located at the rural landscape.



Figure 3.3 Satellite Image of Chongqing



Figure 3.4 Satellite Image of Nanjing

3.3 Working procedures

Schematic diagram of working procedures for the research is shown in Figure 3.5. The first section will discuss ASTER data and its pre-processing procedure. A thorough description of the image object analysis, which is critical to the effective undertaking of object-oriented classification, is followed. Process of accuracy assessment for object-oriented classification is then delivered.

3.3.1 Data

ASTER images of Chongqing (July 21 2000) and Nanjing (Nov 6 2001) were acquired from the EROS Data Center's (EDC) Land Processes Distributed Active Archive Center (LP-DAAC). ASTER is the abbreviation of Advanced Spaceborne Thermal Emission and Reflection Radiometer which has been operating on NASA's Terra Spacecraft since December 1999. ASTER Level-1B data, which means that data set has been pre-processed with basic radiometric calibration and geometric resampling, is used for the research (ASTER Users Handbook, 2002).

ASTER data acquired is stored in Hierarchical Data Format (HDF) (ASTER Users Handbook, 2002), which has to be transferred into Pix format using OrthoEngine in PCI Geomatics V. 9.1.0[®]. City proper is clipped out from the whole image of 60 X 60 km using Subset operation equipped in PCI V. 9.1.0[®] ImageWorks. Clipped images of Chongqing and Nanjing are shown in Figure 3.3 and 3.4, respectively.

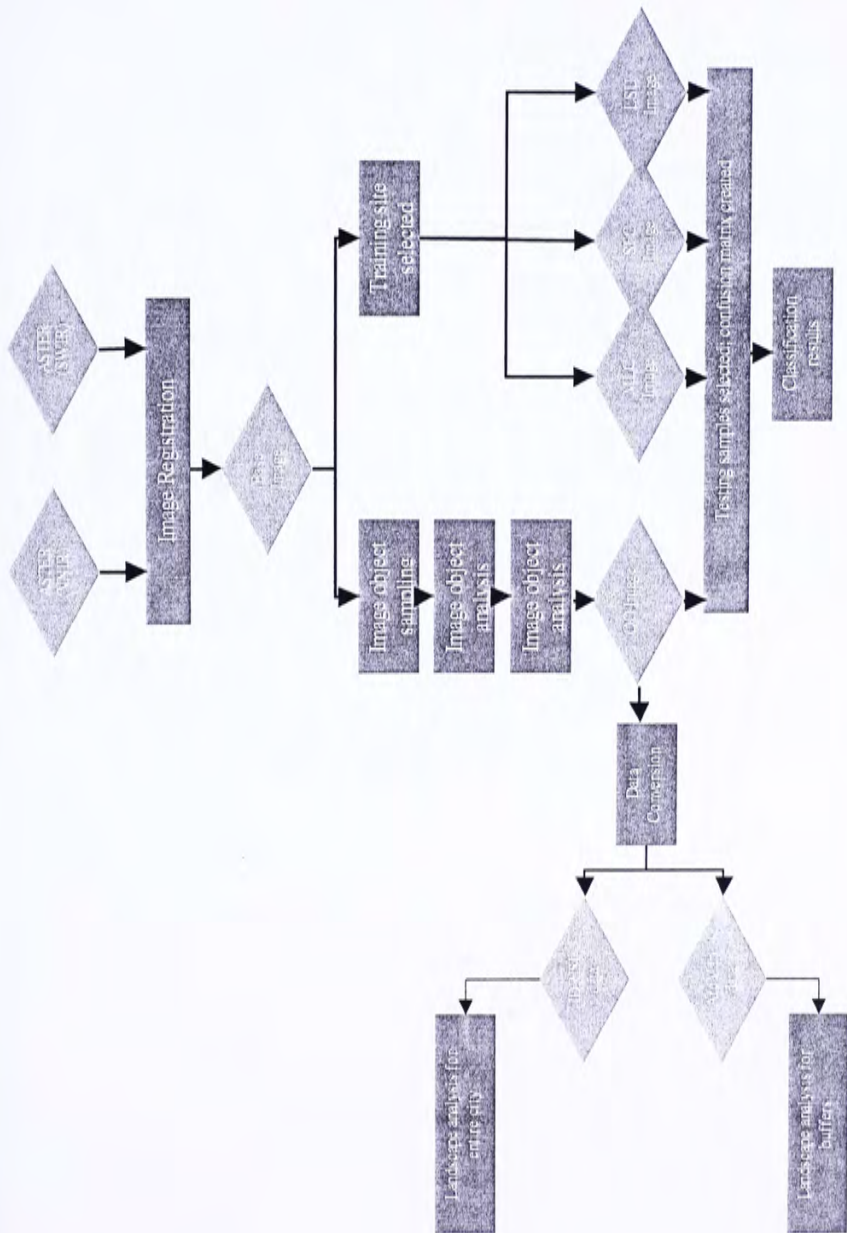


Figure 3.5 Schematic diagram of working flow

ASTER covers a total of 14 spectral bands from visible to the thermal infrared electromagnetic region (ASTER Handbook, 2002). In the research, three visible plus near infrared (VNIR) channels are used in object-oriented classification approach, whereas 6 more shortwave infrared (SWIR) channels are added, that is to say a totality of 9 spectral channels, are used in conventional classification approaches, including maximum likelihood classification (hereafter MLC), linear spectral unmixing method (hereafter LSU), and supervised fuzzy classification (hereafter SFC). Brief comparison of VNIR and SWIR channels are shown in Table 3.5. VNIR channels and SWIR channels are pre-processed separately.

Table 3.5 Basic information of VNIR and SWIR channels

Spectral channels	Band No.	Spectral Range (μm)	Spatial Resolution, m	Quantization Levels
VNIR	1	0.52-0.60	15	8 bits
	2	0.63-0.69		
	3N	0.78-0.86		
SWIR	4	1.60-1.70	30	8 bits
	5	2.145-2.185		
	6	2.185-2.225		
	7	2.235-2.285		
	8	2.295-2.365		
	9	2.360-2.430		

Source: ASTER Users Handbook, 2002

3.3.1.1 VNIR channels

In theory, a good image registration, or georeferencing, should be based on a set of ground control points, which have accurate X- and Y-coordinates, and altitude/height values (usually derived from Digital Elevation Model) with a particular local map projection. In this research reliable DEM or other topographic data of neither Chongqing nor Nanjing is available. Therefore, Level-1B VNIR data is used, which is L1A data being radiometrically and geometrically corrected (ASTER User Handbook, 2002).

Universal Traverse Mercator (UTM) is loaded on the interface of PCI ImageWorks to indicate coordinates of the images.

3.3.1.2 SWIR channels

SWIR channels will be used as additional input channels for conventional classification methods. As previously mentioned, unavailability of topographic data in both study sites deems formal image registration unfeasible. Instead, 15 m resolution VNIR data (Level-1B) is assumed geometrically correct and utilized as reference data and SWIR channels are directly translated into the PIX file containing VNIR channels.

3.3.1.3 Data Fusion

SWIR data (30 m resolution) is “scaled up” to 15 m resolution so as to match with 15 m VNIR data. In the research, image fusion technique called Smoothing Filter-based Intensity Modulation (SFIM) is used (Liu, 2000). It preserves spectral information of the lower resolution image while sharpening its edge information. Algorithm for SFIM is in the following:

$$IMAGE_{SFIM} = \frac{IMAGE_{low} \cdot IMAGE_{high}}{IMAGE_{mean}} \quad \text{(equation 3.1)}$$

where $IMAGE_{low}$ is a pixel of a lower resolution image while $IMAGE_{high}$ is the corresponding pixel of a co-registered higher resolution image. $IMAGE_{mean}$ is a smoothed pixel of $IMAGE_{high}$ using averaging filter over a neighborhood equivalent to the actual resolution of the $IMAGE_{low}$. Kernel size depends on the resolution ratio between lower resolution image and higher one, which is 2 x 2 in this case.

SFIM procedure is operated in PCI Xspace. Average data of the higher resolution image can be produced using PCI Xspace Average Filter. Equation 3.1 can be written in PCI Xspace Image Modelling. A comparison between raw SWIR image and SFIM SWIR image is shown in Figure 3.6.

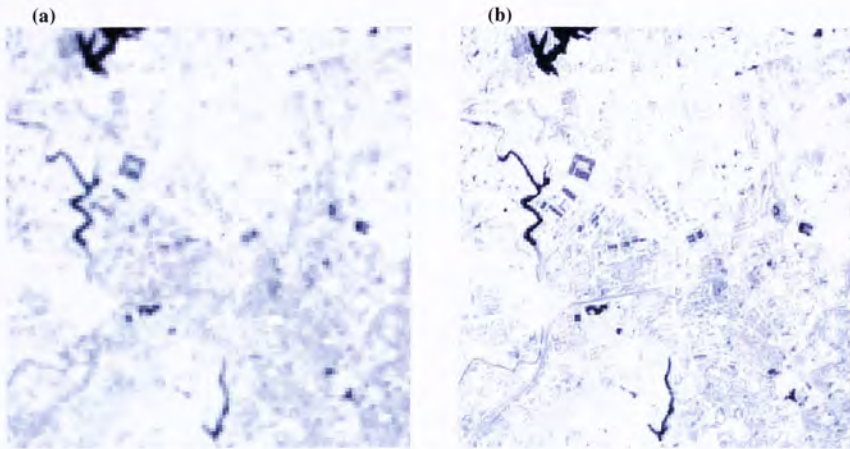


Figure 3.6 Comparison between original SWIR data and SFIM SWIR data. (a) is raw SWIR channel 4. Edge details of lakes, roads and buildings are blurred. After SFIM, edges are sharpened, very much like a normal 15 m VNIR image, which is shown in (b)

3.3.2 Designing Hierarchical Classification System

Conceptually, a hierarchical classification scheme is designed, which organizes land cover classes expected to be extracted from the satellite imagery. Schematic classification systems of Chongqing and Nanjing are shown in Table 3.6, in which general classes in level 1 are further classified into more detailed classes in levels 2 and 3.

3.3.2.1 Chongqing

Eight land cover classes are targeted. The 8 expected classes are set up based on secondary data such as Chongqing City Proper 1996-2010 Urban Master Plan (Chongqing Zhenfu Gongzhong Xinxiwang, 2003), and preliminary visual inspection of the satellite image. At the top level, the image will be classified into 3 general classes: "Water", "vegetation" and "non-vegetation". These three classes will be further divided into more detailed classes at the medium class level. At the lowest class level, it is expected that "impervious" is further sub-divided into three urban classes: "industrial", "high density urban" and "low density urban".

3.3.2.2 Nanjing

Difference in classification system between Chongqing and Nanjing is expected due to local distinctiveness. 11 instead of 8 classes are formulated based on Nanjing City Proper 1991-2010 Urban Master Plan (Nanjing Urban Planning Bureau, 2003) and visual inspection of the image. It is found that in Nanjing, "agricultural crops" and "wetland" which have higher spectral values than "woodland" and "grassland" are observed so that they can be added in the classification system. Besides, "fallowed land" are widely distributed in agricultural land covers. They are thus added in the classification scheme as well.

Table 3.6 Three-tiered classification scheme for object-oriented classification in Chongqing (a) and Nanjing (b)

(a)

LEVEL I	LEVEL II	LEVEL III
Water	Lake River	
Vegetation	Woodland Grassland/Crops	
Non-vegetation	Bare soil Impervious	Bareland Industrial sites High density urban Low density urban

(b)

LEVEL I	LEVEL II	LEVEL III
Water	Lake River	
Vegetation	Bright vegetation	Agricultural crops I Agricultural crops II Wetland Woodland Grassland
	Dull vegetation	
Non-vegetation	Bare soil Impervious	Fallowed land Bareland High density urban Low density urban

3.3.3 Object-oriented Classification

3.3.3.1 Introduction

In Object-oriented classification, image objects of different scales at different locations and resolutions are hierarchically linked up and the inter-relationships between objects explicitly defined in object level hierarchy (Definiens-Imaging, 2003). A diversity of features is available to assist the interpretation of each object. Class hierarchy can then be designed which defines each land cover with those object features and its relationship with another class. In class hierarchy, the whole classification can be divided into several levels which are closely linked with object level hierarchy, such that a decision tree can be constructed.

Two major operations are involved during the formation of object level hierarchy, which are Multiresolution Segmentation and networking of image objects.

Multiresolution Segmentation is a bottom up region-growing technique starting with one-pixel objects. Smaller image objects are merged into bigger ones with minimal heterogeneity until it exceeds the threshold defined by the scale parameter (Definiens-Imaging, 2003; Blaschke et al., 2000). Heterogeneity is pre-defined by users and calculated in terms of spectral or shape. Spectral heterogeneity is calculated using the following algorithm:

$$h = \sum_c w_c \cdot \sigma_c \quad \text{(equation 3.2)}$$

where w_c is weight of each channel while σ_c is standard deviation of spectral values in each channel of pixels within each object. Spatial heterogeneity is a deviation of an object from either a compact or smooth shape (Definiens-Imaging, 2003). A deviation from compact shape is calculated using the following algorithm:

$$h = \frac{l}{\sqrt{n}} \quad \text{(equation 3.3)}$$

where l stands for border length of the image object while \sqrt{n} is the square root of the number of pixels forming the image object. A deviation from smoothness can be calculated using the following algorithm:

$$h = \frac{l}{b} \quad \text{(equation 3.4)}$$

where b stands for the shortest possible border length given by the bounding box of the image object.

Merging of image objects inevitably increase heterogeneity within an image object. Scale parameter, which is also pre-defined by users, takes the role of controlling the maximum heterogeneity within object tolerated (Definiens-Imaging, 2003). Technically, it determines the maximum average object size allowed during each segmentation process.

Networking of Image Objects organizes image objects generated at different scales through “object level hierarchy” so that each object is related explicitly to its “neighborhood” at the same segmentation level, its “sub-objects” at lower level, and its “super-object” at higher level, enabling adaptation of the scale of observation to the phenomena of interest (Definiens-Imaging, 2003; Li & Wu, 2004; Wu & David, 2002).

Ivits et al. (2002) claim that multiresolution segmentation and hierarchical image object network are particularly expedient in patch-scale landscape ecological studies because different segmentation levels allow for visualization of landscape objects at

different scales. They assert that tiny patches of habitat, which are usually smoothed out from visual interpretation, are able to be assessed about their presence, distributions and connectivity with the help of segmentation and object level hierarchy.

In this research, object levels are produced by segmentation with reference to the corresponding levels of classification. That is to say three object levels are generated. Object level 1 is anticipated to be used for Level I classification; Object level 2 is proposed for level II classification; and so on. However, as mentioned in Ivits et al. (2002), image segmentation is a problem with infinite possible solutions. It is up to researchers who define weights of spectral and shape, plus scale parameter/average object size during each segmentation operation. Which spectral-shape ratio and scale parameter can produce the best representation of land cover of interest is by and large unknown and becomes a critical research question to be addressed.

3.3.3.2 Procedure of Object-oriented Classification

The whole classification involves the following procedure:

3.3.3.2.1 Analysis of Image Objects

Image objects segmented using multiresolution segmentation are primitive image objects, plethora of spectral, shape and textural features potentially conducive to intelligent classification (Definiens-Imaging, 2003). However, it is not informed that which of these features are truly usable to distinguish each land cover. Thus, systematic analyses of segmentation and image objects are undertaken to select the best spectral-shape ratio and scale parameters for segmentation.

Total number of image objects generated and average object size are calculated for entire images of Chongqing and Nanjing at increasing segmentation scales and at different spectral-shape ratios for segmentation. Besides, a series of analyses are operated in an attempt to increase the understanding of behavior of a list of spectral, shape, and textural features (shown in Table 3.7) of different land cover class as segmentation scale increases in the object-oriented classification. Similar methodology has been approached by Neel et al. (2004) to evaluate responses of a suit of landscape metrics equipped in FRAGSTATS to a gradient of fragmentation levels and class-area proportions. However, their tests mainly resort to neutral landscape models for simulating the variations in landscape ecological condition; while tests of this research use real cases (Chongqing city and Nanjing) to explore the behavior of spectral, spatial and textural features of objects belonging to different classes at varying object sizes. Algorithms of these features will be listed in Appendix 1.

The analysis is conducted for three main purposes: First, selecting the spectral-shape ratio for segmentation which best represents the spatial variation of an image; second, choosing the most suitable scale parameters to generate 3 segmentation levels; and third, picking up a list of spectral, shape and textural features, which best distinguish each class, to set up classifying rules for each class in the decision tree classification structure. It involves the following procedure:

Table 3.7 Features calculated for image object analyses

Features calculated for the entire image	Features calculated for each class	
Total Number of Objects	Spectral Features:	
	<i>Spectral Mean</i>	
	<i>Standard Deviation</i>	
Average Object Size	<i>Mean Difference to Neighbor</i>	
	Shape Features:	
	<i>Area</i>	
	<i>Border Length/Perimeter</i>	
	<i>Length/width Ratio</i>	
	<i>Shape Index</i>	
Average Object Size	<i>Density</i>	
	Textural Features:	
	<i>GLCM Homogeneity</i>	<i>(all direction)</i>
	<i>GLCM Contrast</i>	<i>(all direction)</i>
	<i>GLCM Dissimilarity</i>	<i>(all direction)</i>
<i>GLCM Entropy</i>	<i>(all direction)</i>	
	<i>GLCM Angular Second Moment</i>	<i>(all direction)</i>

3.3.3.2.2 Image Segmentation

The first step is to generate 10 segmentation levels for images of Chongqing and Nanjing across a gradient in scale parameter (SP = 2 – 20 in 2 increments) using 6 different color-shape combinations (0.1:0.9; 0.3:0.7; 0.5:0.5; 0.7:0.3; 0.9:0.1; 1.0:0.0). Except at color-shape ratio of 1.0:0.0, I additionally duplicate two more segmentations at SP = 10 with varying smoothness-compactness ratios (0.1:0.9; 0.5:0.5 and 0.9:0.1), whereas the ratio of 0.5:0.5 is used to generate other segmentation levels. Overall, a total of 70 segmentation combinations have been generated for each site in this analysis.

3.3.3.2.3 Selection of Features and Data Conversion

The second step is to export objects generated from these 70 segmentation combinations. Spectral, shape and textural features listed above are selected as attributes of each object generated from the image concerned. Values of these features of each object will then be calculated automatically and exported from TIFF format to ArcView SHP format. Total number of image objects and Average object size at each segmentation level and spectral-shape ratio are recorded manually on Excel files.

3.3.3.2.4 Class-based Objects Sampling

30 to 50 samples are targeted for each land use class to recognize their variations in object features along segmentation sizes. A total of 400 samples are drawn using Stratified Systematic Random Sampling method on IDRISI interface. Some land use classes, such as “lakes” and “industrial”, have low proportional shares of total area of the study site and may have insufficient samples for themselves. Additional random sample points are selected and digitized for these classes. Samples thus generated are converted into ArcView SHP format.

3.3.3.2.5 Class-based Objects Analysis

Objects analysis is mainly carried out in ArcMap 9.0. Sample vectors of a particular land use class are selected. Object polygons of that land use class are then extracted using *Select by Attribute* function, which selects all image object polygons intersecting sample vectors of that land use class. After that, database of selected object polygons, composed of each polygon’s spectral, shape, and textural features listed above (in DBF format), is exported to Office Excel, in which means of these features are calculated for all objects belonging to each land use class. Distribution of means are plotted along segmentation

gradient and used to interpret the changes in object characteristics for each land cover class. The result will be presented in the next chapter.

3.3.3.2.6 Designing Object Level Hierarchy

Selection of optimal spectral-shape ratio for segmentation is guided by total number of objects generated, Average object size resulted and segmented image interpretation for different spectral-shape ratios. The three object levels for the creation of object level hierarchy are then selected based on the findings about the variations of object features along increasing segmentation levels.

3.3.3.2.7 Designing Class Hierarchy

Class-based objects analysis will help derive classifying rules for classes expected. Object features which best differentiate a particular class from the others will be identified. Besides, comparison of feature values between land cover classes at different object levels helps illustrate the optimal object level for classification of each expected class. Based on the information, class hierarchy well linked with object hierarchy can then be designed for the three-tiered classification system.

3.3.3.2.8 Decision Tree Classification Structure

Decision tree classification is a branch of rule-based classification system (Lawrence & Wright, 2001). In the system, classifying rules are such hierarchically structured that remote sensing dataset is recursively and dichotomously split into increasingly homogeneous subsets. Output classes are contained by the nodes at the bottom of the hierarchy, or "terminal nodes". This classification structure is in a sense like that of a tree and thus called tree-based classifier (Borak & Strahler, 1999).

In this research, Tree-based approach is adopted. However, while tree-based approach can be implemented automatically in computer using training data (Borak & Strahler, 1999; Lawrence & Wright, 2001), it is accomplished manually in this research by setting up a class hierarchy. In class hierarchy, all classes are defined manually and hierarchically organized. Decision rules/class properties for each class, which determine membership of image object to the class, can be set up by users based on the spectral, spatial and textural features of the class previously mentioned. Function of inheritance, that is to say a passing down of class properties from higher level class to lower ones, is provided to reduce redundant effort in setting up class properties. Decision rules of a particular class will translate pertinent feature values of image objects into fuzzy/membership values at a close interval [0 ; 1] during classification. The output of the classification will include a crisp classification, where each object has exactly one class assignment, and fuzzy values to the three most possible classes which indicate class mixing. (Definiens-Imaging, 2003).

3.3.4 Comparison with other classification algorithms

Besides object-oriented classification approach, three more classifications are generated using maximum-likelihood classification (hereafter MLC), linear spectral unmixing (hereafter LSU), and supervised fuzzy classification (SFC) for comparisons. These three algorithms are widely used in image classification because of their ease of operation. Methods of producing MLC and SFC are very similar. Training samples for each class are selected randomly from the image, with the multispectral values of training samples utilized to model feature space for classification. While MLC generates Gaussian distribution of multispectral values for each class, SFC utilizes multispectral values to model the membership functions for classification (Lillisand, et al., 2004). LSU adopts a

different methodology in which Endmembers, which are multispectral values of pure classes, are required from image. Linear equation is then generated, under which class assignment of each pixel is based on the relative composition of the pure classes in that pixel (Roberts et al., 1998). These three algorithms are merited for their automated and relatively transparent characteristic during operation, and so are used in this research as reference of comparisons (Schiewe et al., 2001). MLC is generated in PCI ImageWorks while the other two in IDRISI.

Accuracy Assessment of all classification methods are carried out in PCI ImageWorks. Congalton's (1991; quoted by Jensen, 1996) suggestion about sample size for significant accuracy assessment is followed such that 50 independent samples for each land use class are selected randomly with Stratified Systematic Random Sampling (on IDRISI interface). 400 random samples are then selected in Chongqing while 500 random samples are selected in Nanjing. The sample vectors are imported into PCI ImageWorks, with their reference land use classes obtained by visual inspection of the image. Confusion matrix, producer's and user's accuracies, and kappa coefficient are then automatically generated, which will be presented in the CHAPTER V.

3.4 Landscape Analyses

The whole procedure of landscape analyses are implemented using FRAGSTATS 3.3 (McGarigal, 2001). Two analysis approaches to investigate the study sites are undertaken. The first approach describes landscape structural and compositional characteristics of a particular study site as an entirety. The result indicates the average situation of the cities. The second approach is through buffer analysis by which variations of landscape characteristics with increasing distance from city centers will be analyzed.

3.4.1 Selection of Landscape Metrics

Although hundreds of landscape metrics have been developed to analyze the landscape structure, most of which are strongly correlated with one another (Leitao & Ahern, 2002). In studies of McGarigal and McComb, (1995) 15 out of 25 landscape metrics selected for quantification of landscape configuration are tested redundant after a series of statistical analyses. Their findings are confirmed by Cifaldi et al.'s (2004) studies in which 25 landscape variables are input into Principal Component Analysis (PCA) to identify their major relationships to changes in land cover patterns. Five PCs contain nearly 80% of the land cover variations of landscape, which are sufficiently described by within 10 landscape metrics.

Additional to high correlation of them, many landscape metrics fail to behave in a way universally expected. It is widely accepted that landscapes are heterogeneous in respect of various components, which can be grouped into two elements: non-spatial composition and spatial configuration (Leitao & Ahern, 2002; Li & Reynolds, 1995; Neel et al., 2004). Researches of both Li and Reynolds (1995) and Neel et al. (2004) reveal that responses of many landscape indices, which are claimed indicating variations of one landscape element, are prone to the influences of another, resulting in theoretical trends of responses of many landscape metrics to variations in a particular landscape structure component being inconsistent with their observations.

The goal of this research is comparing Chongqing and Nanjing in terms of the spatial dimension of their green space within and neighboring city centers. In light of that, focus should be focused on describing the size, shape, and contagion of vegetation patches. Therefore, a suit of patch- and class-metrics is selected from FRAGSTATS 3.3,

(McGarigal, 2001) which is listed in Table 3.8. Their explanations and equations are listed in Appendix 1.

Table 3.8 Landscape metrics calculated in the research

Patch Metrics		Class Metrics	
Area/Perimeter			
<i>Area</i>		<i>Total Class Area</i>	
<i>Perimeter</i>		<i>Percentage of Landscape</i>	
		<i>Number of Patches</i>	
		<i>Patch Density</i>	
		<i>Largest Patch Index</i>	
		<i>Edge Density</i>	
		<i>Area</i>	<i>(area-weighted mean)</i>
		<i>Area</i>	<i>(coefficient of variation)</i>
		<i>Radius of Gyration</i>	<i>(area-weighted mean)</i>
		<i>Radius of Gyration</i>	<i>(coefficient of variation)</i>
Shape			
<i>Perimeter-Area Ratio</i>		<i>Fractal Dimension Index</i>	<i>(area-weighted mean)</i>
<i>Fractal Dimension Index</i>		<i>Fractal Dimension Index</i>	<i>(standard deviation)</i>
		<i>Perimeter-Area Ratio</i>	<i>(area-weighted mean)</i>
		<i>Perimeter-Area Ratio</i>	<i>(standard deviation)</i>
		<i>Perimeter-Area Fractal Dimension</i>	
Proximity/Isolation			
<i>Proximity Index</i>		<i>Proximity Index</i>	<i>(area-weighted mean)</i>
<i>Euclidean</i>	<i>Nearest-Neighbor</i>	<i>Euclidean Nearest-Neighbor Distance</i>	
<i>Distance</i>			<i>(area-weighted mean)</i>
Contagion			
		<i>Clumpiness Index</i>	
		<i>Interspersion Juxtaposition Index</i>	
		<i>Landscape Division Index</i>	
		<i>Effective Mesh Size</i>	

3.4.2 Landscape Analysis for entire cities

Classified image in PIX format will be exported and converted into IDRISI raster format because FRAGSTATS 3.3 does not accept PIX format data (McGarigal, 2001). Conversion of data format is undertaken in PCI ImageWorks Utility. After that, the interface of FRAGSTATS 3.3 is accessed, in which Input Data Type, Background Value, Patch Neighbor Rules and all landscape metrics can be selected. Output statistics of both different land cover classes and individual patches can be converted into EXCEL format for analysis.

3.4.3 Buffer Analysis

Landscape metrics describing vegetation within and around municipal area are presented according to distance of vegetation patch from the urban center/central business district (CBD). Urban centers of two case study cities are located based on visual interpretation and ancillary information. In Chongqing, this point is located at Yu Zhong district which is the city center ("Zhang ling yang zi zhu lu xing shou ce" bian xie zu, 2002); while in Nanjing, this point is located in the city proper zone defined by Nanjing Master Plan 1981-2000 (Nanjing Urban Planning Bureau, 2003). They are shown in Figure 3.7. Buffers (in forms of both entire circles and rings) of increasing distance to city center are drawn on the imagery. Landscape metrics variables of green patches within each ring are then tabulated and interpreted.

(a)

(b)

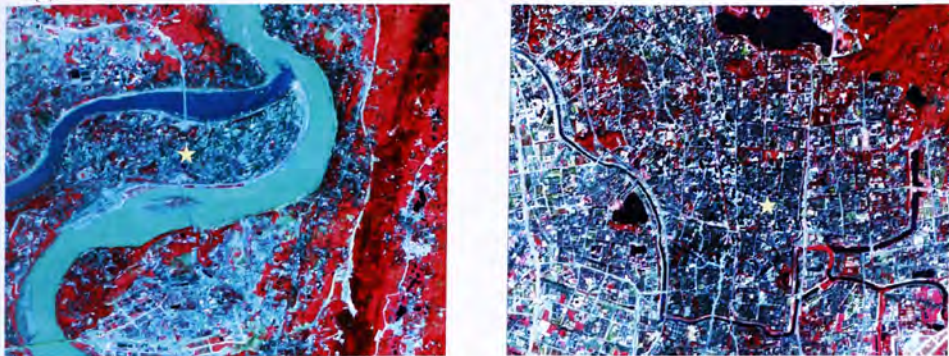


Figure 3.7 City centers of Chongqing (a) and Nanjing (b) are highlighted by stars

This approach is used in an attempt to illustrate the relationship between the spatial and compositional structure of green patches and the distance from urban core, which is a surrogate of descending level of urban density. Similar method was used by Mesev et al. (1995) to study the spread of density and fractal dimension of a variety of urban land use categories from CBD. Also, Zhang et al. (2003) used a series of west-east and south-north transects, which cut across the urban center of Shanghai metropolitan area, to test the hypotheses of Forman and Godron (1986) on the variations of patch density, patch shape complexity, patch size and its variance, and landscape connectivity of an average landscape along urbanization gradient. In this research, concentration is put on green landscape elements within as well as bounding urban boundary.

Buffer analysis involves the following steps. First, classified image in PIX format is exported and converted similar to the first step of landscape analysis for entire cities. The difference, though, is that it will be converted to Arc BIL format. In the interface of

ArcGIS 9 ArcToolbox, the BIL raster file will be converted to SHP vector format using *Conversion: from raster to polygon*.

In the second step, based on the city center, ten buffers are generated using ArcToolbox: Buffer, from 1 kilometer to city center to 10 kilometers to city center, each with 1 kilometer increment (shown in Figure 3.8). Smaller buffers are not included in the analysis because the amount of greenness will be too low. Besides buffer circles, buffer rings are also generated with the same method. However, the base features input for generating buffer are buffer circles of increasing sizes instead. While buffer rings can be used to study the changes in landscape structure of green space at specific distance from city centers, they may seriously distort the spatial configuration of green space. Therefore, the interpretation of some metrics about green space extracted from buffer rings may not be valid, especially those which quantify shape complexity of green space. In this situation, buffer circles have to be used instead, although they tend to suppress the large variations of green space structure at a particular distance from city centers.

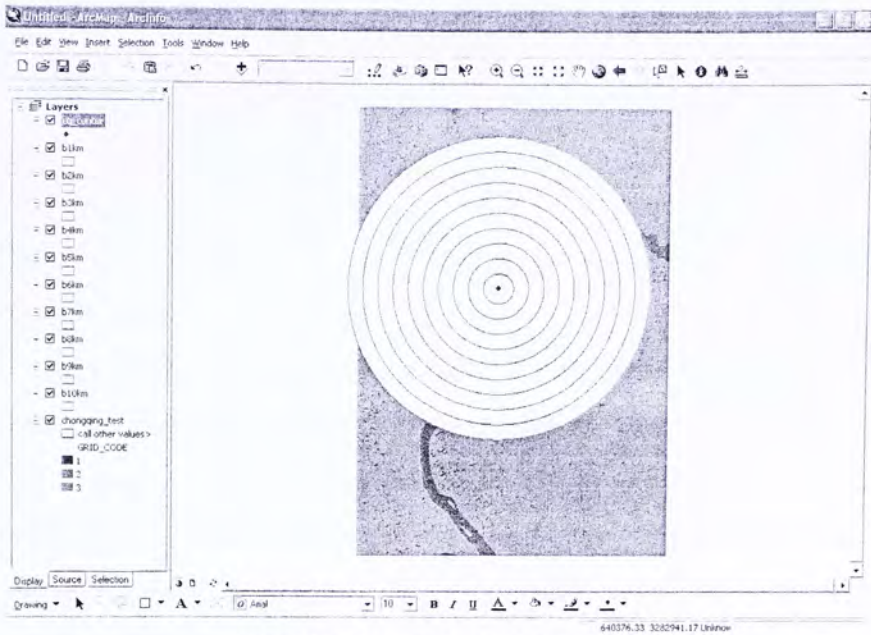


Figure 3.8 Buffer analysis on ArcMap interface

After that, classified image covered by buffers are clipped out using ArcToolbox: Clip function. They are finally converted to ArcGrid format using Conversion: *from feature to raster*, which are input to FRAGSTATS 3.3 for landscape metrics calculation in the same manner as landscape analysis for entire cities.

3.5 Conclusion

In this chapter, methodology of this research is introduced, with the expected flow of the research explained, as well as all the object features and landscape metrics involved in listed. Besides, a crude comparison between the two study sites, Chongqing and Nanjing, has been accomplished. Results and findings of this research will be presented in the next 3 chapters.

CHAPTER 4. Results and Discussion I

Variations of Image Object Signatures for Sampled Land Covers

4.1 Introduction

This chapter will discuss the interpretation of image object features, and their variability along the ascending scale of segmentation. Having detailed in Chapter III, in object-oriented classification concept, each segmented object has its own feature, which is defined by a list of spectral, textural and shape variables, integrating into "object signature" (Definiens-Imaging, 2003). As an image object grows larger and absorbs neighboring pixels/objects, its object signature becomes heterogeneous. The change in signature/nature of the original image object concerned will be reflected on the variations in values of the spectral, textural and shape variables. The pattern of change in object signatures along segmentation scales may in itself vary for different land cover classes, and with different spectral-shape ratio at which segmentation is operated. This chapter is going to search for the optimal scales and spectral-shape ratio for multi-level segmentation.

Moreover, the application of object signature can be extended to define land cover class signature. Inferring from the above assumption, land covers are distinct from each other in terms of spectral, textural, or even shape variables. Image objects of the same land cover category thus have common object signatures, which are different from those of other categories. In this sense, object signatures can be utilized to derive land cover

class signatures, which may be useful for formulating dichotomous classifying rules, quintessential elements of decision tree classifier which will be discussed in the next chapter.

Features of sampled image objects and segmentation levels will be studied case-by-case, Chongqing being the first and Nanjing comes the second. Within each case, focus is set on the alteration of the object signatures at different sizes and spectral-shape ratios for different image object variables as well as land cover categories. Besides, common class signature of each land cover is extracted based on the findings. Limitations of this analysis and comparisons between Chongqing and Nanjing come as a small conclusion for this chapter.

4.2 Chongqing

4.2.1 Spectral-shape ratio

The first objective of image object analysis is to select the best spectral-shape ratio for multi-scale segmentation. Merging of pixels/image objects with ascending segmentation level inevitably increases heterogeneity within an image object. If high spectral-shape ratio is set for segmentation, higher weight will be put on preserving spectral similarity within object during segmentation. On the other hand, low spectral-shape ratio weighs higher on keeping the shape of objects as close to square/circle as possible (Definiens-Imaging, 2003). Therefore, different spectral-shape ratio may lead to totally different representation of land cover objects by image. In this section, how different spectral-shape ratios for image segmentation affects overall image quality is presented.

4.2.1.1 Selection Criteria

The choice of spectral-shape ratio is decided by summarizing the total number of image objects created, Standard deviation of spectral means of objects (which shows the intra-object spectral variances) and differences in image appearance at 6 different spectral-shape ratios, which is listed as follows:

- 0%--the weight of shape on spectral-shape ratio is 0%;
- 10%--the weight of shape is 10%;
- 30%--the weight of shape is 30%;
- 50%--the weight of shape is 50%;
- 70%--the weight of shape is 70%; and
- 90%--the weight of shape is 90%.

Some important observations concerning with different spectral-shape ratios and segmentation levels are presented in the following:

4.2.1.2 Observations

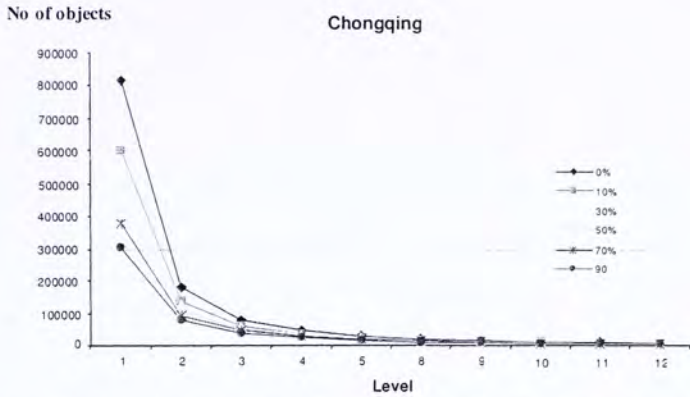
1. **A decrease in spectral-shape ratio yields smaller number of image objects and larger average size of image object at each segmentation level.**

Figure 4.1 shows the relationship between amount of segmented image objects and segmentation levels at varying spectral-shape ratios. An increase in segmentation level leads to generation of larger image objects, which is reflected on the decrease of number of objects in the figure. This relationship is most obvious when segmentation level proceeds from 1 to 2, that is to say when scale parameter is switched from 2 to 4; while

the decrease in number of image objects becomes negligible at segmentation levels 5 to 12.

With an increasing weight of shape in the spectral-shape ratio, this exponential relationship is getting more evident. At segmentation level 1, over 800,000 image objects are generated when the weight of shape is 0%, while only 600,000 image objects are generated with 10% weight of shape for segmentation at level 1. When the ratio increases to 90%, the number of image objects generated at level 1 is reduced to 300,000, nearly three times fewer than the amount that segmentation at the spectral-ratio of 10 to 0 can produce.

Larger number of image objects segmented with higher spectral-shape ratio also implies that image objects produced are in average smaller in size at every segmentation level if higher spectral-shape ratio is set. This fact is supported by average object size generated at different segmentation levels with different spectral-shape ratios, which is shown in Appendix 3.



0%--0% weight of spectral-shape ratio; 10%--10% weight of spectral-shape ratio; 30%--30% weight of spectral-shape ratio; 50% --50% weight of spectral-shape ratio; 70%--70% weight of spectral-shape ratio; 90%--90% weight of spectral-shape ratio.

Figure 4.1 Number of image objects generated along segmentation levels in Chongqing

2. Decreasing the spectral-shape ratio leads to the surge of Standard Deviation of spectral values of image objects at every segmentation level.

The variability of Standard Deviation is selected to indicate the change in within-object variances along segmentation levels. Figure 4.2 shows the change in SD (VNIR 3) for three classes: "lake", "woodland" and "low density urban". Standard Deviation calculates the variance of the spectral values of all pixels forming an image object. Standard Deviation increases with the weight of shape throughout the segmentation gradient, with 90% weight of shape resulting in the most heterogeneous image objects. When spectral-shape ratio is set at 10:0, a comparatively consistent increase in Standard Deviation is observed. Further, Standard Deviation of it is the lowest throughout all land covers shown. Standard Deviation of other VNIR channels and land covers are shown in Appendix 3.

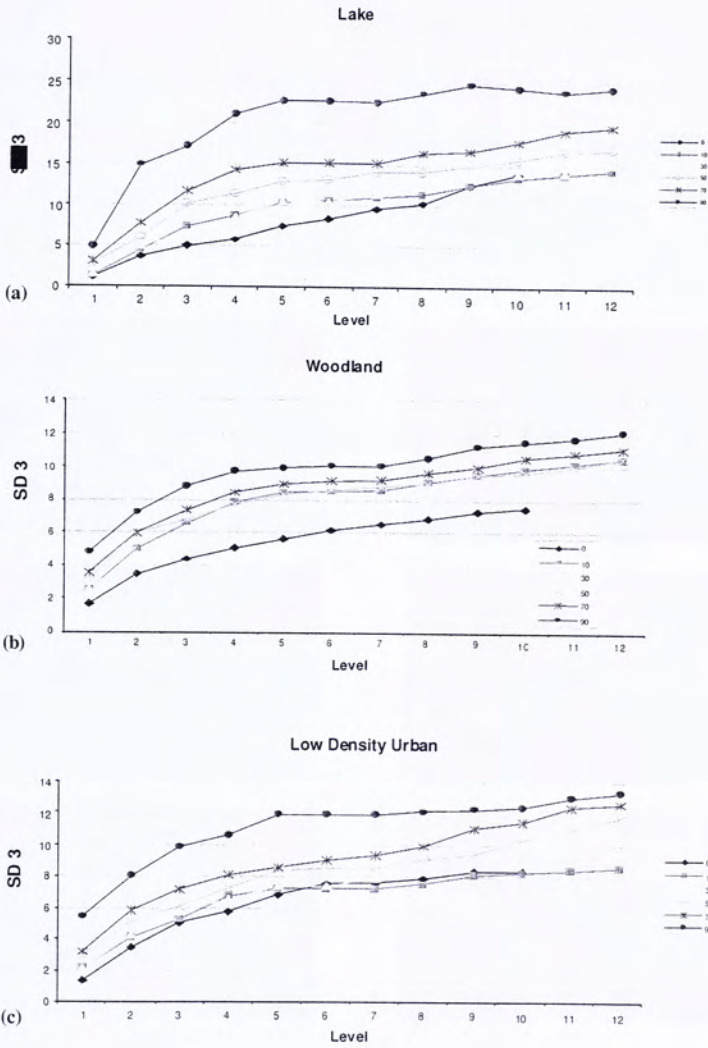


Figure 4.2 Variability of Standard Deviation (VNIR 3) of image objects along segmentation gradient for land cover classes: “Woodland” (a), “Lake” (b) and “Low density urban” (c). Case in Chongqing

3. Low spectral-spatial ratio generates segmented objects with very regular shapes; while 10:0 spectral-shape ratio produces too fractal objects.

When high weight of shape is selected, segmentation will preserve the shape of image objects as close as squares/circles (shown in Figure 4.3). However, segmentation with no weight on shape may create image objects which are too complex (Definiens-Imaging, 2003), which can also be validated in Figure 4.3.

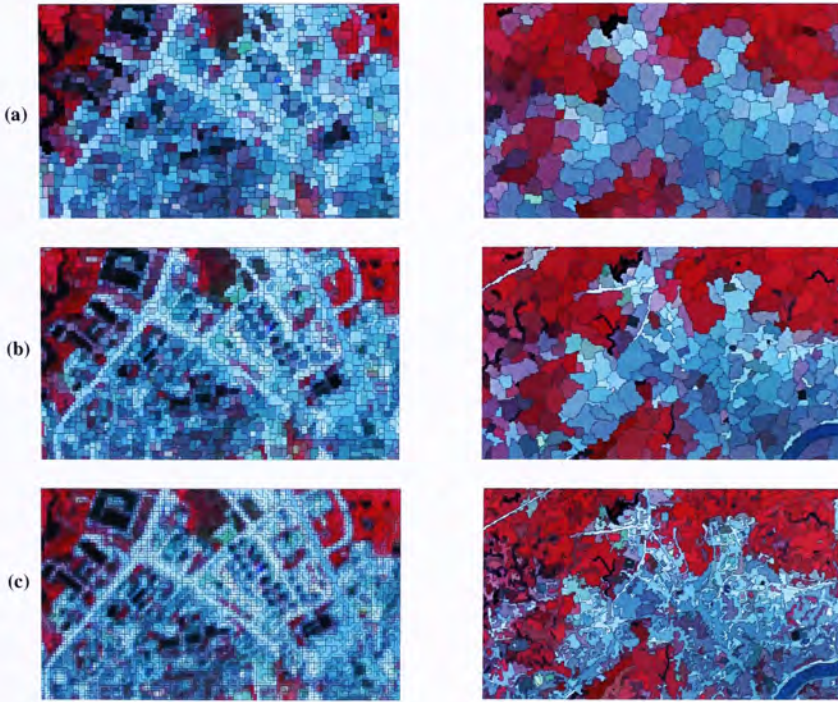


Figure 4.3 Segmented images at the lowest segmentation level (left) and highest segmentation level (right). Top figures are segmented at spectral-shape ratio of 1:9 (a); the bottom ones are segmented at 10:0 (c); the middle at 5:5 (b). Notice that as spectral-shape ratio goes down, the images become more distorted from reality, esp. at high segmentation levels.

In short, high spectral-shape ratio leads to more objects of smaller size segmented at every segmentation level. It also yields smaller spectral variances within objects (revealed by Standard Deviation of objects) across segmentation gradient. It is possible that complexity of the distribution of different land covers can be better preserved if a high spectral-shape ratio is selected. However, 10:0 spectral-shape ratio creates objects too complex in shape. Balancing these factors, 9:1 spectral-shape ratio is recommended for multi-level segmentation.

4.2.2 Segmentation levels

The second objective is to select three segmentation levels for multi-level classification. Having mentioned in Chapter III, classification scheme is a three-tiered system, top level being designed for parent classes, or general classes, such as "water"; while bottom level for child classes, or more detailed classes, such as "low density urban". The aim of this chapter is to create a match between object levels and classification levels. That is to say for each classification level, with specific degree of generalization, a suitable segmentation level with corresponding degree of generalization, or critical segmentation level, is selected.

4.2.2.1 Selection Criteria

Five object features are analyzed for selecting critical segmentation levels, namely: Standard Deviation (SD), GLCM Homogeneity (HOM), GLCM Contrast (CON), GLCM Entropy (ENT) and GLCM Angular Second Moment (ASM). VNIR 2 and 3 are considered for they can explain most of the differences between land covers. Variability of these variables is interpreted for three classes: "lake", "grassland" and "high density urban" because they are representative to classes of water, vegetation and urban

respectively. Variability for other classes are shown in Appendix 3. These variables describe the relationships among pixels forming an object. When segmentation level increases, these variables will change. Sharp change indicates drastic variation of image objects when object scale increases while small change indicates object nature stabilizes. A break point can be located at a segmentation scale where the change of these variables switches obviously, which forms the critical segmentation level.

4.2.2.2 Observations

1. Most of the object variables under study break at segmentation level 5.

It is found that in most of the object variables' variations mentioned above, break point can be clearly located at segmentation level 5, or when scale parameter is set at 10. Variables which have break point at level 5 include: SD for all the three classes, ASM for all the three classes, ENT for all the three classes, CON of VNIR 2 for all the three classes, and HOM for "lake" and "grassland". Only HOM for "high density urban" and CON of VNIR 3 do not break at level 5.

Figure 4.4 shows the variations of SD and ASM for "lake", "grassland" and "high density urban". Critical level is apparent at level 5 for the three classes through which rapid change in the object variable switch into much slower change. It is especially so for ASM, which measures the orderliness of pixel-pairs of different values within GLCM table. ASM sharply drops from level 1 to 4 and changes suddenly into slight change at level 5 onwards. Such a drastic variation of objects substantiates level 5 being one of the three critical segmentation levels.

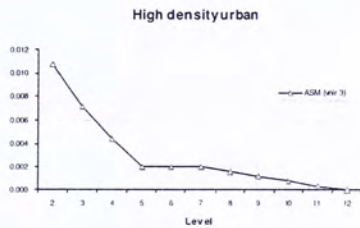
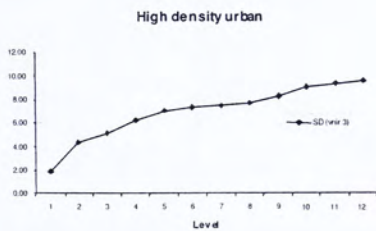
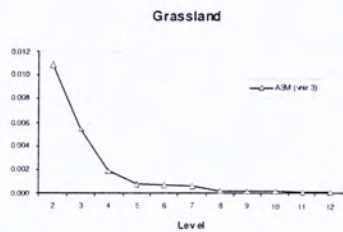
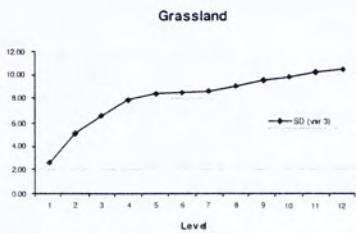
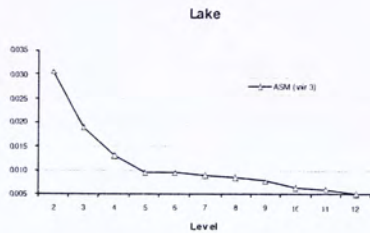
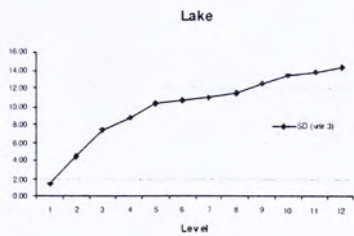


Figure 4.4 Variability of Standard Deviation (on the left) and Angular Second Moment (on the right) of VNIR 3 for the classes: "lake", "grassland" and "high density urban". Case in Chongqing

2. Break points are not clearly defined after segmentation level 5.

Break points after segmentation level 5 are different for different variables and land covers. However it is observed that most of the object variables which show break points break at levels 8, 9 or 10. The findings are listed in the following:

Variables which show break points at level 8 include:

- HOM (VNIR 3) for grassland
- HOM (VNIR 3) for lake
- CON (VNIR 3) for grassland
- CON (VNIR 2) for grassland

For instance, Figure 4.5 shows that HOM (VNIR 3) for grassland turns from horizontal trend to rapid rise again at level 8.

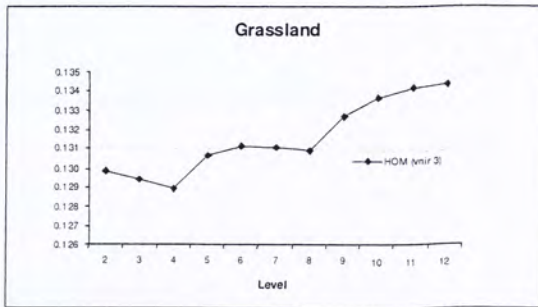


Figure 4.5 Variability of HOM (VNIR 3) for "grassland" in Chongqing

Variables which show break points at level 9 include:

- CON (VNIR 2) for lake
- CON (VNIR 2) for high density urban
- CON (VNIR 3) for lake
- ASM (VNIR 3) for grassland
- SD (VNIR 2) for high density urban

For example, Figure 4.6 shows that SD of VNIR 2 for grassland suddenly rises at level 9 and then stabilizes afterwards, indicating objects change to another stage of heterogeneity.

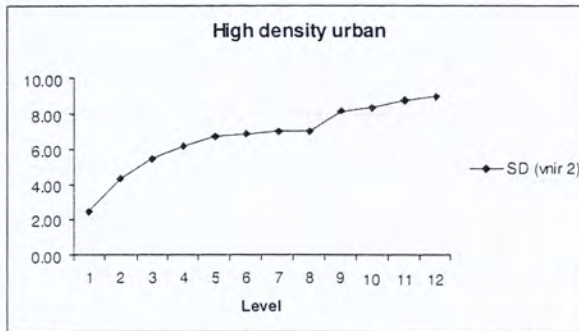


Figure 4.6 Variability of Standard deviation (VNIR 2) for "high density urban in Chongqing

Variables which show break points at level 10 include:

- HOM (VNIR 2) for high density urban
- HOM (VNIR 2) for grassland
- ENT (VNIR 2) for high density urban

For example, HOM (VNIR 2) for “grassland” increases its speed of falling at level 10 (Figure 4.7), indicating that object of grassland starts becoming more heterogeneous at that level.

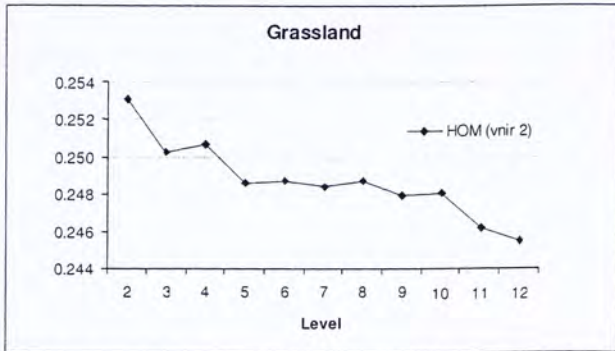


Figure 4.7 Variability of HOM (VNIR 2) for “grassland” in Chongqing

Summing up the above findings, break points are commonly found at levels 8, 9, or 10 for GLCM HOM and CON. Among them, it is applicable for only “grassland” and “lake” when level 8 is set as critical; while it can be applied to only “grassland” and “high density urban” when level 10 is set as critical. Level 9 can be applied to define break points for all of the three classes. Therefore, it is selected as another critical segmentation level.

3. Within-object homogeneity is high at segmentation level 1

Object SD (VNIR 2 and 3) is used to interpret the homogeneity of pixels forming objects at segmentation level 1. As shown in Figure 4.8, SD at level 1 is low for classes “grassland”, “woodland” and “low density urban”. SD of VNIR 2 is the highest for “Low density urban”, reaching as high as 4; while SD for other classes is seldom over 2 at segmentation level 1.

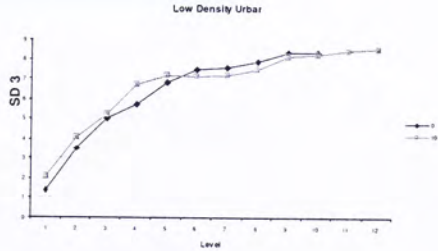
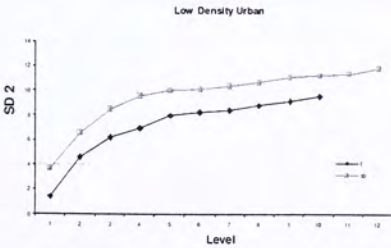
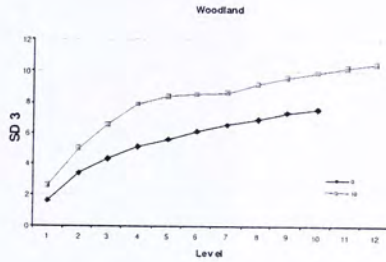
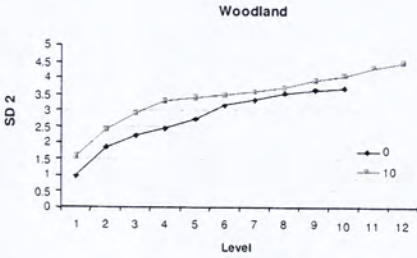
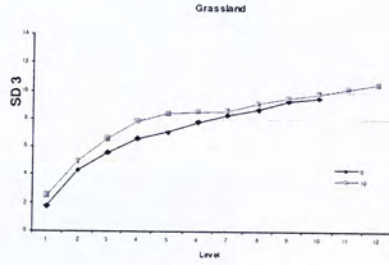
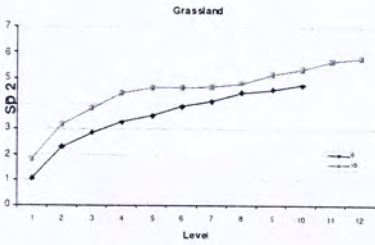
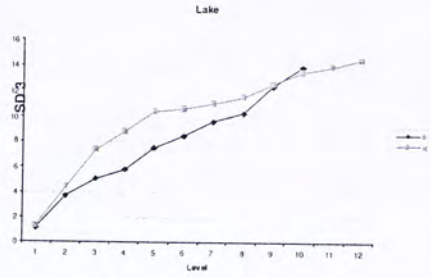
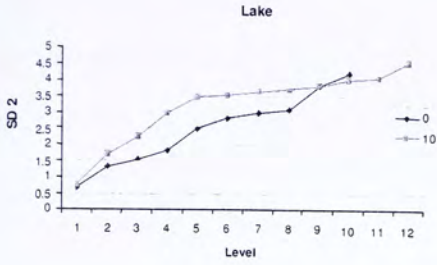
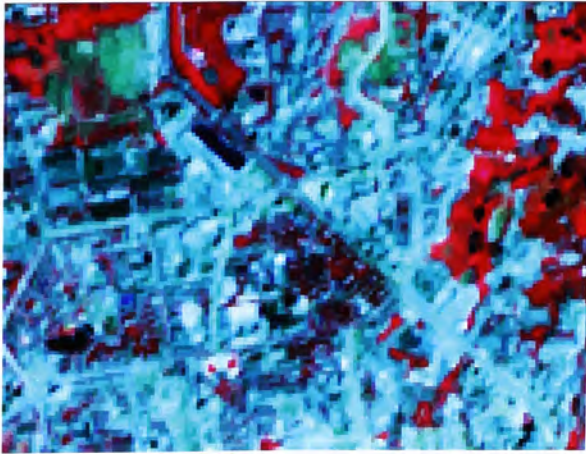


Figure 4.8 Standard Deviation of VNIR 2 (left) and VNIR 3 (right) for “lake”, “grassland”, “woodland” and “low density urban” in Chongqing. Key: 0%–0 % weighting of shape for segmentation; 10%–10 % weighting of shape for segmentation

Figure 4.9 shows the comparison of segmented image at segmentation level 1 with pixel image in Chongqing. It is found that they are not much different with each other from visual inspection. However, considering that many patches of “woodland”, “grassland” and urban covers are of very small size and they often mix with one another in image, scale parameter 1, that is pixel level, is set for segmentation to generate the lowest object level.



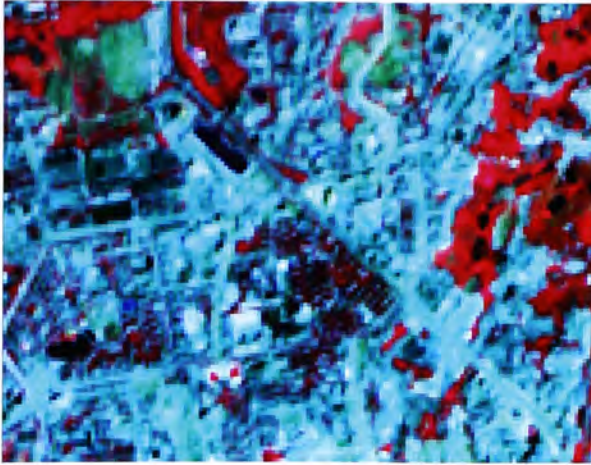


Figure 4.9 Image segmented at scale parameter 2 (Upper) and without segmentation (Lower) in Chongqing

In short, three segmentation levels are selected as object levels for multi-tiered classification. The largest level is level 9; the middle level being level 5; and the lowest level being the pixel level.

4.2.3 Classifying Rules

The third objective is to extract some indicators which can be used to distinguish land covers among one another. Having selected the three object levels for classification, object signature for each class is investigated in order to identify class signatures for different classes at each object level, which will serve as classifying rules for the decision tree classification at the next stage.

4.2.3.1 Selection Criteria

Tables 4.1 to 4.3 present values of a list of spectral, shape and textural features for designated land covers at object levels 9, 5 and 1. A particular feature will be selected as class signature of a class when value of this feature for the class concerned is

discerningly different from other classes. Features suitable for being class signature are bolded in tables and will be explained in the following sections.

4.2.3.2 Level 9

Level 9 is suitable for classifying water body and “industrial”. As shown in Table 4.1, “lake” has obviously large values of SD and GLCM CON of VNIR 3. Its Spectral means of all VNIR channels, as well as Area, are among the lowest. “River” is distinguished by its large values of HOM of all VNIR channels and low values of both CON and SD of VNIR 1 and 2. Besides, Area of “river” is the largest of all classes. “Industrial” is obviously small in both Area and VNIR 3 Spectral mean.

Table 4.1 Values of Spectral (a), Shape (b) and Textural (c) indicators for different land cover classes at segmentation level 9 in Chongqing

Variables	Meanvnr 1	Meanvnr 2	Meanvnr 3	Stdvnr 1	Stdvnr 2	Stdvnr 3	Mdiffvnr 1	Mdiffvnr 2	Mdiffvnr 3
Lake	71.48	40.38	51.64	4.44	3.84	12.56	-14.81	-12.38	-46.13
River	105.03	85.20	63.76	2.18	2.33	2.34	1.09	2.88	-3.18
Grassland	87.39	52.72	108.61	3.92	5.16	9.52	-0.83	-1.89	6.14
Woodland	81.36	46.78	99.56	3.53	3.91	7.54	-3.18	-3.81	0.75
Bareland	98.80	70.23	88.23	6.05	7.58	7.32	2.09	4.75	-3.07
Industrial	89.00	58.27	59.41	5.53	5.81	8.57	-12.86	-12.53	-20.78
High density urban	98.49	68.54	74.64	7.19	8.15	8.25	-1.17	-0.37	-4.08
Low density urban	111.48	81.25	83.02	10.45	11.13	8.12	11.14	12.77	-5.71

Variables	Area	Border length	Length width	Shape index	Density
Lake	36636.21	1566.21	5.16	2.05	1.39
River	285912.93	3311.38	4.53	1.80	1.73
Grassland	97854.39	2350.53	4.11	1.98	1.69
Woodland	91575.00	2276.55	4.50	1.99	1.66
Bareland	73924.34	2235.79	6.44	2.15	1.47
Industrial	33440.63	1191.25	2.70	1.63	1.68
High density urban	74187.00	2130.00	4.06	2.03	1.68
Low density urban	58175.00	2070.00	6.85	2.21	1.49

Table 4.1 Values of Spectral (a), Shape (b) and Textural (c) indicators for different land cover classes at segmentation level 9 in Chongqing (Continued)

(c)

Variables	HOMvnr 1	HOMvnr 2	HOMvnr 3	CONvnr 1	CONvnr 2	CONvnr 3	DISvnr 1	DISvnr 2	DISvnr 3
Lake	0.268	0.314	0.172	50.048	41.808	398.374	4.546	3.893	13.518
River	0.427	0.457	0.484	5.907	7.673	32.344	1.696	1.741	2.376
Grassland	0.293	0.248	0.133	21.158	33.670	112.080	3.075	3.924	7.477
Woodland	0.322	0.325	0.169	17.135	23.275	69.141	2.756	3.055	5.841
Barcland	0.216	0.177	0.161	48.797	74.102	73.217	4.720	5.975	6.119
Industrial	0.220	0.213	0.176	60.889	67.306	120.099	5.212	5.485	7.758
High density urban	0.164	0.145	0.136	60.646	75.112	80.720	5.632	6.384	6.723
Low density urban	0.111	0.103	0.142	146.279	172.254	70.703	8.850	9.656	6.323

Variables	ENTvnr 1	ENTvnr 2	ENTvnr 3	ASMvnr 1	ASMvnr 2	ASMvnr 3
Lake	5.088	4.732	5.986	0.018	0.022	0.008
River	3.923	3.889	3.554	0.036	0.042	0.060
Grassland	5.030	5.443	6.541	0.012	0.008	0.000
Woodland	4.805	4.811	6.162	0.016	0.019	0.002
Barcland	5.674	6.064	6.180	0.006	0.003	0.001
Industrial	5.379	5.420	5.740	0.008	0.009	0.007
High density urban	6.042	6.253	6.360	0.002	0.001	0.001
Low density urban	6.521	6.614	6.230	0.000	0.000	0.000

Key: Meanvnr—spectral mean; Stdvnr—standard deviation of spectral value; Mdiffvnr—mean difference of spectral values; HOMvnr—GLCM homogeneity; CONvnr—GLCM contrast; DISvnr—GLCM dissimilarity; ENTvnr—GLCM entropy; ASM—GLCM angular second moment.

Table 4.2 Values of Spectral (a), Shape (b) and Textural (c) indicators for different land cover classes at segmentation level 5 in Chongqing

Variables	Meanvnr 1	Meanvnr 2	Meanvnr 3	Stdvnr 1	Stdvnr 2	Stdvnr 3	Mdiffvnr 1	Mdiffvnr 2	Mdiffvnr 3
Lake	70.70	39.78	49.22	3.94	3.48	10.38	-14.07	-11.80	-42.18
River	105.03	84.84	62.68	1.87	1.86	1.83	0.83	1.81	-1.98
Grassland	87.36	52.57	109.30	3.48	4.60	8.41	-0.35	-1.25	5.87
Woodland	80.94	46.28	99.31	3.14	3.41	6.65	-2.97	-3.43	0.05
Bareland	98.96	70.99	87.46	5.55	7.14	6.71	1.20	3.88	-4.14
Industrial	86.98	56.50	54.15	4.22	4.40	5.99	-12.62	-12.14	-23.19
High density urban	99.12	69.42	73.23	6.06	6.76	7.08	-0.98	-0.22	-4.96
Low density urban	113.74	83.26	83.98	9.61	10.03	7.18	11.43	12.43	-2.01

Variables	Area	Border length	Length width	Shape index	Density
Lake	28846.55	1252.76	4.91	1.89	1.41
River	137424.19	2036.13	3.65	1.56	1.82
Grassland	43782.25	1517.18	4.32	1.88	1.59
Woodland	51157.76	1593.10	4.12	1.84	1.63
Bareland	34507.89	1374.47	5.56	1.91	1.47
Industrial	15957.00	680.40	2.67	1.39	1.58
High density urban	33741.00	1412.40	4.24	1.94	1.60
Low density urban	27558.33	1380.00	7.71	2.15	1.33

Table 4.2 Values of Spectral (a), Shape (b) and Textural (c) indicators for different land cover classes at segmentation level 5 in Chongqing (Continued)

Variables	HOMvnr 1	HOMvnr 2	HOMvnr 3	CONvnr 1	CONvnr 2	CONvnr 3	DISvnr 1	DISvnr 2	DISvnr 3
Lake	0.282	0.326	0.188	49.208	41.409	368.142	4.423	3.808	12.691
River	0.434	0.471	0.499	5.888	7.010	24.618	1.672	1.654	2.092
Grassland	0.293	0.249	0.131	19.596	31.928	114.062	3.016	3.871	7.536
Woodland	0.323	0.331	0.171	16.243	21.422	68.670	2.701	2.932	5.816
Bareland	0.210	0.165	0.157	47.868	76.157	70.410	4.722	6.154	6.149
Industrial	0.236	0.231	0.186	56.122	60.715	120.340	4.933	5.109	7.668
High density urban	0.168	0.146	0.139	58.962	71.915	74.690	5.534	6.262	6.490
Low density urban	0.102	0.099	0.141	167.080	190.790	74.437	9.552	10.220	6.455

Variables	ENTvnr 1	ENTvnr 2	ENTvnr 3	ASMvnr 1	ASMvnr 2	ASMvnr 3
Lake	4.839	4.547	5.659	0.022	0.026	0.010
River	3.686	3.578	3.269	0.043	0.052	0.075
Grassland	4.809	5.197	6.170	0.014	0.010	0.001
Woodland	4.620	4.599	5.883	0.019	0.024	0.003
Bareland	5.407	5.786	5.830	0.007	0.003	0.003
Industrial	4.788	4.824	5.069	0.015	0.015	0.013
High density urban	5.715	5.903	5.971	0.004	0.001	0.002
Low density urban	6.134	6.169	5.832	0.001	0.001	0.002

Key: Meanvnr—spectral mean; Stdvnr—standard deviation of spectral value; Midfvnr—mean difference of spectral values; HOMvnr—GLCM homogeneity; CONvnr—GLCM contrast; DISvnr—GLCM dissimilarity; ENTvnr—GLCM entropy; ASM—GLCM angular second moment.

Table 4.3 Values of Spectral (a) and Shape (b) and indicators for different land cover classes at segmentation level 1 in Chongqing

(a)	Variables	Meanvnr 1	Meanvnr 2	Meanvnr 3	Stdvnr 1	Stdvnr 2	Stdvnr 3	Mdiffvnr 1	Mdiffvnr 2	Mdiffvnr 3
	Lake	68.07	37.50	42.59	0.82	0.76	1.35	-2.78	-2.49	-7.91
	River	104.86	84.66	61.87	1.01	1.03	0.96	-0.10	-0.05	-1.15
	Grassland	87.44	51.89	113.19	1.42	1.80	2.57	-0.07	-0.73	3.47
	Woodland	79.82	45.03	99.06	1.49	1.57	2.25	-1.23	-1.44	0.32
	Barmland	99.91	73.59	84.58	2.02	2.57	1.94	0.47	2.00	-3.19
	Industrial	84.26	53.80	49.78	1.39	1.31	1.31	-3.40	-3.19	-6.79
	High density urban	97.86	67.78	69.69	2.21	2.53	1.93	-0.33	-0.14	-2.42
	Low density urban	119.73	88.92	84.63	3.19	3.68	2.09	5.58	5.70	0.28

(b)	Variables	Area	Border length	Length width	Shape index	Density
	Lake	3600.00	280.34	2.27	1.22	1.31
	River	8673.39	383.23	2.01	1.15	1.51
	Grassland	1559.54	187.33	2.32	1.22	1.11
	Woodland	2312.07	229.66	2.36	1.24	1.21
	Barmland	1344.08	176.05	2.66	1.22	1.04
	Industrial	2772.00	237.60	2.18	1.18	1.24
	High density urban	1521.00	190.80	2.46	1.24	1.10
	Low density urban	1050.00	154.44	2.56	1.21	1.00

Key: Meanvnr—spectral mean; Stdvnr—standard deviation of spectral value; Mdiffvnr—mean difference of spectral values

Figure 4.10a visualizes the values of SD VNIR 1 on image. "River" can be distinguished by its dark color, which indicates its significantly low value compared with other land covers. In Figure 4,10b, most of "lakes", especially those on eastern bank of Changjiang, becomes bright when GLCM CON of VNIR 3 is visualized. Low spectral value of VNIR 3 for industrial compared with other classes can also be shown in Figure 4.10c.

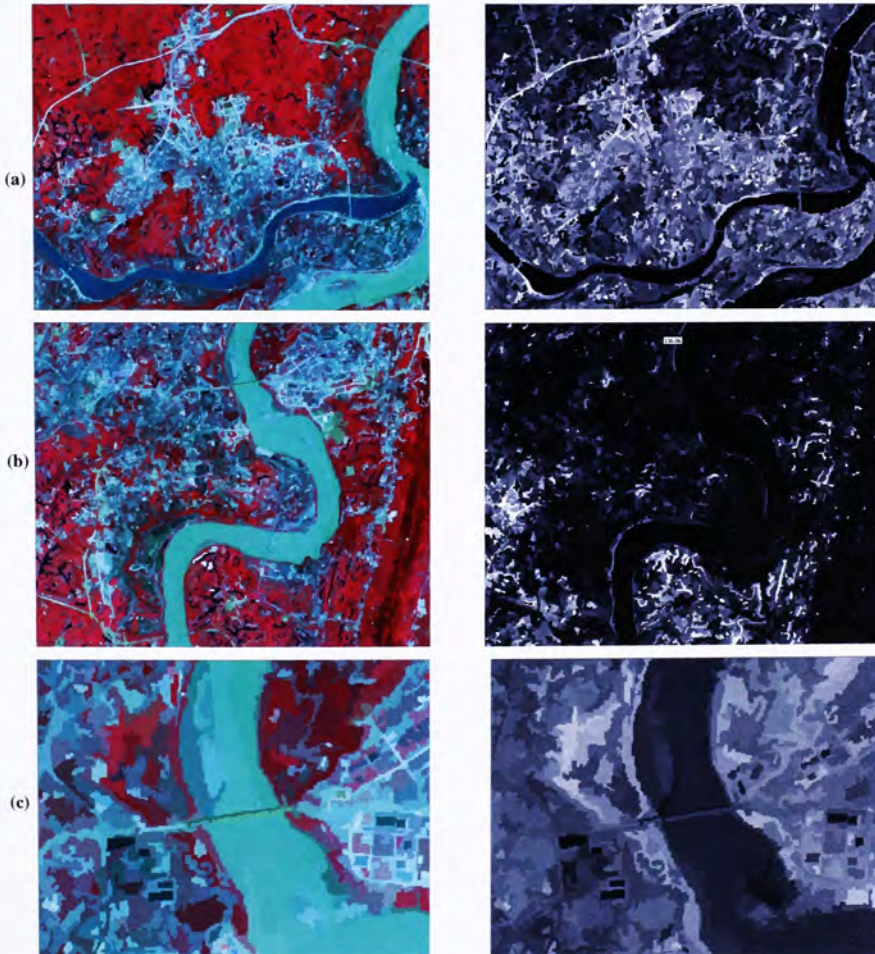


Figure 4.10 Image objects of "river" (a), "lake" (b) and "industrial"(c) and their visualization

It is worth noticing that Area serves best classifying “lake” and “industrial” from other classes at segmentation level 9 because their differences from other classes are not so significant at level 5 or level 1 (shown in Figure 4.11). These two classes can then be divided from each other by Mean difference to neighbor in VNIR 3 and Density (higher value of it indicating that the shape of object approaches circle), as shown in Table 4.1.

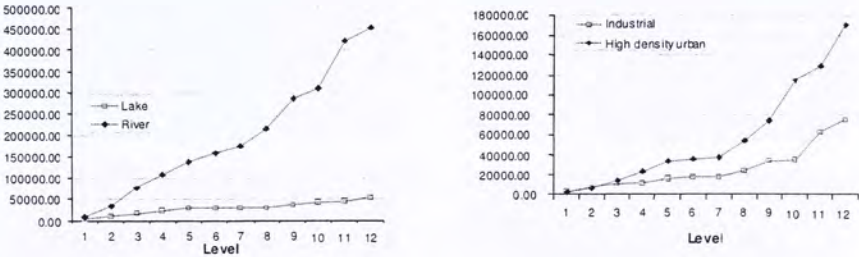


Figure 4.11 Comparisons of Area: between Lake and River (Left) and between Industrial and High density urban (Right) in Chongqing

4.2.3.3 Level 5

After “lake”, “river” and “industrial” are classified at segmentation level 9, in this level object features are identified to differentiate among the remaining classes, that is “grassland”, “woodland”, “bareland”, “high density urban” and “low density urban”.

As shown in Table 4.2, level 5 can be used to distinguish vegetation from other classes because both “grassland” and “woodland” have high value in VNIR 3 Spectral mean and low value in VNIR 2 Spectral mean compared to other classes. Figure 4.12 shows the visualization of values of VNIR 3/VNIR 2 ratio. The contrast between vegetation and non-vegetation can be clearly seen. Thus, it can be utilized to depict the border of green space.

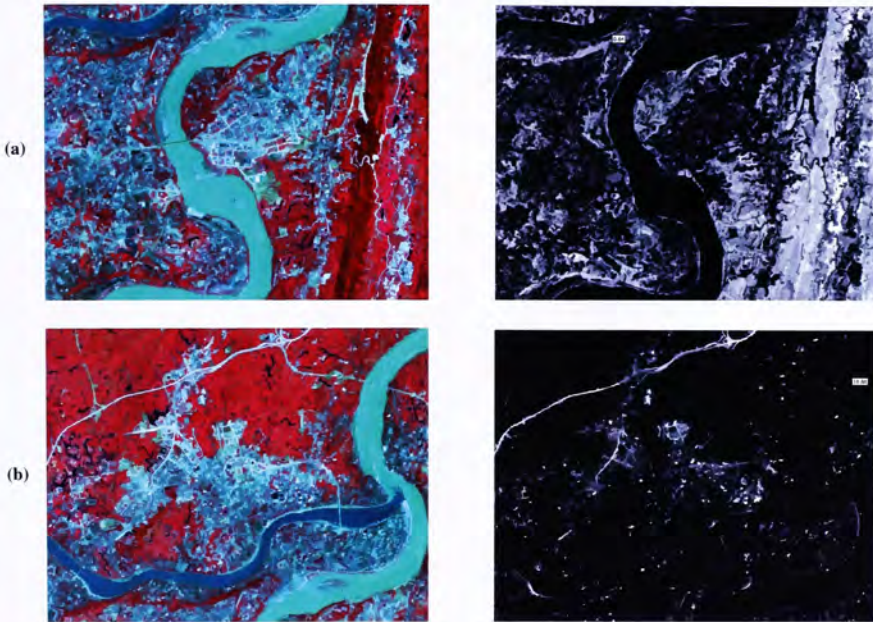


Figure 4.12 Visualization of contrast between “vegetation” and “non-vegetation” at segmentation level 5 using VNIR 3/VNIR 2 ratio (a); and between “low density urban” and other non-vegetation classes using GLCM contrast VNIR 2 (b). Case in Chongqing

For the non-vegetation classes, “low density urban” can be classified out of “high density urban” and “bareland” as it has obviously high value in both Spectral means and GLCM Contrast in VNIR 1 and 2. As shown in Figure 4.12b, “low density urban”, especially the new highway on the north, reveals high contrast against other urban fabric on the south. Thus, “low density urban” can be classified at this level.

4.2.3.4 Level 1

“Lake”, “river”, “industrial”, “vegetation”, and “low density urban” have been identified at the top 2 object levels. The remaining classes, which are “grassland”, “woodland”, “bareland” and “high density urban”, are left at object level 1 to be classified.

At level 1, both textural and shape features are not suitable to be used because it is in fact pixel-level. Thus, only spectral means can be utilized to classify those classes. From Table 4.3, spectral means of all VNIR channels VNIR 3 is not very sensitive to the difference between “woodland” and “grassland”. Therefore, Spectral means of VNIR 1 and 2 are main class descriptors of these two classes at level 1. Equivalently, although Table 4.3 indicates that spectral mean of every channel can be used to divide between “high density urban” and “bareland”, Figure 4.13 shows that contrast between them under VNIR 3 spectral mean is not sufficiently strong. Therefore, spectral means of VNIR 1 and 2 will be used to classify them.

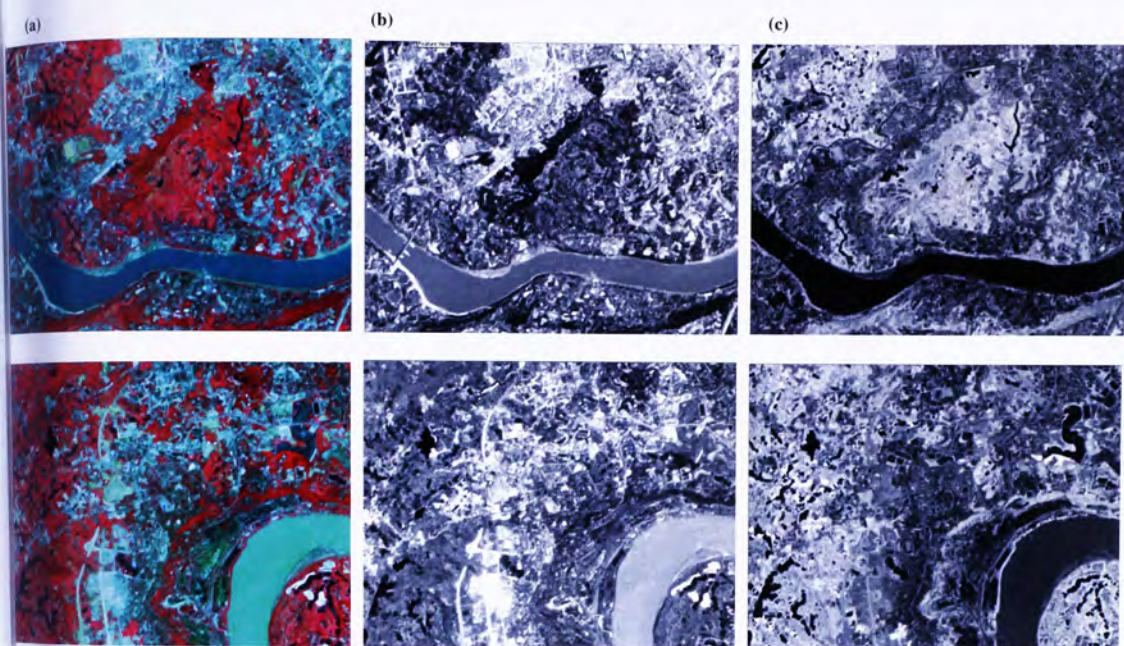


Figure 4.13 Comparison between the original image (a), visualization of spectral mean VNIR 2 (b) and visualization of spectral mean VNIR 3 (c) for “woodland”-“grassland” contrast (Upper) and “high density urban”-“bareland” contrast (Lower). Notice the low contrast for VNIR 3.

4.3 Nanjing

4.3.1 Spectral-shape ratio

Like the case of Chongqing, the first objective of image object analysis in Nanjing is to optimize spectral-shape ratio to minimize the distortion of image by segmentation. The impact of different spectral-shape ratios on the representation of land cover objects in the image is studied.

4.3.1.1 Selection Criteria

In order to optimize the spectral-shape ratio, the total number of image objects generated, Standard deviation of spectral means of objects and appearance of the resultant segmented image at the same 6 spectral-shape ratios as those investigated in Chongqing are studied.

4.3.1.2 Observations

1. **An increase in weight of shape on spectral-shape ratio generates smaller number of image objects and larger average size of image object at every segmentation level. But the difference between spectral-shape ratio of 10:0 and 9:1 is not significant.**

Like the case study in Chongqing, an increase in segmentation level results in a rise of average size of image object, which is reflected on the descending number of objects across segmentation gradient as shown in Figure 4.14. Decrease in number of objects generated is most obvious from segmentation level 1 to level 2, followed by negligible variation in object amount after level 5.

Another shared characteristic between Chongqing and Nanjing is the negative relationship between the weight of shape on spectral-shape ratio and number of objects generated, which is most discerning at segmentation level 1. What is different from Chongqing is that when the weight of shape is increased from 0% to 10%, the decrease in number of objects is not significant throughout the segmentation levels. But when the weight of shape is increased to 90%, number of objects generated at segmentation level 1 falls by half from 100,000 to 50,000.

It is deduced that with decreasing spectral-shape ratio, image objects generated by segmentation tend to be larger in average size at every segmentation level, which is shown in Appendix 4. However, the difference in number of objects generated, and thus average size of objects, is not obvious between spectral-shape ratio of 10:0 and 9:1.

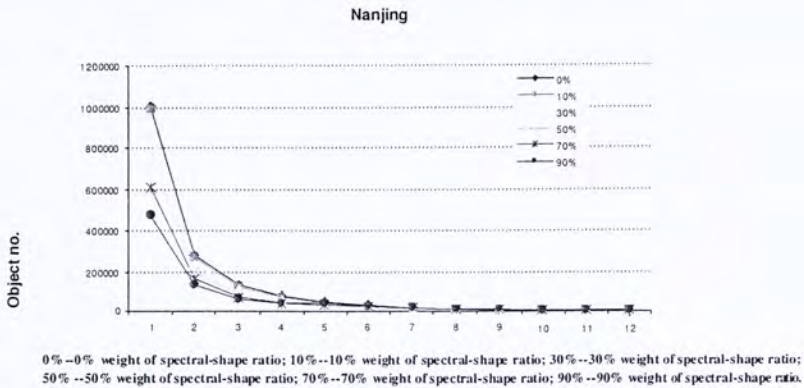


Figure 4.14 Object number generated by varying spectral-shape ratio across segmentation gradient. Case in Nanjing

- Decreasing in the spectral-shape ratio increases Standard deviation of spectral values of image objects at every segmentation level. Difference in SD between spectral-shape ratio of 10:0, 9:1 and 7:3 is slight when the segmentation level is low.

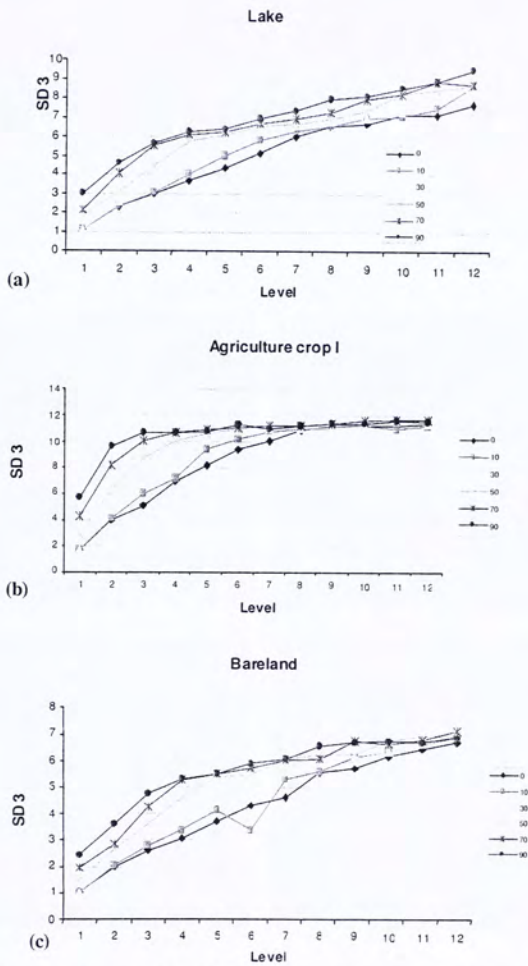
The relationships between pixels' spectral variances within objects of different scales and spectral-shape ratios, which are measured by Standard deviation of VNIR 3, for three classes: "lake", "agricultural crop I" and "bareland" are illustrated in Figure 4.15. These three classes are chosen because they represent land covers of water, vegetation and non-vegetated land respectively. VNIR 3 is sensitive to the differences

between water, vegetation and non-vegetation. So SD of it is used to study the heterogeneity of pixels within objects. SD of other VNIR channels and land cover objects are shown in Appendix 4.

In spite of minor abnormalities in case of "bareland", all classes follow the same pattern of increase in SD with the weight of shape on spectral-shape ratio. When the weight of shape is 90%, SD is the largest for all classes throughout the segmentation gradient. Besides, it rises most rapidly from segmentation 1 to 4. Spectral heterogeneity of objects is the lowest when the weight of shape is 0% at every segmentation level. However, very similar same values of SD are observed when the weight of shape is switched to 10% or 30%, especially when segmentation level is lower than 3.

- 3. Segmented objects are in regular shapes when spectral-shape ratio is low; 10:0, 9:1 and 7:3 segmentation are very similar to pixel image at low segmentation scale.**

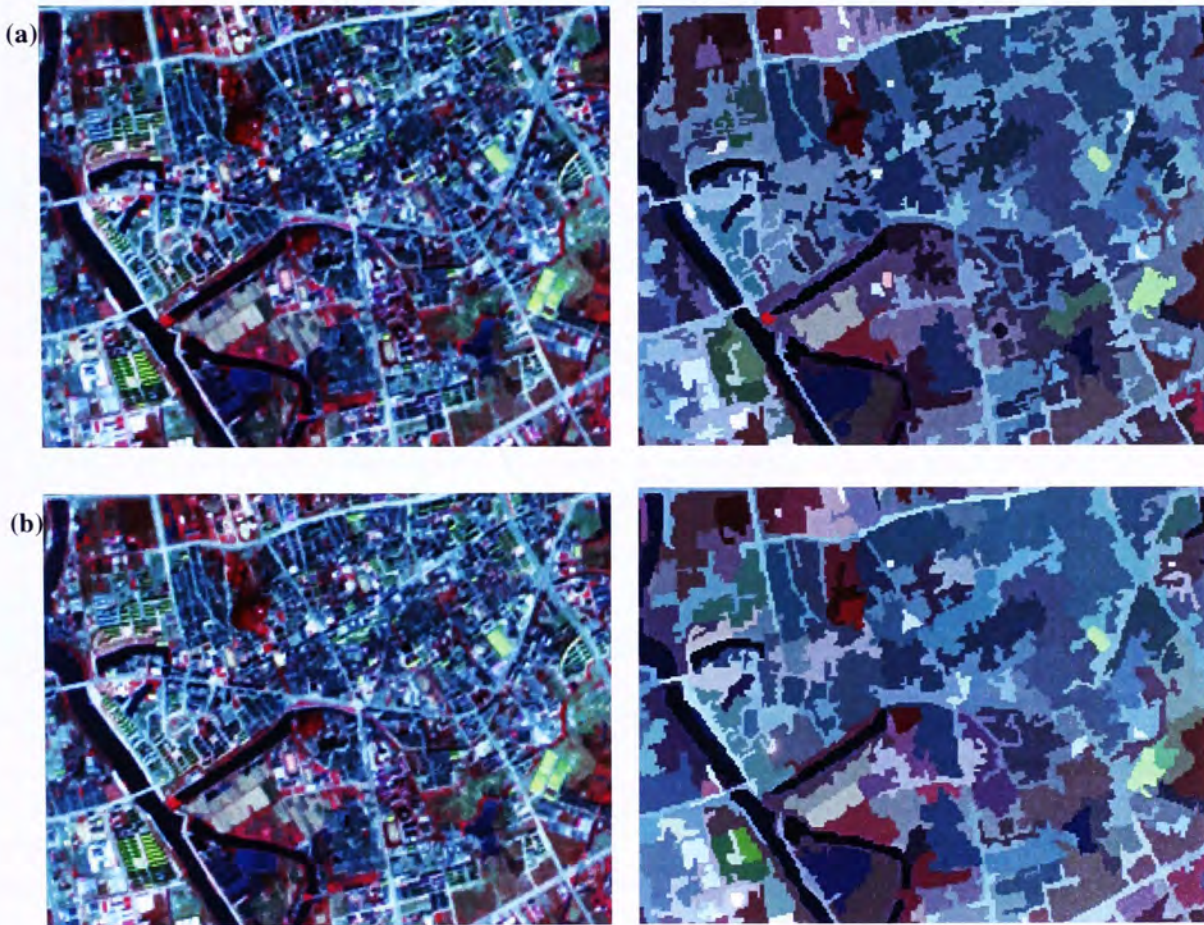
Appearance of segmented images at different spectral-shape ratios are shown in Figure 4.16. They confirm that high weight of shape tends to generate objects which contain pixels of high spectral variances, especially when segmentation level is high.



0%--0% weight of spectral-shape ratio; 10%--10% weight of spectral-shape ratio; 30%--30% weight of spectral-shape ratio; 50%--50% weight of spectral-shape ratio; 70%--70% weight of spectral-shape ratio; 90%--90% weight of spectral-shape ratio.

Figure 4.15 Variability of Standard deviation (VNIR 3) of land covers "Pond" (a), "Agricultural crop I" (b) and "Bareland" (c). Case in Nanjing

Segmented images at level 1 represent the original pixel image equally well when spectral-shape ratio is set 10:0, 9:1 and 7:3. However, objects at level 12 are too complex in shape when the spectral-shape ratio is set to 10:0 or 9:1; while 7:3 produces segmented image more conformable to human view of landscape at smaller scale.



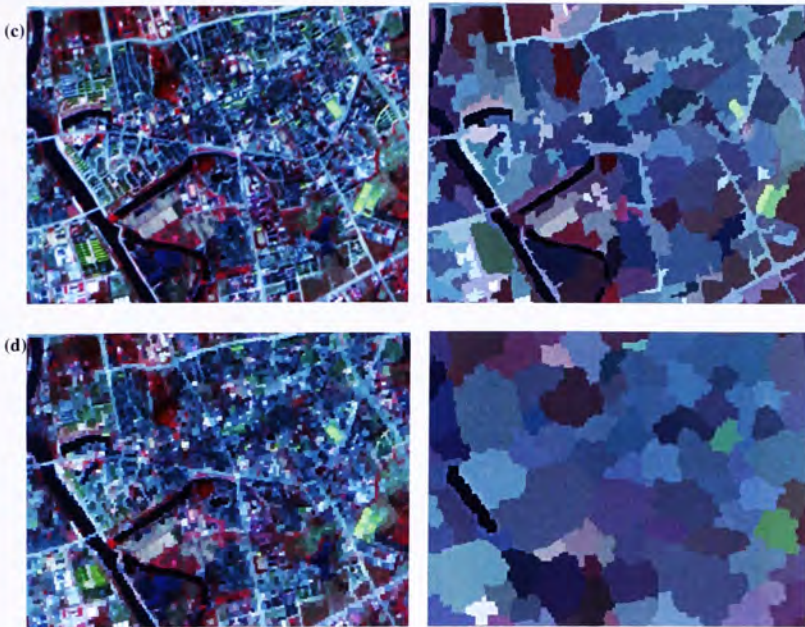


Figure 4.16 Segmented images of Nanjing at segmentation level 1 (left) and 12 (right). They are generated at spectral-shape of 10:0 (a), 9:1 (b), 7:3 (c) and 1:9 (d). Notice: First the regular shapes of objects at 1:9; second the similarity of image quality at level 1 for 10:0, 9:1 and 7:3 and third the fractal objects at both 10:0 and 9:1.

In summary, the higher the spectral-shape ratio more objects of smaller sizes are segmented at every segmentation level. Besides, smaller spectral variances between pixels forming an object are resulted when spectral-shape ratio is increased. However, the differences between the spectral-shape ratios of 10:0, 9:1 and 7:3 are negligible regarding both object number and spectral SD, particularly at segmentation levels lower than 3. Both 10:0 and 9:1 spectral-shape ratios result in objects too complex in shape at high segmentation level; while the appearance of image at 7:3 is closer to human view of landscape at lower “map” scale. Therefore, 7:3 spectral-shape ratio is recommended for multi-level segmentation.

4.3.2 Segmentation Levels

The second objective is to select three critical segmentation levels for the three classification levels of different degrees of generalization. As in the case of Chongqing, a match between each classification level and an object level of suitable degree of generalization is to be found in this part of study.

4.3.2.1 Selection Criteria

The same object features as in the case of Chongqing are analyzed in Nanjing, which are: Standard Deviation (SD), GLCM Homogeneity (HOM), GLCM Contrast (CON), GLCM Entropy (ENT) and GLCM Angular Second Moment (ASM) of VNIR 2 and 3. They can depict the spectral variations of pixels within objects along segmentation levels. Classes which are focused are “lake”, “agricultural crop II” and “low density urban” because they are highly responsive to the change in segmentation scale. Variations of these features for other classes are referred to Appendix 4. Like the case of Chongqing, the selection criterion is whether break points, or critical segmentation levels, can be identified at a segmentation scale where the trends of these variables changes significantly.

4.3.2.2 Observations

1. **Most of the object variables break at segmentation level 5. But break points can also be frequently observed at segmentation level 4.**

Most of the object features listed above are still found breaking at segmentation level 5 just as the case of Chongqing. However, fewer variables have break points at level

5 for all classes. (Only SD of VNIR 2 and ENT VNIR 3) Others variables break at level 5 for 1 or 2 classes, which are shown in Table 4.4.

Table 4.4 Object variables and the classes which have break points at segmentation level 5 in Nanjing

Object variables which break at level 5	Classes
SD (VNIR 2)	All classes
SD (VNIR 3)	Lake, low density urban
HOM (VNIR 2)	Agricultural crop II
HOM (VNIR 3)	Agricultural crop II
CON (VNIR 3)	Lake, agricultural crop II
ENT (VNIR 2)	Lake, low density urban
ENT (VNIR 3)	All classes
ASM (VNIR 2)	Low density urban
ASM (VNIR 3)	Low density urban

5 object variables are found breaking at segmentation level 4 instead of 5. They include: SD (VNIR 3) for “agricultural crop II”, CON (VNIR 2) for “lake”, ENT (VNIR 2) for “agricultural crop II” and ASM (VNIR 2 and 3) for “agricultural crop II and lake”.

Figure 4.17 shows variability of CON (VNIR 3) and ASM (VNIR 3) for “lake” and “agricultural crop II”. The former breaks at level 5 while the latter level 4. Although more features are found breaking at level 5, it is also found that image at level 5 is too coarse to illustrate the contrast between different types of vegetation (shown in Figure 4.18). Segmentation level 4 is thus selected as critical level.

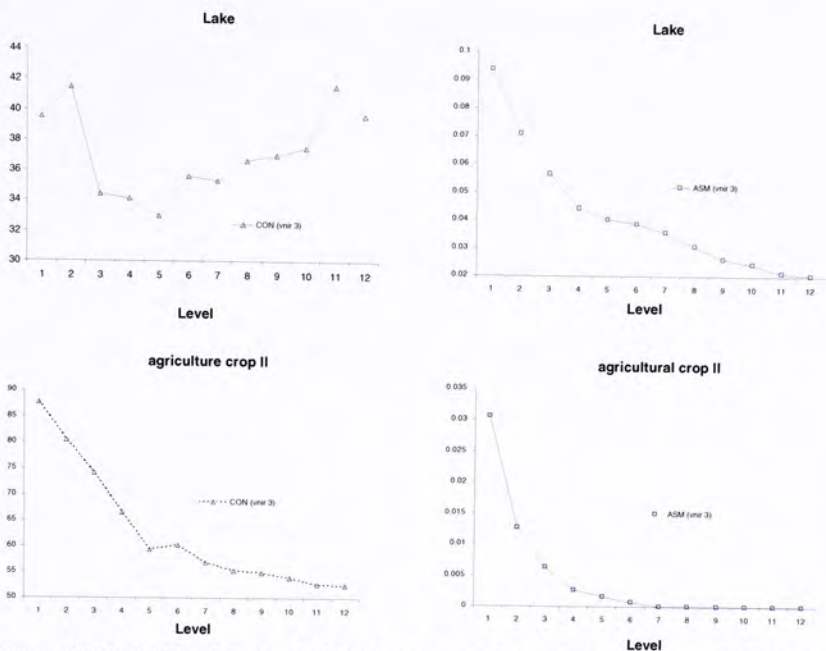


Figure 4.17 Variability of Contrast (VNIR 3) (Left) and Angular Second Moment (VNIR 3) (Right) for lake (a) and agricultural crop II (b) in Nanjing

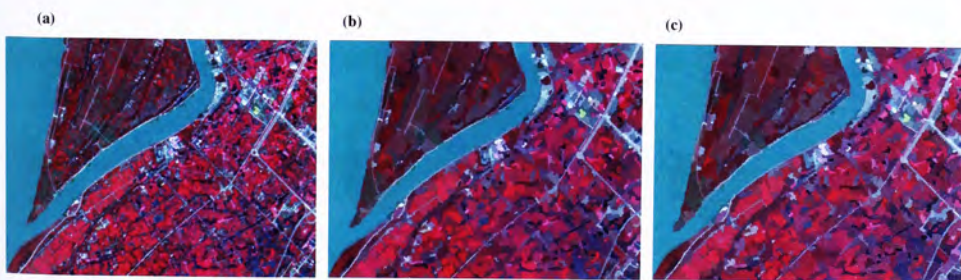


Figure 4.18 Image of “agricultural crop II” from pixel image (a) to segmentation level 4 (b) to level 5 (c) in Nanjing. Notice the gradual loss in details

2. Most of the break points can be found at segmentation levels 8 and 9.

Most of the object variables show break points at level 8 or 10. The findings are listed in the following:

Variables which break at level 8 include:

- SD (VNIR 2) for agricultural crop II
- HOM (VNIR 2) for lake
- HOM (VNIR 3) for lake and low density urban
- CON (VNIR 2) for agricultural crop II

For instance, Figure 4.19 shows that CON (VNIR 2) for “agricultural crop II” starts to increase sharply after level 8.

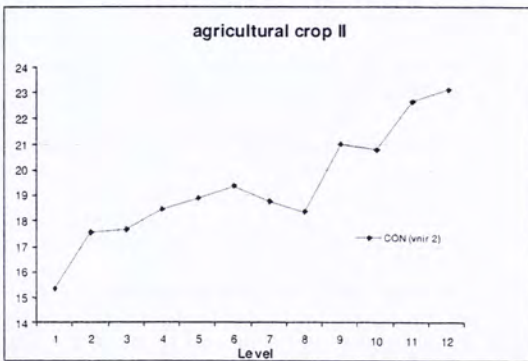


Figure 4.19 Variability of CON (VNIR 2) for “agricultural crop IP” in Nanjing

Variables breaking at level 10 include:

- SD (VNIR 2) for lake
- SD (VNIR 3) for lake and low density urban
- CON (VNIR 2) for lake
- CON (VNIR 3) for lake

Figure 4.20 shows that CON (VNIR 2) for “lake” keeps at about 20 from level 4 onwards and rises sharply at level 10 to over 25 and stays around that value to level 12.

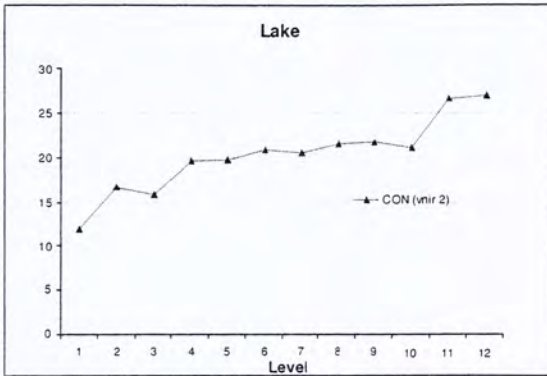


Figure 4.20 Variability of CON (VNIR 2) for “lake” in Nanjing

When level 8 is set at critical level, break points can be defined for the three classes tested; while they can only be defined for “lake” and “low density urban” when segmentation level 10 is set at critical level. Besides, level 8 is more capable of preserving contrast between different types of land covers. Therefore, level 8 is selected as another critical segmentation level.

3. Within-object homogeneity is high at segmentation level 1.

The lowest critical segmentation level can be determined after analyses of spectral variances of objects for “lake”, “agricultural crop II” and “low density urban”, which are graphically shown in Figure 4.21. Focusing on segmentation level 1 discovers that spectral variances within objects are low. Most of the classes have SD of about 1.

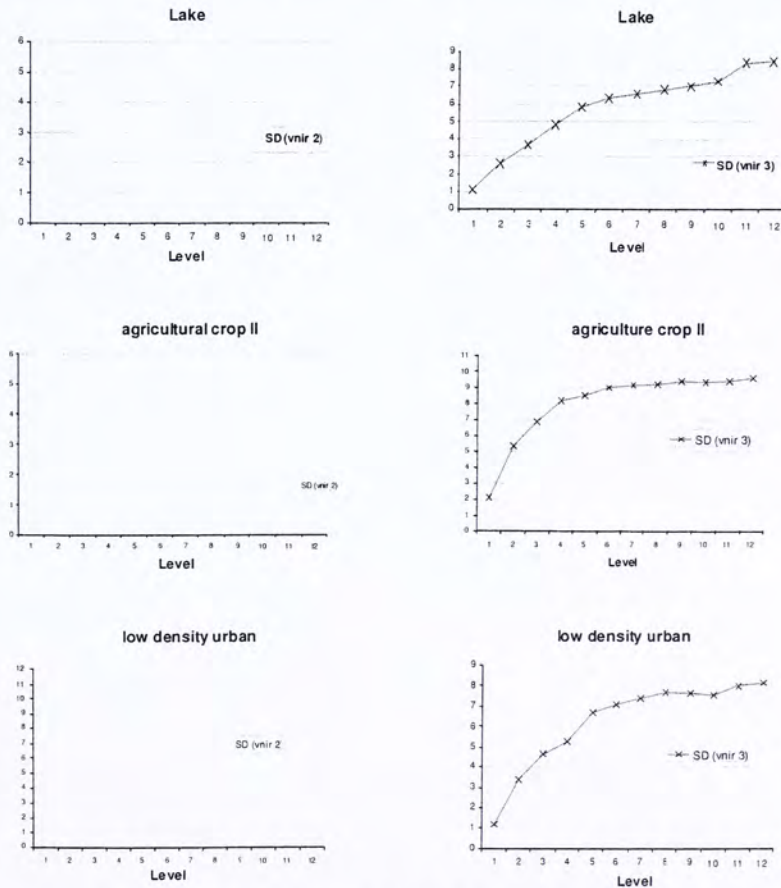


Figure 4.21 Variation of Standard Deviation of VNIR 2 (Left) and VNIR 3 (Right) for “lake” (a), “agricultural crops II” (b) and “low density urban” (c) in Nanjing

This finding is also established for other land covers that have not been presented in this chapter (referring to Appendix 4), which implies that the lowest object level can be set at segmentation level 1 or scale parameter: 2. In fact, visual inspection in the Nanjing image also cannot find out significant differences between pixel-level and segmentation level 1 (Figure 4.22). Therefore, segmentation level 1 is selected as critical level.

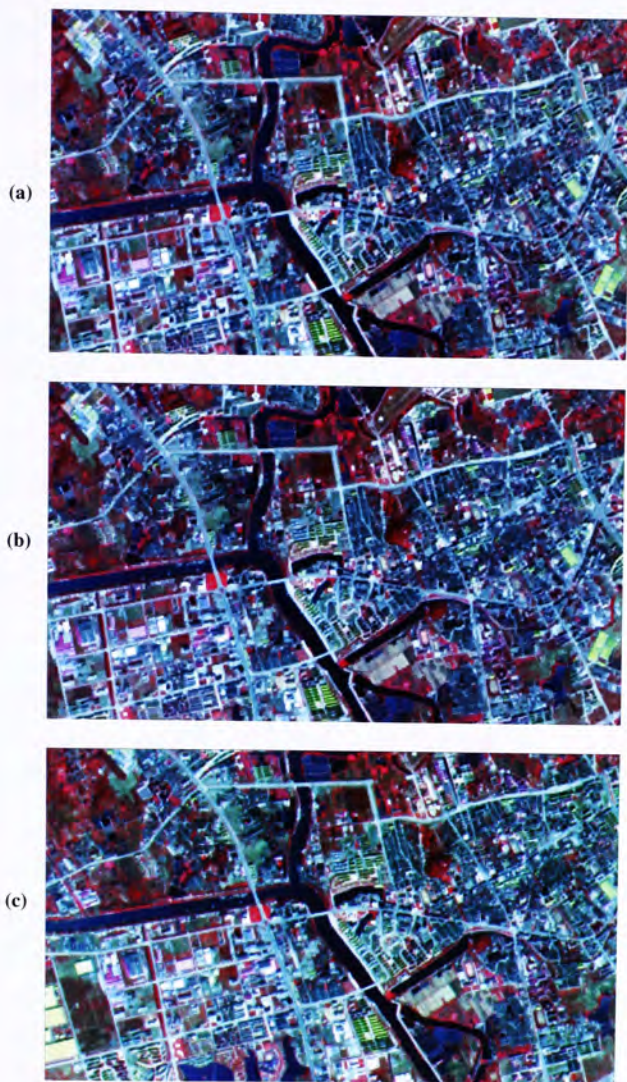


Figure 4.22 Comparison between pixel image of Nanjing (a), segmented image at segmentation level 1 at spectral-shape ratio of 7:3 (b), and segmented image at segmentation level 1 at spectral-shape ratio of 9:1 (c). Difference is hardly found even at large scale

Summing up, three segmentation levels are selected as object levels for classification, which are level 8, level 4 and level 1.

4.3.3 Classifying Rules

The third objective is to extract indicators to classify land covers. Classifying rules will be extracted from spectral, shape and textural features which best define each land cover at pre-selected object levels, which are levels 8, 4 and 1.

4.3.3.1 Selection Criteria

Tables 4.5 to 4.7 show spectral, shape and textural values for different land cover classes at object levels 8, 4 and 1. As in the case of Chongqing, if a feature value of a particular class is obviously different from other classes, that feature will be used as classifying rules for that class during the design of decision tree. Features which can be used to differentiate a class have their values bolded in the table for illustration.

4.3.3.2 Level 8

The top object level can be used to identify water body. Both “river” and “lake” have low spectral values in VNIR 3. Besides, they are particularly low in CON and SD of VNIR 1. The ability of spectral value (VNIR 3) in distinguishing water body from “high density urban”, which also has low values in other spectral channels, is illustrated in Figure 4.23.

Water body can then be further divided into "river" and "lake" by its larger area, higher spectral value in VNIR 1 and higher HOM in all channels. From the image there are smaller river channels which Area cannot be used to classify. They can be distinguished instead by its larger value in length-width ratio, which is shown in Figure 4.24.

Table 4.5 Values of Spectral (a), Shape (b) and Textural (c) indicators for different land cover classes at segmentation level 8 in Nanjing

(a)	Variables	Meanvnr 1	Meanvnr 2	Meanvnr 3	Stdvnr 1	Stdvnr 2	Stdvnr 3	Mdiffvnr 1	Mdiffvnr 2	Mdiffvnr 3
	River	69.472	53.614	28.323	2.516	2.487	3.061	1.146	1.309	-2.648
	Lake	56.910	36.310	30.956	3.627	4.260	6.843	-1.223	-2.543	-6.991
	Woodland	53.815	34.766	43.010	4.185	4.713	6.698	-2.057	-2.262	-0.377
	Agri crop I	56.973	36.275	56.686	3.572	4.629	11.113	-1.627	-3.000	7.823
	Agri crop II	59.529	39.034	49.104	3.899	4.413	9.207	-1.437	-2.081	2.782
	wetland	58.048	37.069	50.565	5.333	5.927	9.339	-0.242	-2.453	9.284
	Grassland	59.592	41.216	44.367	5.040	5.699	6.988	-0.659	-0.587	-0.074
	Fallowland	59.683	41.920	42.935	4.753	5.773	6.802	-0.545	-0.102	-0.508
	Barland	63.034	48.114	43.027	6.637	7.727	5.946	0.839	2.239	-0.777
	Low density urban	68.968	50.753	43.758	9.277	9.580	7.642	4.101	4.288	1.558
	High density urban	62.144	43.352	37.995	7.496	7.675	7.127	-1.125	-1.230	-2.304

(b)	Variables	Area	Length width	Border length	Shape index	Density
	River	637.816	1.447	125.211	1.305	2.054
	Lake	367.533	1.289	94.933	1.285	2.027
	Woodland	347.623	1.360	93.325	1.281	2.015
	Agri crop I	275.452	1.322	78.903	1.296	2.000
	Agri crop II	431.100	1.327	102.733	1.281	2.057
	wetland	322.793	1.550	86.966	1.297	1.943
	Grassland	363.750	1.353	93.591	1.273	2.026
	Fallowland	495.565	1.303	110.652	1.287	2.062
	Barland	320.034	1.349	90.414	1.290	1.999
	Low density urban	279.759	1.341	81.963	1.292	1.961
	High density urban	343.135	1.442	92.423	1.294	1.963

Table 4.5 Values of Spectral (a), Shape (b) and Textural (c) indicators for different land cover classes at segmentation level 8 in Nanjing. (Continued)

(c)

Variables	HOMvnr 1	HOMvnr 2	HOMvnr 3	CONvnr 1	CONvnr 2	CONvnr 3	DISvnr 1	DISvnr 2	DISvnr 3
River	0.506	0.520	0.543	12.050	12.689	12.704	1.764	1.759	1.802
Lake	0.395	0.376	0.305	15.949	21.423	36.641	2.395	2.759	3.991
Woodland	0.352	0.336	0.214	18.866	22.220	33.464	2.692	2.953	4.231
Agri crop I	0.349	0.294	0.144	11.838	17.545	83.802	2.397	3.022	6.787
Agri crop II	0.321	0.299	0.155	15.317	18.374	55.374	2.716	2.999	5.682
wetland	0.324	0.319	0.183	26.360	27.023	60.569	3.190	3.292	5.522
Grassland	0.301	0.268	0.208	24.949	28.338	37.198	3.271	3.631	4.454
Fallowland	0.314	0.274	0.214	23.056	29.639	36.425	3.032	3.587	4.399
Bareland	0.275	0.241	0.266	34.139	42.159	26.122	3.826	4.351	3.569
Low density urban	0.170	0.158	0.171	83.226	87.494	48.147	6.414	6.706	5.241
High density urban	0.195	0.184	0.181	58.653	58.872	42.185	5.293	5.469	4.896

Variables	ENTvnr 1	ENTvnr 2	ENTvnr 3	ASMvnr 1	ASMvnr 2	ASMvnr 3
River	3.369	3.181	3.185	0.077	0.097	0.109
Lake	4.436	4.591	5.146	0.036	0.037	0.031
Woodland	4.718	4.874	5.784	0.018	0.017	0.004
Agri crop I	4.605	5.065	6.382	0.020	0.012	0.001
Agri crop II	4.897	5.109	6.436	0.014	0.012	0.000
wetland	4.926	5.014	5.998	0.016	0.017	0.003
Grassland	5.098	5.381	5.858	0.013	0.009	0.003
Fallowland	5.045	5.456	5.937	0.013	0.008	0.003
Bareland	5.414	5.723	5.406	0.010	0.005	0.009
Low density urban	6.068	6.160	5.991	0.003	0.002	0.001
High density urban	5.865	5.971	5.971	0.004	0.003	0.002

Key: Meanvnr—spectral mean; Stdvnr—standard deviation of spectral value; Mdiffvnr—mean difference of spectral values; HOMvnr—GLCM homogeneity; CONvnr—GLCM contrast; DISvnr—GLCM dissimilarity; ENTvnr—GLCM entropy; ASM—GLCM angular second moment

Table 4.6 Values of Spectral (a), Shape (b) and Textural (c) indicators for different land cover classes at segmentation level 4 in Nanjing

(a)

Variables	Meanvnr 1	Meanvnr 2	Meanvnr 3	Sidvnr 1	Sidvnr 2	Sidvnr 3	Mdiffvnr 1	Mdiffvnr 2	Mdiffvnr 3
River	69.109	53.090	27.533	1.642	1.621	2.101	0.077	-0.070	-2.366
Lake	56.249	35.244	28.908	2.563	3.082	4.816	-2.259	-3.767	-6.750
Woodland	52.560	33.345	43.522	2.915	3.292	5.421	-2.336	-2.590	0.081
Agri crop I	55.794	34.119	63.649	2.584	3.418	9.020	-2.214	-4.226	11.745
Agri crop II	60.123	38.907	52.716	3.072	3.600	8.218	-0.633	-1.558	4.504
wetland	56.846	34.727	54.705	3.326	3.292	7.554	-0.508	-2.889	10.584
Grassland	59.312	41.082	44.734	3.661	4.250	5.740	-0.812	-0.601	0.411
Fallowland	60.817	43.527	42.912	3.882	4.698	5.363	0.153	0.900	-1.169
Bareland	63.002	49.384	41.842	4.170	5.121	3.881	-0.847	0.828	-2.429
Low density urban	73.417	55.078	44.029	7.246	7.299	5.288	6.364	6.375	1.011
High density urban	61.804	43.214	36.703	5.906	6.160	5.608	-1.173	-0.983	-2.523

(b)

Variables	Area	Length width	Border length	Shape index	Density
River	267.211	1.382	76.105	1.227	1.971
Lake	146.333	1.337	56.867	1.225	1.884
Woodland	132.870	1.428	53.922	1.239	1.826
Agri crop I	88.613	1.288	42.452	1.177	1.801
Agri crop II	118.867	1.432	52.400	1.254	1.814
wetland	96.931	1.438	46.414	1.240	1.768
Grassland	127.910	1.375	53.323	1.235	1.842
Fallowland	118.848	1.328	51.000	1.240	1.815
Bareland	84.333	1.351	42.867	1.220	1.760
Low density urban	66.167	1.542	38.741	1.262	1.665
High density urban	106.538	1.483	49.346	1.240	1.787

Table 4.6 Values of Spectral (a), Shape (b) and Textural (c) indicators for different land cover classes at segmentation level 4 in Nanjing (Continued)

(c)

Variables	HOMvnr1	HOMvnr2	HOMvnr3	CONvnr1	CONvnr2	CONvnr3	DISvnr1	DISvnr2	DISvnr3
River	0.513	0.532	0.550	7.547	8.229	12.622	1.547	1.538	1.760
Lake	0.417	0.404	0.331	14.438	19.655	34.110	2.228	2.569	3.748
Woodland	0.367	0.354	0.216	16.954	20.093	32.619	2.537	2.766	4.161
Agri crop I	0.368	0.308	0.139	10.345	16.384	98.884	2.233	2.899	7.317
Agri crop II	0.332	0.301	0.144	14.908	18.476	66.535	2.645	2.987	6.219
wetland	0.357	0.364	0.181	19.277	16.047	63.726	2.729	2.603	5.641
Grassland	0.307	0.270	0.209	21.156	25.393	96.097	3.069	3.485	4.403
Fallowland	0.292	0.249	0.215	28.142	36.878	34.222	3.323	3.968	4.271
Bareland	0.274	0.235	0.289	29.540	40.799	21.323	3.629	4.356	3.238
Low density urban	0.141	0.136	0.171	111.657	111.147	47.440	7.571	7.679	5.241
High density urban	0.183	0.172	0.178	54.292	56.090	40.830	5.265	5.478	4.871

Variables	ENTvnr1	ENTvnr2	ENTvnr3	ASMvnr1	ASMvnr2	ASMvnr3
River	3.012	2.830	2.849	0.091	0.112	0.122
Lake	3.863	3.982	4.472	0.051	0.054	0.044
Woodland	4.170	4.276	5.236	0.028	0.027	0.008
Agri crop I	4.071	4.458	5.664	0.031	0.025	0.005
Agri crop II	4.396	4.634	5.846	0.022	0.018	0.003
wetland	4.217	4.190	5.413	0.030	0.033	0.006
Grassland	4.617	4.879	5.336	0.018	0.014	0.008
Fallowland	4.661	4.979	5.253	0.018	0.012	0.008
Bareland	4.732	5.038	4.633	0.015	0.011	0.016
Low density urban	5.338	5.360	5.151	0.007	0.007	0.009
High density urban	5.412	5.487	5.427	0.006	0.006	0.006

Key: Meanvnr—spectral mean; Stdvnr—standard deviation of spectral value; Midfvnr—mean difference of spectral values; HOMvnr—GLCM homogeneity; CONvnr—GLCM contrast; DISvnr—GLCM dissimilarity; ENTvnr—GLCM entropy; ASM—GLCM angular second moment.

Table 4.7 Values of Spectral (a) and Shape (b) indicators for different land cover classes at segmentation level 1 in Nanjing

Variables	Meanvnr 1	Meanvnr 2	Meanvnr 3	Stdvnr 1	Stdvnr 2	Stdvnr 3	Mdiffvnr 1	Mdiffvnr 2	Mdiffvnr 3
River	68.941	52.822	25.593	0.764	0.710	0.787	0.249	0.225	-1.402
Lake	55.719	33.778	24.312	0.651	0.648	1.138	-0.638	-1.256	-3.401
Woodland	51.032	31.480	42.094	0.847	0.909	1.561	-1.249	-1.478	-1.216
Agri crop I	54.936	31.884	71.827	0.686	0.599	1.724	-0.805	-1.583	4.706
Agri crop II	60.434	37.969	58.970	0.966	1.064	2.153	-0.231	-1.062	4.463
wetland	58.000	34.866	64.016	0.979	0.857	1.664	0.471	-0.224	5.960
Grassland	58.864	40.545	45.758	1.042	1.143	1.591	-0.595	-0.609	0.301
Fallowland	61.058	44.562	40.620	0.946	1.243	1.297	0.204	0.919	-1.496
Barcland	63.135	50.733	41.287	1.150	1.346	0.997	-0.029	0.826	-0.230
Low density urban	77.466	59.180	44.915	1.293	1.180	1.160	4.661	4.251	1.195
High density urban	59.842	41.249	32.942	1.225	1.335	1.298	-1.592	-1.746	-2.518

(b)

Variables	Area	Length width	Border length	Shape index	Density
River	47.895	1.585	31.158	1.222	1.589
Lake	25.167	1.626	20.733	1.202	1.335
Woodland	9.052	1.883	14.208	1.237	1.133
Agri crop I	7.839	1.856	11.935	1.143	1.131
Agri crop II	6.833	1.869	12.200	1.210	1.086
wetland	9.267	1.704	14.000	1.196	1.175
Grassland	7.677	1.741	12.842	1.206	1.120
Fallowland	8.304	1.836	13.783	1.250	1.135
Barcland	8.433	1.968	13.533	1.220	1.151
Low density urban	3.815	1.713	9.037	1.173	0.942
High density urban	5.385	1.918	11.269	1.240	1.018

Key: Meanvnr—spectral mean; Stdvnr—standard deviation of spectral value; Mdiffvnr—mean difference of spectral values

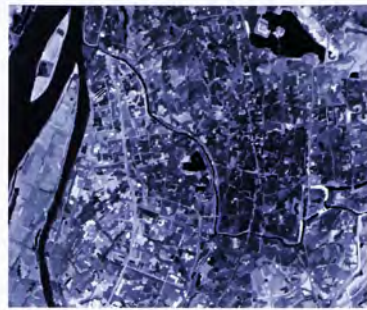
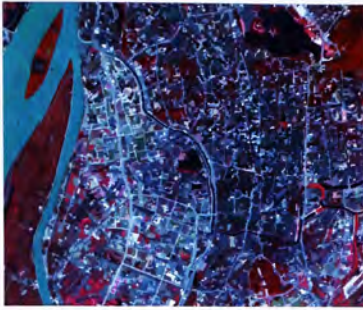


Figure 4.23 Image of Nanjing showing “river”, “lake” and “high density urban” and their values in terms of spectral mean VNIR 3

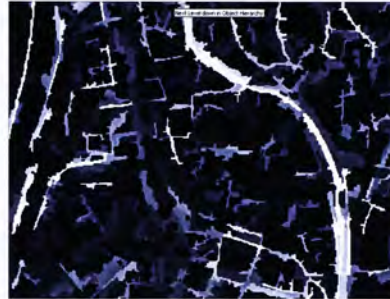


Figure 4.24 Image showing small river channels and lakes; and how they are divided from each other by length-width ratio

4.3.3.3 Level 4

“River” and “lake” are classified at the top object level. So, level 4 will be used to classify the remaining classes. Table 4.6 shows that all vegetation classes have ratio vegetation index (RVI, i.e. $VNIR\ 3/VNIR\ 2$) larger than 1 while other classes (“fallow land”, “bareland”, “high density urban” and “low density urban”) have RVI lower than 1. At this level, therefore, vegetation classes can be grouped together to form a parent class “vegetation” which is defined by RVI, based on which different types of vegetation can be further classified.

Further, from Table 4.6 it is found that 5 classes of vegetation can be divided into 3 super-categories at level 4. They are signified in the table. The first super-category is actually "agricultural crop I" which has particularly high values in terms of both spectral mean and CON of VNIR 3, which is printed in *Italic* form; The second super-category is composed of "agricultural crops II" and "wetland", which have medium VNIR spectral mean and CON values, which is emphasized with dots; The third is constituted by "woodland" and "grassland", which have the lowest values in VNIR 3 spectral mean and CON, which are shaded in grey. Visualization of these three categories in terms of CON VNIR magnitude is shown in Figure 4.25.

Level 4 is also the object level where "low density urban" can be separated from other non-vegetation class because of its significantly high CON values of both VNIR 1 and 2, which is shown in Figure 4.26.

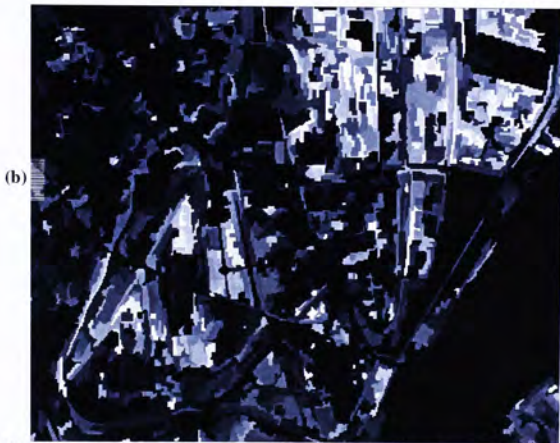


Figure 4.25 Three super-categories of vegetation and visualization of their varying magnitude in CON (VNIR 3)

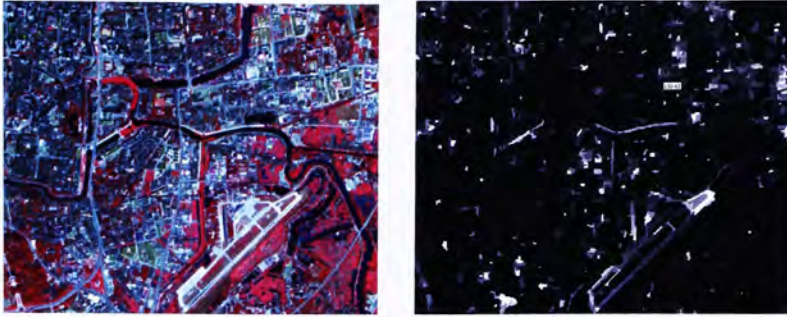


Figure 4.26 Image showing “low density urban” and “high density urban”. Notice the relative brightness of “low density urban” in the visualization of CON VNIR 1

4.3.3.4 Level 1

Level 1 will be used to further classify vegetation category 2 into “agricultural crop II” and “wetland”; vegetation category 3 into “woodland” and “grassland”; and the remaining non-vegetation into “fallow land”, “bareland” and “high density urban”.

At level 1, object size is too small and thus shape and texture features cannot be used. From Table 4.7, “wetland” is significantly higher in spectral mean VNIR 3 than “agricultural crop II”; “Woodland” has particularly high values in spectral mean of VNIR 2 compared to “grassland”. So it is used to discriminate between them. “High density urban” has the lowest values in spectral mean of all channels, followed by “fallow land” and “bareland” having the highest values. Therefore these three non-vegetation classes can be classified spectrally. Discrimination of all these classes against one another is shown in Figure 4.27.

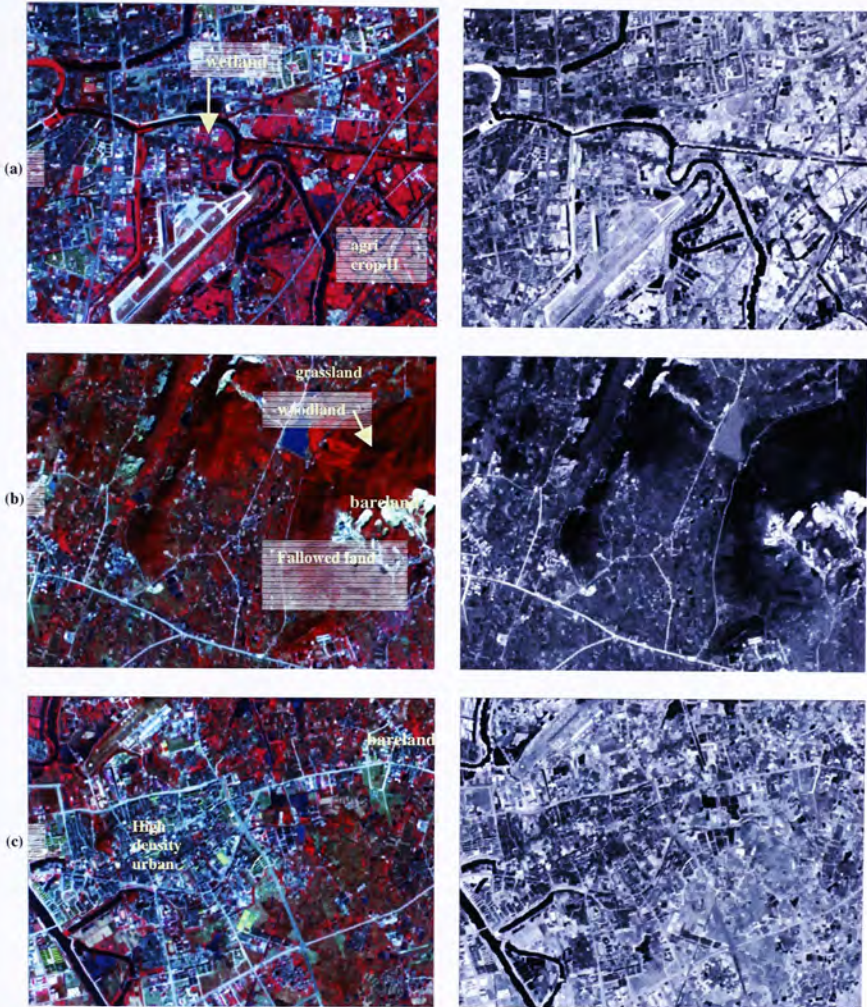


Figure 4.27 Discrimination of land covers using spectral mean at level 1: “wetland” vs. “agri crop II” with VNIR 3 (a); “woodland” vs “grassland” with VNIR 2 and “bareland” vs “fallowed land” with VNIR 1 (b); and “high density urban” vs “bareland” with VNIR 3 (c)

4.4 Discussion

After summary of image objects' features in line with segmentation separately in Chongqing and Nanjing, and their implications on spectral-shape ratio for segmentation, critical segmentation levels, and classifying features for each designated classes, the following section delves into the comparisons between the two study sites in terms of image objects' features.

In this chapter, comparisons between the two study sites, Chongqing and Nanjing, are based on the segmentation specifications presented previously, which include spectral-shape ratio, critical segmentation levels, and classifying rules derived. Explanations will be given on their differences.

Spectral-shape ratio for image segmentation is 9:1 in the case of Chongqing while it is 7:3 for Nanjing. High weight of shape on spectral-shape ratio will produce image objects of larger sizes and within-object spectral variances, which in turn induce more class mixing. On the other hand, too low weight of shape on spectral-shape ratio will generate objects of too complex/fragmented shape. In Nanjing, 10:0, 9:1 and 7:3 generates very similar object average size and object SD. But at 10:0 and 9:1 object shape is too fractal. So 7:3 is adopted instead.

Chongqing and Nanjing differ from each other in critical segmentation levels. The first, second and third object levels for segmentation in Chongqing are defined as scale parameter 1, 10 and 14 respectively; while they are defined as scale parameter 2, 8 and 12 in Nanjing. The difference reflects the two cities' disagreement in urban complexity, which is the result of distinct spatial arrangement of urban elements within a particular

city. Urban planning of Chongqing city center is more chaotic according to visual inspection of the satellite image, which explains the lower scale parameters being defined at the first and second object levels. Higher scale parameter is however defined for the largest object level, considering that many artificial lakes and industrial sites of small size but irregular shape are widespread in the image of Chongqing. Nanjing is characterized by many small patches of vegetation well mixing with concrete urban elements. Such mixing may be hidden by segmentation at the highest object level if scale parameter is set over 12, adversely degrading differentiation between green element and urban element at the highest classification level.

Transferability of classifying rules is to a certain extent possible between Chongqing and Nanjing. For example, water body is suitable to be classified at the highest object level in both sites. Both "river" and "lake" have low values in terms of Contrast and SD, even though in Chongqing CON and SD of VNIR 1 and 2 are used to classify them while CON and SD of VNIR 3 is used in Nanjing. "River" is then distinguished from "lake" by its higher HOM values of all channels and large area. At the medium object level in cases, vegetation and non-vegetation can be discriminated against each other using ratio of VNIR 3 and VNIR 2. Besides, "low density urban" is singled out in both sites because of its particularly high values of CON of VNIR 1 and 2. At the lowest object level, "grassland" and "woodland" are separated with each other utilizing higher spectral means for all VNIR channels for "grassland"; while "high density urban" is discriminated against non-urban classes with its obviously lower spectral means in all spectral channels.

Differences between Chongqing and Nanjing are mainly induced by the local variations between the two sites, and the different seasons in which data was acquired, including: First, industrial land use of regular shape is obvious in Chongqing while it is not so in Nanjing; Second, distinctive agricultural crops and wetland are found in Nanjing while they may mix with “woodland” and “grassland” in case of Chongqing; third, “fallowed land” in agricultural land use is discerning in the image of Nanjing because the acquisition of Nanjing data was in winter while it is not found in the image of Chongqing, which was obtained in summer when green coverage is at maximum.

CHAPTER 5. Results and Discussion II

Image Classification

5.1 Introduction

Having discussed about different patterns of variations in object features with a variety of segmentation specifications (mainly size and spectral-shape ratio) for expected land cover classes in the last chapter, classifying rules for each and every land cover class are conceptualized. These classifying concepts will be put into practice in building up the class hierarchy for object-oriented classification. In the class hierarchy, every class is defined by class description formulated chiefly by the object features. Further, relationships between classes can be explicitly defined (Definiens-Imaging, 2003). The design for classification is composed of three classification levels which link with three object levels. Top classification level will specialize in defining general “super-classes” such as “water”, “land” etc. manipulating the coarseness of high object level. Bottom level will further sub-divide these “super-classes” into destined land cover classes. This procedure of classification adopts the principle of decision-tree classification approach.

This chapter will present the classification in the two study sites, Chongqing and Nanjing. In each site, class hierarchy design will be detailed. Classification flows of three land covers will be studied as a case. After that, comparison of object-oriented classification with other conventional classification methods in terms of classification accuracy and proportion of land cover in the study site will follow. Comments on the transferability of classifying rules based on the classification experience will conclude this chapter.

5.2 Chongqing

5.2.1 Class hierarchy

Class hierarchy is used to organize the structure of the operational decision tree and describe the nature of each land cover category with object rules (Definiens-Imaging, 2003). Based on the classification system, the operational decision tree of Chongqing is formulated (shown in Figure 5.1).

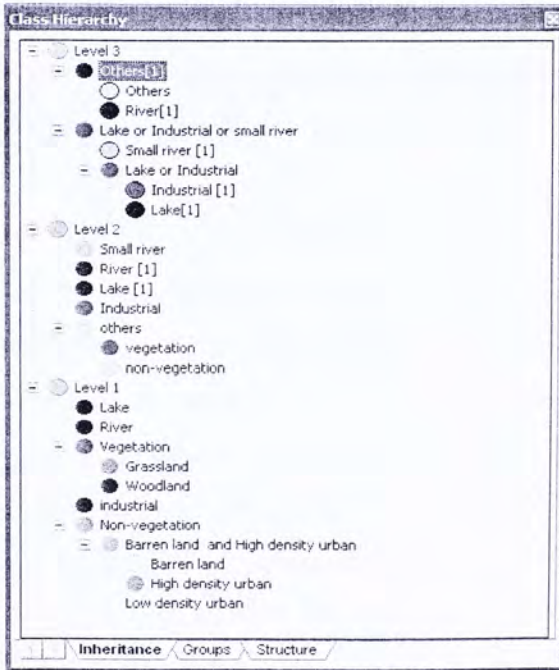


Figure 5.1 Class hierarchy for classification of Chongqing

Source: Definiens-Imaging, 2003

A conceptual decision tree is shown in Figure 5.2, in which a decision tree can be further compartmentalized into series of steps, or *splits*, from the most general land covers to the destined land covers. The *splits* are often dichotomous so that a general class is sub-divided into two classes at the next lower level, one of them being designated

category "X" while another category "Not X", which are complimentary to each other (Borak & Strahler, 1999).

Determination of whether an object belongs to one of the two categories is guided by a list of rules generalized from the findings in CHAPTER IV. Figure 5.2 illustrates the decision tree designed for classification of the Chongqing image. Three destined land cover classes (lake", "grassland and crops" and "low density urban") will be discussed in detail on their flows along the classifying decision tree and classifying rules. Classification flows of other land covers are listed in Appendix 3.

5.2.2 Description of the site

Chongqing is segmented by two big river channels, Jialing River running east-west and Changjiang running north-south. The main city is located at the intersection of these two rivers at the center of the image. "Low density urban" is mainly the new development zone to the north of main city and on the eastern bank of the Changjing to the south of main city. Industrial facilities of regular shape are distributed within the urban area and have low reflectance. Numerous small lakes of different shapes are distributed in the suburban area around the city. Main woodland zone is along Nan Shan north-south to the east of the city. Main vegetation types bounding the city are grassland and crops, with patchy woodland distributed on them. Appearance of "lake", "grassland" and "low density urban" on the image is shown in Figure 5.3.





 Intermediary class
 Destined class

Figure 5.2 Conceptual Decision Tree for Classification of Chongqing

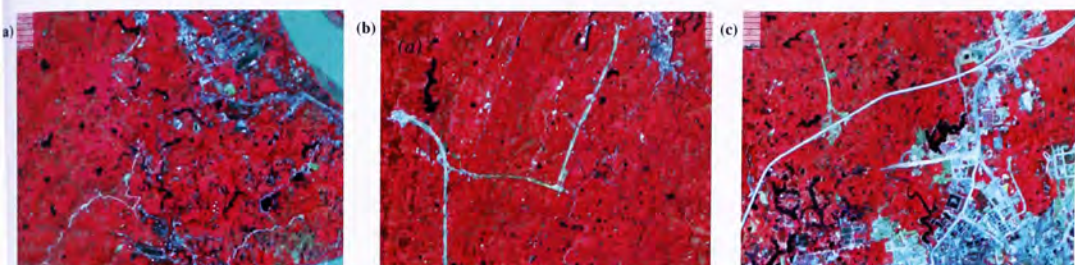


Figure 5.3 Appearance of “lake” (a), “grassland” (b) and “low density urban” (c) in Chongqing

5.2.3 Classification of “lake”

It is observed that “lake” in Chongqing is distinguishable by its low reflectance of VNIR 3, small size and high scores in GLCM Contrast VNIR 3. Specific to these characteristics, classification of “lake” is operated as follows: It is first classified as “lake, industrial, or small river” in classification level 3, which is coincident with object level 3 (that is Segmentation level 9, referring to CHAPTER III). “Lake, industrial, or small river” has the following classifying rules:

- *Mean difference to neighbor (VNIR 3): smaller than -18 (Spectral)*
- *Spectral mean (VNIR 3) x Spectral mean (VNIR 2): smaller than 4400 (Spectral)*
- *Spectral mean (VNIR 3) / Spectral mean (VNIR 2): smaller than 1.95 (Spectral)*
- *Area: smaller than 119,000 (pixels) (Shape)*

Because “lake” is spectrally very similar to “small river”, which also has low reflectance value of VNIR 3, the next step of classifying “lake” is to distinguish “lake and industrial” (which are both more compact in shape) from “small river” (which is elongated in shape) using Shape feature:

- *Density: smaller than 0.91 (Shape)*

Finally, "lake" and "industrial" have to be separated from each other even though they resemble each other in terms of both spectral and shape variables. Compared to "industrial", "lake" has higher reflectance in VNIR 3 along segmentation gradient, and a higher score of GLCM dissimilarity VNIR 3. Classifying rules are thus set as follows:

- *GLCM Dissimilarity (VNIR 3): greater than 10 (Textural)*
- *Spectral mean (VNIR 3) / Spectral mean (VNIR 2): greater than 1.0 (Spectral)*

5.2.4 Classification of "crops and grassland"

According to Chongqing (City proper) Urban Master Plan 1996-2001 (Chongqing Gueihua Sheji Yanjiouyuan, 1995), there are also "agricultural crops" and "wetland" distributed around Chongqing city proper. However, they are found mixing with "grassland" from the Chongqing image. It may be because the image is obtained in summer when different types of vegetation are thriving. Spectral reflectances of "grassland", "agricultural crops" and "wetland" are very similar. Therefore, these three classes are grouped together to form a class "crops and grassland".

"Crops and grassland" is easily dissected from non-vegetation using Ratio Vegetation Index (RVI, i.e. VNIR 3 / VNIR 2). However, dichotomous split of vegetation and non-vegetation cover at Classification level 3 imposes serious effect on overall classification accuracy. It is because there are many tiny patches of vegetation neighboring bare soil. Many of them are grouped as the same objects at high object level, which induces excessive class mixing between vegetation and non-vegetation. Therefore, the dichotomous split between "vegetation" and "non-vegetation" starts at classification level 2, that is Segmentation level 5 as follows:

- *Spectral mean (VNIR 3) / Spectral mean (VNIR 2): greater than 1.25 (Spectral)*

Further segmenting “vegetation” into “woodland” and “crops and grassland” is done at Classification level 1, considering that “woodland” is very patchy and fragmented from the image of Chongqing. Classification of them thus has to be accomplished at pixel level (that is Scale parameter 1). Classifying rules of “crops and grassland” are as follows:

- *Not “woodland”, which is classified by:*
 - *Spectral mean (VNIR 1): smaller than 86.1 (Spectral)*
 - *Spectral mean (VNIR 2): smaller than 50.1 (Spectral)*
 - *Spectral mean (VNIR 3): smaller than 112 (Spectral)*

5.2.5 Classification of “low density urban”

Classifying “low density urban” requires first separation of land objects from water objects and industrial sites at Classification level 1. These two super-classes are separable in both spectral and shape terms. Classifying rules of *land* are as follows:

- *Not “lake, industrial or small river”, which is classified by:*
 - *Mean difference to neighbor (VNIR 3): smaller than -18 (Spectral)*
 - *Spectral mean (VNIR 3) x Spectral mean (VNIR 2): smaller than 4400 (Spectral)*
 - *Spectral mean (VNIR 3)/Spectral mean (VNIR 2): smaller than 1.95 (Spectral)*
- *Then, Not “river”, which is classified by:*
 - *Standard deviation (VNIR 1): smaller than 4.51 (Spectral)*

- *Standard deviation (VNIR 2): smaller than 4.51 (Spectral)*
- *Standard deviation (VNIR 3): smaller than 4.51 (Spectral)*
- *Spectral mean (VNIR 3): Spectral mean (VNIR 2): smaller than -19.9 (Spectral)*

Second, “low density urban” is grouped in the class “non-vegetation” with other non-vegetated land covers at Classification level 2 using RVI. Applying such a vegetation index is particularly effective because “low density urban” is comprised of highways, new buildings and construction sites which are all notably non-vegetated cover. Classifying rules of “non-vegetation” is as follows:

- *Not “vegetation”, which is classified by:*
 - *Spectral mean (VNIR 3)/Spectral mean (VNIR 2): greater than 1.2 (Spectral)*

Lastly, a way is sought to separate “low density urban” from “bare land” and “high density urban”. It is accomplished finally by using specifically high GLCM contrast values in both VNIR 1 and 2 at Classification level 1 (that is pixel-level). Values of GLCM contrast are actually very unstable at this object level and thus CON should be used at medium classification level. Nonetheless, after trial-and-error it is found that CON of VNIR 1 and 2 are most effective in identifying “low density urban” at pixel level. Therefore, classifying rules of “low density urban” are as follows:

- *GLCM contrast (VNIR 1): greater than 80 (Textural)*
- *GLCM contrast (VNIR 2): greater than 90 (Textural)*

6.3.3 Classification Result

Classified image of Chongqing using object-oriented classification approach is shown in Figure 5.4, which is compared with classified image using conventional classification algorithm. (MLC—maximum likelihood classification; SFC—supervised fuzzy classification; LSU—linear spectral unmixing) LSU fails to classify all our designated land covers so the classification scheme is modified in case of LSU: “river” and “lake” are aggregated into more general class “water” while “industrial” is discarded. Their classification overall accuracies and kappa coefficients are presented in Table 5.1.

Table 5.1 Comparison of classification accuracy between different classification algorithms. Case in Chongqing

Classification Algorithms	Overall Accuracy (%)	KAPPA
Object-oriented approach	64.16	.514
Maximum Likelihood Classification	62.66	.478
Supervised Fuzzy Classification	52.88	.409
Linear Spectral Unmixing	42.00	.228

Object-oriented classification approach attains the highest overall accuracy, followed in descending order by MLC, SFC and LSU. However, the differences between object-oriented approach and other algorithms are not sufficiently large to assert its superiority. It is especially NOT so when object-oriented classification is compared with MLC, where the difference is less than two percent in overall accuracy.



Figure 5.4 Classified images of Chongqing using different approaches: Object-oriented classification (a), maximum-likelihood classification (b), supervised fuzzy classification (c) and linear spectral unmixing (d)

5.2.7 Error matrix

From the error matrix and class-based accuracy statistics produced by Object-oriented approach and MLC (Tables 5.2 and 5.3), class mixture between “crops and grassland” and “woodland”, “bare land” and urban land covers are serious: In MLC, 45 out of 102 sample points which are “woodland” are classified as “crops and grassland”; 35 out of 49 “bare land” sample points are classified as “crops and grassland”; of 35 “high density urban” sample points 21 are classified as “crops and grassland”; 13 “low density urban” sample points are mixed with “crops and grassland”. In object-oriented classification, the mixture problem between “crops and grassland” with other land covers does not seem to be significantly improved: Of 87 “woodland” sample points, 37 are classified as “crops and grassland”; while 49 of 78 points of “bare land” are classified as “crops and grassland”.

5.2.8 Class Proportion

Areal proportion of each land cover is presented in Table 5.4. “Crops and grassland” occupies the most area of Chongqing (over 50%), followed by “woodland” (18.67%) and “high density urban area” (7.09%). “Lake” and “industrial” take the least proportions of total area: 1.75% and 0.62% respectively. Urban landscape (including “bareland”, “industrial”, “low density urban” and “high density urban”) occupies about 20% of the whole landscape, which is about 121 km², which is much lower than the amount documented in China City Statistical Yearbook (2003). It is because the image of Chongqing classified delineates mainly the city proper, excluding many districts, prefecture-level cities and prefectures which are administered by Chongqing municipality.

Table 5.2 Error matrix (upper) and accuracy statistics (lower) for MLC. Case in Chongqing

Classified Data	Lake	River	Crops & grassland	Woodland	Bare land	Industrial	High den. urban	Low den. urban	Total
Lake	2	0	0	0	0	0	1	0	3
River	0	26	0	0	0	0	0	0	26
Crops and grassland	5	0	133	45	35	0	21	13	252
Woodland	0	0	8	56	3	0	1	0	68
Bare land	0	1	0	0	6	0	0	0	7
Industrial	0	1	0	0	0	0	0	0	1
High density urban	0	0	0	1	0	1	5	0	7
Low density urban	0	0	1	0	5	0	7	22	35
Totals	7	28	142	102	49	1	35	35	399

Class Name	Producer's Accuracy (%)	User's Accuracy (%)
Lake	28.6	66.7
River	92.9	100.0
Crops & grassland	93.7	52.8
Woodland	54.9	82.4
Bare land	12.2	85.7
Industrial	0.0	0.0
High density urban	14.3	71.4
Low density urban	62.9	62.9

- Overall Accuracy: 62.66%
- Kappa: 0.478

Table 5.3 Error matrix (upper) and accuracy statistics (lower) for Object oriented classification. Chongqing as a case

Classified Data	Lake	River	Crops & grassland	Woodland	Bare land	Industrial	High den. urban	Low den. urban	Total
Lake	3	0	3	0	0	0	0	0	6
River	0	25	0	0	0	0	0	0	25
Crops and grassland	1	0	115	37	49	0	7	5	214
Woodland	2	0	13	50	6	0	2	0	73
Bare land	0	0	0	0	16	0	8	11	35
Industrial	2	0	0	0	0	1	0	1	4
High density urban	0	3	0	0	3	0	14	3	23
Low density urban	0	0	0	0	4	0	2	13	19
Totals	8	28	131	87	78	1	33	33	399

Class Name	Producer's Accuracy (%)	User's Accuracy (%)
Lake	28.6	33.3
River	89.3	100.0
Crops & grassland	90.1	59.8
Woodland	56.9	79.5
Bare land	26.5	37.1
Industrial	100.0	25.0
High density urban	40.0	60.9
Low density urban	42.9	78.9

- Overall Accuracy: 64.16%
- Kappa: 0.514

Table 5.4 Class proportion (by Object-oriented approach). Case in Chongqing.

Class Name	Area (in km ²)	Class proportion
Lake	10.64	1.75%
River	36.36	5.97%
Grassland	325.90	53.52%
Woodland	113.61	18.67%
Bare land	41.12	6.76%
Industrial	3.77	.62%
High density urban	43.16	7.09%
Low density urban	34.07	5.60%
Total	608.63	

5.2.9 Post-classification Aggregation

Although object-oriented classification produces the best classification result among the classification methods selected and tested, 64% accuracy is insufficient to validate us further analyzing the classified image with landscape metrics. Post-classification aggregation is thus required. "Lake" and "river" will be aggregated into "water"; "woodland" and "crops and grassland" are grouped into "green space"; "bare land", "industrial" and two urban land covers are mixed up into the class "land". Resultant image after aggregation is shown in Figure 5.5 whereas accuracy statistics are shown in Table 5.5. Overall classification accuracy increases to 86% after aggregation.

Table 5.5 Accuracy Statistics for Object-oriented Classification after Aggregation. Case in Chongqing

Class Name	Producer's Accuracy	User's Accuracy	Kappa Statistic
Water	77.14 %	87.10 %	.859 %
Urban Green Space	97.17 %	84.81 %	.601 %
Land	64.96%	89.41 %	.850 %

Overall Accuracy: 86%

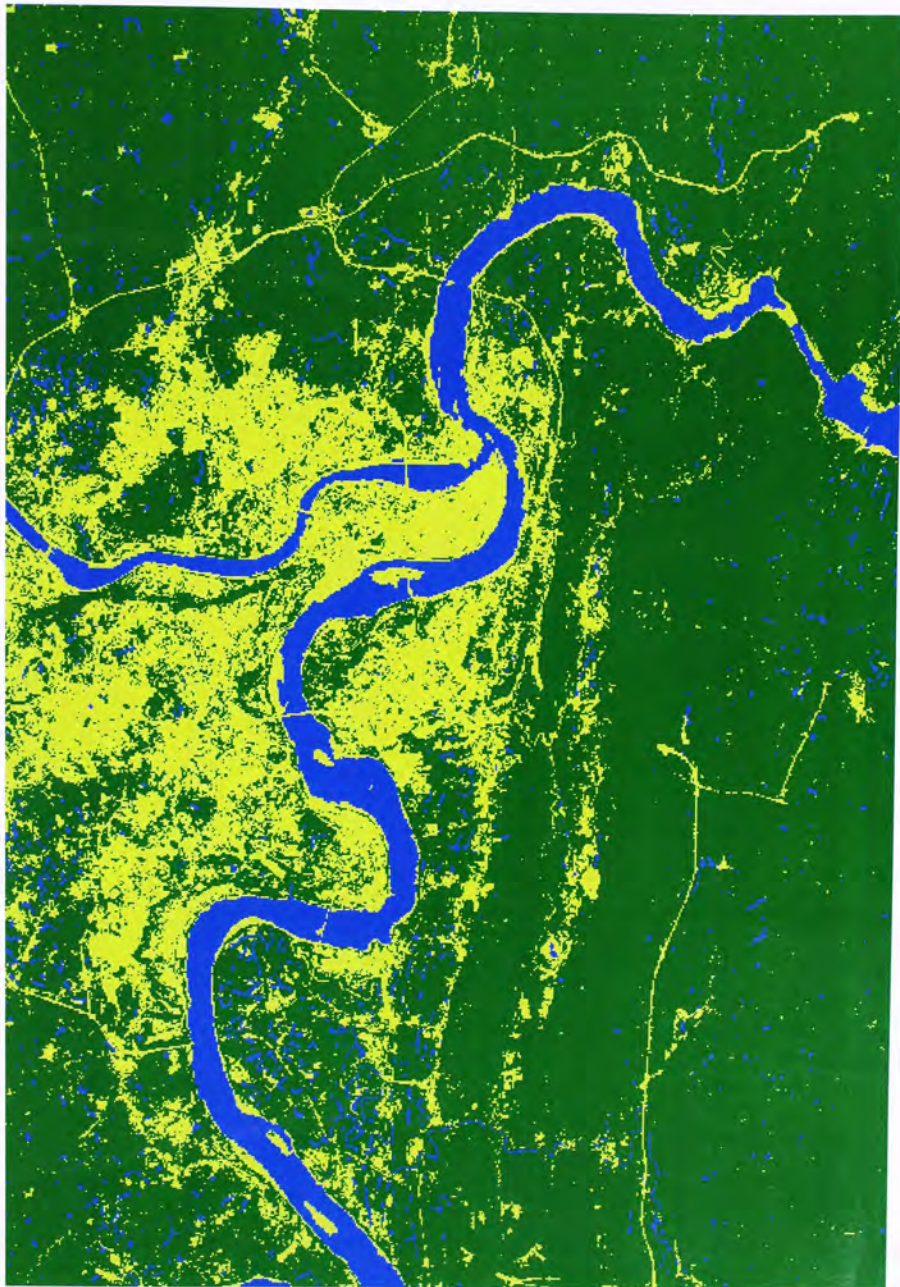


Figure 5.5 Classified Image of Chongqing after class aggregation

5.3 Nanjing

5.3.1 Class Hierarchy

Figure 5.6 shows the operational decision tree of Nanjing while Figure 5.7 is the conceptual decision tree for object-oriented classification of the city.

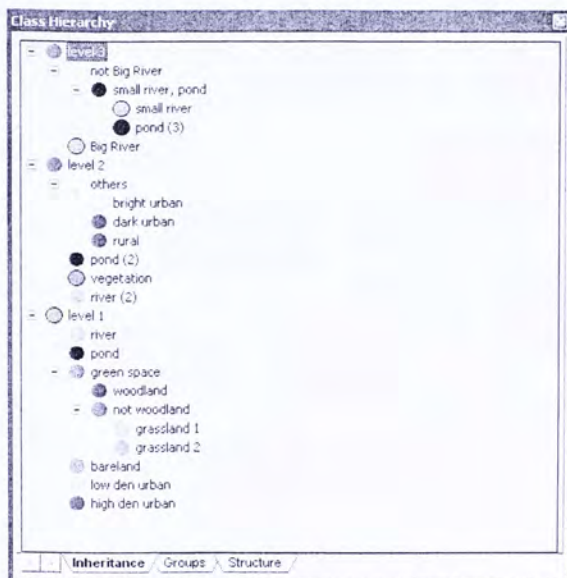
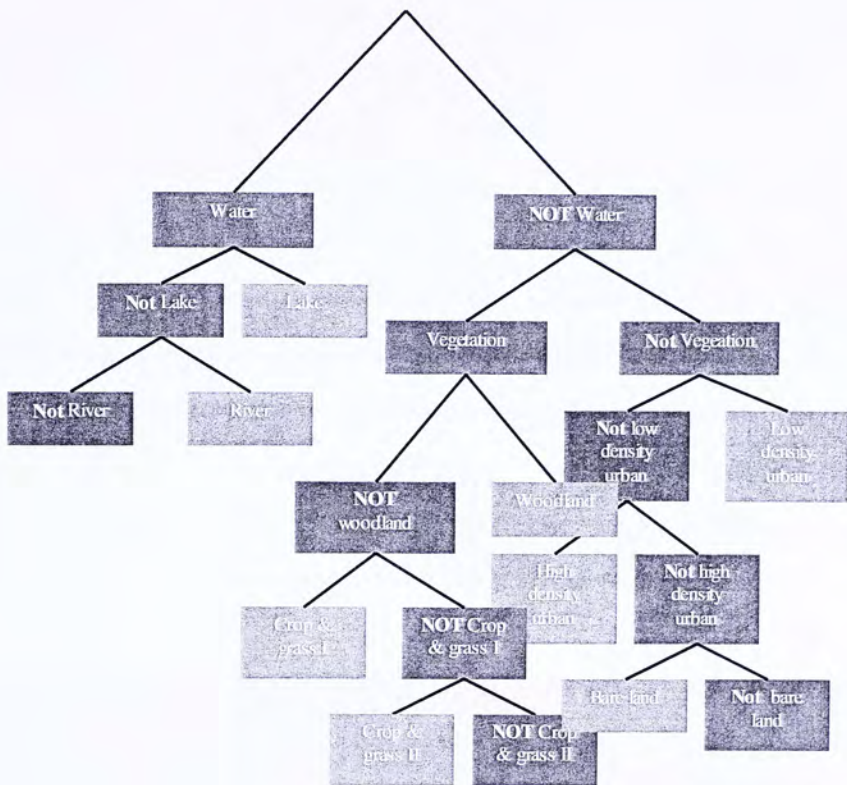


Figure 5.6 Class hierarchy for Classification of Nanjing

Source: Definiens-Imaging, 2003

Like the case of Chongqing in previous section, only three destined land cover classes will be detailed on their flows along the classifying decision tree and classifying rules, which are: "lake", "grassland and crops II" and "low density urban". Classification of other land cover categories are detailed in Appendix 3.



- Intermediary classes
- Destined classes

Figure 5.7 Conceptual decision tree for classification of Nanjing

5.3.2 Description of the site

Referring back to CHAPTER III, classification system of Nanjing is different from that of Chongqing because of the local uniqueness of Nanjing city is. Sizes of lakes in Nanjing are much larger than those in Chongqing. Besides, industrial facilities cannot be differentiated from “high density urban” from the image as in the case of Chongqing. Main city is located on the eastern bank of Changjiang, with “low density urban” abutting by the south. “Low density urban” can also be found on the new development zone to the southeast of the main urban zone. Most of all, unlike Chongqing, agricultural land uses are clearly observed on the suburb, which include different types of agricultural crops and wetland easily distinguished from grassland spectrally; and “fallowed land” distributed patchily on farmlands which may be left uncultivated in winter time. Figure 5.8 shows the appearance of agricultural crops, lakes, and low density urban on the image.

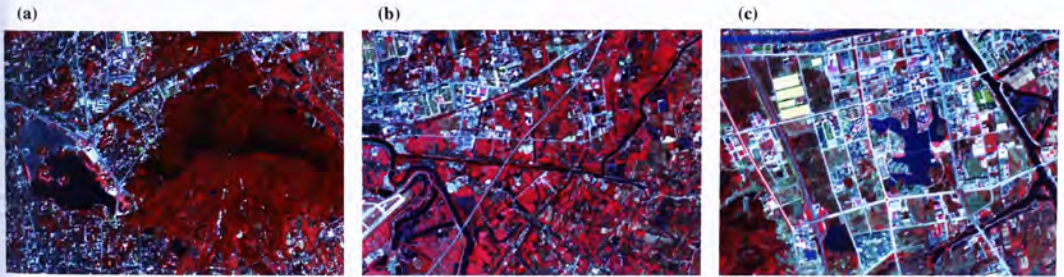


Figure 5.8 Appearance of “lake” (a), “agricultural crop II” (b) and “low density urban” (c) in Nanjing

5.3.3 Classification of lake

Unlike in case of Chongqing, classification of “lake” in case of Nanjing cannot be accomplished solely at the highest classification level. It is because “lake” is very much like some of “high density urban” objects in spectral characteristics: both of very low spectral reflectance. Mixing happens especially between high building shadows and

“lake”. Solution is finally found through trial-and-error: delineating city regions manually in PCI in Bitmap format, which is transformed into an image channel named *urban boundary*. Rule that “lake” is out of urban zone is then set to discriminate “lake” against building shadow at classification level 2. Also, “lake” and “small river” have similarly low spectral values in all VNIR channels so that Shape features are resorted to differentiate between them. Therefore, classifying rules of “lake” are as follows:

At Classification Level 3:

- *Not “Big River”, which is:*
 - *Spectral Mean (VNIR 1): smaller than 78 (Spectral)*
 - *Spectral Mean (VNIR 3): smaller than 37 (Spectral)*
 - *Standard Deviation (VNIR 3): smaller than 8 (Spectral)*
 - *Spectral Mean (VNIR 3) - Spectral Mean (VNIR 2): smaller than -17 (Spectral)*

- *Classified as “Small river and lake”, which is:*
 - *Urban boundary: 0*
 - *Spectral Mean (VNIR 3): smaller than 28 (Spectral)*
 - *Spectral Mean (VNIR 3) / Spectral Mean (VNIR 2): smaller than 1.01 (Spectral)*

- *Not “Small river”, which is:*
 - *Density: smaller than 1.81 (Shape)*

At Classification Level 2:

- *Existence of “Lake” super-object:1 (Relation to Super-object)*

OR:

- *Spectral Mean (VNIR 3): smaller than 32 (Spectral)*
- *Urban boundary: 0*
- *Spectral mean (vnir 3) / Spectral mean (vnir 2): smaller than 1.01(Spectral)*

5.3.4 Classification of “crops and grassland II”

Mixing between crops, wetland vegetation and ordinary grassland is complicated. Separating them in object-oriented classification would seriously lower the overall classification accuracy. Eventually, different types of vegetation are re-grouped into two main vegetation categories: “crops and grassland I” which have very high spectral values especially in VNIR 3, composed of mainly “agricultural crop I” and “wetland”; and “crops and grassland II” with comparatively lower VNIR 3 spectral values while higher VNIR 1 values, which is composed of “agricultural crop II” and “grassland”. Classification of “crops and grassland II” starts with discrimination of “land” against “water bodies” by the following classifying rules:

- *Not “Big River”, which is:*
 - *Spectral mean (VNIR 1): smaller than 78 (Spectral)*
 - *Spectral mean (VNIR 3): smaller than 37 (Spectral)*
 - *Standard deviation (VNIR 3): smaller than 8 (Spectral)*
 - *Spectral mean (VNIR 3)-Spectral mean (VNIR 2): smaller than -17 (Spectral)*
- *Not “small river, lake”, which is:*
 - *Urban boundary: 0*
 - *Spectral mean (VNIR 3): smaller than 28 (Spectral)*

- *Spectral mean (VNIR 3)/Spectral mean (VNIR 2): smaller than 1.01 (Spectral)*

At Classification level 2, it is classified as “vegetation” using the following rules:

- *Spectral mean (VNIR 3) / Spectral mean (VNIR 2): greater than .98 (Spectral)*

At Classification level 1:

- *Not “woodland”, which is:*
 - *Spectral mean (VNIR 1): smaller than 53 (Spectral)*
 - *Spectral mean (VNIR 2): smaller than 36 (Spectral)*
 - *Spectral mean (VNIR 3): smaller than 51 (Spectral)*

- *Then, Not “crops and grassland I”, which is:*
 - *NDVI: greater than 0.3 (Spectral)*
 - *Spectral mean (VNIR 1): smaller than 61 (Spectral)*

5.3.5 Classification of “low density urban”

The image of Nanjing reveals lower brightness contrast between “low density urban” and “high density urban”. Much of the “high density urban” objects are found mixed with “low density urban” objects even at the lowest object level. Therefore, the *urban boundary* channel has to be used again to delineate urban boundary. Classification of “high density urban” is implemented at Classification level 2 in the following:

- *Not “Big River”, which is:*
 - *Spectral mean (VNIR 1): smaller than 78 (Spectral)*
 - *Spectral mean (VNIR 3): smaller than 37 (Spectral)*

- *Standard deviation (VNIR 3): smaller than 8 (Spectral)*
- *Spectral mean (VNIR 3)-Spectral mean (VNIR 2): smaller than -17 (Spectral)*

- *Not “small river, lake”, which is:*
 - *Urban boundary: 0*
 - *Spectral mean (VNIR 3): smaller than 28 (Spectral)*
 - *Spectral mean (VNIR 3)/Spectral mean (VNIR 2): smaller than 1.01 (Spectral)*

At Classification level 2, it is classified as:

- *Not “vegetation”, which is:*
 - *Spectral mean (VNIR 3)/Spectral mean (VNIR 2): greater than .98 (Spectral)*

Then, further classified as the destined class “low density urban” by:

- *GLCM Dissimilarity (VNIR 1): greater than 4 (Textural)*
- *Spectral mean (VNIR 1): greater than 66 (Spectral)*
- *Spectral mean (VNIR 2): greater than 50 (Spectral)*
- *Spectral mean (VNIR 3): greater than 35 (Spectral)*

5.3.6 Classification Result

Classified image of Nanjing using object-oriented classification approach is shown in Figure 5.9, which is compared with classified image using conventional classification

algorithm (MLC, SFC and LSU). Their classification accuracies and kappa coefficients are presented in Table 5.6. Compared to Chongqing, classification result of Nanjing is poorer across all classification methods selected. Linear spectral unmixing produces the lowest classification accuracy, which is barely above 20%, followed by supervised fuzzy classification whose overall accuracy is about 35%. MLC, however, rank the top in accuracy rate (straightly 50%) over object-oriented classification. In spite of it, these two methods do not have significant difference in terms of overall accuracy.

Table 5.6 Comparison of classification accuracy between different classification algorithms. Case in Nanjing

Classification Algorithms	Overall Accuracy (%)	KAPPA
Object-oriented approach	47.40	.327
Maximum Likelihood Classification	50.00	.340
Supervised Fuzzy Classification	34.80	.239
Linear Spectral Unmixing	20.00	.144

5.3.7 Error Matrix

Comparison between object-oriented classification and maximum-likelihood classification in terms of both error matrix and class-based accuracy (in Table 5.7 and 5.8) lead us to very similar conclusion to that for Chongqing: Inter-class mixing is easily observed. In MLC, of 79 points which are “woodland”, 29 are classified as “crops and grassland II” while 11 are classified as “bareland”, which results in low producer’s accuracy for “woodland” (36.7%). For the non-vegetation classes, 23 out of 70 sample points of “bareland” are classified as “crops and grassland II”. Only 10 of 43 “low density urban” sample points are correctly classified, with the remainder mostly mixed

with “crops and grassland II”, “bareland” and “high density urban”, which account for a very low producer’s accuracy for “low density urban” (23.3%).

For Object-oriented classification, nearly half of the “woodland” sample points are classified as “crops and grassland II”, which explains the low accuracy rate for the class (34%). 32 out of 70 points of “bareland” are classified as “crops and grassland II” while another 14 points mix with “low density urban”, which explains the very low rate of class accuracy (27%). Accuracy of “high density urban” is dragged down to about 28% because 12 out of 35 points are classified as “low density urban” while 9 of them mix with “crops and grassland II”.

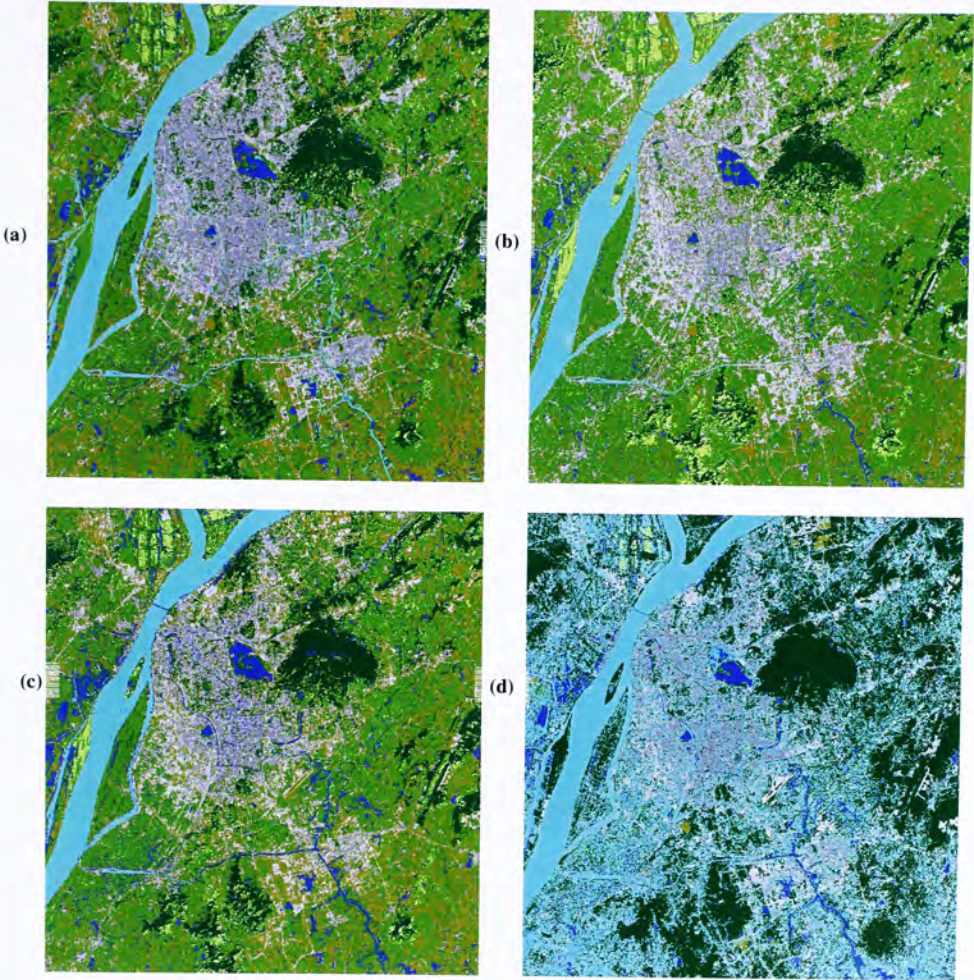


Figure 5.9 Classified images of Nanjing using different approaches: Object-oriented classification (a), maximum-likelihood classification (b), supervised fuzzy classification (c) and linear spectral unmixing (d)

Table 5.7 Error matrix (upper) and accuracy statistics (lower) for Object-oriented classification. Case in Nanjing

Classified Data	Lake	River	Woodland	Crops & grass I	Crops & grass II	Bare land	Low den. urban	High den. urban	Total
Lake	3	0	1	1	4	3	3	1	41
River	2	35	0	0	3	0	1	0	16
Woodland	1	0	29	1	21	3	1	1	57
Crops & grassland I	0	0	1	3	2	1	0	0	7
Crops & grassland II	4	3	29	7	107	23	12	6	191
Bare land	8	2	11	1	39	32	7	3	103
Low density urban	1	1	4	1	15	6	10	6	44
High density urban	0	2	4	1	5	2	9	18	41
Totals	19	43	79	15	196	70	43	35	500

Class Name	Producer's Accuracy (%)		User's Accuracy (%)	
Lake	15.79		18.75	
River	81.40		85.37	
Woodland	36.71		50.88	
Crops & grass I	20.00		42.86	
Crops & grass II	54.59		56.02	
Bare land	45.71		31.07	
Low density urban	23.26		22.73	
High density urban	51.43		43.90	

- Overall Accuracy: 50%
- Kappa: 0.34

Table 5.8 Error matrix (upper) and accuracy statistics (lower) for Maximum-likelihood Classification. Case in Nanjing

Classified Data	Lake	River	Woodland	Crops & grass I	Crops & grass II	Bare land	Low den. urban	High den. urban	Total
Lake	1	0	1	0	2	2	0	1	7
River	2	35	0	0	1	0	0	0	38
Woodland	0	0	27	1	6	2	0	0	36
Crops & grassland I	1	0	5	6	5	1	0	0	18
Crops & grassland II	7	3	36	4	135	32	16	9	242
Bare land	4	1	3	1	21	19	5	3	57
Low density urban	4	3	5	1	24	14	17	12	80
High density urban	0	1	2	2	2	0	5	10	22
Totals	19	43	79	15	196	70	43	35	500

Class Name	Producer's Accuracy (%)		User's Accuracy (%)	
Lake		5.26		14.29
River		81.40		92.11
Woodland		34.18		75.00
Crops & grass I		40.00		33.33
Crops & grass II		68.88		55.79
Bare land		27.14		33.33
Low density urban		39.54		21.25
High density urban		28.57		45.46

- Overall Accuracy: 47.4%
- Kappa: 0.327

5.3.8 Class Proportion

Areal proportion occupied by each destined land cover class in Nanjing is shown in Table 5.9. "Lake", as in case of Chongqing, occupies the least area (3.65%), which together with "river" making about 11% of area in Nanjing from image occupied by water body. Among vegetation covers, "crops and grassland II" takes the largest areal share (37.11%), followed by "woodland" which takes 11% of the area. "Bare land" occupies over 18% while the two urban classes each take 9%. In sum, non-vegetation land takes 36% of the total area of study site. Built-up area, including "low density urban", "high density urban" and "bareland" is about 342 km². Compared to the built-up area of 439 km² documented in China City Statistical Yearbook (2003), the figure calculated in this research is much smaller because large area of green space which is within Nanjing city has not been counted.

Table 5.9 Class proportion (by Object-oriented approach). Case in Nanjing

Class Name	Area (km ²)	Class proportion
Lake	32.89	3.65%
River	72.34	8.02%
Woodland	102.06	11.32%
Crops & grassland I	17.18	1.91%
Crops & grassland II	334.67	37.11%
Bareland	171.19	18.98%
Low density urban	89.88	9.97%
High density urban	81.52	9.04%
Total	901.73	

5.3.9 Post-classification Aggregation

Like the case of Chongqing, "lake" and "river" will be aggregated into "water"; "woodland" and "crops and grassland" are grouped into "green space"; "bare land", "industrial" and two urban land covers are mixed up into the class "land". Resultant

image after aggregation is shown in Figure 5.8 whereas accuracy statistics are shown in Table 5.10. Overall classification accuracy increases to 66.8% after aggregation. Aggregated classified image will then be the basis for landscape analyses in the next step.

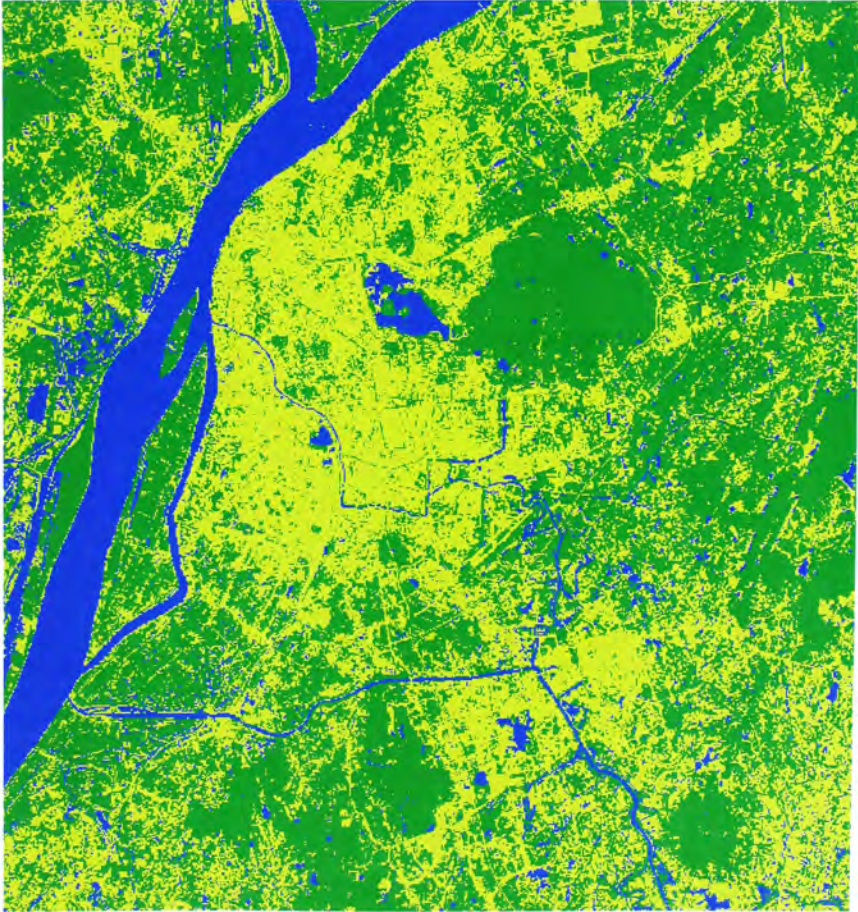


Figure 5.10 Classified Image of Nanjing after class aggregation

Table 5.10 Accuracy Statistics for Object-oriented Classification after Aggregation. Case in Nanjing

Class Name	Producer's Accuracy	User's Accuracy	Kappa Statistic
Water	64.52%	70.18 %	.660 %
Urban Green Space	68.97 %	78.74 %	.494 %
Land	63.51%	49.74 %	.286 %

Overall Accuracy: 66.8%

5.4 Discussion

Based on the two case studies in Chongqing and Nanjing, this section will discuss the pros and cons of object-oriented classification and transferability of classifying rules between different sites.

5.4.1 Problems of object-oriented classification

The result of case studies show object oriented classification cannot produce classification accuracy significantly higher than that produced by conventional classifiers, especially maximum likelihood classification. In the case of Nanjing, using object-oriented approach actually lowers the overall accuracy percentage. Some intrinsic weaknesses which may critically affect the classification quality are highlighted.

The fundamental assumption is that if an image object belongs to a particular land cover class, it will carry an object signature comprised by a set of spectral, textural, and shape variables. Image objects of the same class should have similar object variables which should also be significantly different those of another class. Under this assumption, each land cover class can be defined by identifying corresponding value ranges in the

multi-dimensional feature space. In the real case, however, features of different land covers are quite ambiguous, deeming them ineffective in distinguishing each land cover class. Within-class variations in many object variables of some land cover are too large, while between-class variations too narrow, to serve as good class signatures.

The design of class hierarchy is such that classification levels links to object/segmentation levels. That is to say classification of parent classes/super classes is implemented at the highest object level with the largest-sized objects, while destined classes are classified at the lowest object level based on the parent classes at the top class hierarchy. Inter-linkage between parent classes and destined classes on the one hand, and between class hierarchy and object level hierarchy on the other, implies that the classification accuracy of the destined classes strongly depends on the classification accuracy of the parent classes at the highest object levels. As object level increases, within-object heterogeneity is then increased and thus the problem of class mixing within the larger objects will aggravate accordingly. Classification of parent classes may be adversely affected if within-object heterogeneity is too high, which in turn imposes impact on the classification accuracies of destined classes at the lower classification levels. This problem aggravates when it is unknown at which object level can the classification quality of parent classes be best preserved

5.4.2 Strengths of object-oriented classification

Despite the defects discussed above, object-oriented classification significantly multiplies the variety and amount of information for classification. Objects are generated from pixels through segmentation from which a diversity of information about the objects can be extracted. In this research, spectral, shape and textural features are studied to derive useful classifying rules for the formulation of object-based decision tree.

In this chapter, shape and textural features are proved applicable to classify some of the classes if pixels are grouped into suitable scales. For example, two shape features (Area and Density) are critical in the discrimination of "lake" against "river" at the top object level in the images of both sites. Standard Deviation of spectral values within object is used to define "river" at the same level in both sites as well. GLCM texture features (CON and DISS) are used at the lowest object level in both sites to discriminate "low density urban" against other non-vegetation covers. Besides shape and texture features, object-oriented classification also allows information about relationship between objects of different object levels to be utilized for classification. For instance, the concept 'Existence of "lake" Super-objects' is used to classify "lake" at medium classification level in the case of Nanjing. All these information cannot be used for other pixel-based classification algorithms.

In short, object-oriented classification concept greatly increases the complexity of classification task and the time it needs, especially in searching for the most suitable segmentation levels at which class mixing of pixels within objects can be kept at minimum and object features for each destined class which best differentiates it from

other classes, the concept allows a lot more information about local regions of satellite image to be extracted from the image, which are proved effective in classifying some of the land covers in the two case studies of this research.

5.4.3 Transferability of classifying rules

Comparing two cases, we find that most classifying rules are transferable from one place to another. Most of the common land covers can be defined by the object variables which can be used in both Chongqing and Nanjing, even though activation values of the classifying rules need to be adjusted with site-specific situation. For example, small river channel and “lake” can be separated by shape variables *Density* at the top object level; big “river” can be defined by spectral variable *Standard Deviation* of spectral channel (especially of VNIR 3) for its relatively high spectral homogeneity within an average image object; urban, especially “low density urban” is distinguished from other land covers by its distinctively high *GLCM CONDISS* concerning VNIR 1 and 2; “woodland” is separable from “crops and grassland” for its lower spectral values in all VNIR channels. However, whether classifying variables of these classes can be reused again in other places is perhaps topics for further research.

CHAPTER 6. Results and Discussion III

Landscape Structure of “Urban Green Space”, Chongqing and Nanjing

6.1 Introduction

CHAPTER VI provides the classification maps of Chongqing and Nanjing. Both cities are classified into three classes: “water”, “urban green space” and “land”. In this chapter, “urban green space” will be focused. Class-based metrics will be used to anatomize landscape structure of green space in the city area and their variation tendency as a function of distance from old city centers. The objective of this chapter is twofold: First, studying the configuration of “urban green space” in both cities from city center to periphery with the aid of class-based metrics. We will focus on mainly four aspects of green space condition: landscape composition, fragmentation pattern, contagion and patch shape complexity. Other class-based metrics are listed in Appendix 6 and 7. Second, comparing entire “urban green space” in the two cities and explaining their similarities/disparities in line with their patterns of urban development.

6.2 Chongqing

6.2.1 Landscape composition

Class total area (CA) measures the absolute land occupation of green space along distance from city center (Figure 6.1). It increases linearly with distances from city center,

which is expected because the buffer ring is getting increasingly bigger in size away from center. Absolute area of green space should increase accordingly.

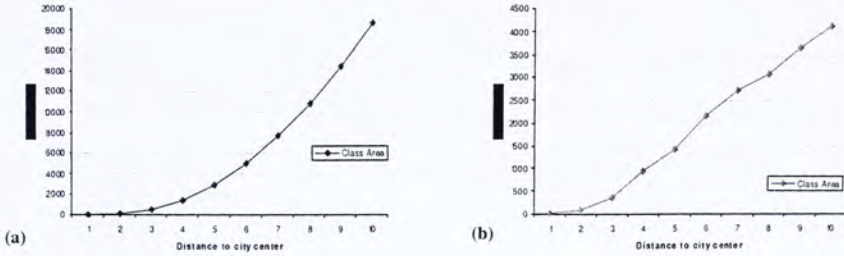


Figure 6.1 Total class area of "urban green space" along distance to city center for circle (a) and ring (b) buffers. Chongqing as a case

Proportion of landscape (PLAND) occupied by "urban green space" shows the relative abundance of green area. From Figure 6.2b, it is found that "urban green space" occupies less than 50% of land covered by buffer rings within 5 km of city center. After 5 km, PLAND increases to about 70%. Besides, increase in PLAND within 2 km of urban center is negligible. All these indicate that there is not enough space for expansion of green space within Yu zhong, city center district of Chongqing.

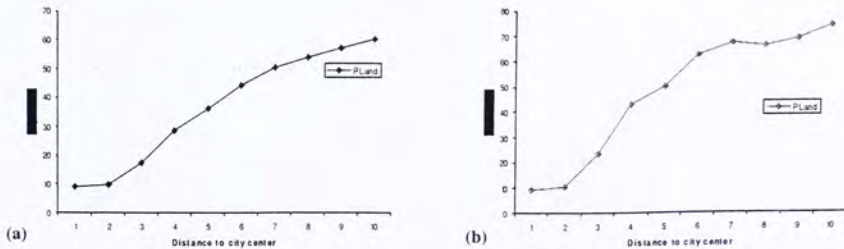


Figure 6.2 Proportion of landscape occupied by "urban green space" along distance to city center for circle (a) and ring (b) buffers. Chongqing as a case

6.2.2 Fragmentation

Fragmentation is a description of the process and tendency of a landscape component to break into small patches (Frohn, 1998). It can be revealed in Chongqing by a sharp increase in Patch number of green area from below 200 patches to over 400 at 3 km buffer ring. Accompanying with the fact that PLAND increases from 10% to over 20% at the same buffer ring, sharp increase in PN may imply that more space is available for landscaping. They are however small and scattering, which can be shown by small mean patch area in the same ring (Figure 6.3c). They are urban parks (such as E ling gungyuan) and small-scale green areas in residential and industrial land uses. Multiplication of small green patches also increases the Patch density at 3 km, which measures the amount of green patches in relative terms.

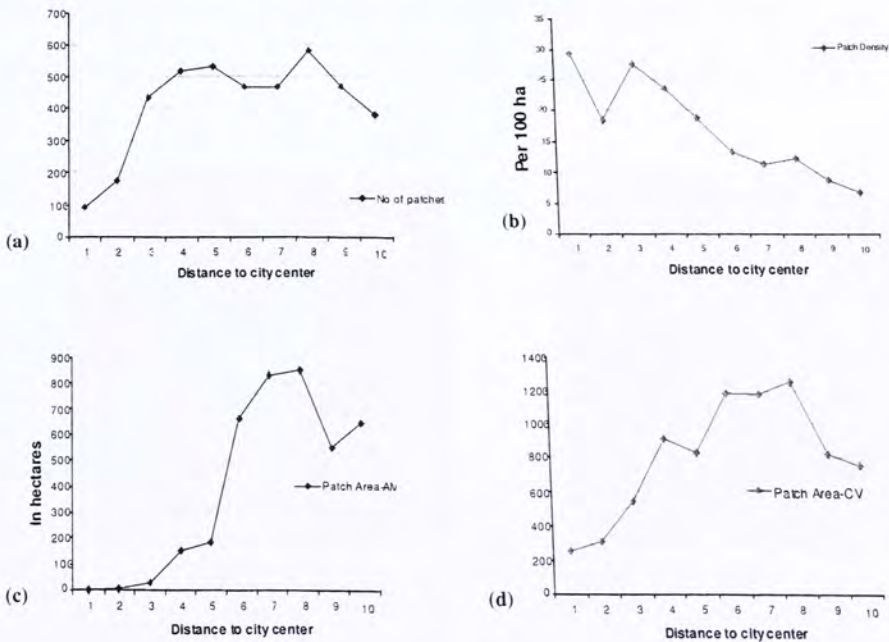


Figure 6.3 Number of Patch (a), Patch Density (b), Area-weighted mean (c) and Coefficient of Variation (d) (*ring*) for the class “urban green space”. Chongqing as a case

Sharp rise in Mean patch size (MPS) and Coefficient of Variation in Patch size (Patch Area-CV) is observed at 6 km ring, implying that some large patches of green space begin to emerge at 6 km from city center to lift both MPS and variations of patch size significantly. It is observed that green areas become extensive and contiguous at 6 km ring (Figure 6.4a), which are mainly mountain areas in Nanan District, Yubei District and Jiangbei District. Combining it with the facts of constant increase in PLAND and decrease in PD, it is apparent that fragmentation of “urban green space” is related to the small green patches at 3 km from city center; while mountains (such as Nan shan) provide extensive space for greening at 6 km from city center.

MPS decreases sharply to about 550 ha at 9 km from city center. Obvious increase in Patch number occurs at 8 km from city center. These indicate that green space becomes more patchy compared to that at 6 km ring. This phenomenon can be explained by new urban zones are developed at the north, west and south of original urban area, although contiguous green area can be found at east and southeast (Figure 6.4b).

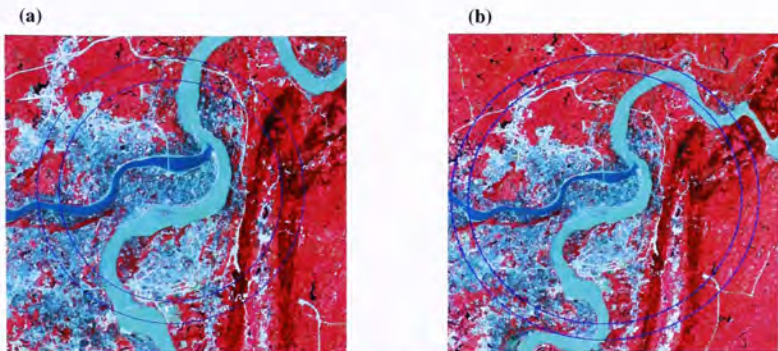


Figure 6.4 6 km (a) and 9 km (b) buffer rings of Chongqing

6.2.3 Contagion

Contagion, or class aggregation, refers to the tendency of a class to occur in large and aggregated distribution. It measures the extent to which pixels/grids of the same class are aggregated (McGarigal, 2002).

“Urban green space” of Chongqing is not highly aggregated throughout the buffer distances. Clumpiness Index (ring) does not rise above 0.9 at any buffer ring distance (Figure 6.5). Clumpiness Index consistently increases from 1 km to 7 km, during which Mean patch size is increasing as well. It may imply that emergence of large green areas is related to the increment of aggregation of “urban green space”. Nevertheless, the slight increment of Clumpiness Index (from 0.67 to 0.85) means that green areas are not well connected even at the peripheral region of Chongqing.

Landscape Division Index decreases from 97% to 88% at 6 km from city center, where sharp increase in MPS occurs coincidentally. It then rises again to the secondary peak (93%) at 9 km, where decrease in MPS is observed. It confirms that emergence of large green patches helps lower the probability of observing dissected green patches. Nevertheless, the index is high throughout the buffers of Chongqing city center, indicating that disaggregated green areas are dominating the landscape.

6.2.4 Patch Shape Complexity

Buffer in ring shape may artificially change the shape of green space, which affects the interpretation of patch shape indices. So indices in this section reflect the cumulative shape of green patches as buffer circle grows larger away from city center.

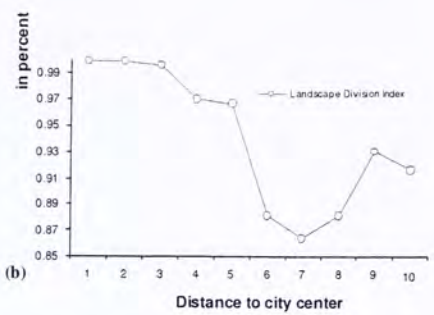
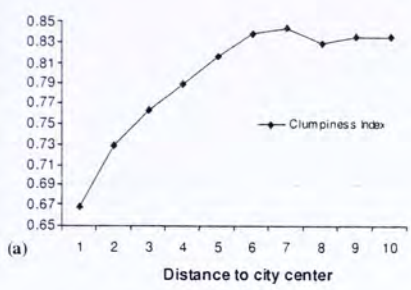


Figure 6.5 Clumpiness Index and Landscape Division Index (ring) of “urban green space” in Chongqing

Fractal Dimension Index (circle) increases from 1 km to 5 km from the city center. It implies that vegetation patches tend to become increasingly more fractal until the maximal fractal dimension is reached after 5 km, which is reflected from flatness of curve from 6 to 10 km (Figure 6.6). Minimal Fractal Dimension Index is below 1.15 at 1 km while the maximum is hardly over 1.3, indicating overall green space in Chongqing is inclined to be simple in shape.

Perimeter-Area ratio decreases from 900 to 300 before 5 km from city center. It decreases by only about 200 after 5 km. Considering that total area of green space increases exponentially away from the city center (Figure 6.1), smaller decrease in PA ratio after 5 km implies that shape of green patches becomes more complex after 5 km away from city center, where mountain ranges and reservoir regions provide more space for free development of woodland and grassland, such as Nan shan and Jin shan. Besides, most of the northern part of Chongqing has not been developed, which provides extensive and complex green space after 5 km from the city center.

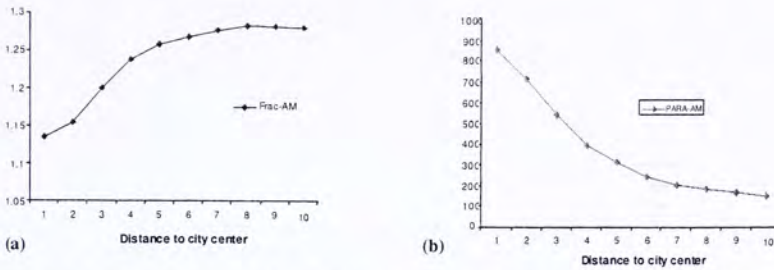


Figure 6.6 Area-weighted mean of Fractal Dimension Index (circle) (a) and Area-weighted mean of Perimeter-Area Ratio (circle) (b) of “urban green space” in Chongqing

6.3 Nanjing

6.3.1 Landscape composition

Class total area (ring) of “urban green space” starts to rise at 2 km buffer. Before 5 km from the city center, class area increases from 0 to about 1000 ha. After 5 km, it increases sharper from 1000 to over 3000 ha at 10 km. It is because the area of buffer ring increases exponentially at the same time (Figure 6.7).

Proportion of land occupied by green area (PLAND) increases from 15% to 25% at 3 km from city center (Figure 6.8). From the image (Figure 6.9a) it is the periphery of old city center where landscaping parks emerge such as Shuihu gungyuan and Chingliang Shan gungyuan. Another sharp rise in PLAND starts to occur after 5 km from city center, where PLAND increases from about 30% to about 55%, where large-scale green areas occur, such as Zijingshan and Lieshi lingyuan (Figure 6.9b).

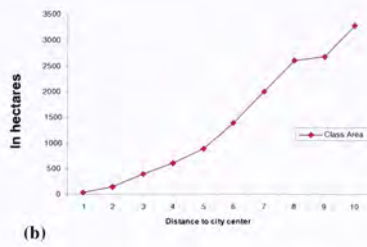
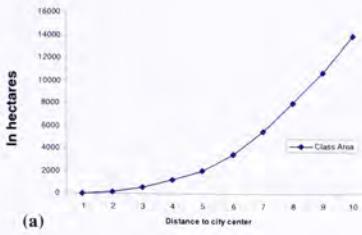


Figure 6.7 Total class area of “urban green space” along distance to city center for circle (a) and ring (b) buffers. Case in Nanjing

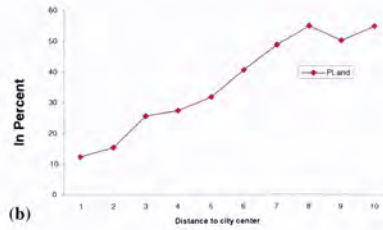
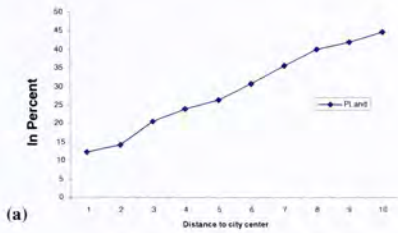


Figure 6.8 Proportion of Landscape occupied by “urban green space” along distance to city center for circle (a) and ring (b) buffers. Case in Nanjing

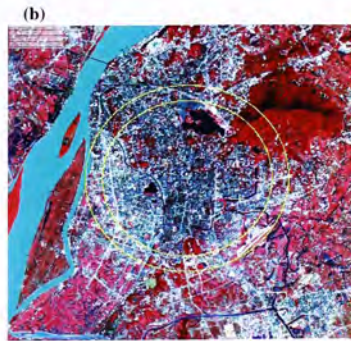
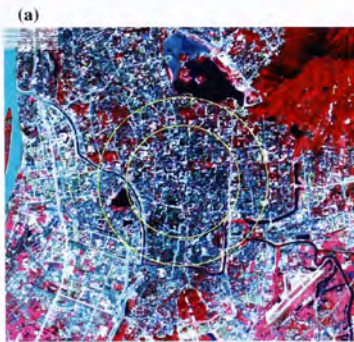


Figure 6.9 3 km (a) and 9 km (b) buffer rings of Nanjing

6.3.2 Fragmentation

Fragmentation pattern of green space in Nanjing resembles that of Chongqing. Number of patches (NP) increases consistently from about 200 at 1 km ring to nearly 1200 at 4 km, an increase 1000 within only 4 km. The greatest increase happens at 4 km from city center, in which many small patches of green space and parks are observed by water bodies, in tourist spots (such as Wang On Shi Guju) and along old city wall. After 4 kilometers, however, rise of NP becomes much slower and less consistent, even though a general ascending trend is still noticeable (Figure 6.10a).

Patch density (PD) shows an overall decreasing trend. The rise in PD happens at 4 km buffer ring, coinciding with the sharpest rise in NP; the greatest slump happens between 4- and 6-km buffer rings, at which NP rise comes to a halt (Figure 6.10b).

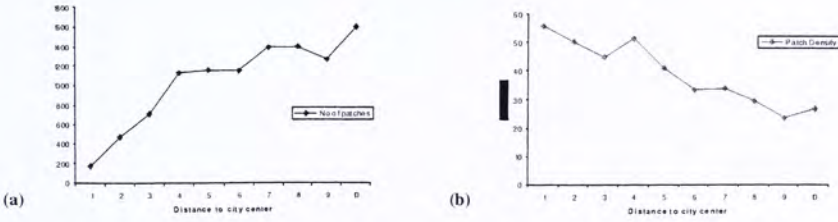


Figure 6.10 Number of patches (a) and patch density (b) of “urban green space” along buffer rings in Nanjing. Notice the coincidence between leveling of NP and falling of PD.

Like the case of Chongqing, decrease in PD coincides with increase in Mean Patch Size and Variation of patch sizes in Nanjing. As illustrated in Figure 6.11a, sharp increase in Patch area happens at 5 km from city center, where a large piece of woodland is found at the southwestern tip of Zi Jing Shan; and at 7 km buffer ring, which passes through the middle of Zi Jing Shan from north to south.

No further rise in MPS and patch size CV occur after the 7-kilometer buffer, indicating that sizes of green patch have already reached maximum. Coefficient of Variation of patch sizes also peaks at 5 km and 7 km (Figure 6.11b). Similar interpretation as in the case of Chongqing can be drawn: green space is highly fragmented within 4 km buffer, notable by low class total area, proportion of landscape and MPS and high patch density; outside this buffer, green space becomes less fragmented because some large green patches emerge to increase both CA and proportion of landscape. They also lower density of green patches.

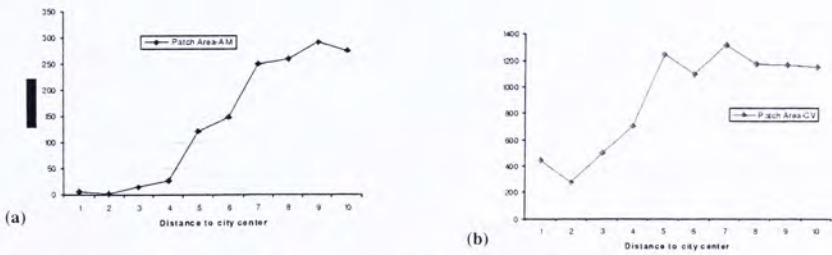


Figure 6.11 Area-weighted mean (a) and Coefficient of variation (b) of patch area for the class “urban green space” in ring buffers in Nanjing

6.3.3 Contagion

Like fragmentation pattern, aggregation of “urban green space” in Nanjing is very similar to that of Chongqing. The most disaggregated region is at 2 km from city center, with Landscape Division Index reaching its maximum (Figure 6.12). Emergence of large vegetation patches at 5 km buffer ring and 7 km buffer ring helps increase the overall contagion in the corresponding regions, which can be reflected on the steep slump of Landscape Division Index at the above rings. However, the scores are very high throughout the buffer zones (all higher than 0.95), indicating that the frequency of small, disaggregated green patches are very high throughout the study site, which is shown in Figure 6.12.

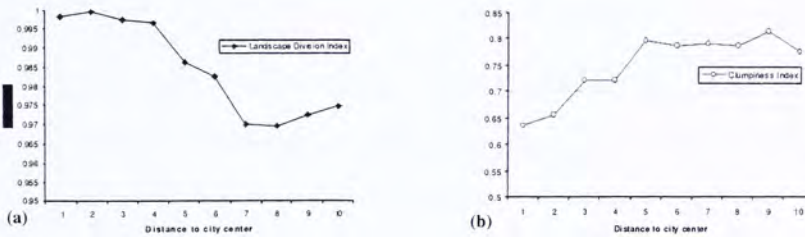


Figure 6.12 Landscape Division Index (a) and Clumpiness Index (b) of “urban green space” for ring buffers in Nanjing

Clumpiness Index before 4 km buffer ring is lower, between about 0.65 (1 km) and 0.7 (3 km). Emergence of larger-scale parks such as Xianwuhu gungyan at 3 km increases both PLAND, Mean Patch size and Clumpiness. Emergence of Zi Jing Shan increases the score to 0.8 after 4 km from the city center, which is then stabilized from 5 km to 10 km. It means that aggregation of green space cannot be further increased. It is because periphery of Nanjing is occupied by agricultural land uses, which are

disaggregated by nature. Besides, new urban development is found in the southern east of Nanjing city, which limits the development of green coverage (Figure 6.13).

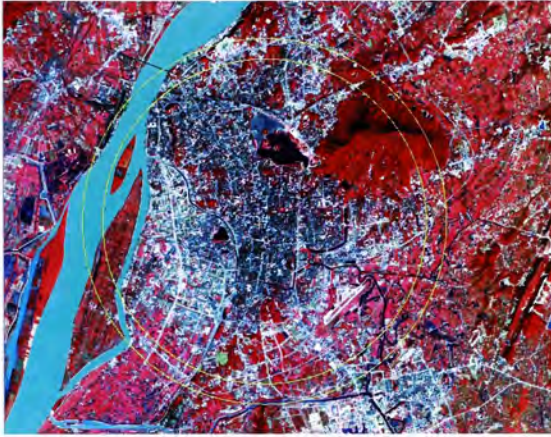


Figure 6.13 Periphery of Nanjing city. 9-km buffer ring is outlined in yellow

6.3.4 Patch Shape Complexity

Similar results about patch shape complexity to Chongqing are observed. Fractal Dimension Index increases with the distance from city center (Figure 6.14a), implying that not only is the total area and landscape proportion of green space increasing, but also the green patches are becoming more complex in configuration in general away from city center. Fractal Dimension Index hardly rises above 1.3, indicating that vegetation patches in Nanjing are overall inclined to be simple in shape.

Decrease in Perimeter-Area ratio becomes less rapid after 5 kilometers, suggesting patches of more complex shape appear (Figure 6.14b). Area around the city center of Nanjing is old developed urban zone, leaving less space for spontaneous growth of vegetation; while in the outskirts area very large green landscape such as Ningdan

gungyuan at the southern tip of Chongqing city allows extensive growth of vegetation, causing them larger in size and comparatively complex in shape.

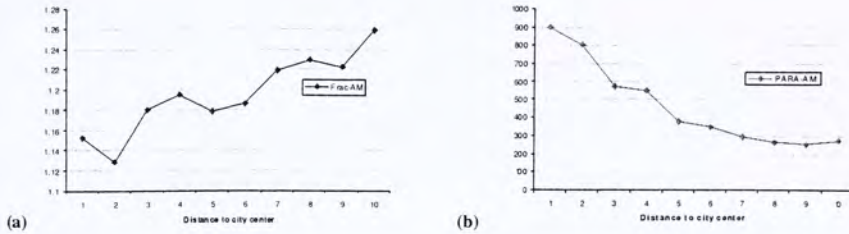


Figure 6.14 Area-weighted mean Fractal Dimension Index (a) and Perimeter-Area Ratio (b) of “urban green space” for buffer circles in Nanjing

6.4 Discussion

In this section, two cities, Chongqing and Nanjing are put together for comparison in terms of landscape structure of urban green space. In fact, from the findings presented above we can observe more similarities than disparities between the two cities, even though they look very different from the imagery.

6.4.1 Similarities

Both cities have very low proportion of landscape occupied by “urban green space” within 2 km buffer (about 10%), which is the city center region, and densely populated and developed urban area. Considering that city center regions of both Chongqing and Nanjing have very long history of urban development (referring to CHAPTER III), niche for vegetation should be scarce. Beyond the 2 km buffer, however, steady increase in landscape proportion of vegetation can be observed until maximum proportion is reached

at 7 to 8 kilometers from the urban centers. Land use gradually changes from high dense urban to low dense urban and agricultural activities, freeing more land for vegetation coverage. This pattern of variation in land uses with distance from city center is consistent with many researches earlier done (e.g. Zhang et al., 2004; Zong et al., 2002:).

Especially similar is the fragmentation pattern, which is revealed by number of patches (NP), patch density (PD) and patch area distribution of the study sites. In both cities, sudden increase in NP occurs at the 3 km region followed by fluctuation of NP from 3- to 10-kilometer buffer rings. It can be interpreted as space for vegetation begins to be more available at 3-kilometer ring. From 4 kilometers onwards, green space of increasingly larger sizes emerge so steep increase in both area-weighted mean and coefficient of variation of patch area can be observed. These large green space patches stabilize NP and lower PD in both urban areas.

Figures 6.15 and 6.16 illustrate the frequency distribution of patch size of “urban green space” within the 10 km buffer circles of city centers of Chongqing and Nanjing respectively. In Chongqing, green patches which are smaller than 1 hectare take up over 92% of total amount of green areas. Only about 70 out of 3500 total green patches are larger than 5 hectares. In Nanjing, green patches smaller than 0.1 hectare are even more dominant, taking over 70% of total amount of green areas. Green areas over 5 ha in area take up barely 1%. These observations confirm that green spaces of both Chongqing and Nanjing are fragmented. Besides, except the large mountains such as Nanshan in Chongqing and Zi Jing Shan in Nanjing provide space for extensive development of green space, most of the green space in both cities is tiny in size, which are mainly roadside planting, green lawns within residential areas or schools and agricultural fields.

More parks and cultural heritage can be found in Nanjing, for example Shiuanwuhu gungyuan, Ming Gugung yiji, etc., which provide space for planting. However, most of them are small in size and far away from one another. Roadside trees fail to provide good connection between them so as to increase aggregation of the overall green landscape.

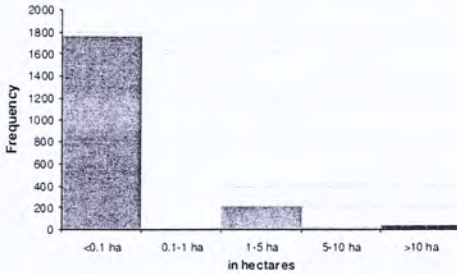


Figure 6.15 Frequency distribution of area of "urban green space" in Chongqing

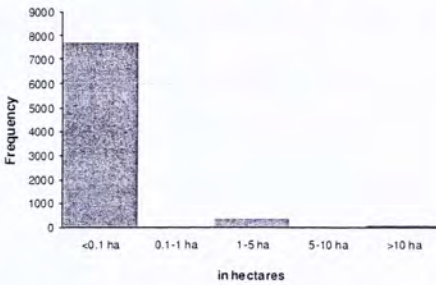


Figure 6.16 Frequency distribution of area of "urban green space" in Nanjing

Equally similar is that green space in both Chongqing and Nanjing is generally simple in shape. Although some large patches of more fractal shape in the outer urban obviously reduce the rate of decrease in Perimeter-Area Ratio at 5 to 6 kilometers from the city centers, shape of an average green space patch tends to be simple, which explains low scores in area-weighted mean FRAC. After all, Chongqing and Nanjing are very established cities. Urban functions such as residential and commercial dominate. Green

space is treated more as human amenity embedded in a planned urban mosaic than a means of ecological conservation. Therefore, free growth of vegetation into fractal shape is generally not allowed.

6.4.2 Differences

Table 6.1 shows the metrics values of “urban green space” within the 10 km buffer circles of both Chongqing and Nanjing. They are different from each other in aspects of landscape composition and fragmentation; while similar in terms of complexity of patch shape. Compared with Chongqing, lower proportion of landscape in Nanjing is occupied by “urban green space”. While green space takes up over 60% of the entire landscape within the 10 km buffer circle of Chongqing, it takes up less than 50% in Nanjing. Besides, the largest patch of green space takes up 30% of 10 km buffer circle of Chongqing; while it takes about 10% in case of Nanjing.

In the case of fragmentation, Nanjing is over 3 times higher in PD and nearly twice the level of ED in Chongqing. Average patch of Nanjing (1079 m²) is about one-fifth the size of Chongqing (5380 m²). Green space in Nanjing has slightly lower Clumpiness Index while higher Landscape Division Index as compared to Chongqing. However, Proximity Index of Nanjing (14480) is significantly higher than that of Chongqing (7979), which may suggest that green space in Nanjing is smaller in size and lower in landscape occupation; while it is better connected with each other compared to that of Chongqing.

Table 6.1 Class-level landscape metrics for “urban green space” in the 10 km buffer circles of Chongqing and Nanjing

Metrics	Chongqing	Nanjing
Landscape Composition		
Class Total Area (ha)	18675.07	14061.38
Proportion of Landscape (%)	60.12	44.76
Largest Patch Index (%)	30.51	10.25
Fragmentation		
Number of Patches	3533	10642
Patch Density (per 100 ha)	11.37	33.87
Edge Density (m per ha)	69.10	138.30
Patch Area-AM (ha)	5380.01	1079.15
Patch Area-CV (%)	3188.74	2856.09
Radius of Gyration-AM (m)	3095.12	1220.31
Radius of Gyration-CV (%)	424.09	303.95
Patch Shape Complexity		
Fractal Dimension Index-AM	1.28	1.27
Fractal Dimension Index-SD	0.05	0.05
Perimeter-Area Ratio-AM	151.26	305.96
Perimeter-Area Ratio-SD	641.08	718.59
Perimeter-Area Fractal Dimension	1.372	1.337
Class Aggregation		
Proximity Index-AM	7979.68	14480.33
Euclidean Nearest Neighbor Distance-AM (m)	22.07	22.60
Clumpiness Index	0.86	0.79
Interspersion & Juxtaposition Index (%)	39.61	35.19
Landscape Division Index	0.90	0.98
Effective Mesh Area (ha)	3234.28	483.01

Different levels and patterns of urban development contribute to the discrepancy between two cities in landscape structure of green space. Being one of the most developed cities in the eastern seaboard of China, Nanjing is experiencing more rapid economic and urban development. From the image, it is easy to notice many large scale constructions and dragging activities operating on western, eastern and northern edges of the city. New urban development can also be observed in Jiangning prefecture, which is to the southeast of Nanjing (Atlas of Cities of China, 1995, Vol. 1). These clues suggest Nanjing is still vibrantly extending. This factor may greatly limit space available for contiguous green space development in Nanjing periphery. Only in large scale mountain ranges such as Zi Jing Shan can the continuous green space coverage be allowed. On the other hand, Chongqing is located in western China, which is much less developed compared to the east. Municipal area is unsurprisingly smaller in size and more compact in shape. From the image, the city is very compact, dissected only by Changjiang and Jianing River. Extension of city seems to be constrained by steep mountain ranges by both the east (Nanshan) and the west (Gele Shan). The only new development zone in Yubei is actually abutting old development zone of Chongqing. The pattern of urban development allows much more niche for development of vegetation cover in suburban zone, greatly increasing both proportion and size of "urban green space".

Aggregation of green space, however, is slightly higher in Nanjing, especially within 5 km from the city center. This phenomenon can be stemmed from the fact that Nanjing is rich in cultural heritage, such as Ming Palace, ancient city wall, etc., which requires vegetation as amenity and preservation. Roadside trees are better developed to improve the urban environment for tourism. Large trees are protected from felling in Nanjing which enable connected "tree-ways" along major commercial centers, such as

Zhongshan Road and Hanzhong Road (Jim & Chen, 2003). All these reasons may help increase the connection of urban green space within old city region of Nanjing. On the other hand, center region of Chongqing mainly serves residential, commercial and industrial functions. Less attention is paid on greening within the district, which is confirmed by the lack of parks in Chongqing city.

“Urban green space” in both cities is similar in terms of shape complexity. Shape of vegetation tends to be simple. It may be because green space in these two cities serves more as amenity to urban settlement, such as public parks, roadside shade, etc., or as agricultural field supporting city with food, rather than ecological reserve, providing habitats for local fauna and flora. Therefore, most of them are inherently simple in shape and artificial in nature.

CHAPTER 7. Conclusion

7.1 Summary on findings

This section sums up the findings of image object analyses, object-oriented classification, comparison between different classification methods and studies of “urban green space” of Chongqing and Nanjing using landscape metrics.

7.1.1 Summary on image object analyses

Image object analyses have been undertaken for the ASTER images of Chongqing and Nanjing. It is observed that in both sites decreasing spectral-shape ratio yields smaller number of image objects of larger average size during segmentation across scales. It also increases spectral variances within image objects at all scales. Pixels/objects of different land covers may merge together as the same object if the weight of shape is set too high for spectral-shape ratio, thus causing severe class mixing. On the other hand, if spectral weight is too dominant in the spectral-shape ratio, objects generated will be too fractal in shape. Guided by these observations, spectral-shape ratio of 9:1 is chosen for Chongqing while 7:3 is set for Nanjing.

Three critical segmentation levels are chosen for the hierarchical classification system in both sites based on the analysis of variations of spectral and textural features along segmentation levels. Critical segmentation level can be identified if break point is observed along the variation. In Chongqing, break point can be identified at segmentation level 5 for most of the object variables under study. Break points at other levels are more difficult to be defined. Level 9 is selected as another critical level because break points can be observed for more classes. Pixel level is selected as the smallest object level to

facilitate the identification of patchy “woodland”. In Nanjing, segmentation level 4 instead of level 5 is chosen as critical level because the latter is found too coarse to differentiate different types of vegetation. Level 8 is selected as another critical level because object variables are found breaking at this level for more classes. Pixel level and segmentation level 1 produces insignificant difference in image resolution so that latter is chosen as object level 1.

Classifying rules are derived for expected classes after segmentation levels are chosen from comparing various object features of different classes at 3 object levels. Many classifying rules are transferable between Chongqing and Nanjing. At the top object level, “river” is distinguishable by its large area and low within-object heterogeneity. “Lake” is characterized by its low spectral values in all VNIR channels and higher spectral variances compared to “river”. At the second object level, vegetation can be separated from non-vegetation using ratio vegetation index (RVI). In case of Nanjing, vegetation can be further divided into 3 sub-categories based on GLCM CON values of vnir 3. This level can also be used to separate “low density urban” from other non-vegetation classes due to its high GLCM CON values in VNIR 1 and 2. At the lowest object level, object size is too small to generate valid shape or textural information and thus spectral means of different VNIR channels are the main information for classification of the remaining classes.

7.1.2 Summary on object-oriented classification

Based on the findings of object analyses, decision tree is designed for classification of the images of both sites. Three classes are chosen to be studied intensively regarding the classifying rules. In Chongqing, “lake”, “crops and grassland” and “low density

urban” are chosen as cases. “Lake” can be classified at object level 3 mainly using features of Area, Density and GLCM DISS. “Grassland” is combined with “crops” to form a class “crops and grassland” which is classified mainly by higher ratio vegetation index (RVI) at object level 2 and then further distinguished from “woodland” at object level 1 using spectral means of all VNIR channels. “Low density urban” is classified at object level 1 instead of level 2 because its higher GLCM CON of VNIR 1 and 2 are most significant at that level. In Nanjing, classification of “lake”, “crops and grassland II” and “low density urban” is studied. For “lake”, it is classified in both object levels 3 and 2 from “small river” using shape feature of density. “agricultural crop II”, “wetland” and “grassland” are difficult to be distinguished so they are combined into the class “crops and grassland II”, which is classified as “vegetation” at object level 2 using RVI and then separated from “woodland” and “crops and grassland I” using mainly spectral means. “Low density urban” is separated from other non-vegetation classes at object level 1 by its higher GLCM DISS in VNIR 1.

Comparisons of different classification methods in terms of accuracy in both Chongqing and Nanjing are similar. Linear spectral unmixing yields the lowest overall accuracy, followed by supervised fuzzy classification. Object-oriented classification yields overall accuracy similar to that of maximum likelihood classification. In Chongqing, object-oriented classification attains 64.14 % overall accuracy while maximum likelihood classification attains 62.66 %, only about 2 % lower. In Nanjing, object-oriented classification attains 47.4 % overall accuracy while MLC increases the overall accuracy to 50 %. From the confusion matrices, it is revealed that serious misallocation occurs between grassland, bare soil and urban. For landscape analyses at the next step, post-classification aggregation is implemented in both cases. All classes are

combined into only three classes: "water", "urban green space" and "land". It increases the overall accuracy of object-oriented classification to over 80 % and 66 % in case of Chongqing and Nanjing respectively.

7.1.3 Summary on landscape studies of "urban green space"

"Urban green space" in Chongqing and Nanjing are studied using landscape metrics in terms of landscape composition, fragmentation pattern, contagion and patch shape complexity. Both cities have low proportion of landscape occupied by "urban green space" within 2 km buffer ring surrounding the city centers. Dense urban development suppresses green coverage at about 10 %. Beyond the 2 km buffer ring, steady increase of landscape proportion of green space can be observed. Maximum of green coverage is reached at about 8 km from the city center, where land use changes into low dense urban and agricultural activities. Green space in both cities is highly fragmented, which is evidenced by high frequency of patches which are below 1 hectare in size. Fragmentation is most serious within the 3 km buffer ring, where patch number suddenly increases. Beyond the 3 km buffer, very large and contiguous green space emerges to reduce both patch number and patch density. Aggregation of green space is low for both cities. Besides, most of the green space is simple in shape, revealed by low fractal dimension index. It is because urban green space is allowed mostly in parks, roadsides and lawns within residential and commercial areas, which are confined in size and simple in shape.

Comparing between Chongqing and Nanjing shows that green space in Nanjing within the 10 km buffer circle ranks lower in landscape proportion and fragmentation. Patch density and edge density are much higher in Nanjing than in Chongqing. It may be because Nanjing is more rapidly developed, which greatly limit space available for large

scale green space development. Suburban Nanjing is occupied mainly by agricultural crops from the image, which are fragmented in nature and small in size. It also contributes to the high patch density and small patch size in Nanjing. On the other hand, Chongqing city proper is more compact, with its development greatly constrained by steep mountain slopes on both eastern and western sides. Continuous vegetation cover is allowed around the city proper of Chongqing, which greatly increases the landscape composition and fragmentation of green space. However, aggregation of green space is slightly higher for Nanjing, especially within 5 km from the city center. It is because Nanjing is endowed with cultural heritage which provide more space for landscaping within city proper. Roadside trees are found more prominent within the old urban center, which connects with the cultural heritage well. On the other hand, fewer planting and parks can be found within city proper which can connect with green space outside the city center.

7.2 Limitations of the research

This research has several limitations in data preparation, image classification and landscape analyses:

7.2.1 Data preparation

Some important first-hand and secondary information cannot be acquired at the stage of data pre-processing. Topographic maps of Chongqing and Nanjing are inaccessible. Coordinates and altitude information of the two sites are not available as well. Without such information, geo-referencing of ASTER data is unable to be undertaken. Land use maps of the two cities used as the reference of this research were issued in 1995, while the images for classification and landscape studies were acquired in

2000 and 2001. Some changes in land covers identified on images cannot be captured in land use maps. Post-classification adjustment and accuracy assessment are made more difficult because of this reason.

7.2.2 Image classification

Object-oriented classification is faced with several problems. Having mentioned in Chapter III, object features of each land cover class are actually averages of thirty to fifty random samples collected for each of expected classes. No consideration has been put on the heterogeneity of features within the same land cover class. During implementation of classification, it is discovered that variances of object features within a class are unexpectedly large for some land cover classes. Facing with the situation, many pre-formulated classifying rules have to be adjusted with trial-and-error method, or even discarded. Some classes which can be easily identified by visual inspection are found difficult to be distinguished from one another in object-oriented classification because they are very similar in respect of some objects' features. For example, in both cases of Chongqing and Nanjing, "vegetation" and "bareland" are mainly divided using ratio vegetation index. (RVI) However, it is found that some "grassland" objects have their RVI very similar to those of "bareland" objects.

Optimal segmentation scales, which minimize class mixing of the segmented images, are difficult to be decided. Especially in case of Nanjing, it is found that severe mixing between "vegetation" and "non-vegetation" occurred at Object level 2. Because Object-oriented classification adopts decision tree methodology, accuracy of classification at higher level strongly influences the classification accuracy at lower level. Serious class mixing between "vegetation" and "non-vegetation" directly lowers the

classification accuracy of “woodland”, “crops and grassland II”, “bareland”, “fallowed land”, “high density urban” and “low density urban” at the lowest classification level, which is the main cause of low overall classification accuracy in case of Nanjing.

Although ASTER image has 15 spectral channels spanning across visible band, near infrared band, shortwave infrared band and thermal infrared band, only 3 visible and near infrared bands have been input into object-oriented classification while 6 more bands in shortwave infrared band are input into other three classifiers. It implies that object-oriented classification is solely dependent on the visible and near infrared information, while much of the information about the different land covers provided in other spectral regions have not been extracted and utilized.

Spectral unmixing and supervised fuzzy classification produced classification accuracy far lower than maximum likelihood classification and object-oriented classification in this research, which is inconsistent in many earlier findings that these two classification approaches attain classification accuracy comparable with that of maximum likelihood classifier (Foody, 1996; Zhang & Foody, 2001; Roberts et al., 1998). Operating spectral unmixing classifier requires spectral data of endmembers. In this research, endmembers can only be collected from the image. Such image endmembers are vulnerable to spectral changes caused by changes in space, illumination and other radiometric conditions, which may affect the classification quality (Roberts et al., 1998). Supervised fuzzy classifier needs intensive fine-tuning of training samples and fuzzy threshold curves. Less effort has been put in these tasks due to time constraint. Because of the above reasons, comparison of classification is mainly made between object-oriented classification and maximum likelihood classifier.

7.2.3 Landscape Analysis

Scrutiny of landscape metrics variables in this research reveals that many metrics are highly correlated with one another and thus redundant. It confirms many researchers' findings (Leitão & Ahern, 2002; McGarigal & McComb, 1995; Cifaldi, et al., 2004). For example, Area-weighted Mean Patch Size, Area-weighted Radius of Gyration and Effective Mesh Size behave nearly the same regardless of the change in distance from city center, even though they are supposed to account for different aspects of landscape configuration. Moreover, most of the metrics selected fail to show obvious patterns for interpretation. In light of the above problems, only a few metrics variables are sifted out to describe four fundamental aspects of landscape structure: landscape composition, fragmentation, contagion/class aggregation and shape complexity of patches. The remainders are put in Appendix 3.

Caution should also be taken on the methodology of landscape studies. As mentioned in CHAPTER III, 10 buffers of extending sizes in forms of both circles and rings are generated around city centers of Chongqing and Nanjing. Both buffers have impacts on the behavior of metrics variables. Metrics for buffer circles reflect cumulative condition of the whole landscape. Large variations in landscape structure due to distance changes tend to be suppressed. On the other hand, buffer rings artificially distort the original configuration of landscape components, severely confounding some metrics variables, especially those which are sensitive to shape of landscape components.

Another problem of landscape studies of this research stems from data of data acquisition. Data of Chongqing is acquired in mid-summer, in which both natural

vegetation and agricultural planting are more exuberant and thus connected; while data of Nanjing is acquired in autumn, leaving much larger area of fallowed land.

Classification accuracy of Nanjing (66%) is lower than that of Chongqing (about 80%). Landscape studies based on a land use map of low accuracy may seriously affect the validity of the findings concerning with landscape variables. In this sense, there is high probability of underestimating the coverage of "urban green space", especially concerning about the 30% error of omission of "urban green space" in Nanjing.

Two cities, Chongqing and Nanjing, are compared only, while there are many cities worth being researched have not been studied in this research. In terms of landscape studies of Chinese cities, this research lacks comprehensiveness due to this reason.

7.3 Suggestions for further research

Further research can be undergoing in the following fields. Object-oriented classification greatly increases the data volume for image classification. Not only spectral values, but also shape and textural features can be generated from image objects at different segmentation scales. In this research, it is found difficult to extract useful knowledge about class properties from such a large database just by human expertise. In future research about object-oriented classification data mining techniques can be adopted to assist in the extraction of classification knowledge. Data mining is an important part of knowledge discovery from database (KDD) which helps discovering interesting patterns from large amounts of data stored in databases, under which some functionalities such as association rule mining, emerging patterns searching, etc., which have been suggested contributive in enhancing the classification accuracy of decision tree

classification. Some algorithms integrating data mining techniques with decision tree inductions have been developed, such as SLIQ and SPRINT, which may improve the existing object-oriented classification (Han & Kamber, 2001).

This research tests the effectiveness of using shape and textural features to classify ASTER images, which have 15 m spatial resolution for VNIR channels and 30 m for SWIR channels. However, it is unknown whether shape and textural features are expeditious in classifying remotely sensed data which has lower spatial resolution. Commercial satellite images nowadays advance greatly in spatial resolution, such as IKONOS which has 1 m spatial resolution for panchromatic image and 4 m for multispectral image. With these low resolution satellite images, future research about object-oriented classification can extend its scope to studying the changes in interpretation of object features with images of different resolutions, from images as low as 1 m resolution to those as high as 1 km resolution (such as AVHRR), and its implications on the usage of object-oriented classification.

Last but not least, there are many Chinese cities which have not been analyzed in respect of their landscape structures of urban green space. Comparisons can be done in many perspectives: cities of different latitudes, cities of different political hierarchies, etc. A more thorough investigation into urban green space in Chinese cities in future research is necessary for directing landscape planning policies of China.

Bibliography

- Antunes, A.F.B., *et al.*, 2003. Object-oriented analysis and semantic network for high resolution image classification, *Anais XI SBSR, Belo Horizonte, Brazil, 05-10 abril 2003*, INPE, pp. 273-279.
- ASTER User Handbook, Version 2, 2002.
- Atkinson, P. M. *et al.*, 1997. Mapping sub-pixel proportion land cover with AVHRR, Imagery, *International Journal of Remote Sensing*, 18(4), pp. 917-933.
- Atkinson, P. M. and Tatnall, A. R. L., 1997. Neural networks in remote sensing, *International Journal of Remote Sensing*, 18(4), pp. 699-709.
- Belanger, L. and Grenier, M., 2002. Agricultural intensification and forest fragmentation in the St. Lawrence valley, Quebec, Canada. *Landscape Ecology*, 17, pp. 495-507
- Bin, Z., *et al.* 2003. The impact of urban planning on land use and land cover in Pudong of Shanghai, China. *Journal of Environmental Sciences*, 15(2), pp. 205-214.
- Blaschke, T. *et al.*, 2000. Object-oriented image processing in an integrated GIS/remote sensing environment and perspectives for environmental applications, *Environmental Information for Planning, Politics and the Public*, Metropolis-Verlag, Marburg, Volume II.
- Borak, J. S. and Strahler, A. H., 1999. Feature selection and land cover classification of a MODIS-like data set for a semiarid environment, *International Journal of Remote Sensing*, 20(5), pp. 919-938.
- Cao, Y., 2001. Ecological measures about green land system construction in metropolis—a case study in Changchun city. *Urban Environment and Urban Ecology*, 14(5), pp. 9-11.
- Che, S. and Song, Y., 2001. Extract of the remote sensing message of urban green space landscape—Shanghai city as the case study. *Environment and Urban Ecology*, 14(2), pp. 10-12.
- Chen, S.S. and Jim, C.Y., 2003. Quantitative assessment of the treescape and cityscape of Nanjing, China, *Landscape Ecology*, 18, pp. 395-412.
- Chuvieco, E., 1999. Measuring changes in landscape pattern from satellite images: short-term effects of fire on spatial diversity, *International Journal of Remote Sensing*, 20(12), pp. 2331-2346.
- Cifaldi, R. L., *et al.*, 2004. Spatial patterns in land cover of exurbanizing watersheds in southeastern Michigan. *Landscape and Urban Planning*, 66, pp. 107-123.

- Cracknall, A. P., 1998. Synergy in remote sensing—what's in a pixel? *International Journal of Remote Sensing*, 19(11), pp. 2025-2047.
- Definiens-Imaging, 2003. *e-Cognition Object Oriented Image Analysis 3.0 User Manual*.
- De Kok, R., *et al.*, 2003. Analysis of urban structure and development applying procedures for automatic mapping of large area data, *The International Archives of the Photogrammetry, Remote Sensing and Spatial Information Sciences*, 34, pp. 41-45.
- De Ridder, K., 2003. BUGS-Benefits of Urban Green Space, First Research Brief.
- Duan, X. 2002. Sustainable development for ecology environment of Chongqing. *Chongqing huan jing ke xue*, 24(2), pp. 6-10.
- Fabos, J. G., 1995. Introduction and overview: the greenway movement, uses and potentials of greenways. *Landscape and Urban Planning*, 33, pp. 1- 13.
- Fang, Y., *et al.* 2001. Approaches of eco-city construction in Chengdu. *Urban Environment and Urban Ecology*, 14(2), pp. 50-53.
- Farina, A., 1998. *Principles and Methods in Landscape Ecology*, 1st edn., London; New York: Chapman & Hall, 1998.
- Feng, W., *et al.* 2003. Investigation about landscape ecology construction in the urban fringe of Chengdu. *Chongqing huan jing ke xue*, 25(11), pp. 84-86.
- Fisher, P., 1997. The pixel: a snare and a delusion, *International Journal of Remote Sensing*, 18(3), pp. 679-685.
- Foody, G. M., 1996. Approaches for the production and evaluation of fuzzy land cover classifications from remotely-sensed data, *International Journal of Remote Sensing*, 17(7), pp. 1317-1340.
- Foody, G. M. and Boyd, D. S., 1999. Detection of partial land cover change associated with the migration of inter-class transitional zones, *International Journal of Remote Sensing*, 20(14), pp. 2723-2740.
- Forman, R.T.T. and Godron, M., 1986. *Landscape Ecology*, New York: Wiley, 1986.
- Franklin, S.E. *et al.*, 2001. Using Spatial Co-occurrence Texture to Increase Forest Structure and Species Composition Classification Accuracy, *Photogrammetric Engineering and Remote Sensing*, 67(7), pp. 849-855.
- Frohn, R.C., 1998. *Remote Sensing for Landscape Ecology: New Metric Indicators for Monitoring, Modeling, and Assessment of Ecosystems*, Boca Raton: Lewis Publishers, 1998.

- Frizzelle, B.G. and Moody, A., 2001. Mapping Continuous Distributions of Land Cover: A Comparison of Maximum-Likelihood Estimation and Artificial Neural Networks, *Photogrammetric Engineering and Remote Sensing*, 67(6), pp. 693-705.
- Fung, T. and Chan, K., 1994. Spatial composition of spectral classes: a structural approach for image analysis of heterogeneous land-use and land-cover types, *Photogrammetric Engineering and Remote Sensing*, 60(2), pp. 173-180.
- Fung, T. and Siu, W., 2001. A Study of Green Space and its Changes in Hong Kong Using NDVI. *Geographical and Environmental Modelling*, 5(2), pp. 111-122.
- Gobster, P. H., 2001. Neighbourhood-Open Space Relationships in Metropolitan Planning: a look across four scales of concern. *Local Environment*, 6(2), pp. 199-212.
- Gomes, A. and Marçal, A.R.S., 2003. Land cover revision through object-based supervised classification of ASTER data, *ASPRS 2003 Annual Conference Proceedings, May 2003, Anchorage, Alaska*.
- Gopal, S. and Woodcock, C., 1994. Theory and methods for accuracy assessment of Thematic maps using fuzzy sets. *Photogrammetric Engineering and Remote Sensing*, 60(2), pp. 181-188.
- Guan, D. *et al.*, 1999. Landscape ecological analysis of urban vegetation in Guangzhou, China, *Journal of Environmental Sciences*, 11(2), pp. 160-166.
- Guo jia tong ji ju, China, 2001. *Zhongguo cheng shi tong ji nian jian*, 2001. Beijing shi : Zhongguo tong ji xin xi zi xun fu wu zhong xin.
- Guo jia tong ji ju, China, 2003. *Zhongguo cheng shi tong ji nian jian*, 2003. Beijing shi : Zhongguo tong ji xin xi zi xun fu wu zhong xin.
- Gulinck, H. *et al.*, 1993. Landscape structural analysis of central Belgium using SPOT data. *Landscape Ecology and GIS*. Taylor and Francis, 1993., ch. 10.
- Han, J. and Kamber, M., 2001. *Data mining: concepts and techniques*. Morgan Kaufmann Publishers. ch. 7.
- He, X., *et al.* 2003. Landscape ecological analysis of mountainous city and town of China. *Urban Environment and Urban Ecology*, 6(6), pp. 198-200.
- Herold, M., *et al.* 2002. Object-oriented mapping and analysis of urban land use/cover using IKONOS data. *Proceedings of 22nd EARSEL Symposium "Geoinformaiton for European-wide integration, Prague, June 2002*.
- Hong, S., *et al.* 2003. Landscape pattern and its effect on ecosystem functions in Seoul Metropolitan area: Urban ecology on distribution of the naturalized plant species, *Journal of Environmental Sciences*, 15(2), pp. 199-204.

- Huang, H., 2001. *Chongqing yu Jing, Jin, Hu jing ji fa zhan bi jiao yan jiu*, 1st edn., Chongqing chu ban she, 2001.
- Ivits, E., et al., 2002. Landscape connectivity studies on segmentation based Classification and manual interpretation of remote sensing data, *e-Cognition User Meeting, October 2002, Munchen*, pp. 1-10.
- Jensen, J. R., 1996. *Introductory Digital Image Processing: a Remote Sensing Perspective*, 2nd edn. Upper Saddle River, NJ: Prentice-Hall.
- Jiangsu Provincial People's Government, 2003. *Jiangsu nian jian, 2003*. Nanjing: Nanjing da xue chu ban she.
- Jim, C. Y., 1989. Tree canopy cover, land use and planning implication in urban Hong Kong, *Geoforum*, 20(1), pp. 57-68.
- Jim, C. Y., 1989a. Tree-canopy characteristics and urban development in Hong Kong, *Geographical Review*, 70, pp. 210-225.
- Jim, C. Y., 2002. Planning strategies to overcome constraints on greenspace provision in urban Hong Kong, *Town Planning Review*, 73(2), 127-152.
- Jim, C.Y. and Chen, S. S., 2003. Comprehensive greenspace planning based on landscape ecology principles in compact Nanjing city, China. *Landscape and Urban Planning* 65, pp. 95-116.
- Jim, C. Y. and Liu, H. T., 2001. Patterns and dynamics of urban forests in relation to land use and development history in Guangzhou city, China, *The Geographical Journal*, 167(4), pp. 358-375.
- Kiema, J. B. K., 2002. Texture analysis and data fusion in the extraction of topographic objects from satellite imagery, *International Journal of Remote Sensing*, 23(4), pp. 767-776.
- Lawrence, R. L. and Wright, A., 2001. Rule-based classification systems using classification and regression tree (CART) analysis, *Photogrammetric Engineering and Remote Sensing*, 67(10), pp. 1137-1142.
- Lein, J. K., 2003. Sensing sprawl: towards the monitoring of urban expansion using Dempster-Shafer Theory, *Geocarto International*, 18(2), pp. 61-70.
- Leitao, A.B. and Ahern, J., 2002. Applying landscape ecological concepts and metrics In sustainable landscape planning, *Landscape and Urban Planning*, 59, pp. 65-93.
- Leung, Y., 1988. *Spatial Analysis and Planning under Imprecision*, Netherlands: Elsevier.
- Leung, Y., et al., 1999. A generic concept-based object-oriented geographical information system, *International Journal of Geographical Information Science*, 13(5), pp. 475-498.

- Li, H. and Reynolds, J.F., 1994. A simulation experiment to quantify spatial heterogeneity in categorical maps, *Ecology*, 75(8), pp. 2446-2455.
- Li, H. and Wu, J., 2004. Use and misuse of landscape indices, *Landscape Ecology*, 19, pp. 389-399.
- Lillesand, T. M., *et al.*, 2004. *Remote Sensing and Image Interpretation*, 5th edn., John Wiley & Sons, Inc.
- Little, C. E., 1990. *Greenways for America*. The Johns Hopkins University Press: Baltimore and London.
- Liu, J.G., 2000. Smoothing Filter-based Intensity Modulation: a spectral preserve image fusion technique for improving spatial details, *International Journal of Remote Sensing*, 21(18), pp. 3461-3471.
- Low, H. K. *et al.*, 1999. A neural network landuse classifier for SAR images using textural and fractal information, *Geocarto International*, 14(1) pp.67-74.
- Luo, X. and Chen, C., 1999. *Xin Chongqing de jue qi yu Zhongguo zhong xi bu jing ji de fa zhan*, Chongqing chu ban she, 1999.
- McGarigal, K., 2001. *FRAGSTATS User Guidelines, Version 3*.
- McGarigal, K. and Marks, B.J., 1994. *FRAGSTATS: Spatial pattern analysis program for quantifying landscape structure*.
- McGarigal, K. and McComb, W.C., 1995. Relationships between landscape structure and breeding birds in the Oregon coast range, *Ecological Monographs*, 65(3), pp. 235-260.
- Mesev, T.V., *et al.*, 1995. Morphology from imagery: detecting and measuring the density of urban land use, *Environment and Planning A*, 27, pp. 759-780.
- Neel, M.C., *et al.*, 2004. Behavior of class-level landscape metrics across gradients of class aggregation and area. *Landscape Ecology*, 19, 435-455.
- Qin, H., 2001. Landscape of Nanning city and the way to ameliorate it. *Urban Environment and Urban Ecology*, 14(2), pp. 44-46.
- Raucoules, D. and Thompson, K. P. B., 1999. Adaptation of the Hierarchical Stepwise Segmentation Algorithm for automatic segmentation of a SAR mosaic, *International Journal of Remote Sensing*, 20(10), pp. 2111-2116.
- Riccotta, C. and Avena, G. C., 1999. The influence of fuzzy set theory on the areal extent of thematic map classes, *International Journal of Remote Sensing*, 20(1), pp. 201-205.

- Roberts, D.A., *et al.*, 1998. Change Identification Using Multitemporal Spectral Mixture Analysis: Applications in Eastern Amazonia, *Remote sensing change detection : environmental monitoring methods and applications*. Ann Arbor Press. ch. 9.
- Schiewe, I. J., *et al.*, 2001. Potential and problems of multi-scale segmentation methods in remote sensing, *GeoBIT/GIS*, 6, pp. 34-39.
- Schumaker, N. H., 1996. Using landscape indices to predict habitat connectivity, *Ecology*, 77(4), pp. 1210-1225
- Selinger-Looten, R., *et al.*, 1999. Structure of plant communities and landscape patterns in alluvial meadows of two flood plains in the north-east of France, *Landscape Ecology*, 14, pp. 213-229.
- Sester, M., 2000. Knowledge acquisition for the automatic interpretation of spatial data, *International Journal of Geographical Information Science*, 14(1), pp. 1-14.
- Shaban, M. A. and Dikshit, O., 2002. Evaluation of the merging of SPOT multispectral and panchromatic data for classification of an urban environment, *International Journal of Remote Sensing*, 23(2), pp. 249-262.
- Sui, D.Z. and Zeng, H., 2000. Modeling the dynamics of landscape structure in Asia's emerging desakota regions: a case study in Shenzhen, *Landscape and Urban Planning*, 758, pp.1-16.
- Teng, C. H. and Fairbairn, D., 2002. Comparing expert systems and neural fuzzy Systems for object recognition in map dataset revision, *International Journal of Remote*, 23(3), pp. 555-567.
- Turner, M. G. *et al.*, 2001. *Landscape Ecology in Theory and practice*, NY: Springer-Verlag.
- Tyrväinen, L. and Väänänen, H., 1998. The economic value of urban forest amenities: an application of the contingent valuation method, *Landscape and Urban Planning*, 43, pp. 105-118.
- Walmsley, A. 1995. Greenways and the making of urban form. *Landscape and Urban Planning*, 33, pp. 81-127.
- Website of Chongqing Zhenfu Gongzhong Xinxiwang, Visit in March 2004. Available at the following website:
<http://www.cq.gov.cn/>
- Website of Definiens-Imaging, e-Cognition 3.3 User Manual, Visit in September, 2004. Available at the following website:
<http://www.definiens-imaging.com>

Website of Nanjing Urban Planning, Visit in December, 2003. Available at the following website:

<http://www.njghj.gov.cn/>

Weiers, S. *et al.*, 2004. Mapping and indicator approaches for the assessment of habitats at different scales using remote sensing and GIS methods. *Landscape and Urban Planning*, 67, pp. 43-65.

Yang, P. 2003. Ecological approach to the construction of Shan shui garden city in Chongqing city. *Chongqing huan jing ke xue*, 25(2), pp. 9-11.

Yu, Q., 1998. Structure of modern urban open space system. *Urban Planning Forum* 6, pp.49-56.

Zang, L. and Feng, B., 2003. Integrity of ecological function in urbanized region. A case study on Jiangning District, Jiangpu County, Nanjing. *Urban Environment and Urban Ecology*, 16(5), pp. 72-74.

Zhang ling yang zi zhu lu xing shou ce" bian xie zu, 2002. *Sichuan Chongqing*, 1st edn., Beijing : Zhongguo qing gong ye chu ban she, 2002.

Zhang, L., *et al.*, 2004. A GIS-based gradient analysis of urban landscape pattern of Shanghai metropolitan area, China. *Landscape and Urban Planning*, 69, pp. 1-16.

Zhang, J. and Foody, G. M., 1998. A fuzzy classification of sub-urban land cover from remotely sensed imagery. *International Journal of Remote Sensing*, 19(14), pp. 2721-2738.

Zhang, Q., 1999. Strategies for the conservation of urban greenspace biodiversity. *Urban Environment and Urban Ecology*, 12(3), pp.36-38.

Zhang, Y., 2001. Texture-integrated classification of urban treed areas in high-resolution color-infrared imagery. *Photogrammetric Engineering and Remote Sensing*, 67(12), pp. 1359-1365.

Zhao, G., 2000. *Chongqing*. Beijing Shi : Min zu chu ban she, 2000.

Zheng, Q., 1999. *Cheng shi yuan lin lu di gui hua*. Beijing shi : Qi xiang chu ban she, 1999.

Zhou, X., *et al.* 2003. *Analysis of the construction of ecological garden city—Chongqing as a case study*. *Chongqing huan jing ke xue* 25(6), pp. 12-17.

Zhou, T. and Tao, K., 2003. Construction of urban greenbelt system in Ningbo city. *Urban Environment and Urban Ecology*, 16(2), pp. 4-6.

Zhongguo Chengshi Dituji Bianji Weiyuan Hui, 1995. *Atlas of Cities of China*, Vol. 1. Zhongguo Ditu Chubanshe.

Zhongguo Chengshi Dituji Bianji Weiyuan Hui, 1995a. *Atlas of Cities of China*, Vol. 2.
Zhongguo Ditu Chubanshe.

Appendix 1—Equations of object features

Spectral Statistics:

- Spectral Mean of a particular spectral layer

$$\bar{C}_L = \frac{1}{n} \cdot \sum_{i=1}^n C_{Li}$$

where C_{Li} is the spectral value of a particular layer of all n pixels forming an image object. The value range is [0 ; 255] for 8 bit data.

- Standard Deviation of a spectral layer—which calculates the variance of the layer values of all n pixels forming an image object.

$$\sigma_L = \sqrt{\frac{1}{n-1} \cdot \sum_{i=1}^n (C_{Li} - \bar{C}_L)^2}$$

- Mean Difference to Neighbors—computing the layer mean difference for each neighboring object and then weighted with regard to the length of the border between the objects:

$$\Delta C_L = \frac{1}{l} \cdot \sum_{i=1}^n l_{Si} \cdot (\bar{C}_L - \bar{C}_{Li})$$

where,

l border length of the image object of concern

l_{Si} border length shared with direct neighbor i

\bar{C}_L layer mean value of the image object of concern

\bar{C}_{Li} layer mean value of neighbor i

n quantity of neighbors

Shape Statistics:

- Area—in nongereferenced data the area of a single pixel is 1. Therefore, the area of an image object is the number of pixels forming it.
- Border Length—defined as the sum of edges of the image object that are shared with other image objects or are situated on the edge of the entire image. In nongereferenced data the length of a pixel edge is 1. Feature value range starts from 4.
- Length/width—there are two ways to compute the ratio:

$$\gamma = \frac{l}{w} = \frac{eig_1(S)}{eig_2(S)}, eig_1(S) > eig_2(S)$$

which is the ratio of the eigenvalues of the covariance matrix of x- and y-coordinates of pixels forming an image object; or:

$$\gamma = \frac{l}{w} = \frac{a^2 + ((1-f) \cdot b)^2}{A}$$

when length/width ratio is approximated using the bounding box, where a and b are length and width of the bounding box, while f is the degree of filling, which is the area A covered by the image object divided by total area of the bounding box. Feature value range is [0 ; 1]

- Shape Index—describing the smoothness of the image object borders:

$$s = \frac{e}{4 \cdot \sqrt{A}}$$

where,

e border length of the image object

A area of the image object

Feature value range starts from 1.

- Density—describing the deviation of the form of the image objects from square, expressed by the area covered by the image object divided by its radius:

$$d = \frac{\sqrt{n}}{1 + \sqrt{\text{Var}(X) + \text{Var}(Y)}}$$

where,

n number of pixels forming the image object

$\text{Var}(X)$ and $\text{Var}(Y)$ are covariance matrix of x - and y -coordinates of all pixels forming the image object respectively. They are used to approximate the radius of the image object.

Textural statistics (Texture after Haralick):

- Homogeneity—high weights are put along the diagonal frequencies, while the weights are decreasing exponentially with distance from the diagonal. It is a measure of smoothness of an image object:

$$H = \sum_{i,j=0}^{N-1} \frac{P_{i,j}}{1 + (i-j)^2}$$

where $P_{i,j}$ is the relative frequency at the $(i,j)^{\text{th}}$ entry, N is spectral quantization of pixels.

- Contrast—the opposite of homogeneity. It is a measure of the amount of local variation within the image object.

$$CON = \sum_{i,j=0}^{N-1} P_{i,j} (i-j)^2$$

- Dissimilarity—similar to contrast, but the weights increase linearly instead of exponentially.

$$Dis = \sum_{i,j=0}^{N-1} P_{i,j} |i-j|$$

- Entropy—high if the frequencies distribute equally. It is low if the elements are close to either 0 or 1.

$$Ent = \sum_{i,j=0}^{N-1} P_{i,j} (-\ln P_{i,j})$$

- Angular Second Moment—using $P_{i,j}$ as a weight for itself. High value if frequencies within the GLCM are very orderly.

$$ASM = \sum_{i,j=0}^{N-1} P_{i,j}^2$$

Appendix 2—Equations for Landscape Metrics

Patch Metrics

Patch Metrics are computed for every patch in the landscape, with patch type/land cover class of each patch also recorded, which includes the following:

- Perimeter-Area Ratio—a simple measure of shape complexity, without standardization to a simple Euclidean shape:

$$PARA = \frac{P_{ij}}{a_{ij}}$$

where P_{ij} equals perimeter (m) of patch ij; a_{ij} equals area (m^2) of patch ij.

- Fractal Dimension Index—reflects shape complexity across a range of patch sizes.

$$FRAC = \frac{2 \ln(0.25 p_{ij})}{\ln a_{ij}}$$

where p_{ij} equals perimeter (m) of patch ij; a_{ij} equals area (m^2) of patch ij.

- Proximity Index—equals the sum of patch area divided by the nearest edge-to-edge distance squared between the patch and the focal patch of all patches of the corresponding patch type whose edges are within a specified distance of the focal patch. It is a dimensionless index considering simultaneously the size and proximity of patches in a specified radius of neighborhood.

$$PROX = \sum_{s=1}^n \frac{a_{ijs}}{h_{ijs}^2}$$

where a_{ijs} equals area (m^2) of patch ijs within specified neighborhood (m) of patch ij . h_{ijs}^2 equals distance (m) between patch ijs and patch ijs , based on patch edge-to-edge distance, computed from cell center to cell center.

- Euclidean Nearest-Neighbor Distance—simple calculating the shortest straight-line distance between the focal patch and its nearest neighbor of the same class.

$$ENN = h_{ij}$$

where h_{ij} is the distance (m) from patch ij to nearest neighbor patch of the same patch type, based on patch edge-to-edge distance, computed from cell center to cell center.

Class Metrics

They are indices computed of every patch type or land cover in the landscape, with the result presented separately for each class. They include the following:

- Patch Number—simply number of patches of a particular patch type/land cover; a crude measure of the level of fragmentation of the patch type.

$$NP = n_i$$

where n_i equals number of patches in the landscape of patch type i .

- Patch Density—expresses number of patches per unit area. (in number per 100 hectares) It facilitates comparisons among different landscapes like our research.

$$PD = \frac{n_i}{A}(10,000)(100)$$

where n_i equals NP of patch type I; A is total landscape area in m^2 , which are converted into 100 hectares by multiplying 10,000 and 100.

- Percentage of Landscape—quantifying the proportional abundance of a particular land cover in the landscape. It measures the non-spatial composition of a landscape.

$$PLAND = P_i = \frac{\sum_{j=1}^n a_{ij}}{A} (100)$$

where P_i is the proportion of the landscape shared by the patch type I; a_{ij} is area (in m^2) of patch ij; A is total landscape area in m^2 .

- Patch Area—equal to the area (m^2) of the patch, divided by 10,000 in order to convert to hectares. Statistics of Patch area will be calculated for each patch type in order to depict an overall situation in each land cover, which includes:
- Area-weighted mean—equal to the sum of all patches of a particular land cover of the corresponding patch metric value multiplied by area of each patch of the class divided by the total sum of patch areas of all patches of that class, that is:

$$AM = \sum_{j=1}^n x_{ij} \left[\frac{a_{ij}}{\sum_{j=1}^n a_{ij}} \right]$$

- Coefficient of Variation—equal to the standard deviation divided by the mean, multiplied by 100 to convert to a percentage, for the patch metric concerned, that is:

$$CV = \frac{SD}{MN} (100)$$

where SD equals standard deviation:

$$SD = \sqrt{\frac{\sum_{j=1}^n \left[x_{ij} - \left(\frac{\sum_{j=1}^n x_{ij}}{n_i} \right) \right]^2}{n_i}}$$

MN equals Means:

$$MN = \frac{\sum_{j=1}^n x_{ij}}{n_i}$$

where x_{ij} refers to metric values of a patch j of class i .

- Radius of Gyration—equal to the mean distance between each cell in the patch and the patch centroid. It is another way of patch size measurement.

$$GYRATE = \frac{\sum_{r=1}^z h_{ijr}}{z}$$

where h_{ijr} is the distance (m) between cell ijr (located within patch ij) and the centroid of patch ij (the average location), based on the cell center-to cell center distance; z is the number of cells in patch ij . Area-weighted mean of Gyrate will be calculated for each land cover class.

- Largest Patch Index—equal to the percentage of the landscape comprised by the largest patch. In this sense, it is a simple way of measuring class dominance.

$$LPI = \frac{\max_{j=1}^n (a_{ij})}{A} (100)$$

where a_{ij} is area in squared meter of patch ij in class i . A is the total landscape area.

- Edge Density—equals the sum of lengths of all edge segments involving the patch class concerned, divided by total landscape area. A “true” edge segment is pixels abutting patches of different classes.

$$ED = \frac{\sum_{k=1}^m e_{ik}}{A} (10,000)$$

where e_{ik} is the total length (m) of edge involving patch class I; A is the total landscape area.

- Fractal Dimension Index—calculation of class-level Fractal Dimension Index is the same as patch-level algorithm. Area-weighted mean, standard deviation and correlation of variation of FRAC will be calculated for each land cover.
- Perimeter-Area Fractal Dimension—another form of measurement of patches’ shape complexity. This index bases its calculation on regression analysis and linear logarithmic relationship between area and perimeter of patches across a large range of patch sizes/scales. The equation is as follows:

$$PAFRAC = \frac{2}{\frac{\left[n_i \sum_{j=1}^n (\ln p_{ij} \cdot \ln a_{ij}) \right] - \left[\left(\sum_{j=1}^n \ln p_{ij} \right) \left(\sum_{j=1}^n \ln a_{ij} \right) \right]}{\left(n_i \sum_{j=1}^n \ln p_{ij}^2 \right) - \left(\sum_{j=1}^n \ln p_{ij} \right)^2}}$$

where a_{ij} is area (m^2) of patch ij ; p_{ij} is the perimeter (m) of patch ij ; and n_i is the number of patches of land cover class i .

- Perimeter-Area Ratio—the calculation in class-level equals that in patch-level. Area-weighted mean and standard deviation of the metric value will be calculated for each land cover class.
- Proximity Index—same as Proximity Index in patch-level metrics. Area-weighted mean of PROX will be calculated for each land cover.
- Euclidean Nearest Neighbor Distance—same as ENND in patch-level. Area-weighted mean for each class will be calculated.
- Clumpiness Index—equals the proportional deviation of the proportion of like adjacencies involving a particular land cover from the expected proportion under spatially random distribution. Clumpy takes on a range between -1 and 1, where -1 means the focal land cover is maximally disaggregated while 1 means another maximal end. It is calculated as follows:

$$\text{Given } G_i = \left(\frac{g_{ii}}{\left(\sum_{k=1}^m g_{ik} \right) - \text{min-}e_i} \right)$$

$$\text{CLUMP} = \left[\begin{array}{l} \frac{G_i - P_i}{P_i} \text{ for } G_i < P_i \text{ \& } P_i < 0.5; \text{ else} \\ \frac{G_i - P_i}{1 - P_i} \end{array} \right]$$

where g_{ii} is the number of like adjacencies between pixels of patch class i based on the double-count method; g_{ik} is the number of adjacencies between pixels of patch class i and k based on double-count method; $\text{min-}e_i$ is minimum perimeter of patch class i for a maximally clumped class; P_i is the proportion of the landscape occupied by patch class i .

- Interspersion and Juxtaposition Index—a proportion between the observed interspersion over the maximum possible interspersion for the given number of patch classes. Unlike Clumpiness Index, it is based on patch adjacencies rather than pixel adjacencies.

$$IJI = \frac{-\sum_{k=1}^m \left[\left(\frac{e_{ik}}{\sum_{k=1}^m e_{ik}} \right) \ln \left(\frac{e_{ik}}{\sum_{k=1}^m e_{ik}} \right) \right]}{\ln(m-1)} = (100)$$

where e_{ik} is the total length (m) of edge between patch classes i and k ; m is the number of patch classes present in the landscape.

- Landscape Division Index—is based on cumulative patch area distribution and is interpreted as the probability that two randomly chosen pixels in the landscape are not situated in the same patch of the corresponding land cover. It is a measurement of spatial autocorrelation of a landscape.

$$DIVISION = \left[1 - \sum_{j=1}^n \left(\frac{a_{ij}}{A} \right)^2 \right]$$

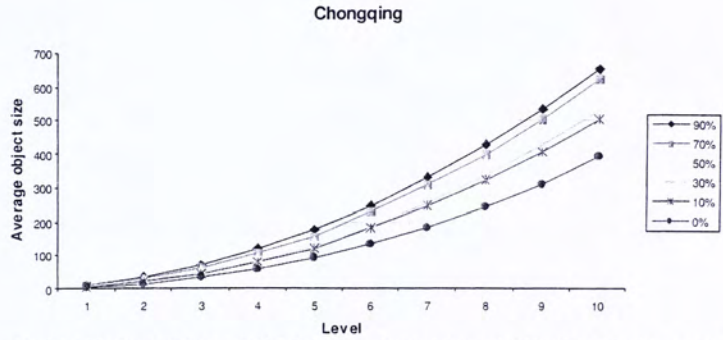
where a_{ij} is area (m^2) of patch ij ; A is total landscape area.

- Effective mesh size—it is absolutely but negatively correlated with DIVISION. While DIVISION represents the probability that a pair of randomly selected pixels is separated in two patches, MESH calculates the resultant size of patches if the landscape is divided according to the corresponding degree of DIVISION. (Jaeger; cited in Neel et al. 2004)

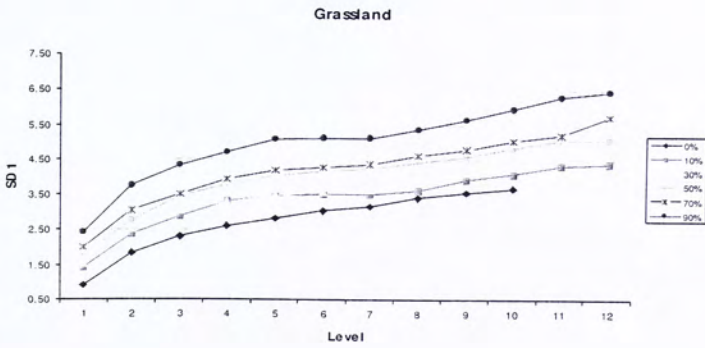
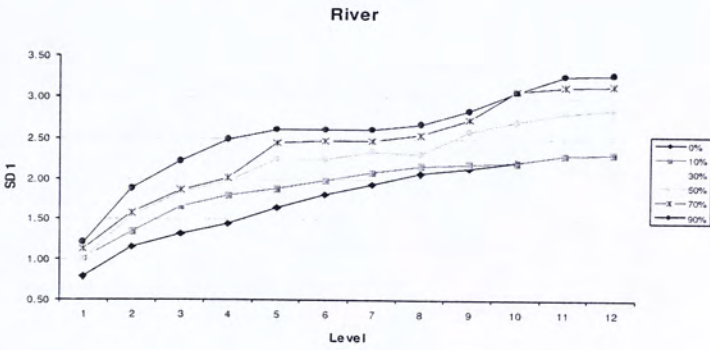
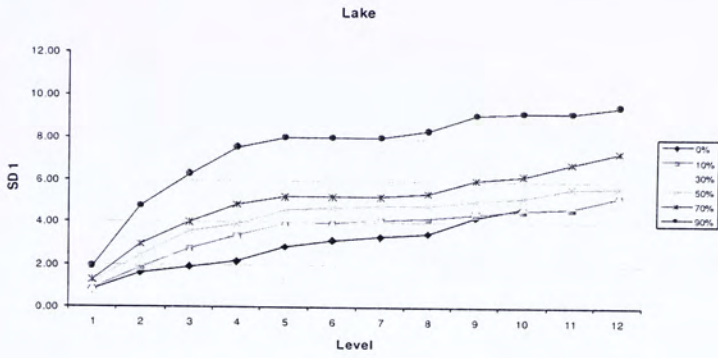
$$MESH = \frac{\sum_{j=1}^n a_{ij}^2}{A} \left(\frac{1}{10,000} \right)$$

where a_{ij} is area (m^2) of patch ij ; A is total landscape area (in squared meters).

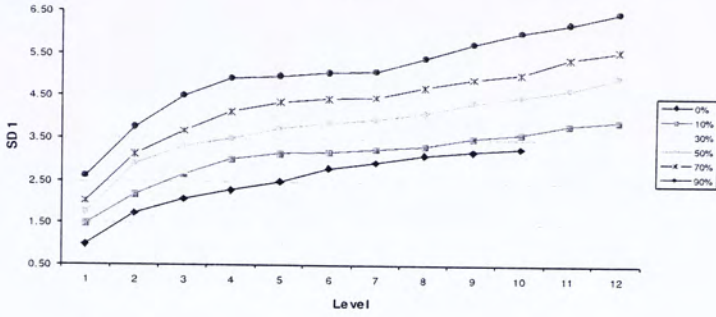
Appendix 3—Variations of Object Features along Segmentation Levels in Chongqing



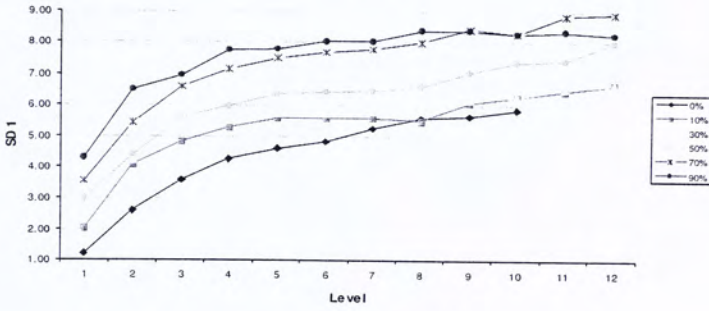
0% --0% weight of spectral-shape ratio; 10% --10% weight of spectral-shape ratio; 30% --30% weight of spectral-shape ratio; 50% --50% weight of spectral-shape ratio; 70% --70% weight of spectral-shape ratio; 90% --90% weight of spectral-shape ratio.
Figure A.1 Variation of average object size along segmentation gradient. Case in Chongqing.



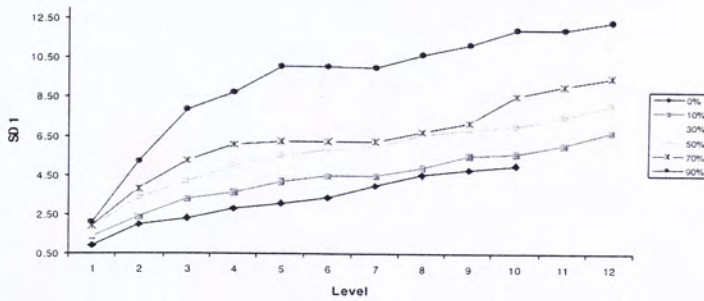
Woodland

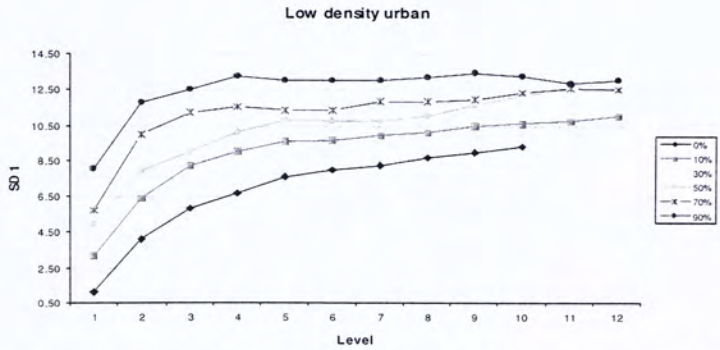
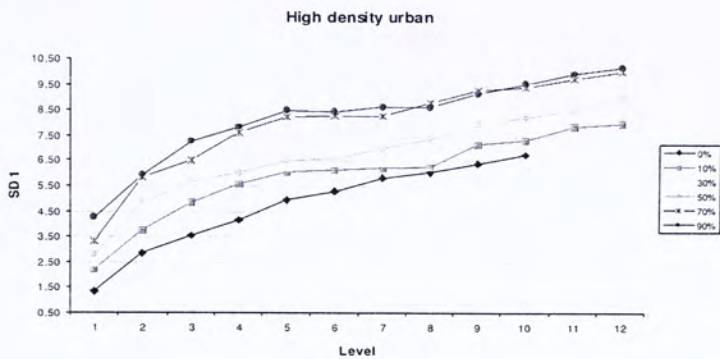


Bareland



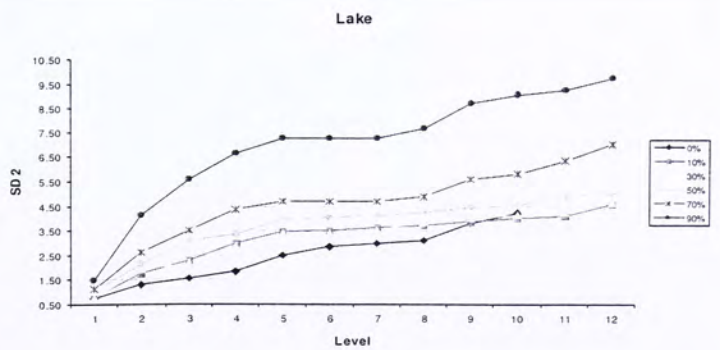
Industrial



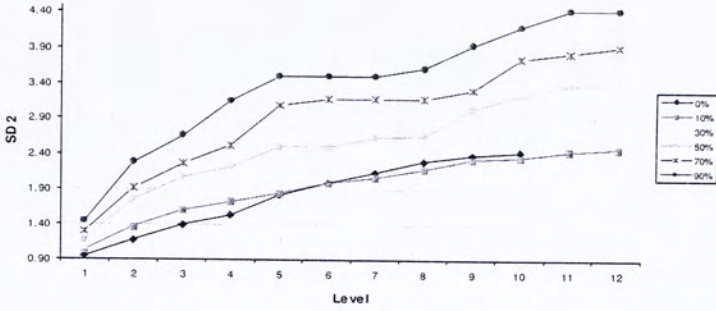


0% --0% weight of spectral-shape ratio; 10% --10% weight of spectral-shape ratio; 30% --30% weight of spectral-shape ratio; 50% --50% weight of spectral-shape ratio; 70% --70% weight of spectral-shape ratio; 90% --90% weight of spectral-shape ratio.

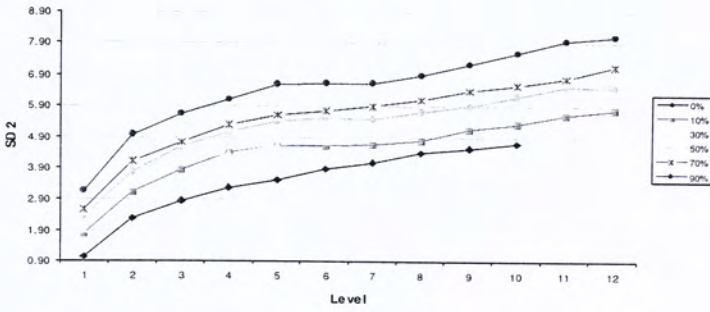
Figure A.2 Variation of Standard Deviation (VNIR 1) for different land cover objects along segmentation gradient. Case in Chongqing.



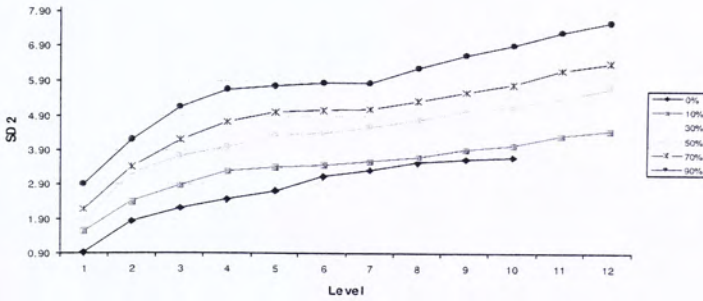
River



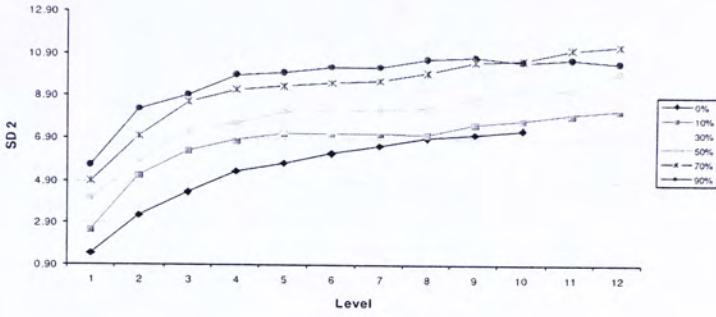
Grassland



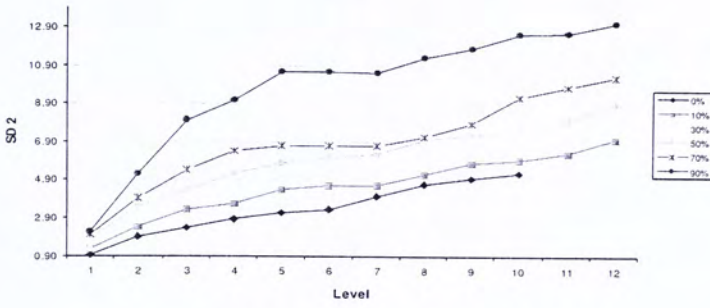
Woodland



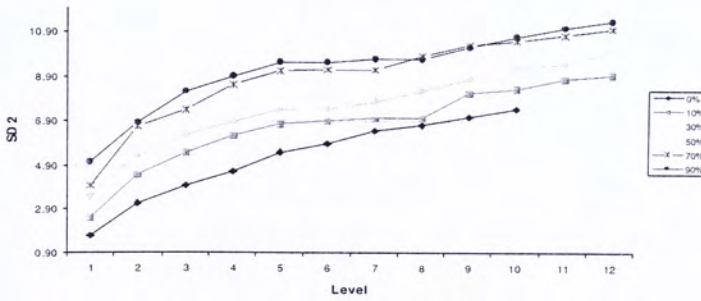
Bareland

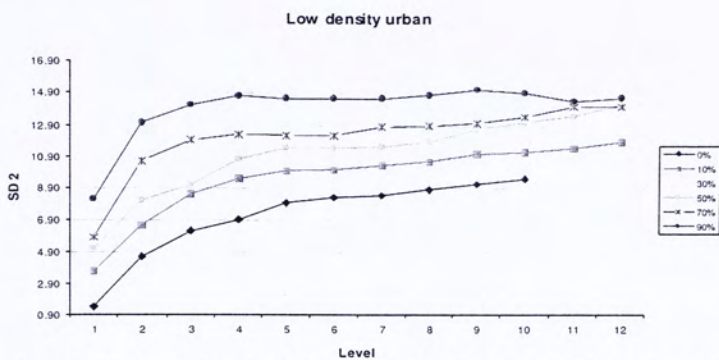


Industrial



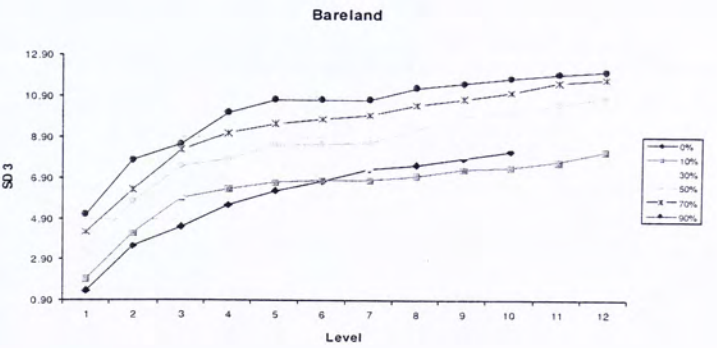
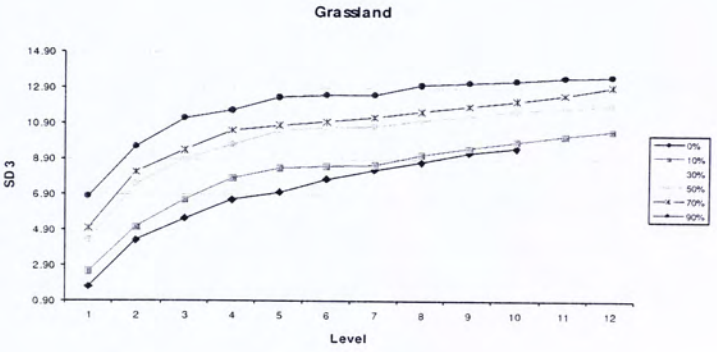
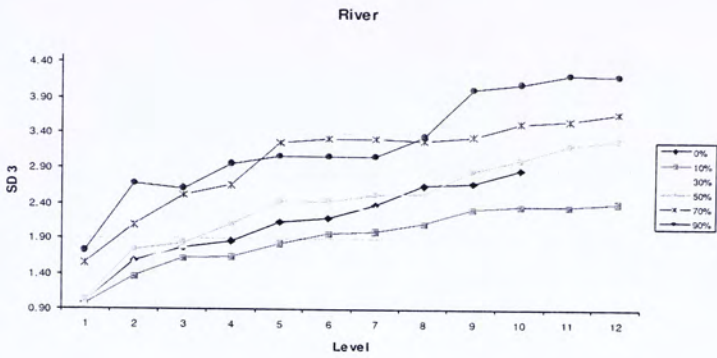
High density urban

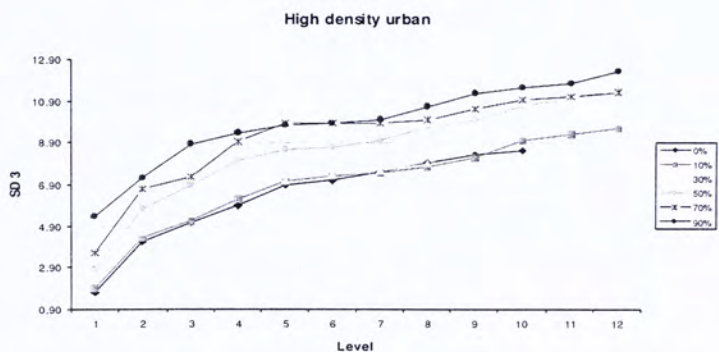
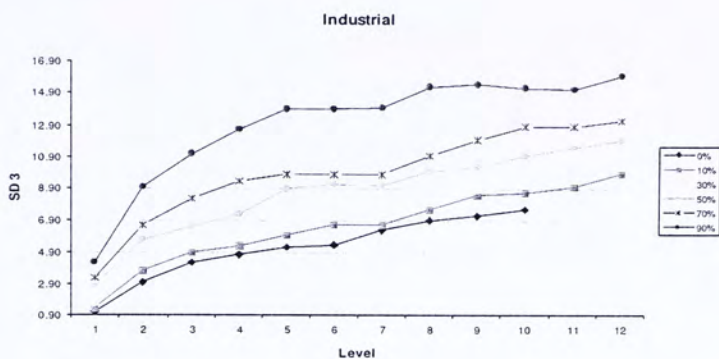




0% --0% weight of spectral-shape ratio; 10% --10% weight of spectral-shape ratio; 30% --30% weight of spectral-shape ratio; 50% --50% weight of spectral-shape ratio; 70% --70% weight of spectral-shape ratio; 90% --90% weight of spectral-shape ratio.

Figure A.3 Variation of Standard Deviation (VNIR 2) for different land cover objects along segmentation gradient. Case in Chongqing.

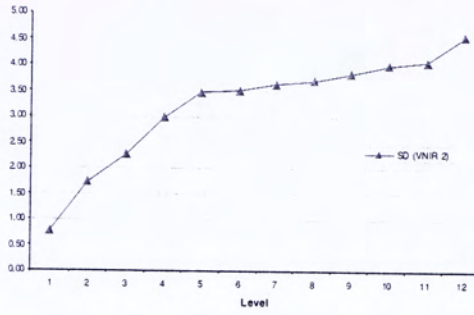




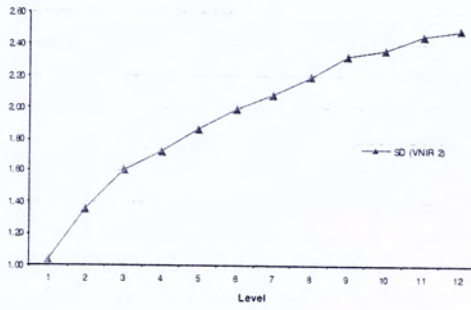
0% --0% weight of spectral-shape ratio; 10% --10% weight of spectral-shape ratio; 30% --30% weight of spectral-shape ratio;
 50% --50% weight of spectral-shape ratio; 70% --70% weight of spectral-shape ratio; 90% --90% weight of spectral-shape ratio.

Figure A.4 Variation of Standard Deviation (VNIR 3) for "river", "grassland", "bareland", "industrial" and "high density urban" along segmentation gradient. Case in Chongqing.

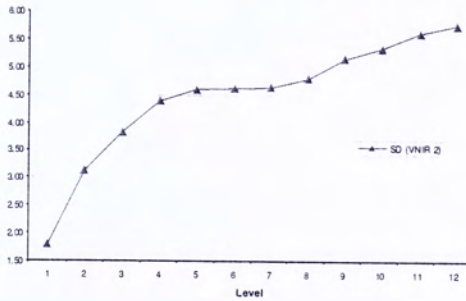
Lake



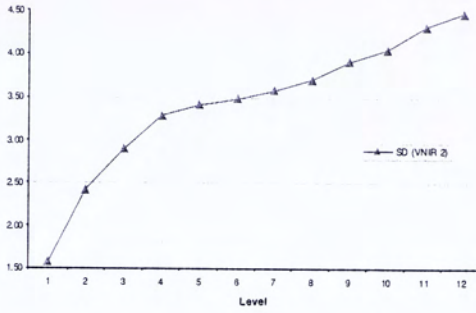
River



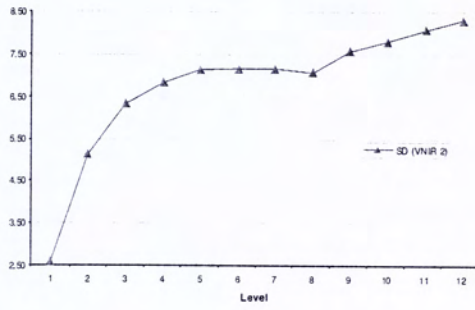
Grassland



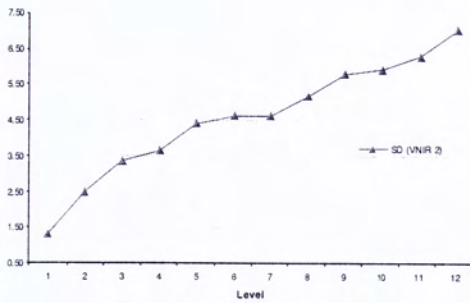
Woodland



Bareland



Industrial



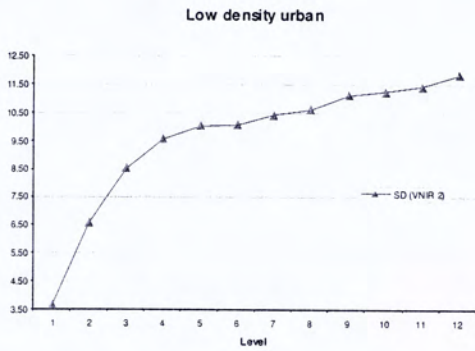
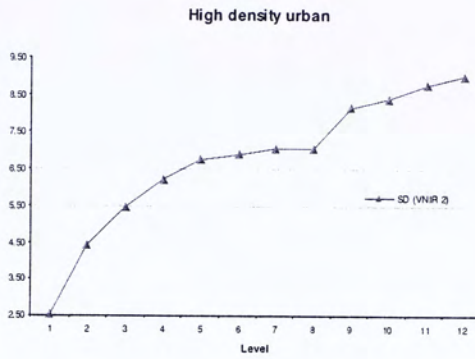
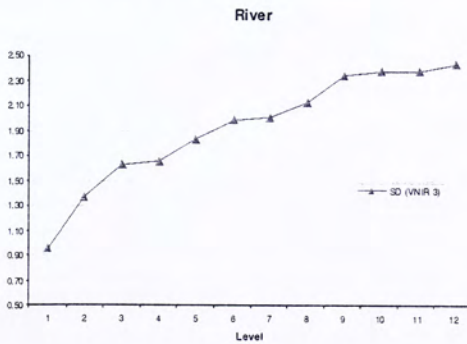
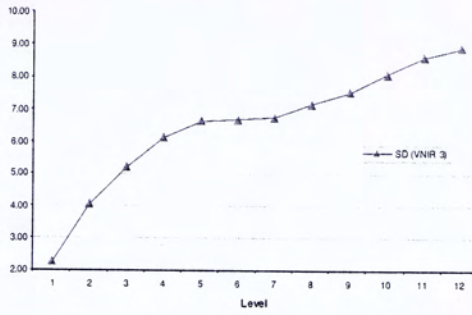


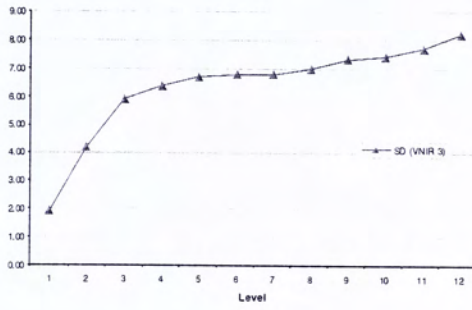
Figure A.5 Variability of Standard Deviation of VNIR 2 for different land cover objects along segmentation gradient (Spectral-shape ratio: 9:1). Case in Chongqing.



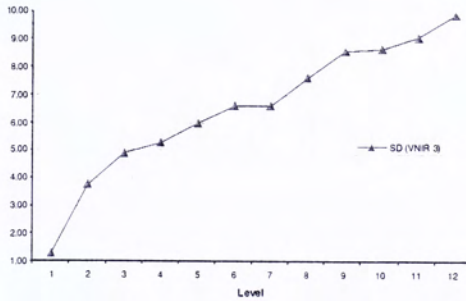
Woodland



Bareland



Industrial



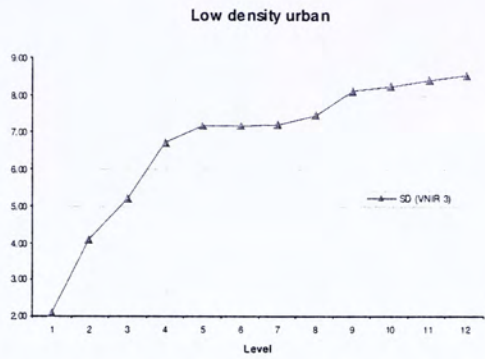
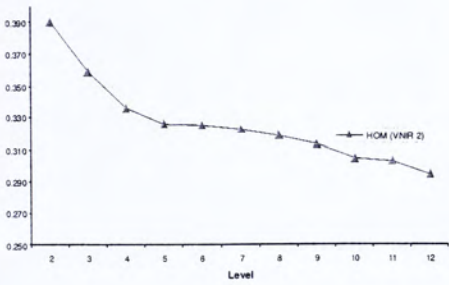
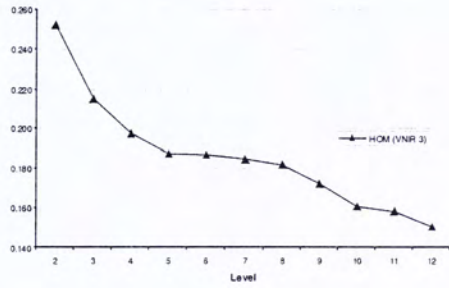


Figure A.6 Variability of Standard Deviation of VNIR 3 for different land cover objects along segmentation gradient (Spectral-shape ratio: 9:1). Case in Chongqing.

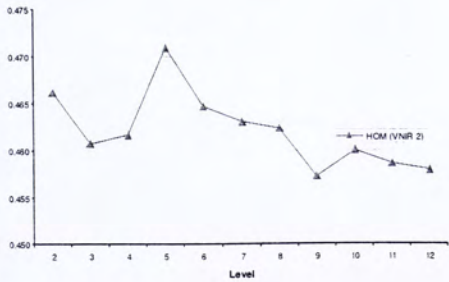
Lake



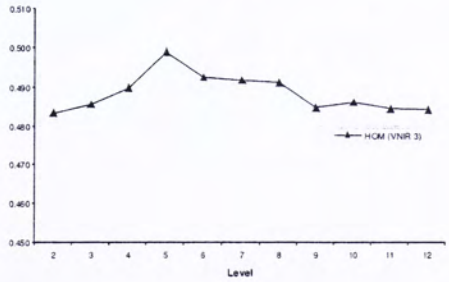
Lake



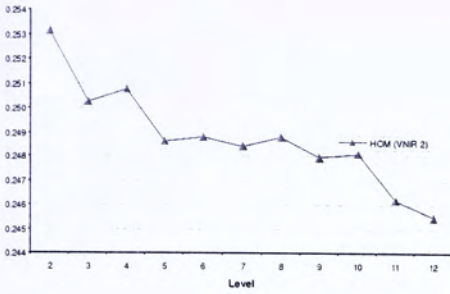
River



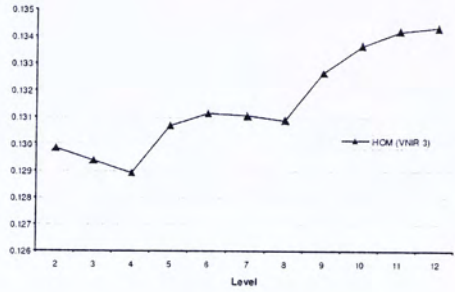
River



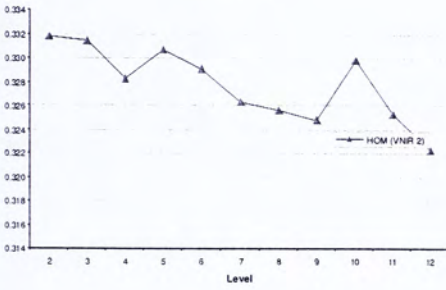
Grassland



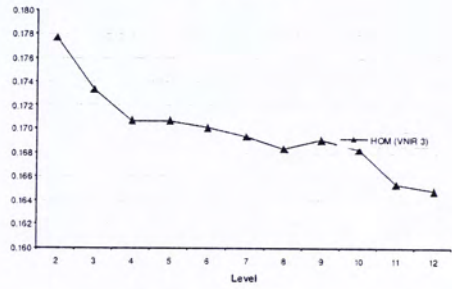
Grassland



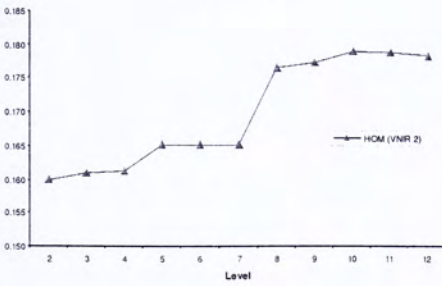
Woodland



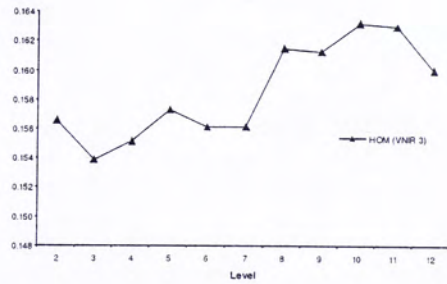
Woodland



Bareland



Bareland



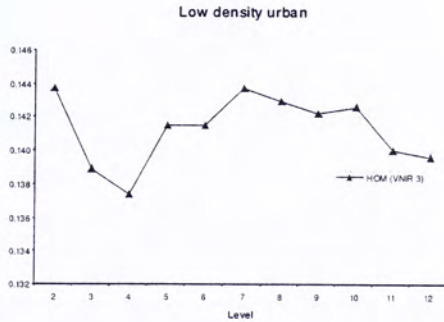
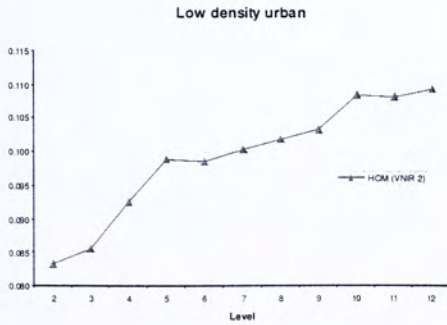
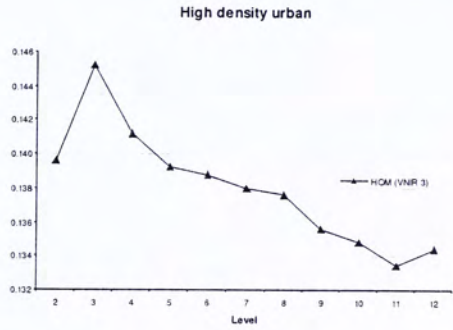
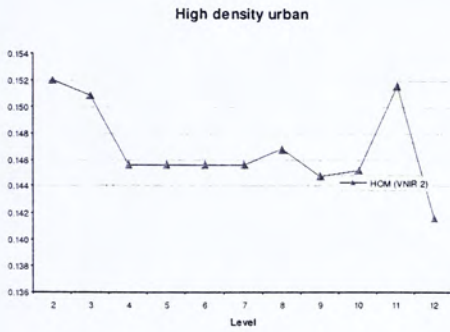
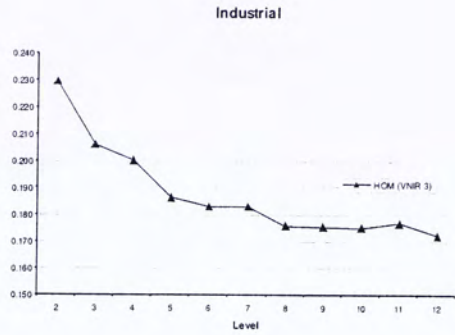
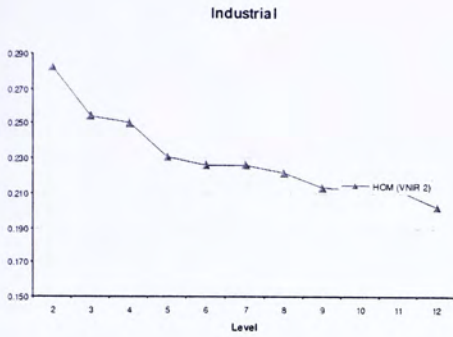
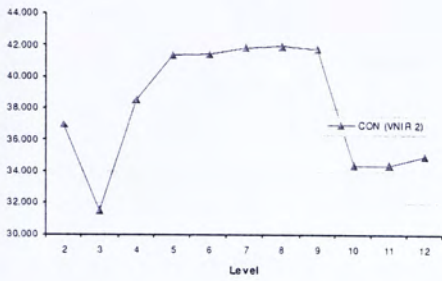
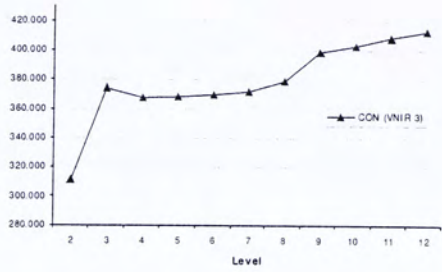


Figure A.7 Variability of GLCM Homogeneity (VNR 2 and 3) for land cover objects along segmentation gradient (Spectral-shape ratio: 9:1). Case in Chongqing.

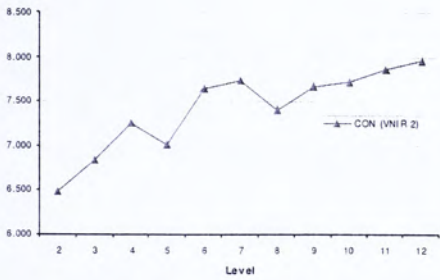
Lake



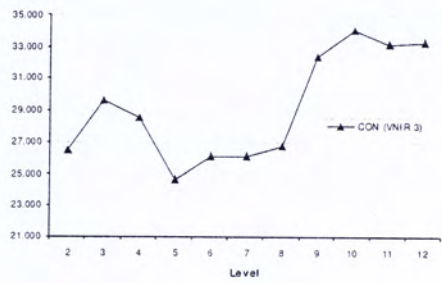
Lake



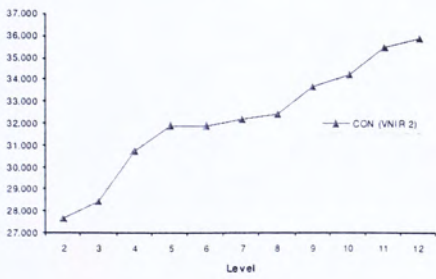
River



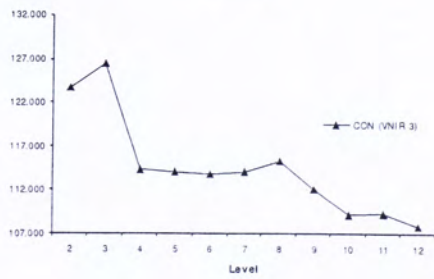
River



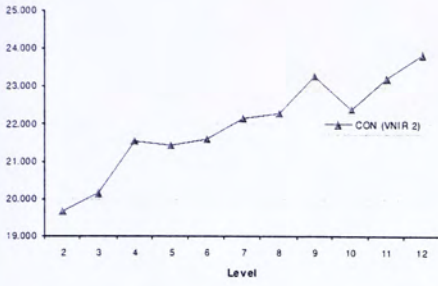
Grassland



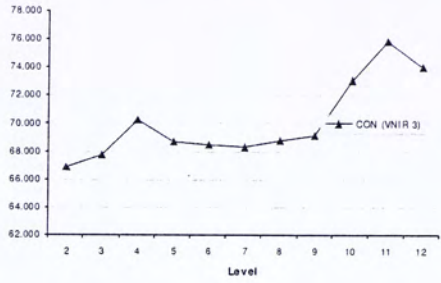
Grassland



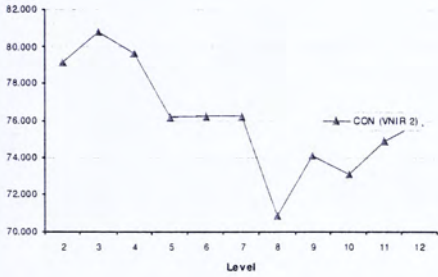
Woodland



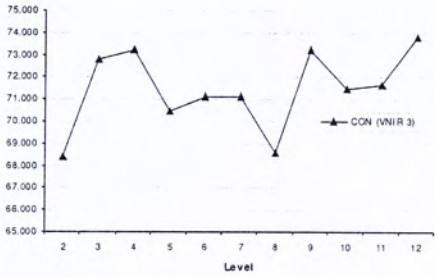
Woodland



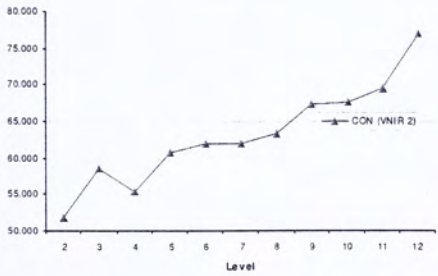
Bareland



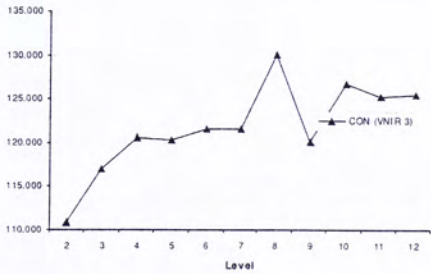
Bareland



Industrial



Industrial



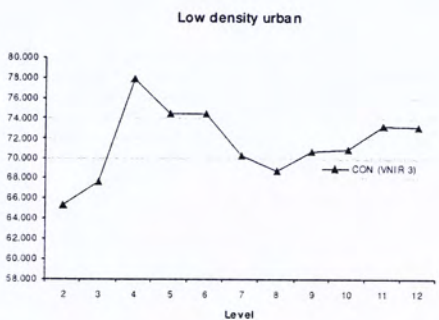
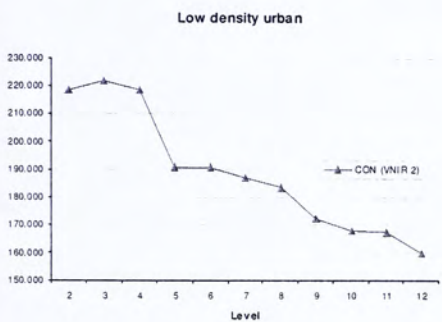
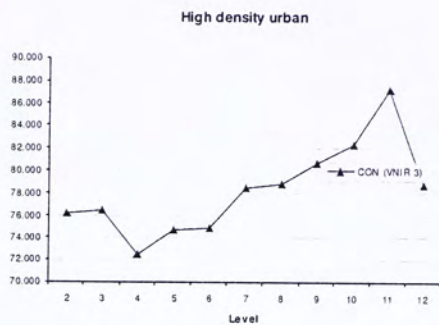
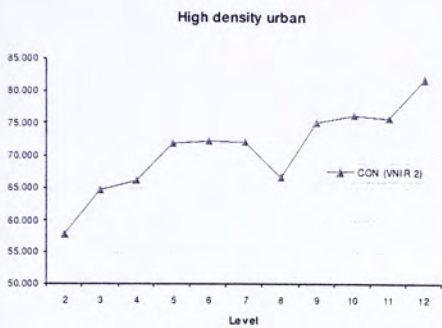
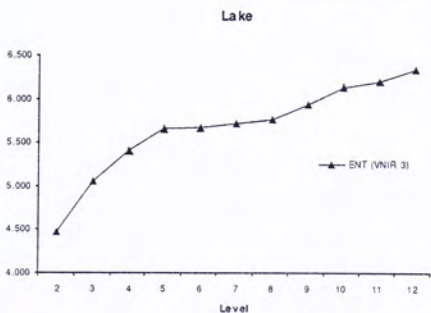
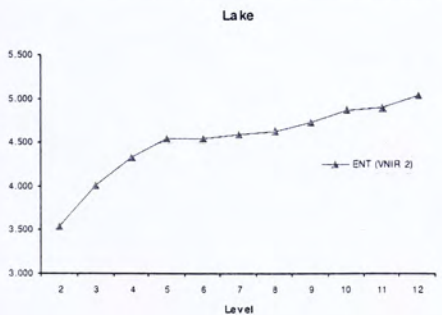
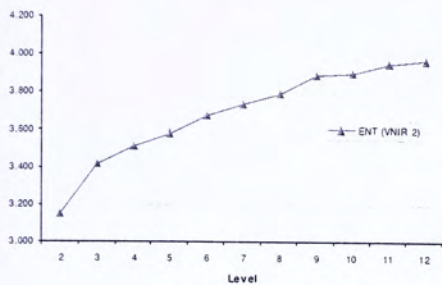


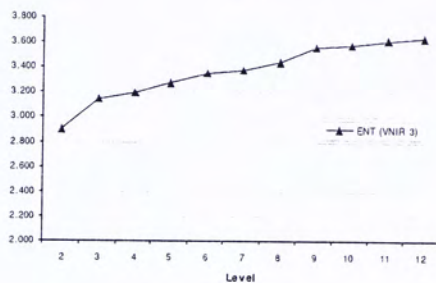
Figure A.8 Variability of GLCM Contrast (VNIR 2 and 3) for land cover objects along segmentation gradient (Spectral-shape ratio: 9:1). Case in Chongqing.



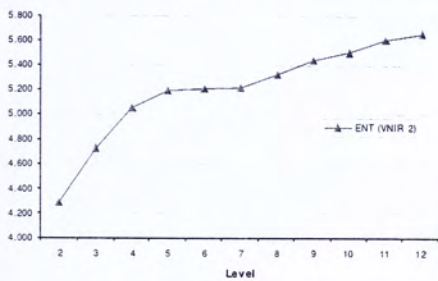
River



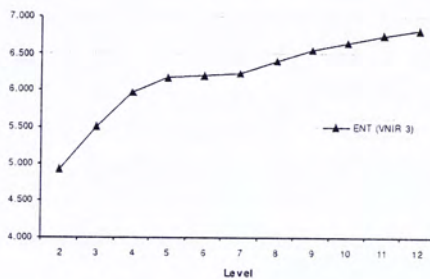
River



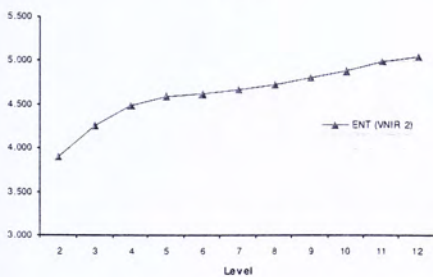
Grassland



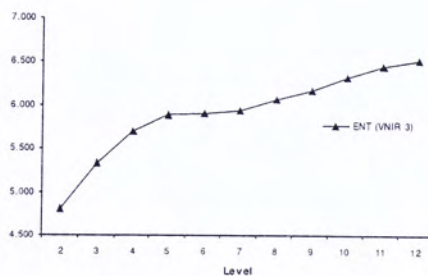
Grassland



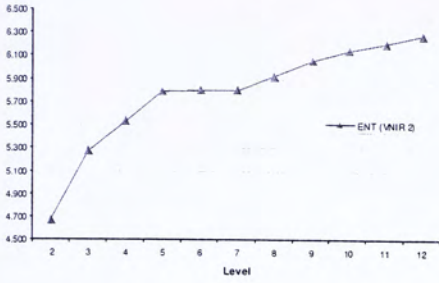
Woodland



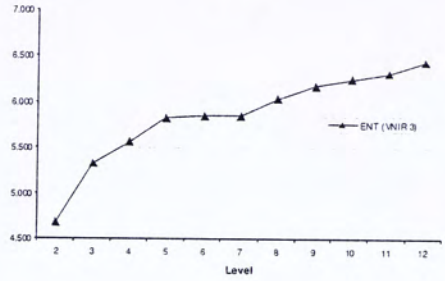
Woodland



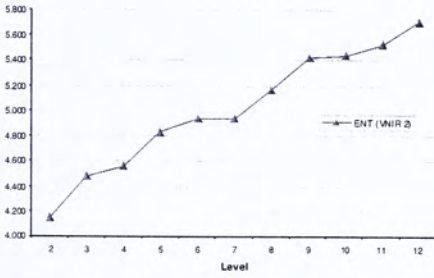
Bareland



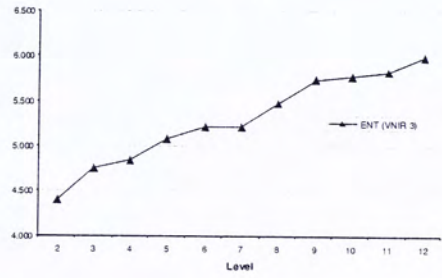
Bareland



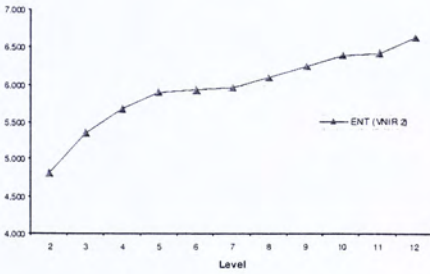
Industrial



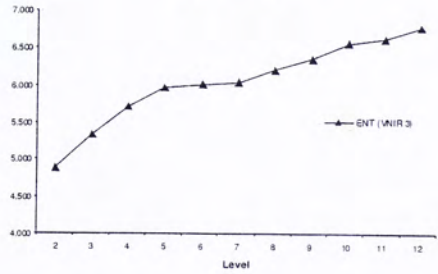
Industrial



High density urban



High density urban



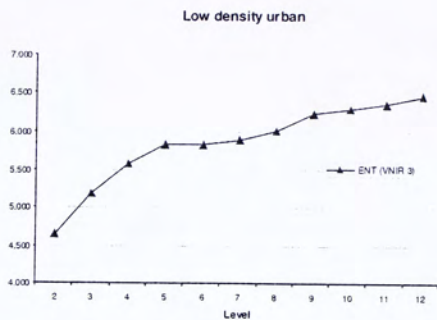
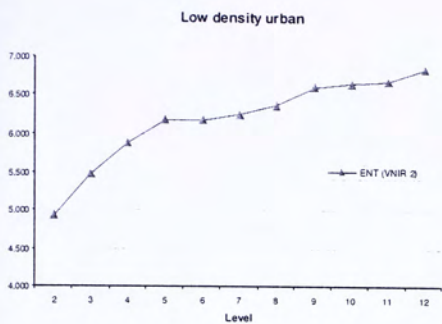
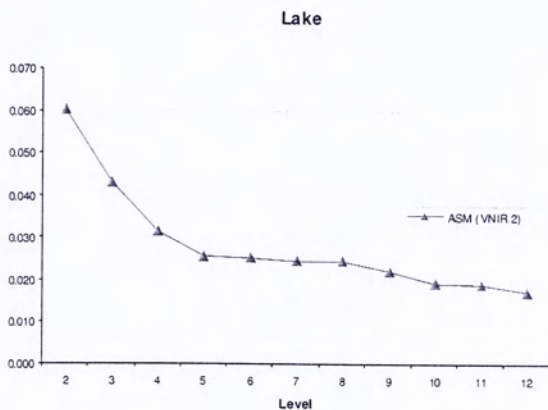
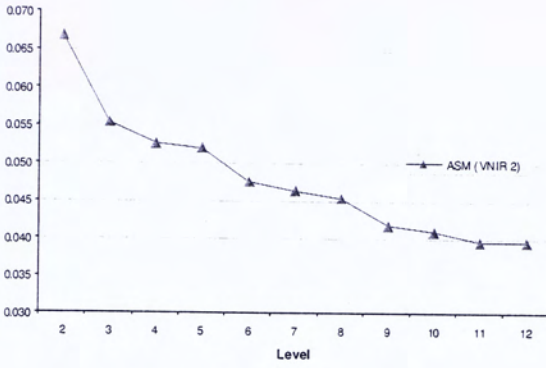


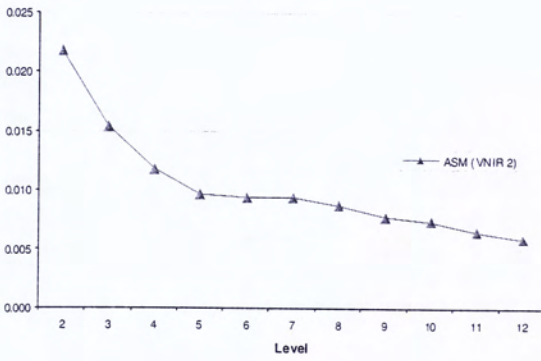
Figure A.9 Variability of GLCM Entropy (VNIR 2 and 3) for land cover objects along segmentation gradient (Spectral-shape ratio: 9:1). Case in Chongqing.



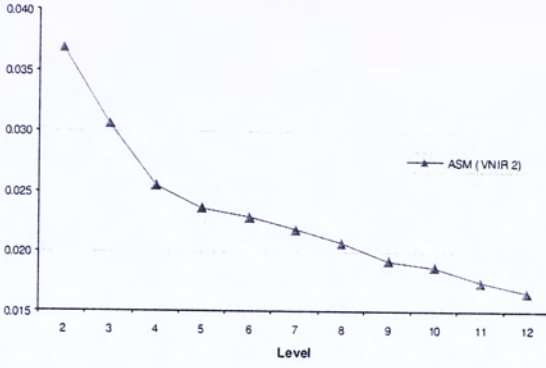
River



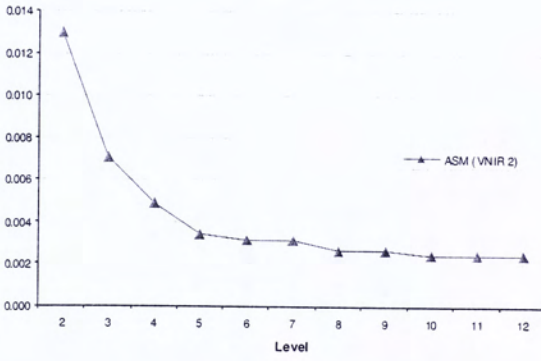
Grassland



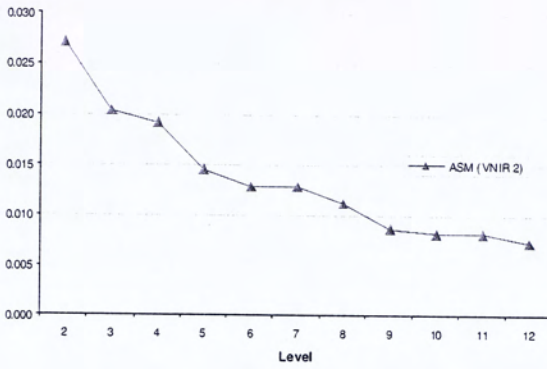
Woodland



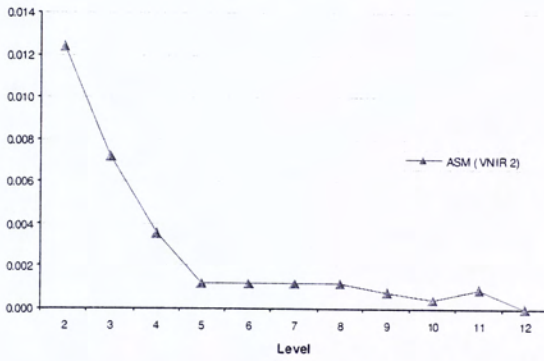
Bareland



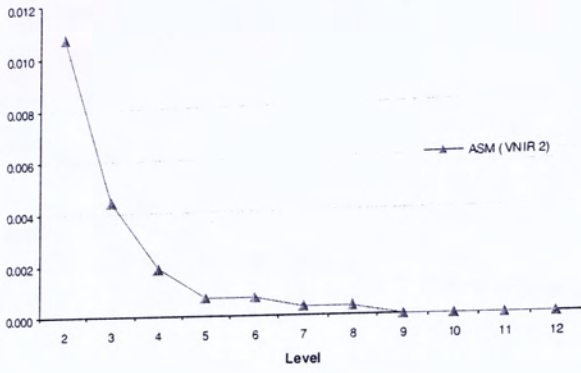
Industrial



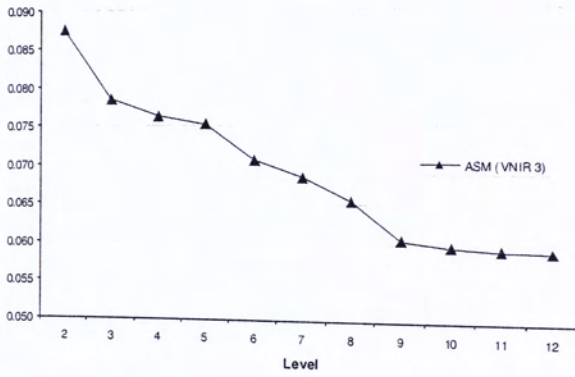
High density urban



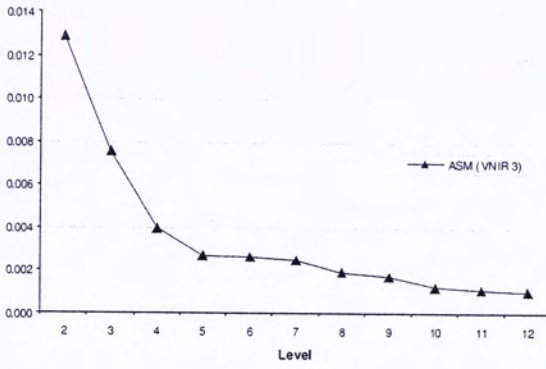
Low density urban



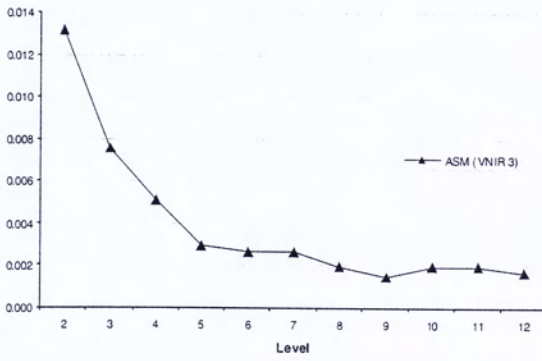
River



Woodland



Bareland



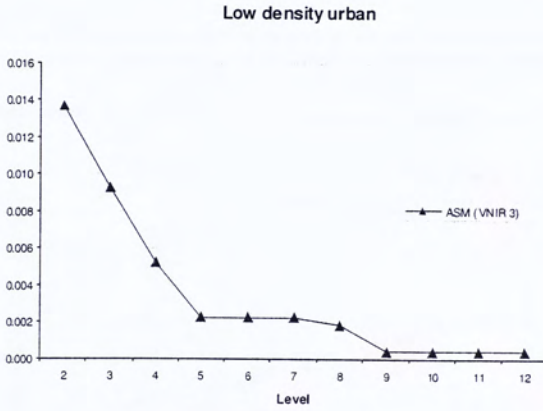
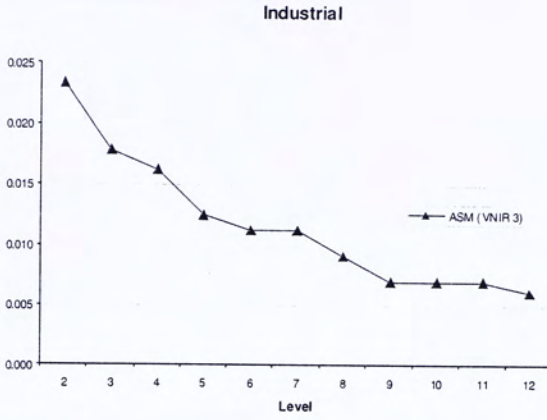


Figure A.10 Variability of GLCM Angular Second Moment (VNIR 2 and 3) for land cover objects along segmentation gradient (Spectral-shape ratio: 9:1). Case in Chongqing.

Appendix 4—Variations of Object Features along Segmentation Levels in Nanjing

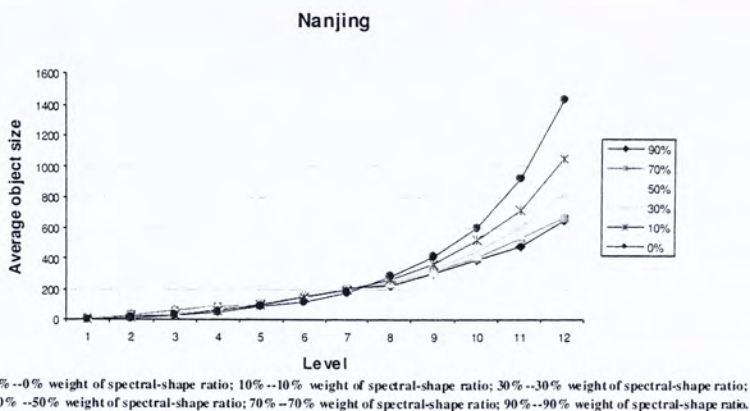
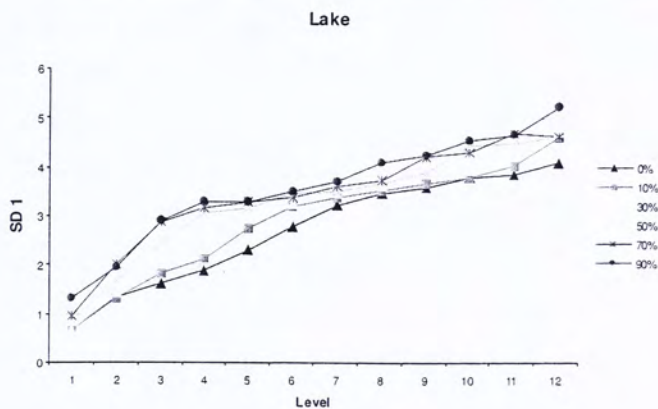
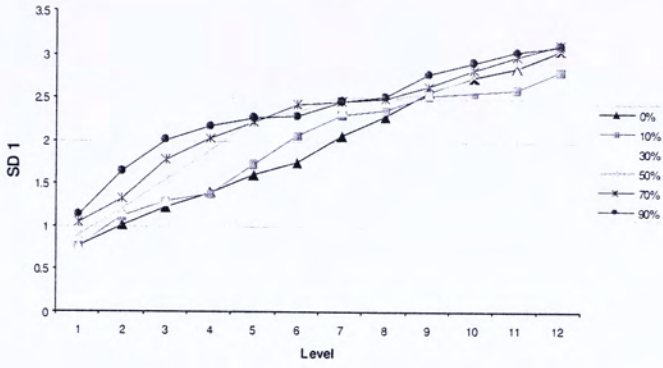


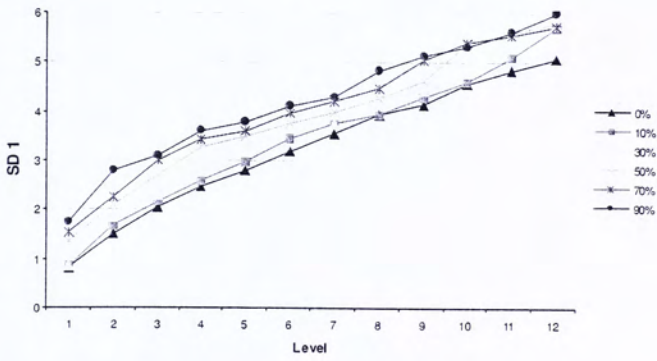
Figure A.11 Variation of average object size along segmentation gradient. Case in Chongqing.



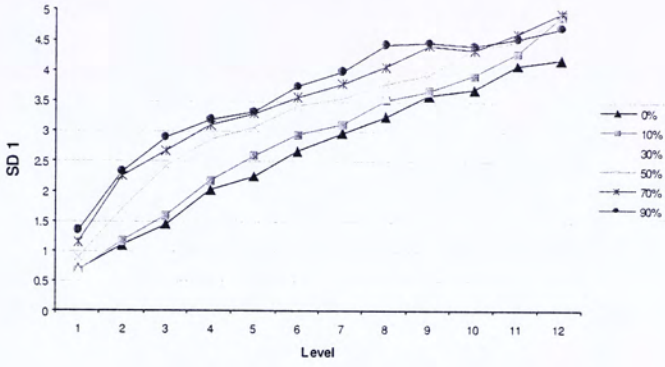
River



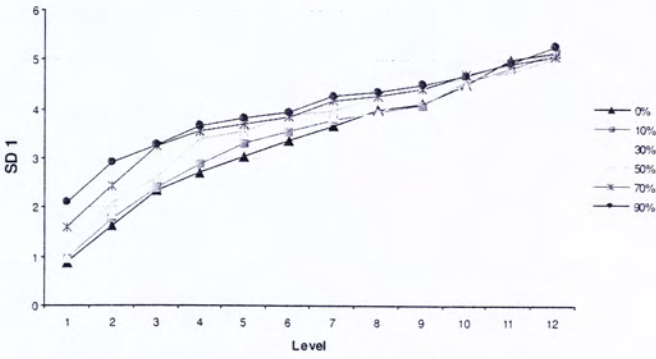
Woodland



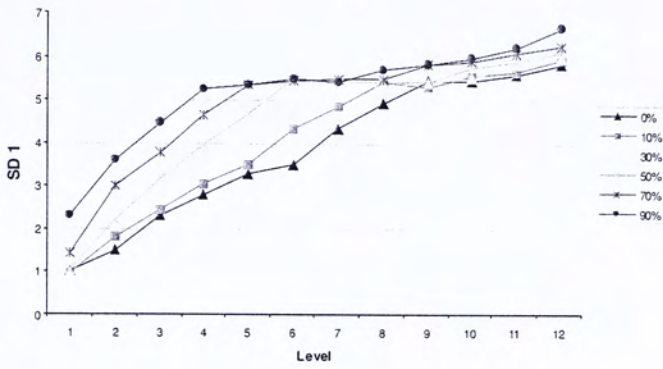
Agricultural crop I



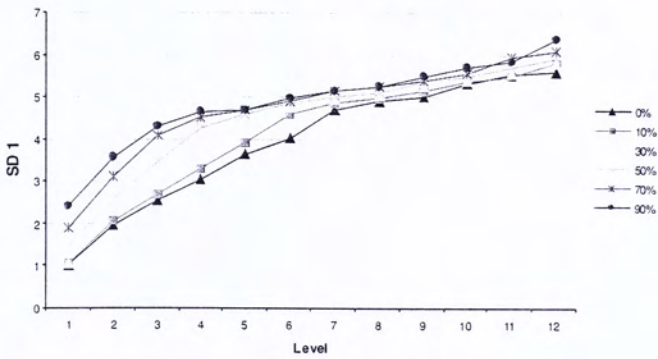
Agricultural crop II

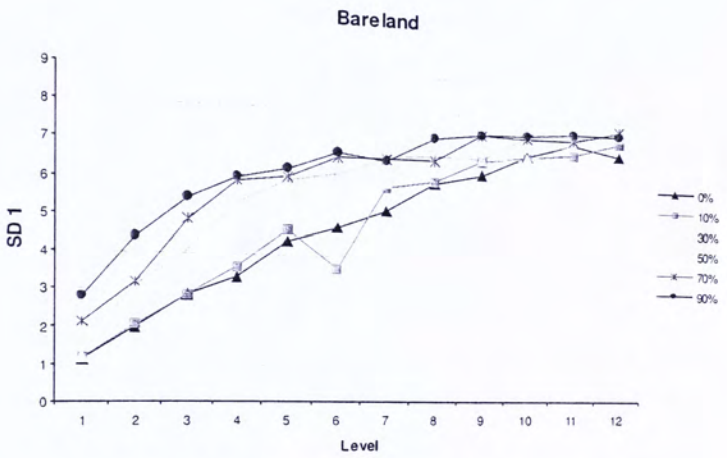
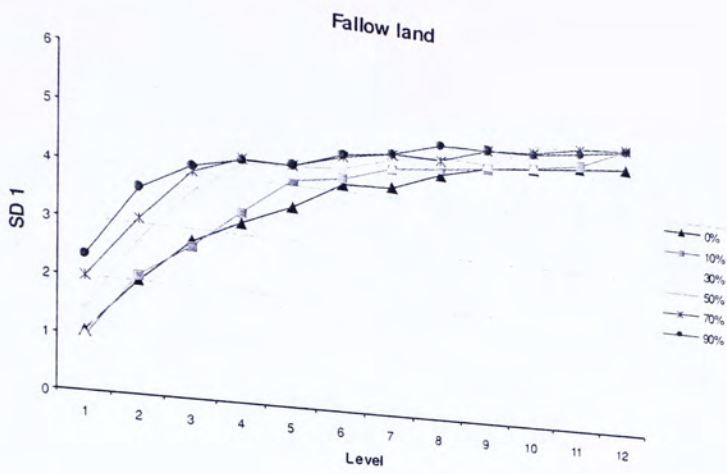


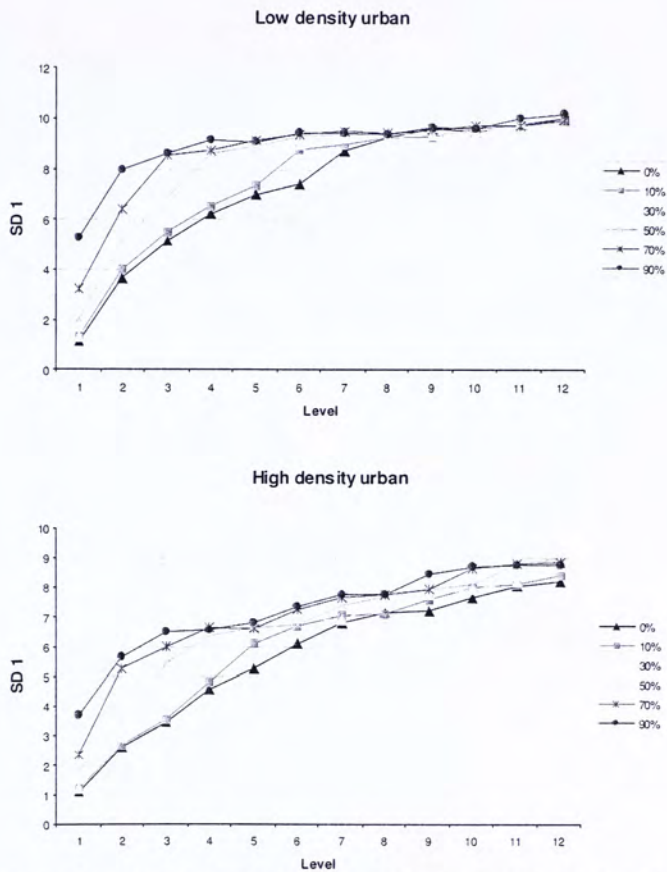
Wetland



Grassland



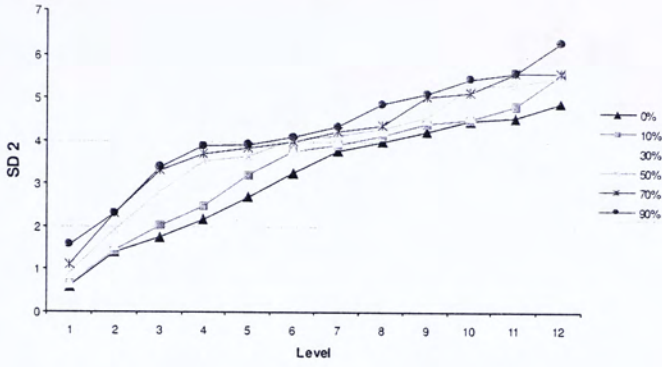




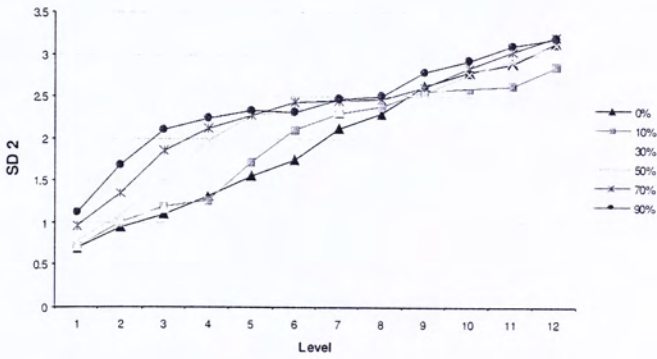
0%--0% weight of spectral-shape ratio; 10%--10% weight of spectral-shape ratio; 30%--30% weight of spectral-shape ratio;
 50%--50% weight of spectral-shape ratio; 70%--70% weight of spectral-shape ratio; 90%--90% weight of spectral-shape ratio.

Figure A.12 Variation of Standard Deviation (VNIR 1) for land cover objects along segmentation gradient. Case in Nanjing.

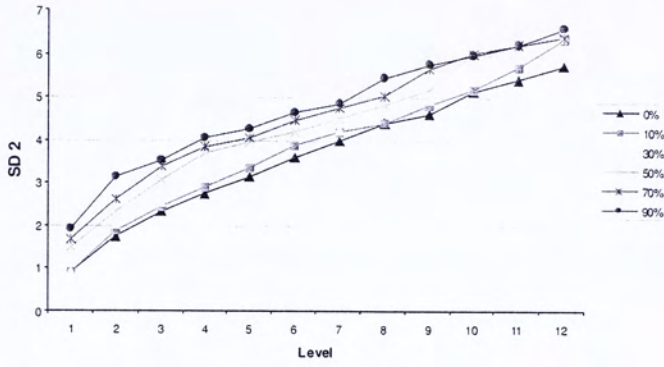
Lake



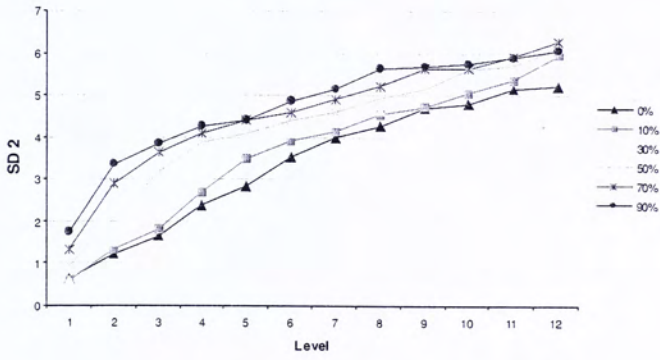
River



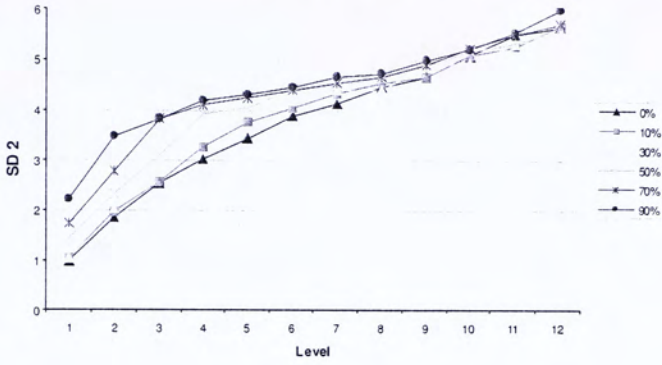
Woodland



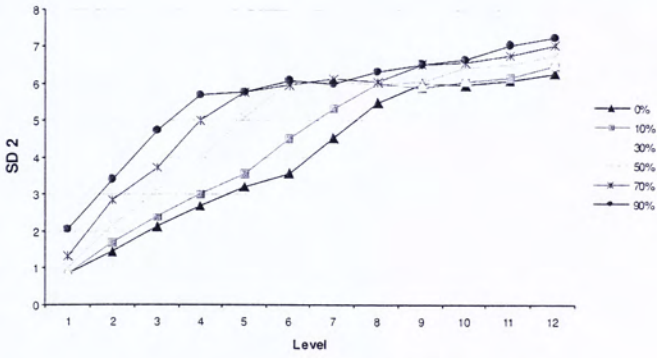
Agricultural crops I



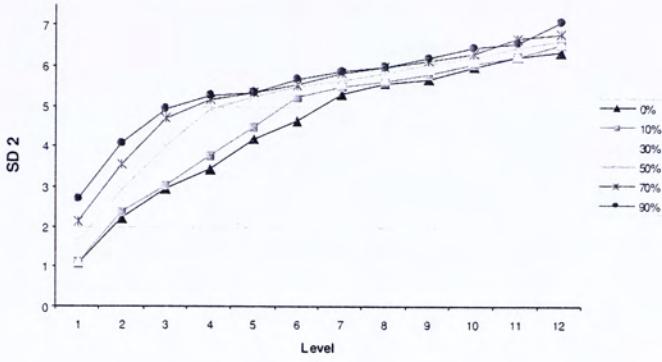
Agricultural crops II



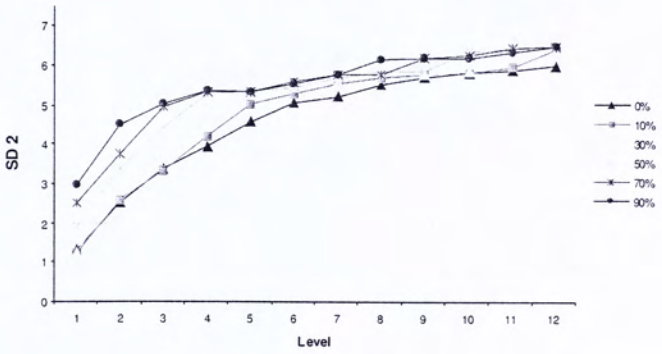
Wetland



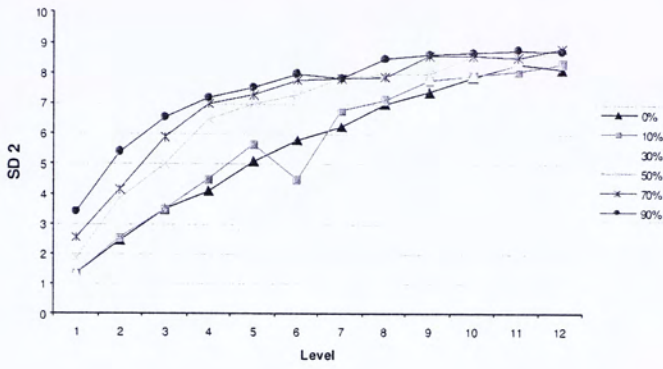
Grassland



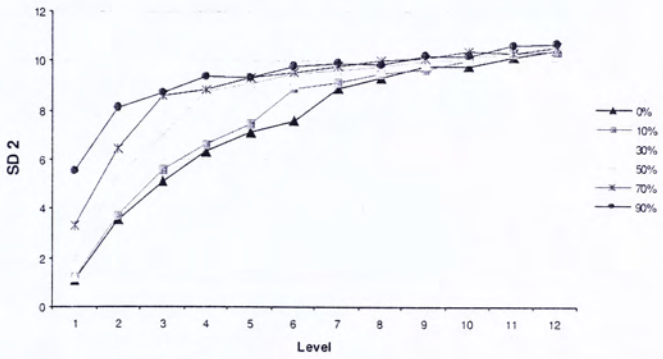
Fallow land

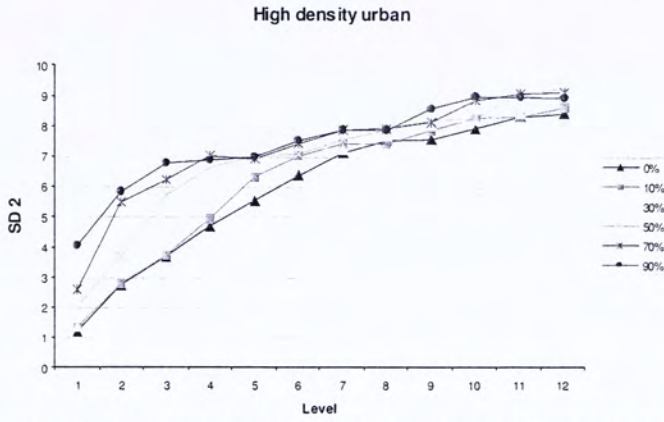


Bareland



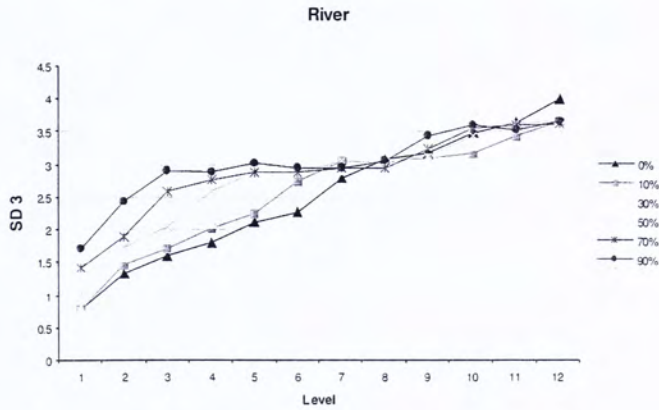
Low density urban



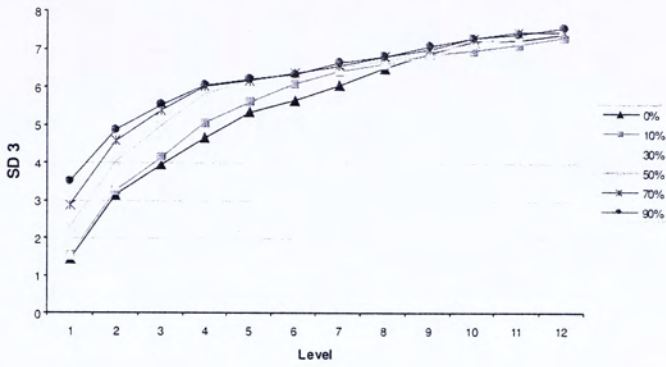


0%--0% weight of spectral-shape ratio; 10%--10% weight of spectral-shape ratio; 30%--30% weight of spectral-shape ratio; 50% --50% weight of spectral-shape ratio; 70% --70% weight of spectral-shape ratio; 90% --90% weight of spectral-shape ratio.

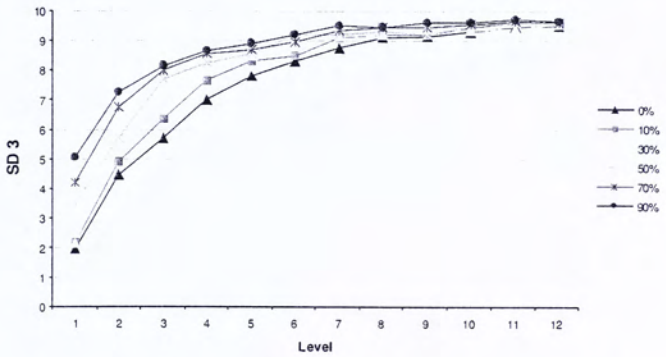
Figure A.13 Variations in Standard Deviation (VNIR 2) for land cover objects along segmentation gradient. Case in Nanjing.

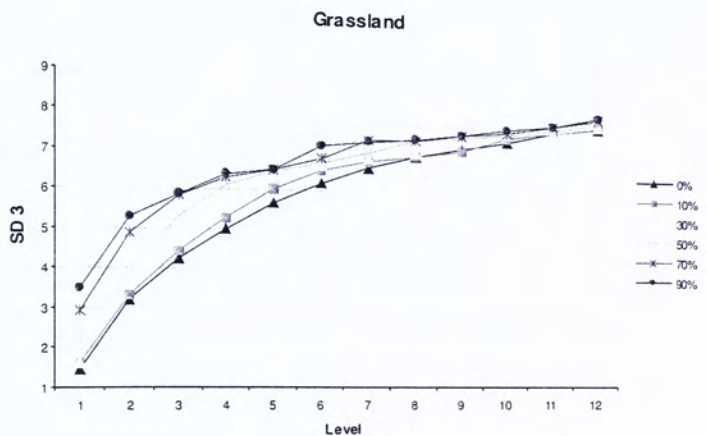
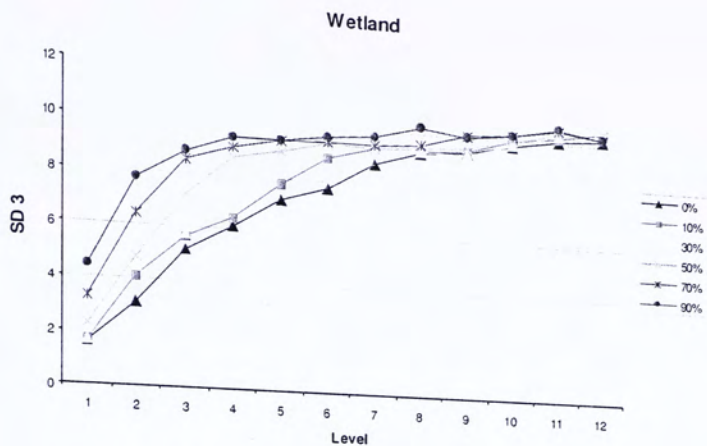


Woodland

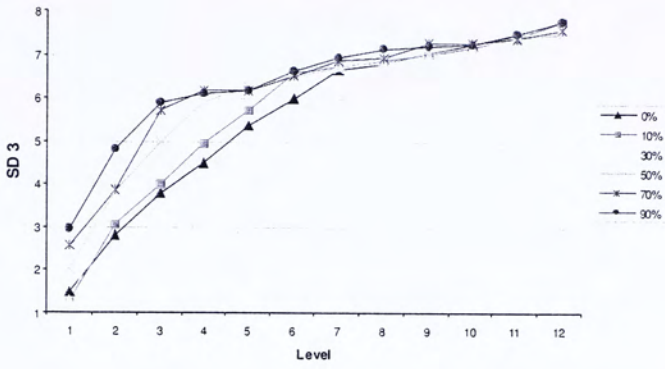


Agricultural crops II

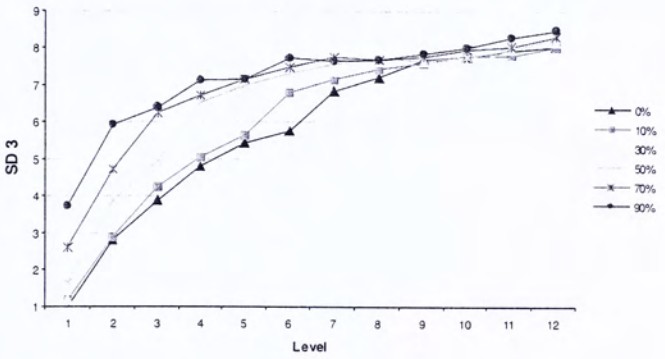




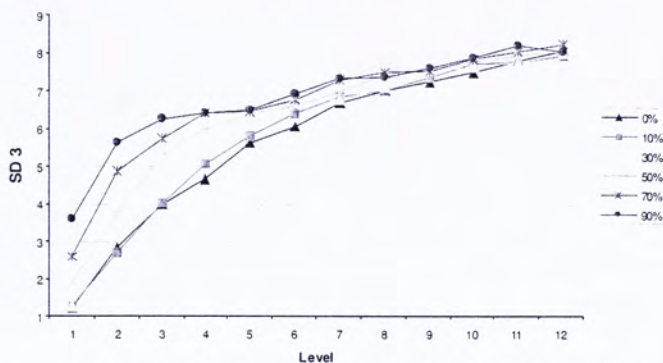
Fallow land



Low density urban



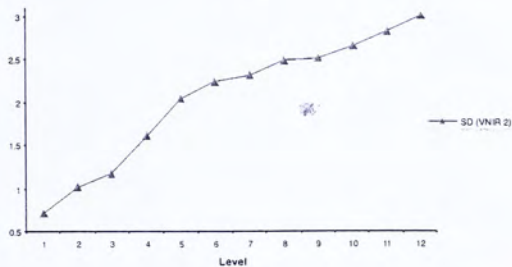
High density urban



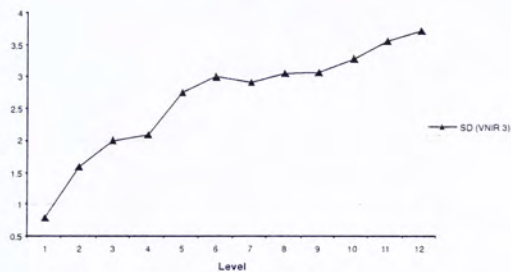
0%--0% weight of spectral-shape ratio; 10%--10% weight of spectral-shape ratio; 30%--30% weight of spectral-shape ratio; 50%--50% weight of spectral-shape ratio; 70%--70% weight of spectral-shape ratio; 90%--90% weight of spectral-shape ratio.

Figure A.14 Variations of Standard Deviation (VNIR 3) for land cover objects along segmentation gradient. Case in Nanjing.

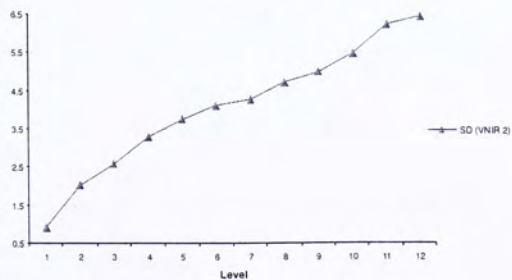
River



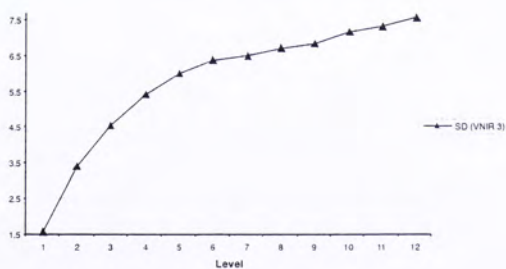
River



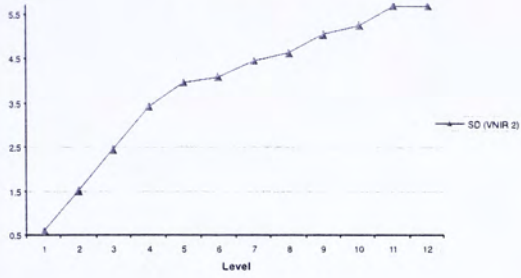
Woodland



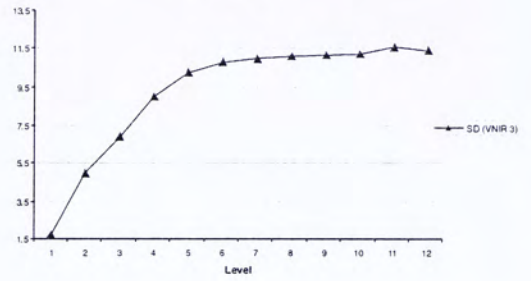
Woodland



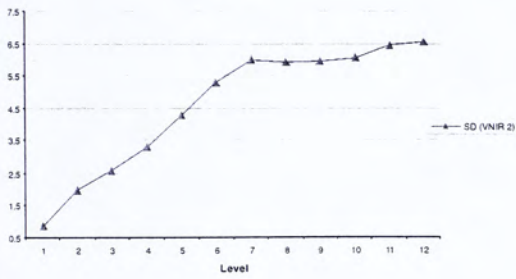
Agricultural crops I



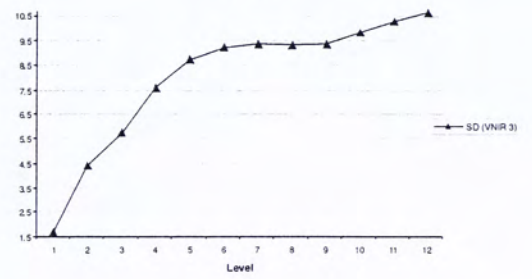
Agricultural crops I



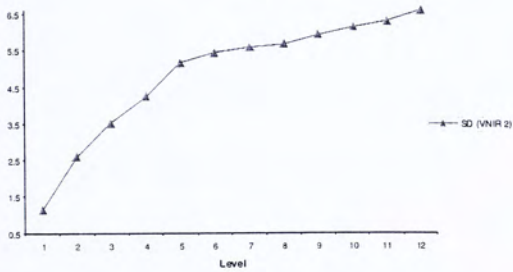
Wetland



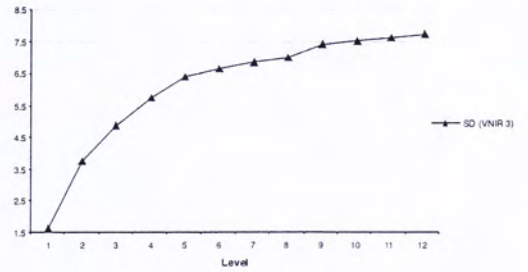
Wetland



Grassland



Grassland



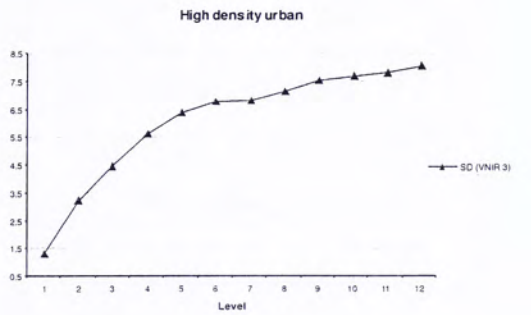
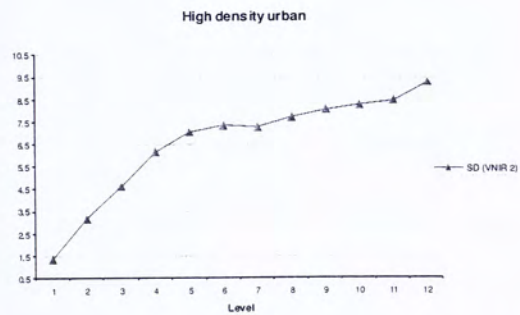
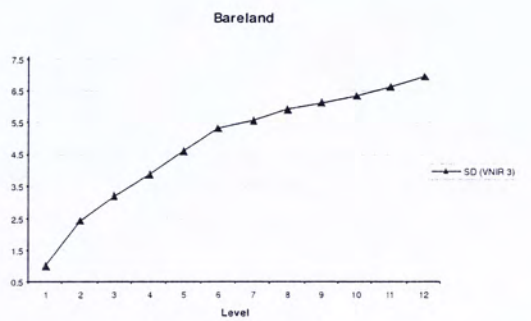
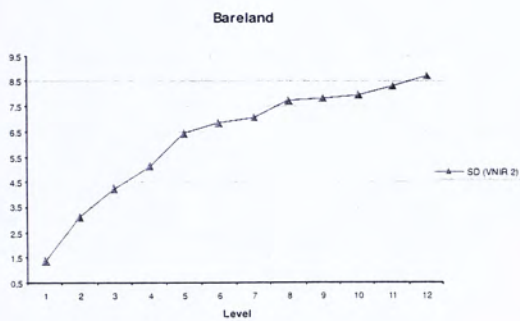
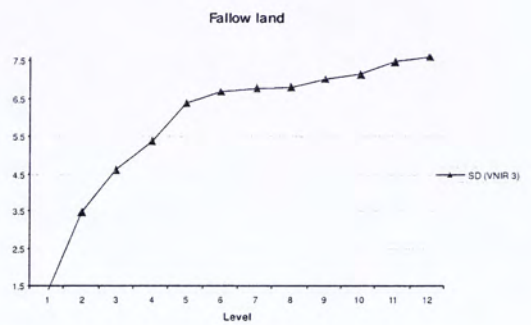
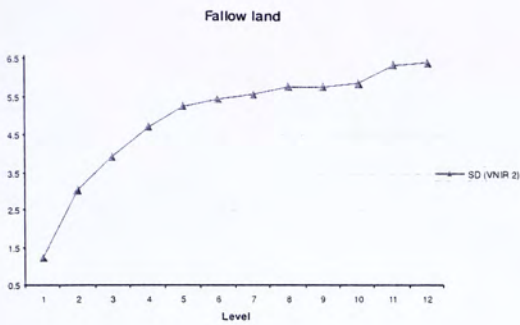
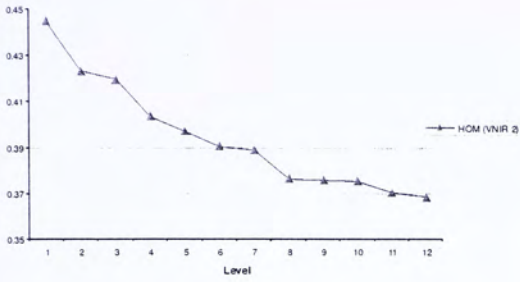
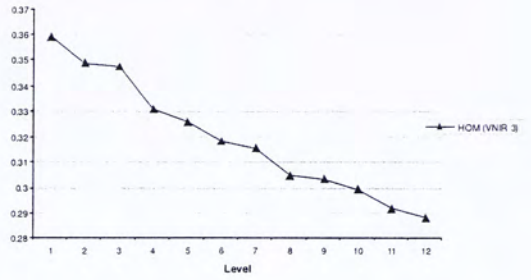


Figure A.15 Variability of Standard Deviation (VNIR 2 and 3) for land cover objects along segmentation gradient (Spectral-shape ratio: 7:3). Case in Nanjing.

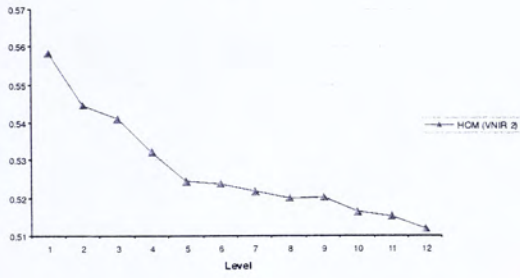
Lake



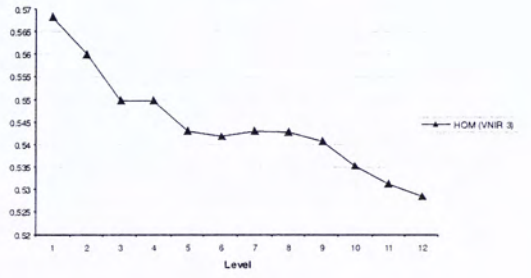
Lake



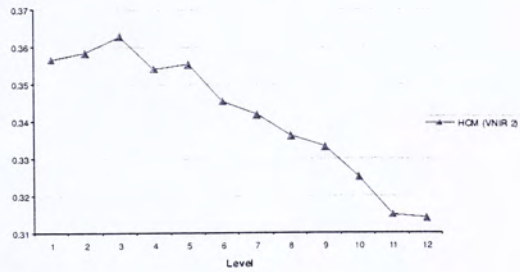
River



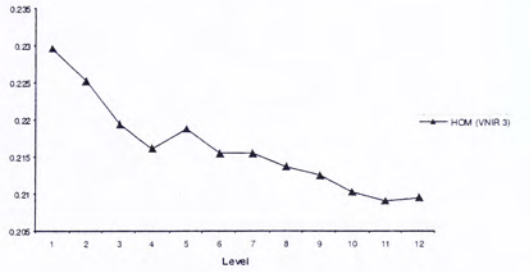
River



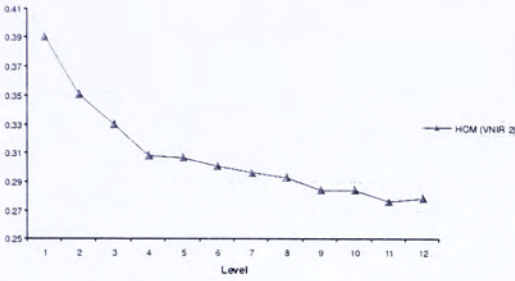
Woodland



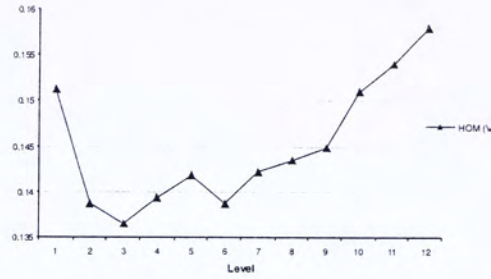
Woodland



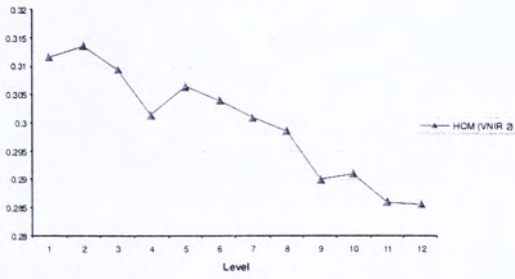
Agricultural crops I



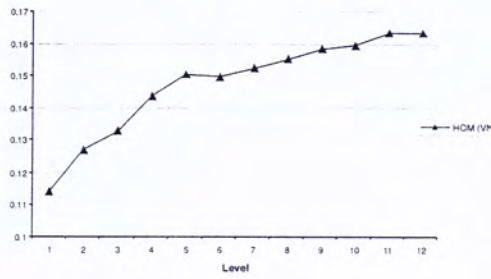
Agricultural crops I



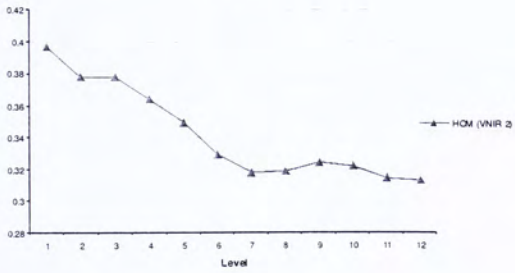
Agricultural crops II



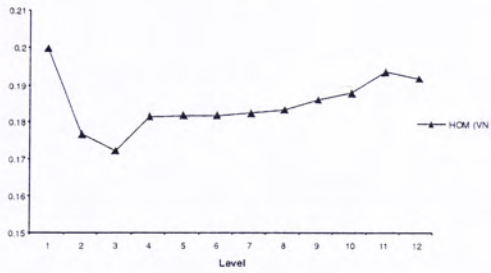
Agricultural crops II



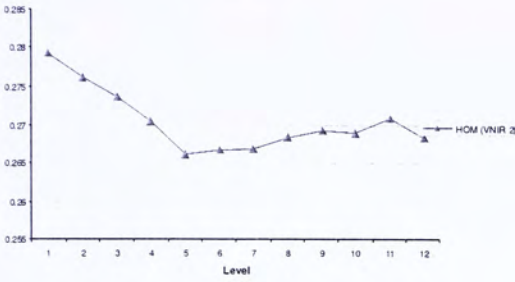
Wetland



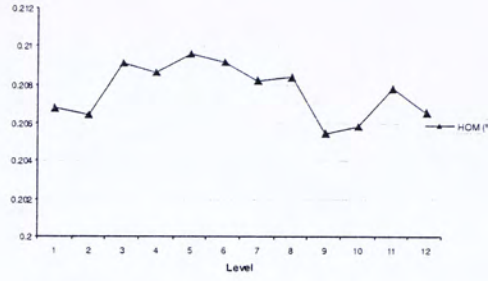
Wetland



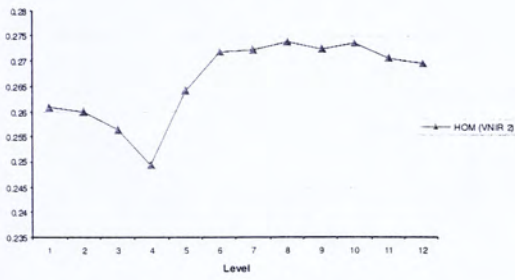
Grassland



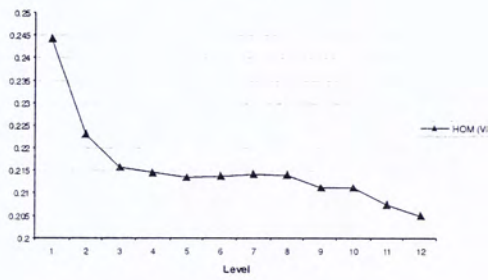
Grassland



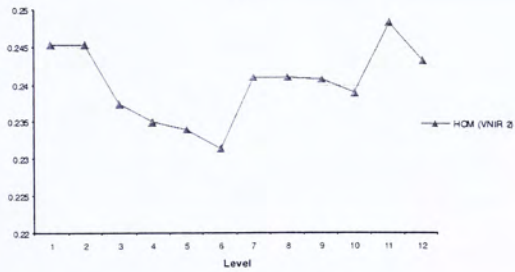
Fallow land



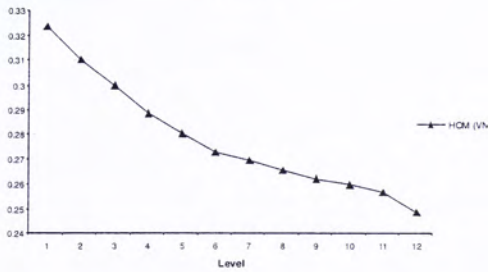
Fallow land



Bareland



Bareland



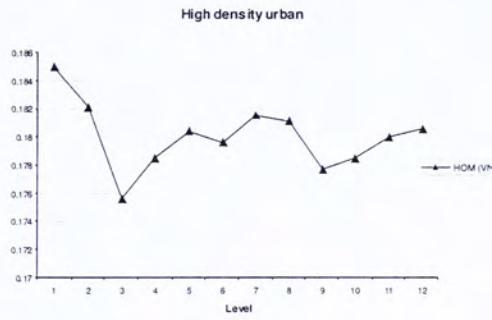
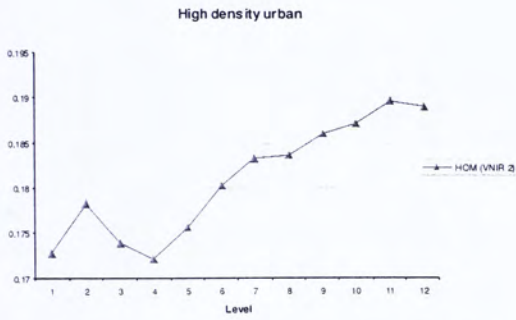
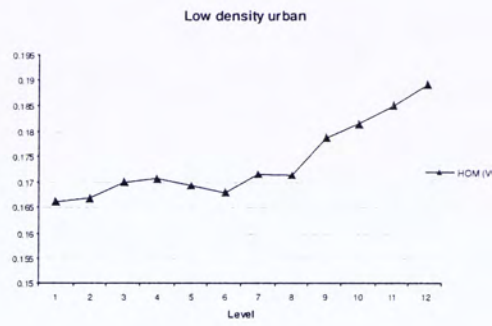
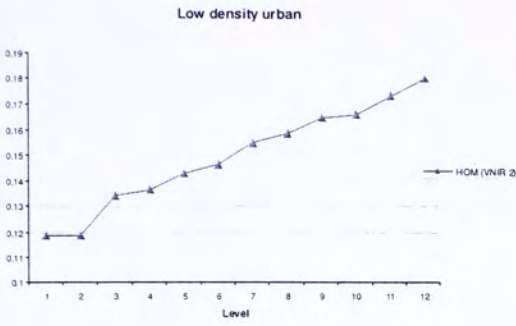
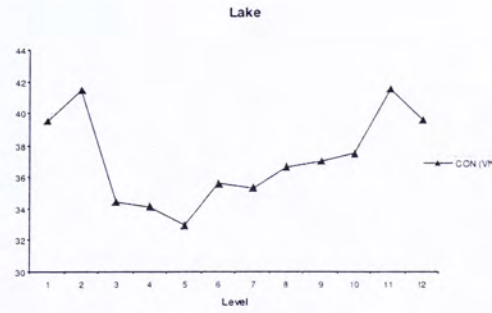
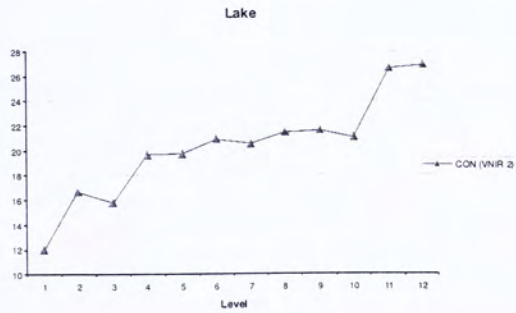
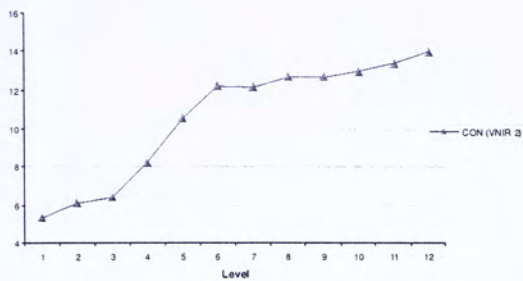


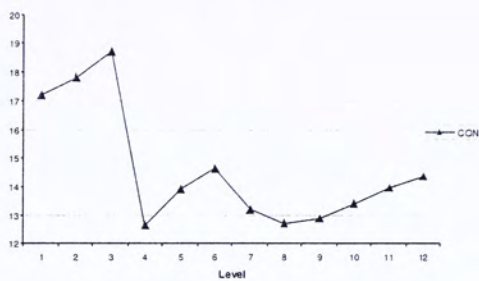
Figure A.16 Variability of GLCM Homogeneity (VNIR 2 and 3) for land cover objects along segmentation gradient (Spectral-shape ratio: 7:3). Case in Nanjing.



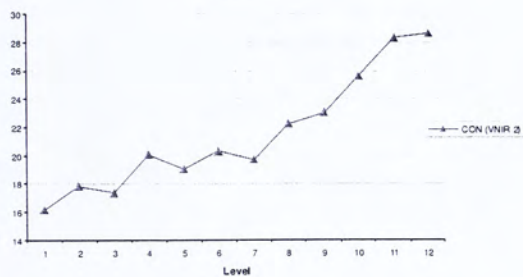
River



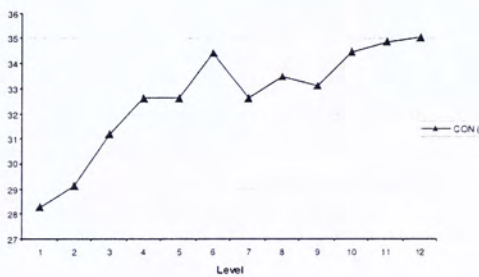
River



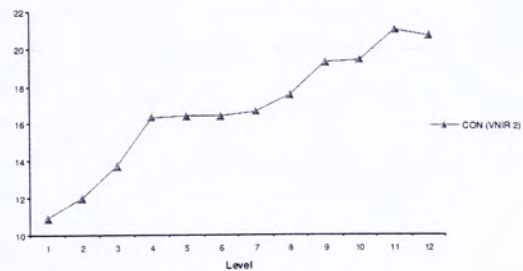
Woodland



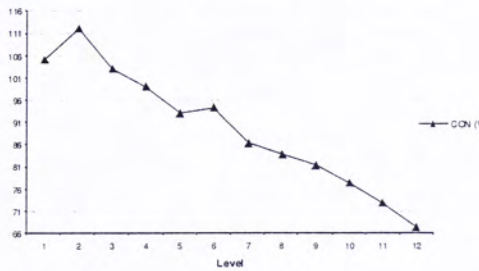
Woodland



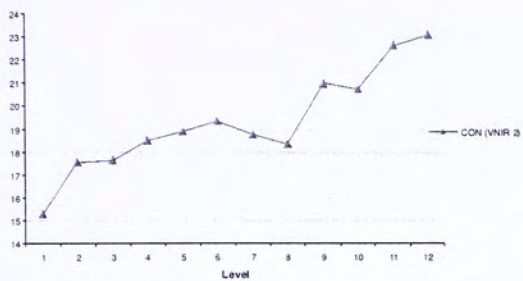
Agricultural crops I



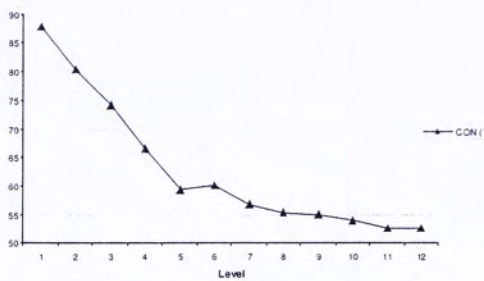
Agricultural crops I



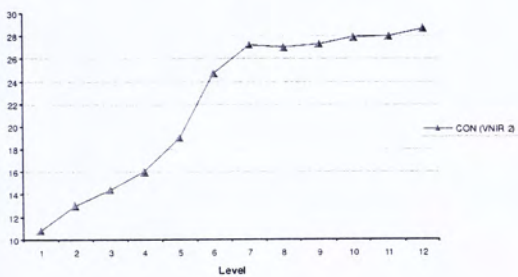
Agricultural crops II



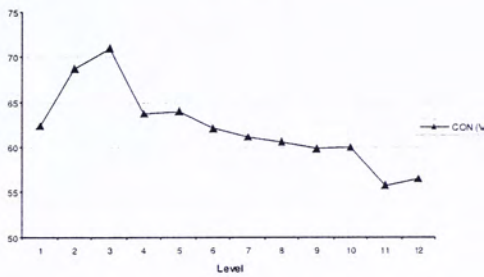
Agricultural crops II



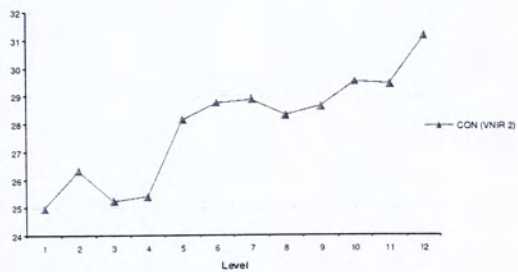
Wetland



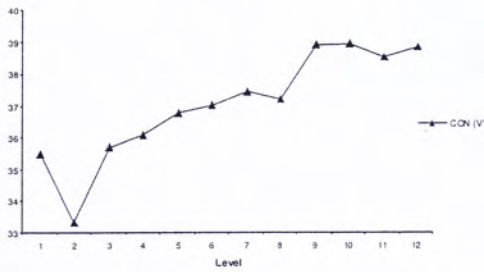
Wetland



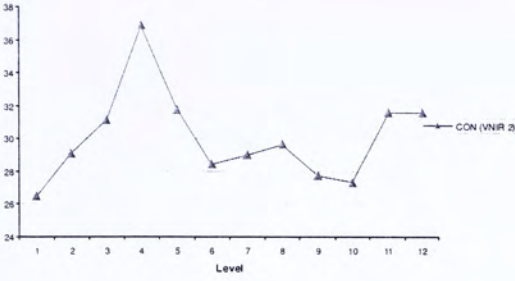
Grassland



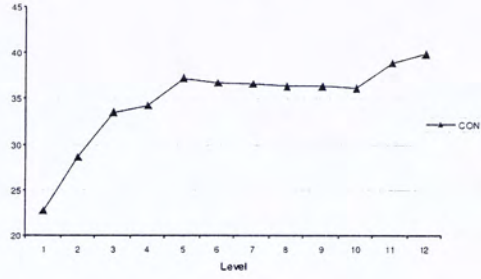
Grassland



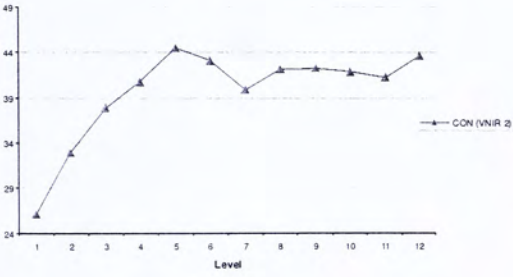
Fallow land



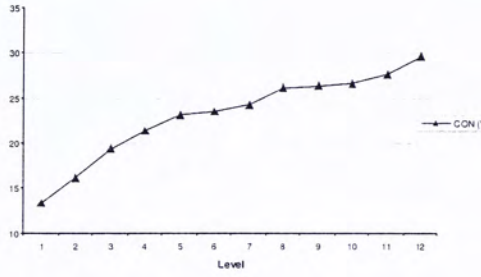
Fallow land



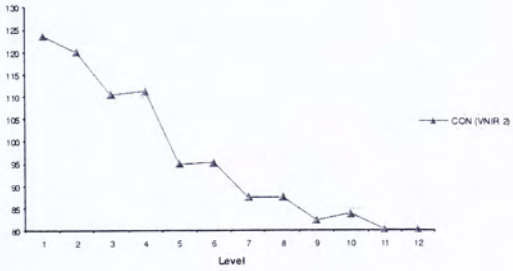
Bareland



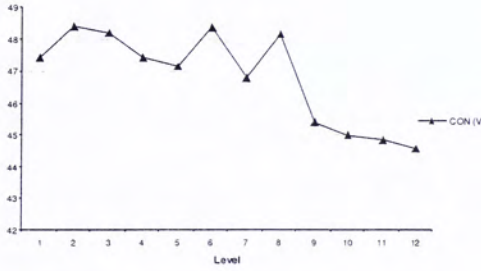
Bareland



Low density urban



Low density urban



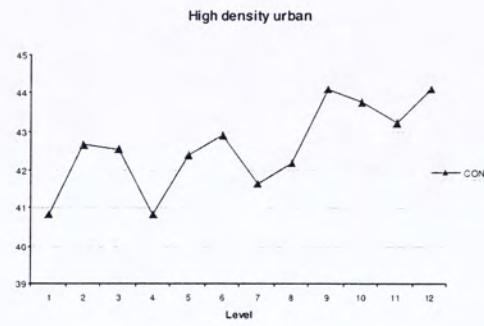
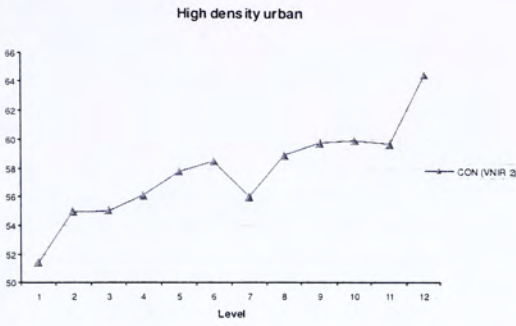
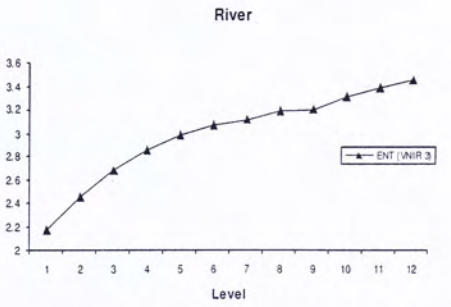
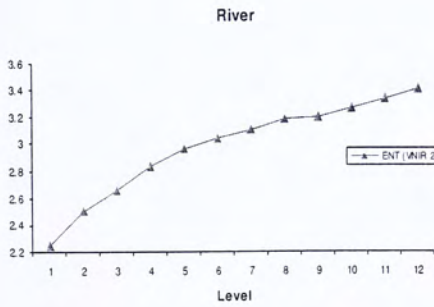
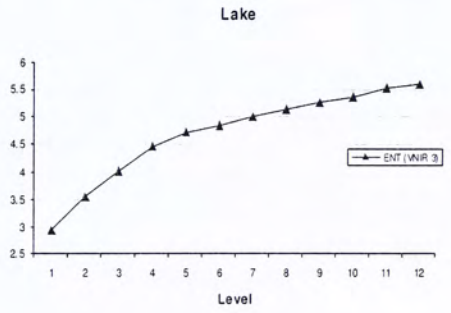
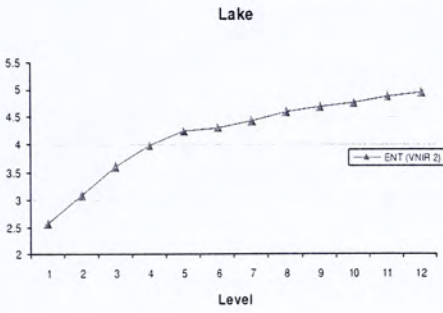
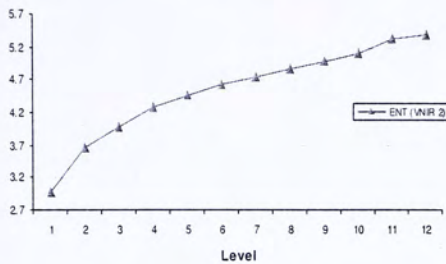


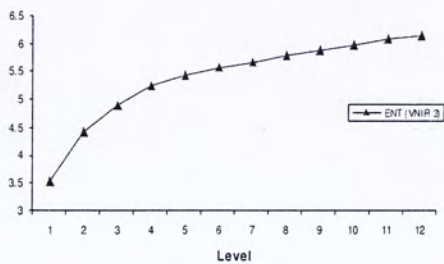
Figure A.17 Variability of GLCM Contrast (VNIR 2 and 3) for land cover objects along segmentation gradient (Spectral-shape ratio: 7:3). Case in Nanjing.



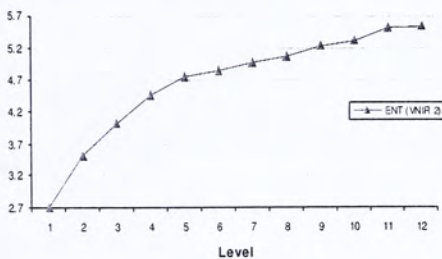
Woodland



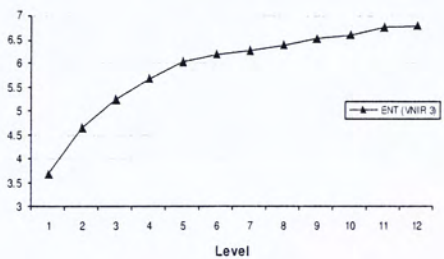
Woodland



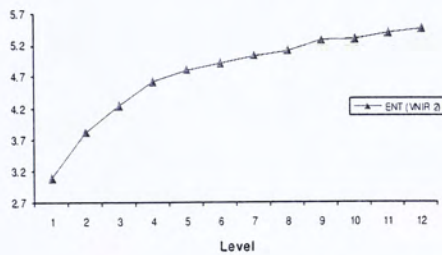
Agricultural crops I



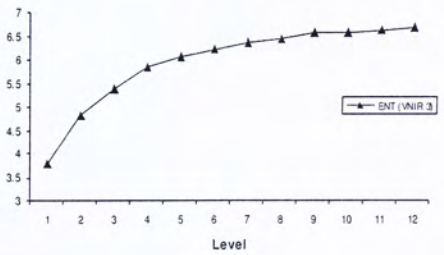
Agricultural crops I



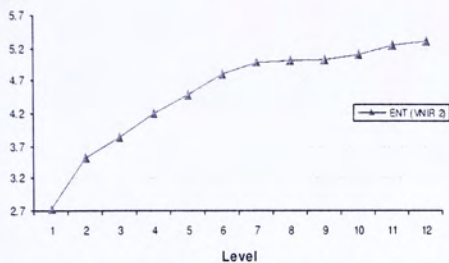
Agricultural crops II



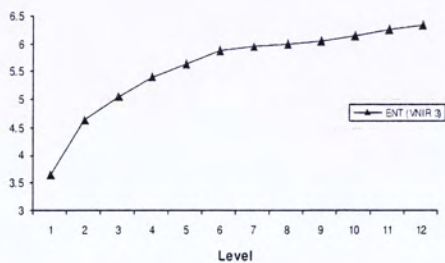
Agricultural crops II



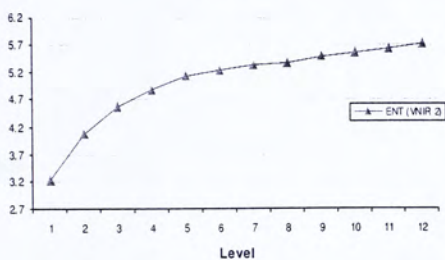
Wetland



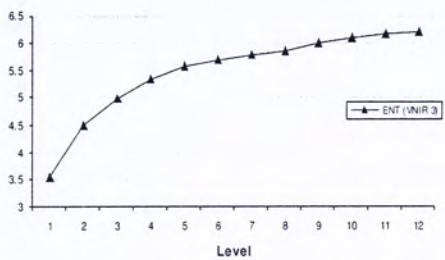
Wetland



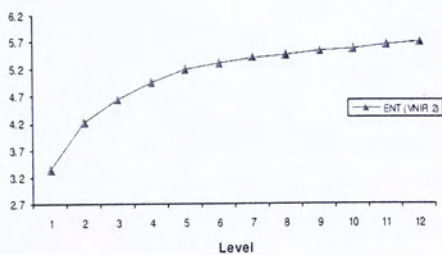
Grassland



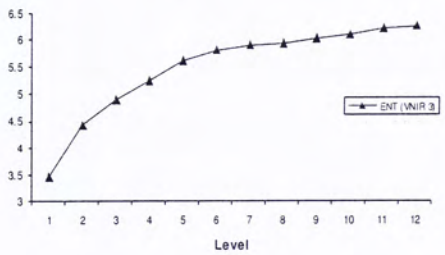
Grassland



Fallow land



Fallow land



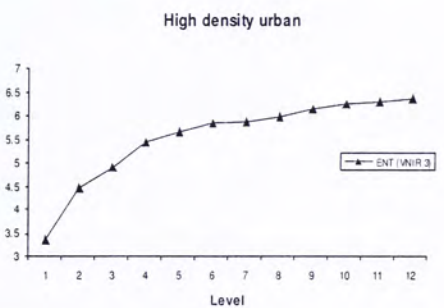
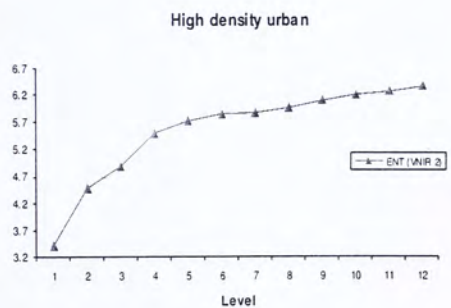
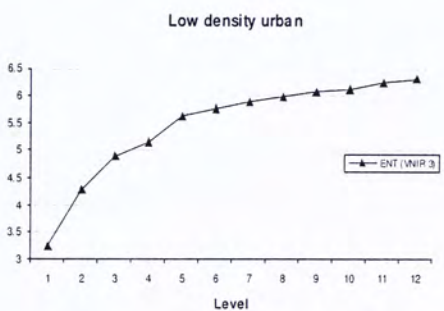
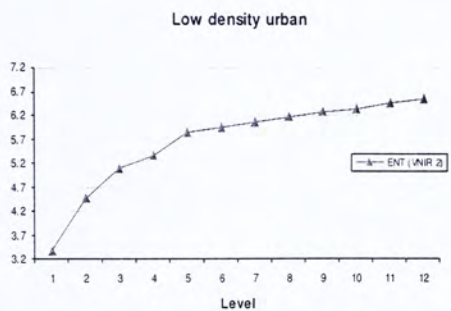
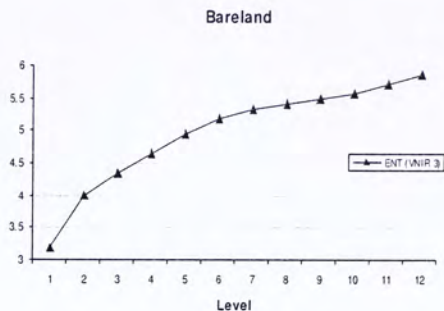
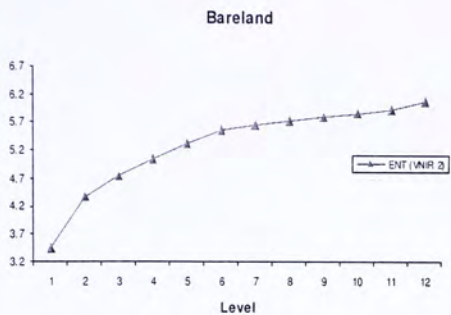
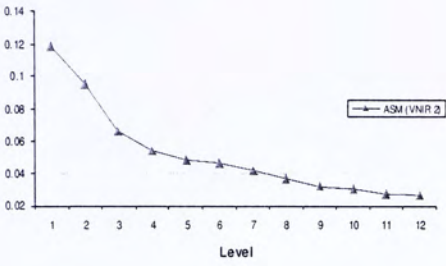
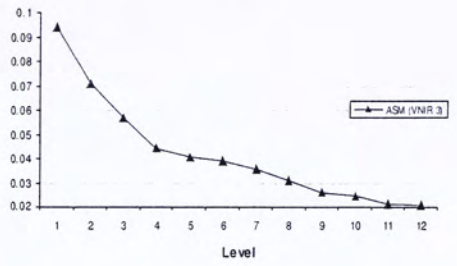


Figure A.18 Variability of GLCM Entropy (VNIR 2 and 3) for land cover objects along segmentation gradient (Spectral-shape ratio: 7:3). Case in Nanjing.

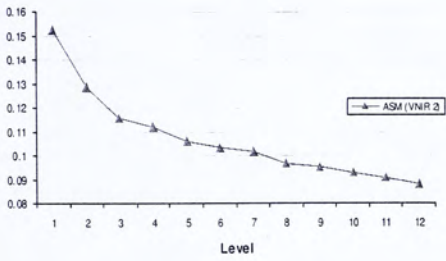
Lake



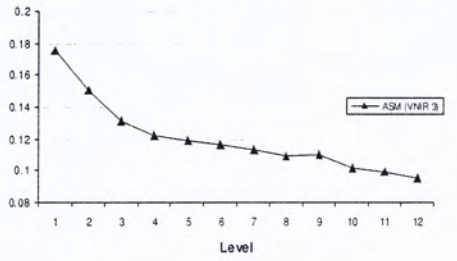
Lake



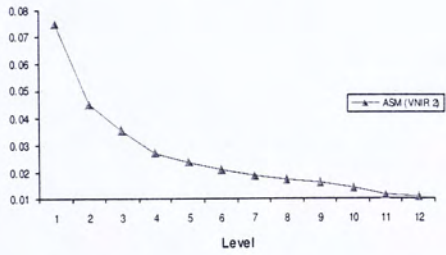
River



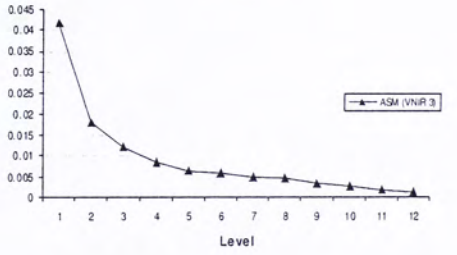
River



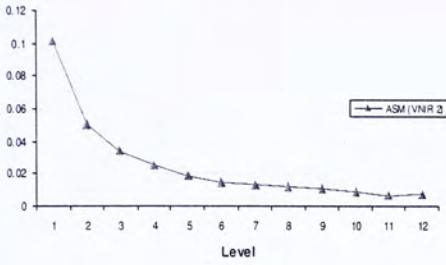
Woodland



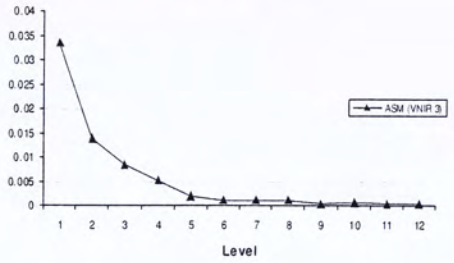
Woodland



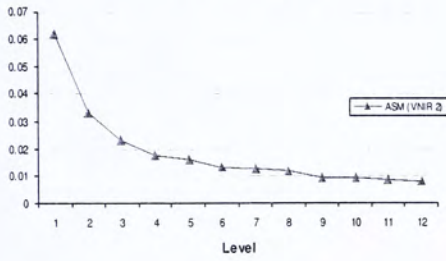
Agricultural crops I



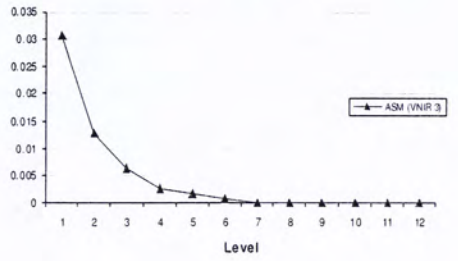
Agricultural crops I



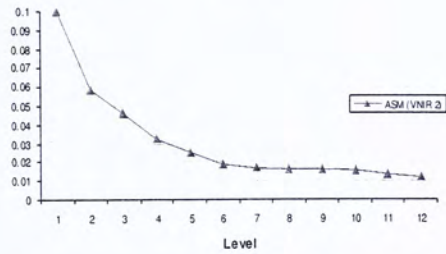
Agricultural crops II



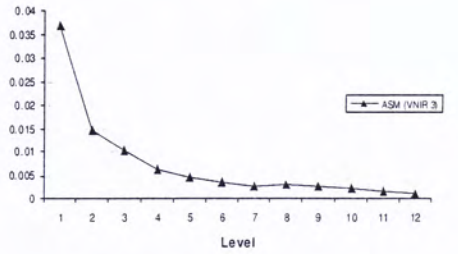
Agricultural crops II



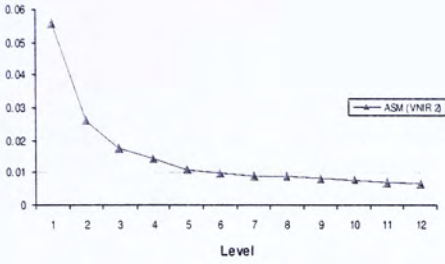
Wetland



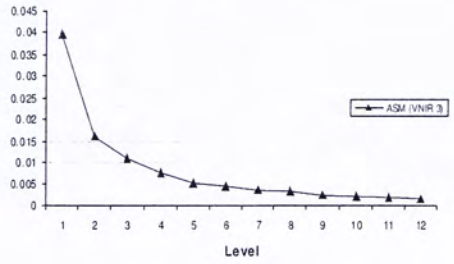
Wetland



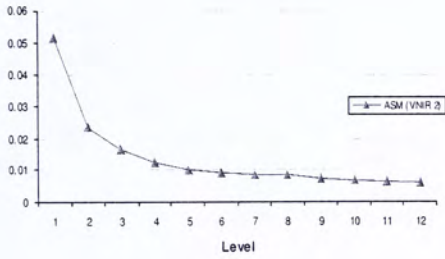
Grassland



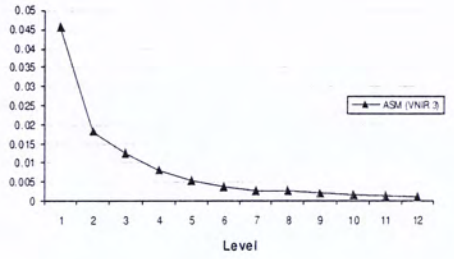
Grassland



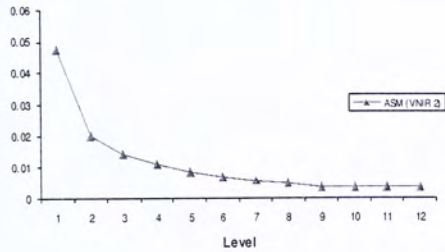
Fallow land



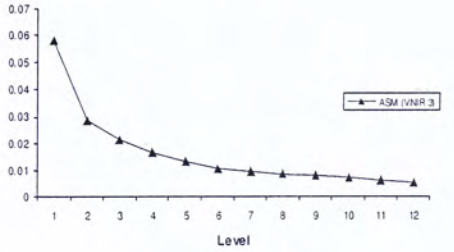
Fallow land



Bareland



Bareland



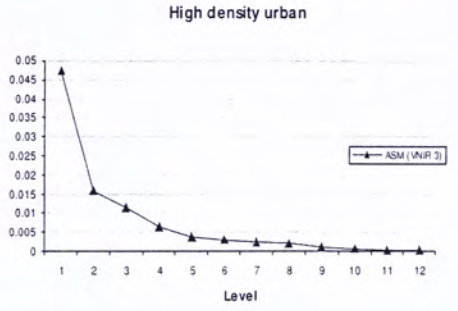
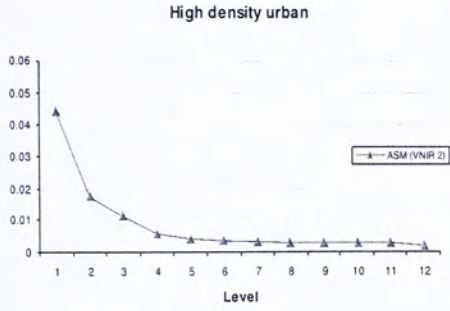
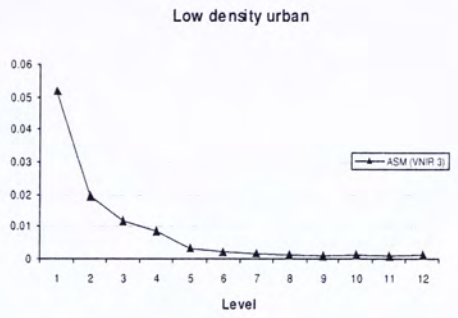
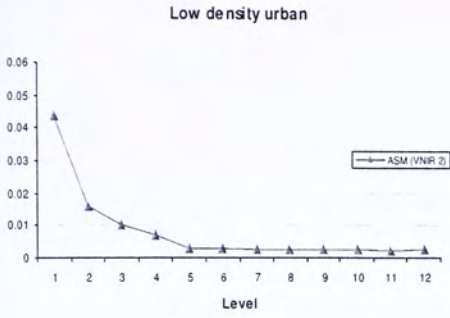


Figure A.19 Variability of GLCM Angular Second Moment (VNIR 2 and 3) for land cover objects along segmentation gradient (Spectral-shape ratio: 7:3). Case in Nanjing.

Appendix 5—Classifying Rules

Chongqing

1. River

Classification Level 1

- NOT “lake, industrial or smaller river”
 - *Area: smaller than 119000 pixels*
 - *Mean difference to Neighbor (VNIR 3): smaller than -18*
 - *VNIR 3 x VNIR 2: smaller than 4400*
 - *VNIR 3 / VNIR 2: 1.95*
- Standard Deviation (VNIR 1): smaller than 4.51
- Standard Deviation (VNIR 2): smaller than 4.51
- Standard Deviation (VNIR 3): smaller than 4.51
- VNIR 3 - VNIR 2: smaller than -19.9

OR

- IS “small river”
 - *Density: smaller than 0.91*

2. Woodland

Classification Level 1

- NOT “lake, industrial or smaller river”
 - *Area: smaller than 119000 pixels*
 - *Mean difference to Neighbor (VNIR 3): smaller than -18*
 - *VNIR 3 x VNIR 2: smaller than 4400*
 - *VNIR 3 / VNIR 2: 1.95*

AND

- NOT “River”
 - *Standard Deviation (VNIR 1): smaller than 4.51*
 - *Standard Deviation (VNIR 2): smaller than 4.51*
 - *Standard Deviation (VNIR 3): smaller than 4.51*

Classification Level 2

- IS “vegetation”
 - *VNIR 3 / VNIR 2: greater than 1.26*

Classification Level 1

- IS “woodland”
 - *VNIR 1: smaller than 86.1*
 - *VNIR 2: smaller than 50.1*
 - *VNIR 3: smaller than 112*

3. Bareland

Classification Level 1

- NOT “lake, industrial or smaller river”
 - *Area: smaller than 119000 pixels*
 - *Mean difference to Neighbor (VNIR 3): smaller than -18*
 - *VNIR 3 x VNIR 2: smaller than 4400*
 - *VNIR 3 / VNIR 2: 1.95*

AND

- NOT "River"
 - *Standard Deviation (VNIR 1): smaller than 4.51*
 - *Standard Deviation (VNIR 2): smaller than 4.51*
 - *Standard Deviation (VNIR 3): smaller than 4.51*

Classification Level 2

- NOT "vegetation"
 - *VNIR 3 / VNIR 2: greater than 1.26*

Classification Level 1

- NOT "low density urban"
 - *GLCM Contrast (VNIR 1): greater than 80*
 - *GLCM Contrast (VNIR 2): greater than 90*
- NOT "high density urban"
 - *VNIR 3: smaller than 71.5*

4. Industrial

Classification Level 1

- IS "lake, industrial or smaller river"
 - *Area: smaller than 119000 pixels*
 - *Mean difference to Neighbor (VNIR 3): smaller than -18*
 - *VNIR 3 x VNIR 2: smaller than 4400*
 - *VNIR 3 / VNIR 2: 1.95*

AND

- NOT "small river"
 - *Density: smaller than 0.91*

AND

- NOT "lake"
 - *GLCM Dissimilarity (VNIR 3): greater than 10*
 - *VNIR 3 / VNIR 2: greater than 1*

5. High density urban

Classification Level 1

- NOT "lake, industrial or smaller river"
 - *Area: smaller than 119000 pixels*
 - *Mean difference to Neighbor (VNIR 3): smaller than -18*
 - *VNIR 3 x VNIR 2: smaller than 4400*
 - *VNIR 3 / VNIR 2: 1.95*

AND

- NOT "River"
 - *Standard Deviation (VNIR 1): smaller than 4.51*
 - *Standard Deviation (VNIR 2): smaller than 4.51*
 - *Standard Deviation (VNIR 3): smaller than 4.51*

Classification Level 2

- NOT "vegetation"
 - *VNIR 3 / VNIR 2: greater than 1.26*

Classification Level 1

- NOT “low density urban”
 - *GLCM Contrast (VNIR 1): greater than 80*
 - *GLCM Contrast (VNIR 2): greater than 90*
- VNIR 3: smaller than 71.5

Nanjing

1. River

Classification Level 1

- IS “big river”
 - *VNIR 1: smaller than 78*
 - *VNIR 3: smaller than 37*
 - *Standard Deviation (VNIR 3): smaller than 8*
 - *VNIR 3 - VNIR 2: smaller than -17*

OR

- IS “smaller river, pond”
 - *Urban Center Boundary=0*
 - *VNIR 3: smaller than 28*
 - *VNIR 3 / VNIR 2: smaller than 1.01*
- Density: smaller than 1.81

2. Woodland

Classification Level 1

- NOT “big river”
 - *VNIR 1: smaller than 78*
 - *VNIR 3: smaller than 37*
 - *Standard Deviation (VNIR 3): smaller than 8*
 - *VNIR 3 - VNIR 2: smaller than -17*

AND

- NOT “smaller river, pond”
 - *Urban Center Boundary=0*
 - *VNIR 3: smaller than 28*
 - *VNIR 3 / VNIR 2: smaller than 1.01*

Classification Level 2

- IS “vegetation”
 - *VNIR 3 / VNIR 2: greater than 0.98*

Classification Level 3

- VNIR 1: smaller than 53
- VNIR 2: smaller than 36
- VNIR 3: smaller than 51

3. Crops and grassland I
Classification Level 1

- NOT “big river”
 - *VNIR 1: smaller than 78*
 - *VNIR 3: smaller than 37*
 - *Standard Deviation (VNIR 3): smaller than 8*
 - *VNIR 3 - VNIR 2: smaller than -17*

AND

- NOT “smaller river, pond”
 - *Urban Center Boundary=0*
 - *VNIR 3: smaller than 28*
 - *VNIR 3 / VNIR 2: smaller than 1.01*

Classification Level 2

- IS “vegetation”
 - *VNIR 3 / VNIR 2: greater than 0.98*

Classification Level 3

- NOT “woodland”
 - *VNIR 1: smaller than 53*
 - *VNIR 2: smaller than 36*
 - *VNIR 3: smaller than 51*
- *VNIR 1: smaller than 61*
- *NDVI: greater than 0.3*

4. Bareland

Classification Level 1

- NOT “big river”
 - *VNIR 1: smaller than 78*
 - *VNIR 3: smaller than 37*
 - *Standard Deviation (VNIR 3): smaller than 8*
 - *VNIR 3 - VNIR 2: smaller than -17*

AND

- NOT “smaller river, pond”
 - *Urban Center Boundary=0*
 - *VNIR 3: smaller than 28*
 - *VNIR 3 / VNIR 2: smaller than 1.01*

Classification Level 2

- NOT “vegetation”
 - *VNIR 3 / VNIR 2: greater than 0.98*

AND

- NOT “bright urban”
 - *GLCM Dissimilarity VNIR 1: greater than 4*
 - *VNIR 1: greater than 66*
 - *VNIR 2: greater than 50*

- *VNIR 3: greater than 35*

OR

- NOT “dark urban”
 - *Urban Center Boundary=1*

**5. High density urban
Classification Level 1**

- NOT “big river”
 - *VNIR 1: smaller than 78*
 - *VNIR 3: smaller than 37*
 - *Standard Deviation (VNIR 3): smaller than 8*
 - *VNIR 3 - VNIR 2: smaller than -17*

AND

- NOT “smaller river, pond”
 - *Urban Center Boundary=0*
 - *VNIR 3: smaller than 28*
 - *VNIR 3 / VNIR 2: smaller than 1.01*

Classification Level 2

- NOT “vegetation”
 - *VNIR 3 / VNIR 2: greater than 0.98*

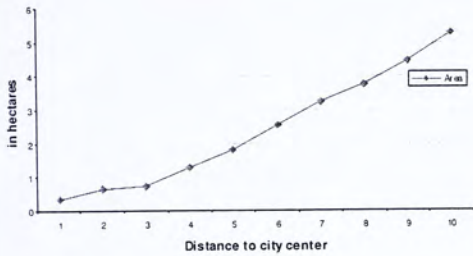
AND

- NOT “bright urban”
 - *GLCM Dissimilarity VNIR 1: greater than 4*
 - *VNIR 1: greater than 66*
 - *VNIR 2: greater than 50*
 - *VNIR 3: greater than 35*
- *Urban Center Boundary=1*

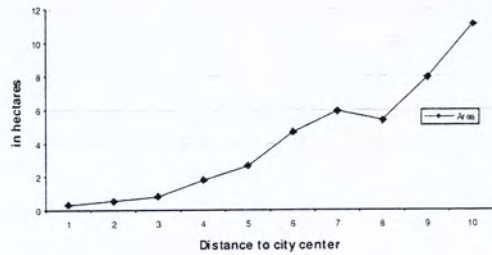
Appendix 6—Variations in Landscape Metrics along Buffers from City Center in Chongqing

Patch-metrics

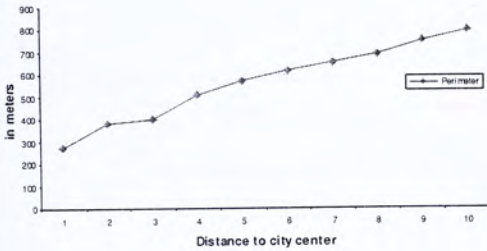
Area



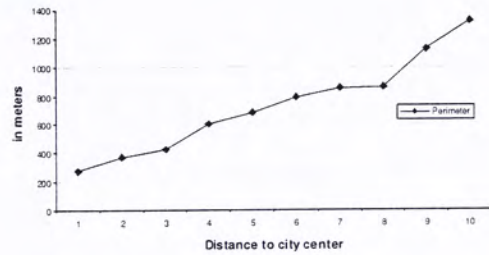
Area



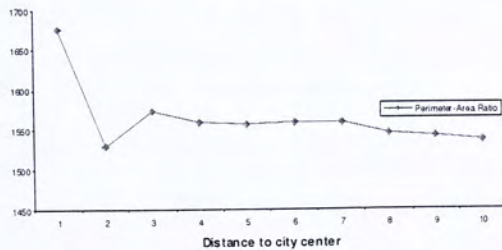
Perimeter



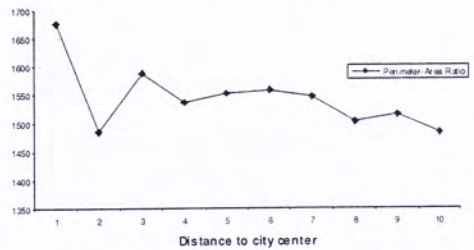
Perimeter



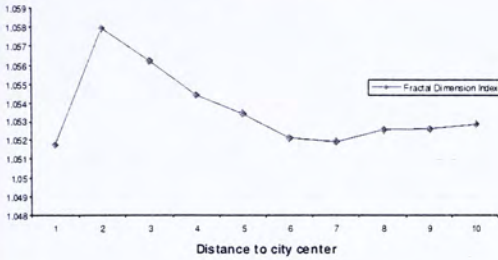
Perimeter-Area Ratio



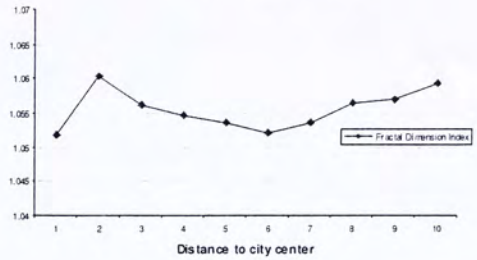
Perimeter-area Ratio



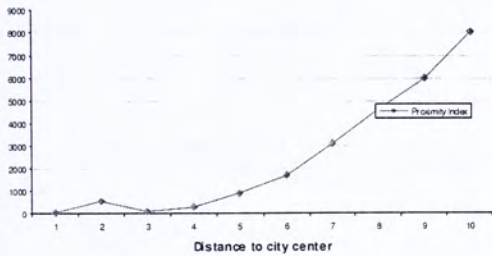
Fractal Dimension Index



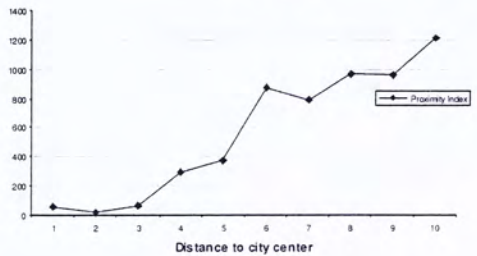
Fractal Dimension Index



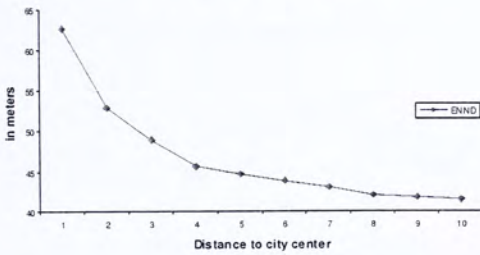
Proximity Index



Proximity Index



Euclidean Nearest Neighbor Distance



Euclidean Nearest Neighbor Distance

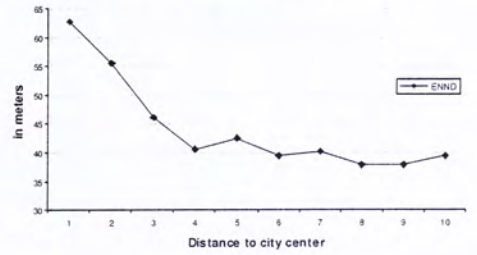
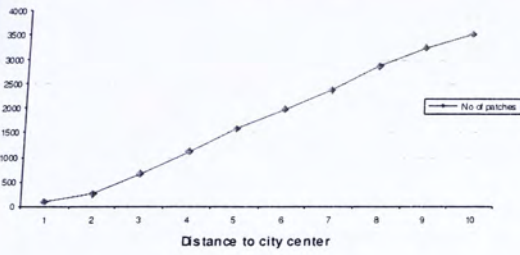


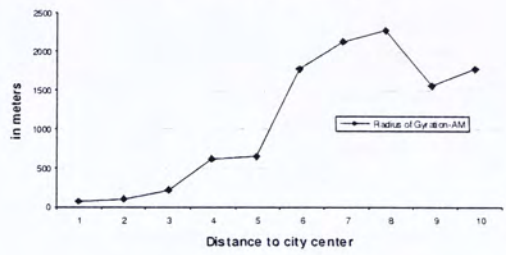
Figure A.20 Variability of patch-metrics along buffer circles (Left) and buffer rings (Right) from the city center of Chongqing.

Class-metrics

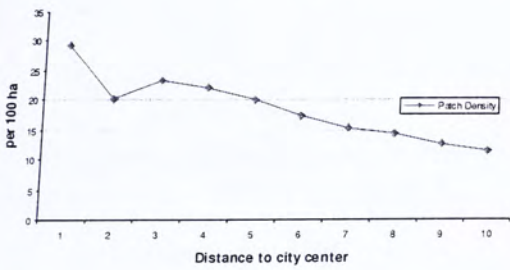
Number of Patches



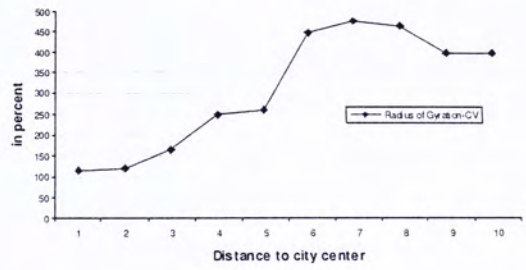
Area-weighted Mean Gyrate



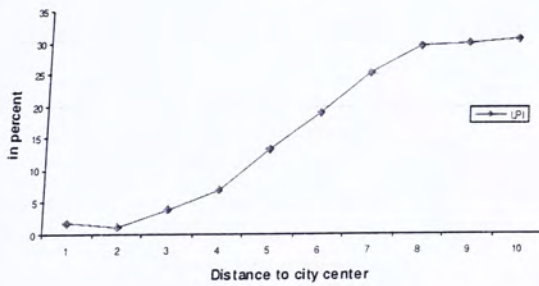
Patch Density



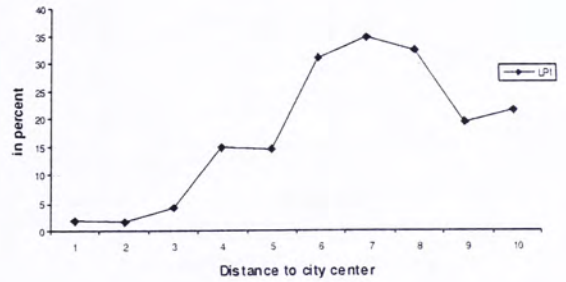
Coefficient of Variation of Gyrate



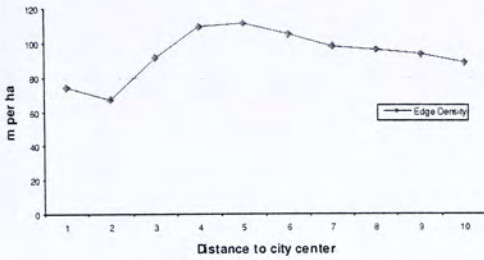
Largest Patch Index



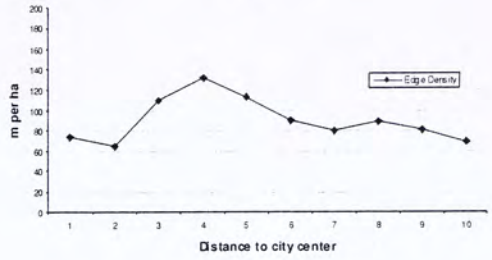
Largest Patch Index



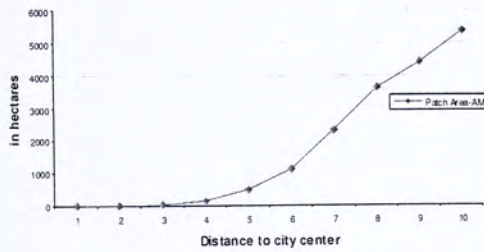
Edge Density



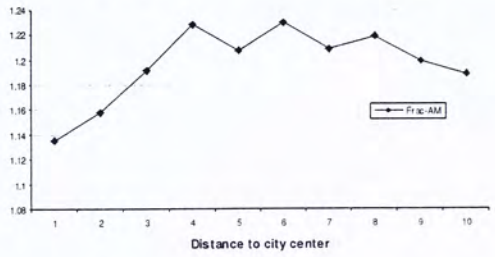
Edge Density



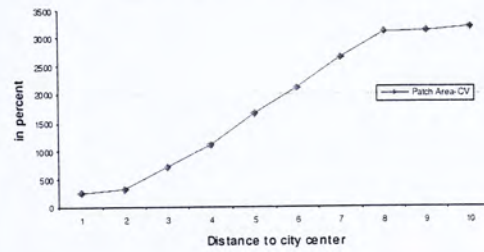
Area-weighted Mean of Patch Area



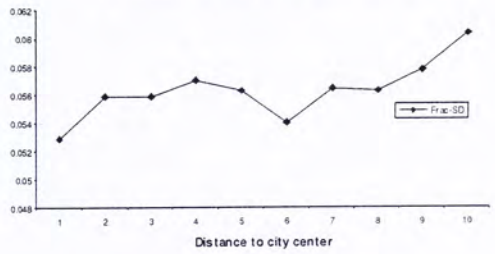
Area-weighted Mean Fractal Dimension Index



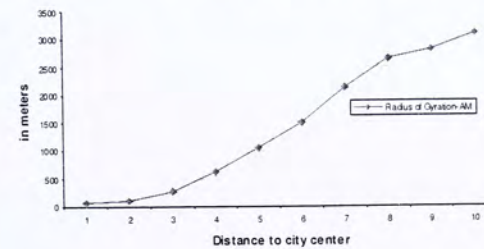
Coefficient of Variation of Mean Patch Area



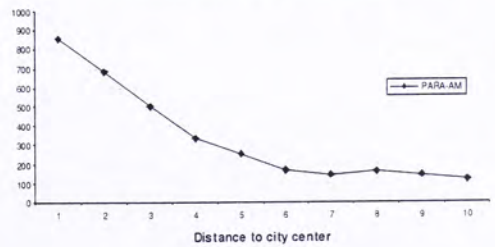
Standard Deviation of Fractal Dimension Index



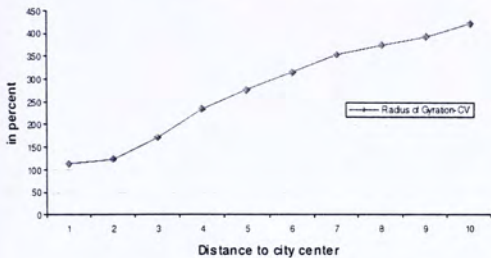
Area-weighted Mean of Gyrate



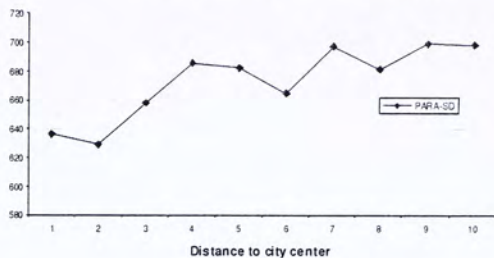
Area-weighted Mean Perimeter-area Ratio



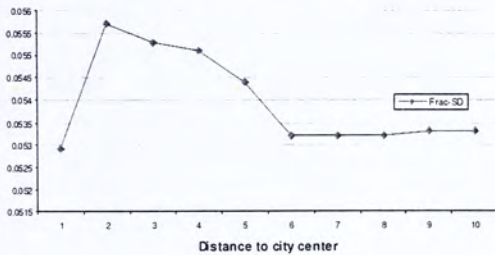
Coefficient of Variation of Gyrate



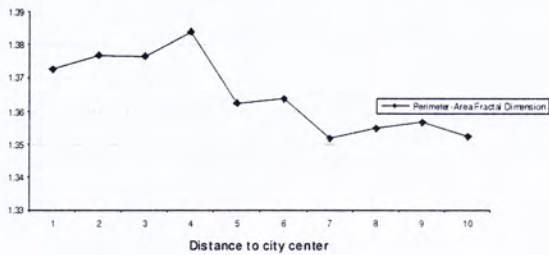
Standard Deviation of Perimeter-area Ratio



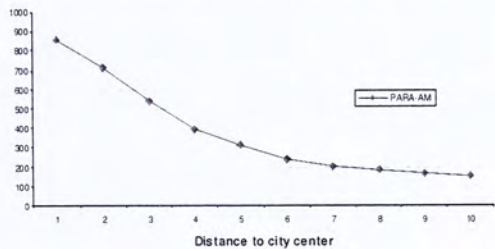
Standard Deviation of Fractal Dimension Index



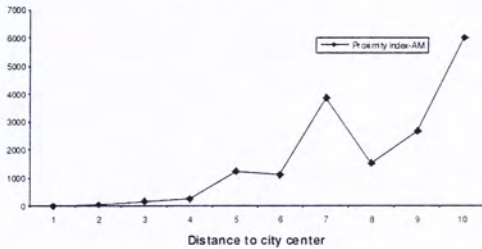
Perimeter-Area Fractal Dimension



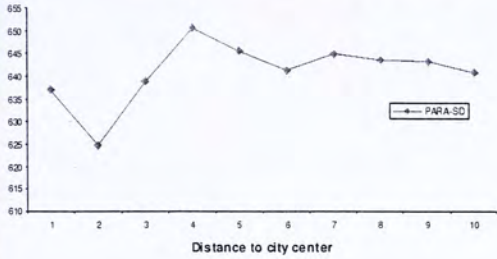
Area-weighted Mean of Perimeter-area Ratio



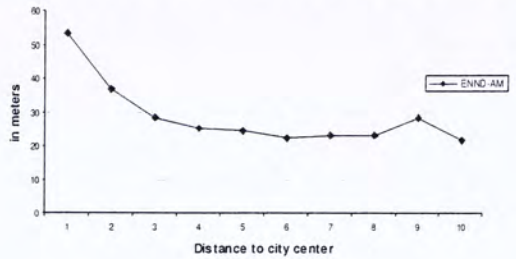
Area-weighted Mean Proximity Index



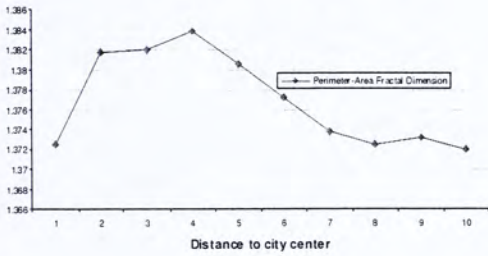
Standard Deviation of Perimeter-area Ratio



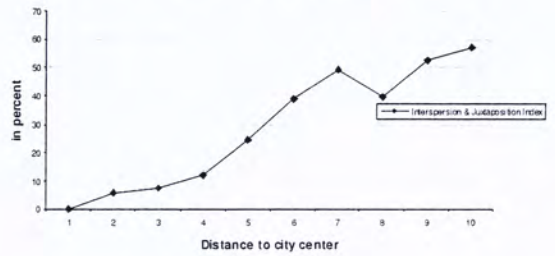
Area-weighted Mean of Euclidean Nearest Neighbor Distance



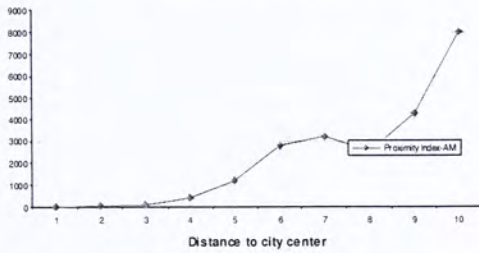
Perimeter-area Fractal Dimension



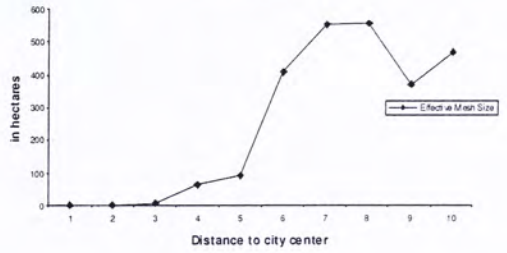
Interspersion and Juxtaposition Index



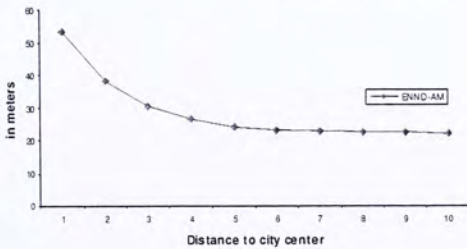
Area-weighted Mean Proximity Index



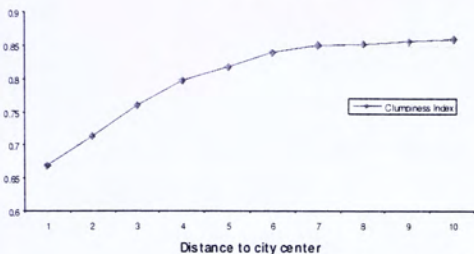
Effective Mesh Size



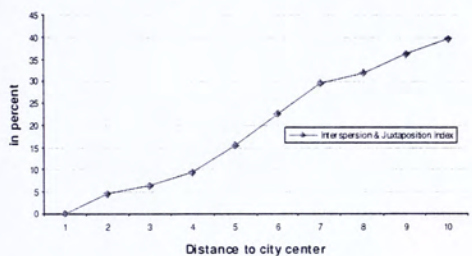
Area-weighted Mean Euclidean Nearest Neighbor Distance



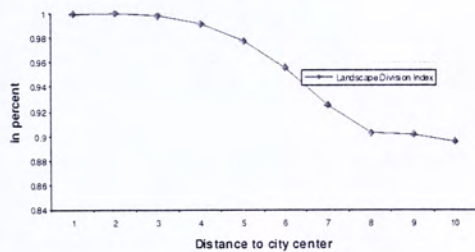
Clumpiness Index



Interspersion and Juxtaposition Index



Landscape Division Index



Effective Mesh Size

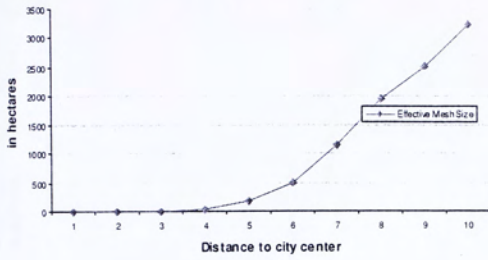
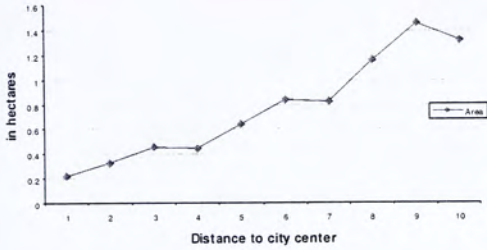


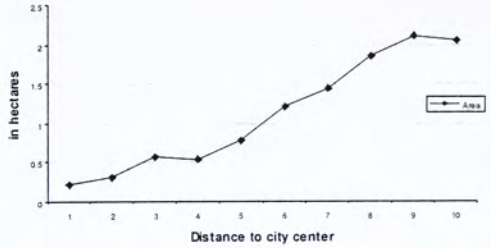
Figure A.21 Variability of class-metrics along buffer circles (Left) and buffer rings (Right) from city center of Chongqing.

Appendix 7—Variations in Landscape Metrics along Buffers from City Center in Nanjing

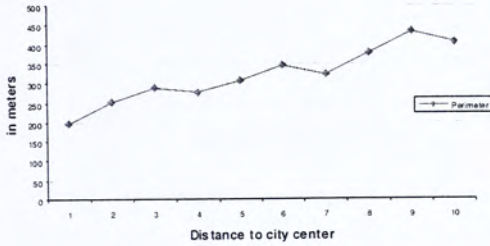
Area



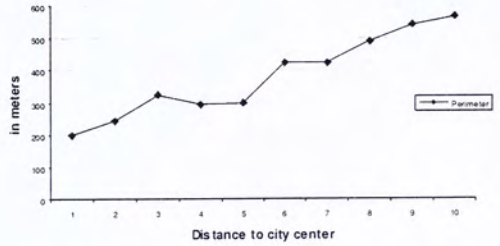
Area



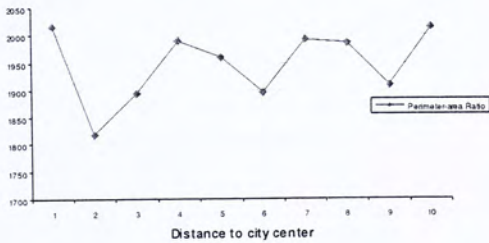
Perimeter



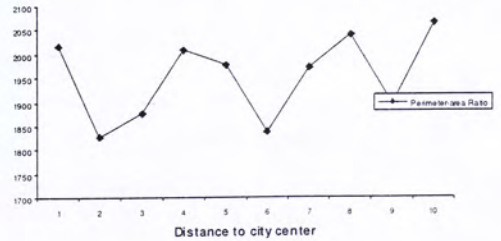
Perimeter



Perimeter-area Ratio



Perimeter-area Ratio



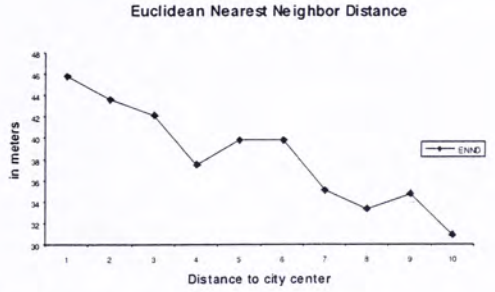
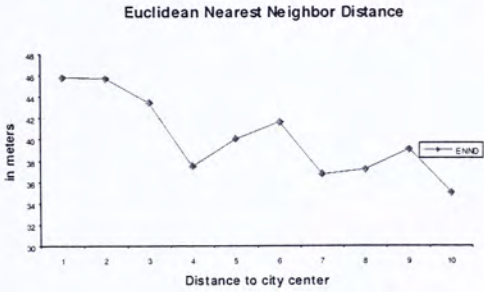
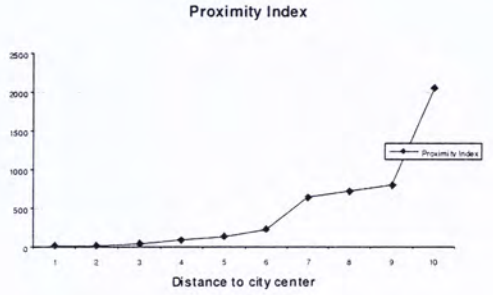
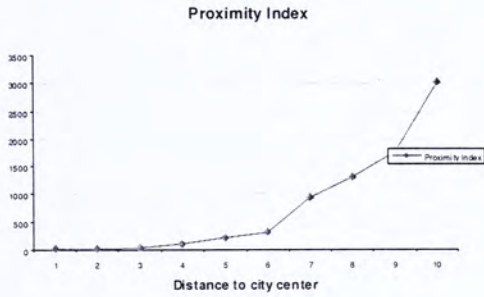
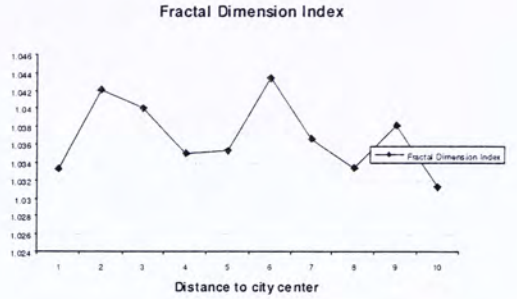
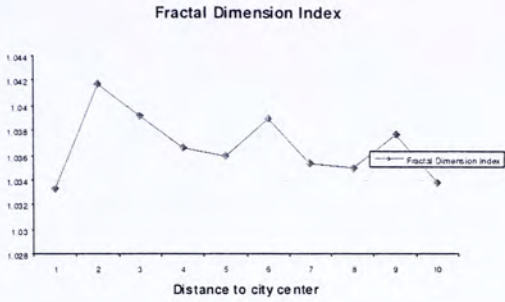
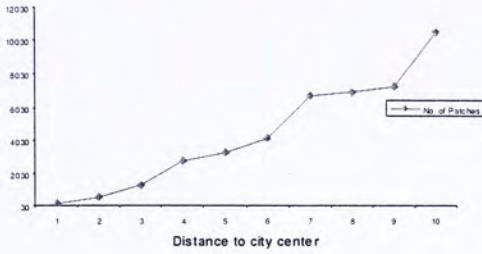
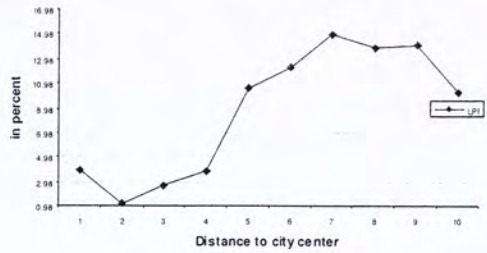


Figure A.22 Variability of patch-metrics along buffer circles (Left) and buffer rings (right) from city center of Nanjing.

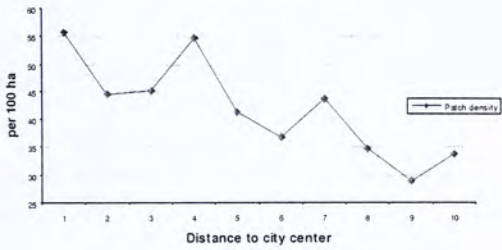
Number of Patches



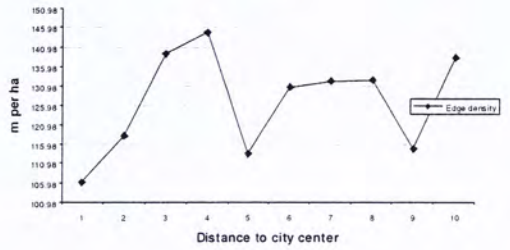
Largest Patch Index



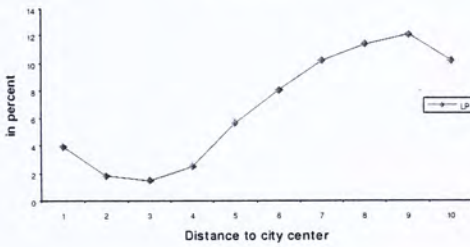
Patch Density



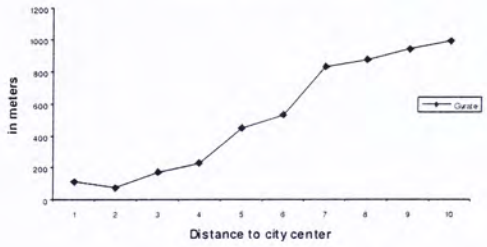
Edge Density



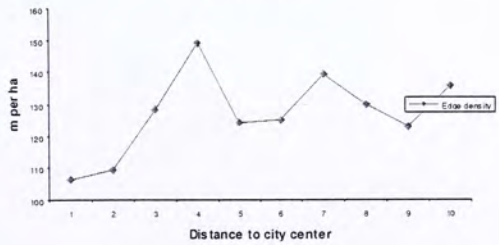
Largest Patch Index



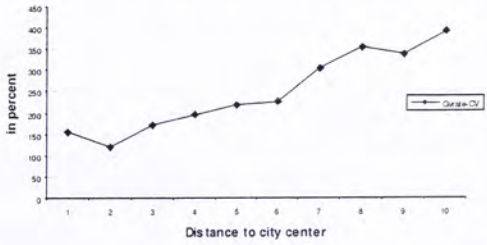
Area-weighted Mean Gyrate



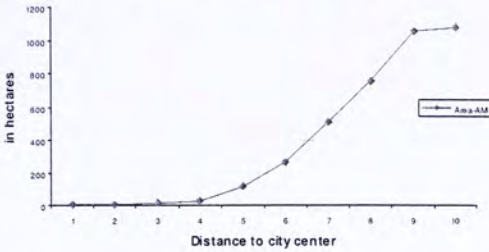
Edge Density



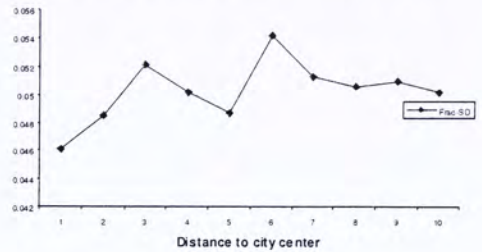
Coefficient of Variation of Gyrate



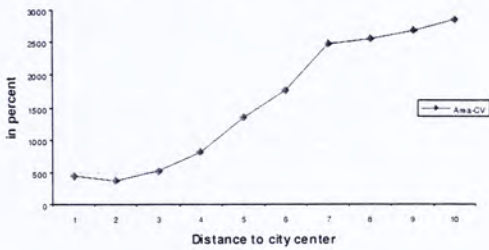
Area-weighted Mean Patch Area



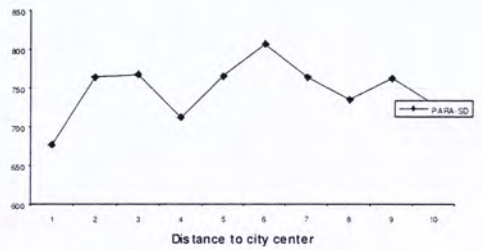
Standard Deviation of Fractal Dimension Index



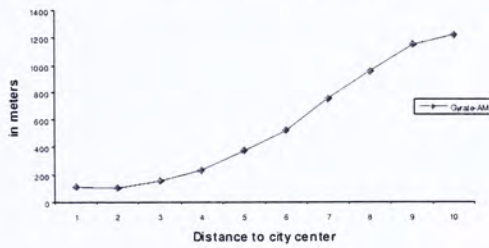
Coefficient of Variation of Patch Area



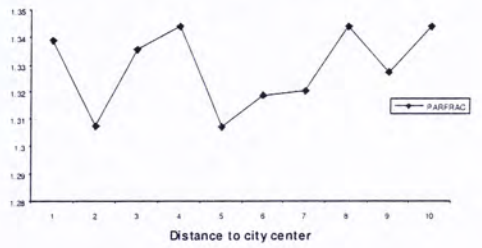
Standard Deviation of Perimeter-area Ratio



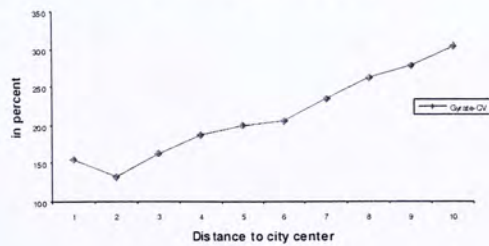
Area-weighted Mean Gyrate



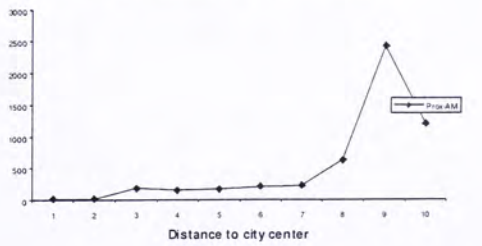
Perimeter-Area Fractal Dimension Index



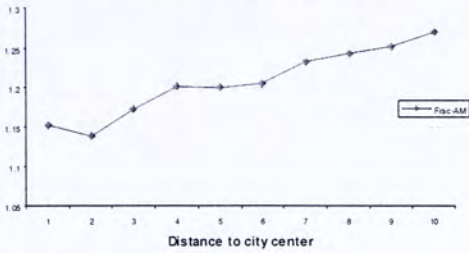
Coefficient of Variation of Gyrate



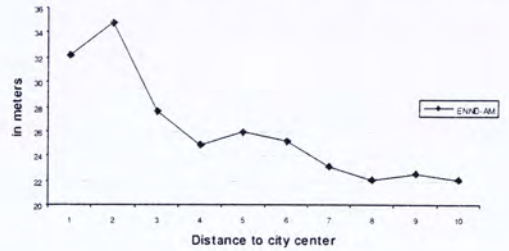
Area-weighted Mean Proximity Index



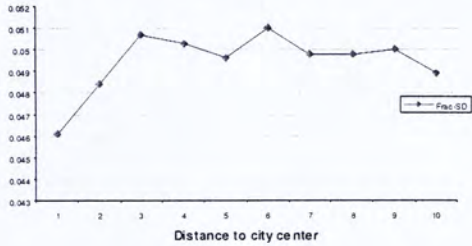
Area-weighted Mean Fractal Dimension



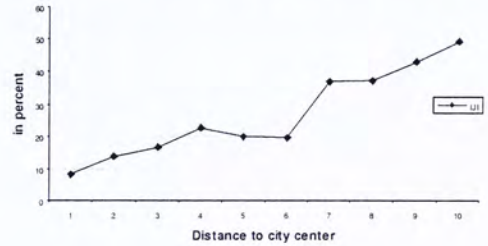
Area-weighted Mean Euclidean Nearest Neighbor Distance



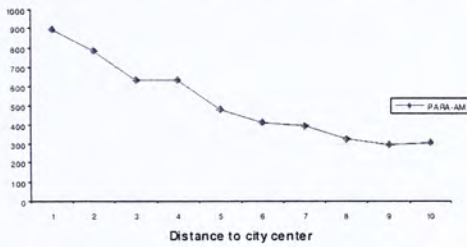
Standard Deviation of Fractal Dimension



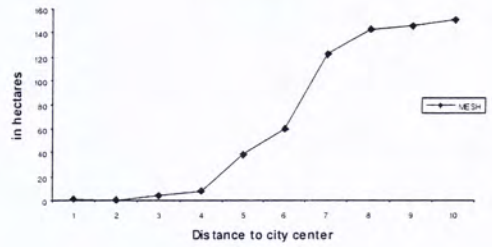
Interspersion and Juxtaposition Index



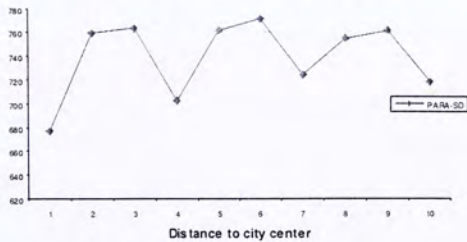
Area-weighted Mean Perimeter-area Ratio



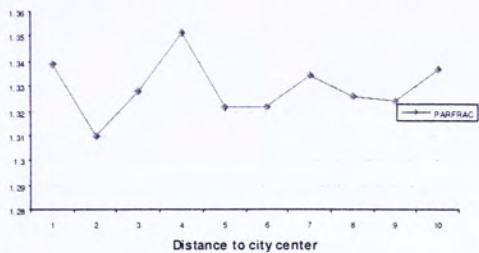
Effective Mesh Size



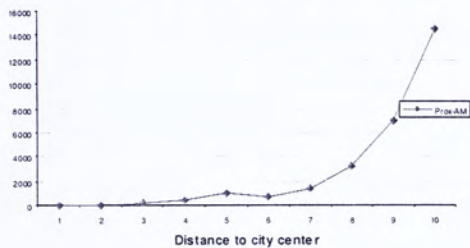
Standard Deviation of Perimeter-area Ratio



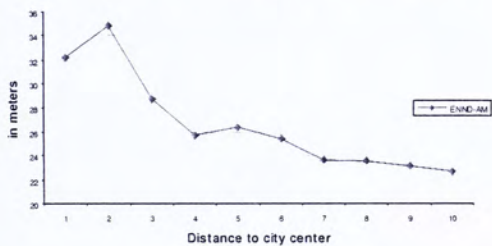
Perimeter-Area Fractal Dimension Index



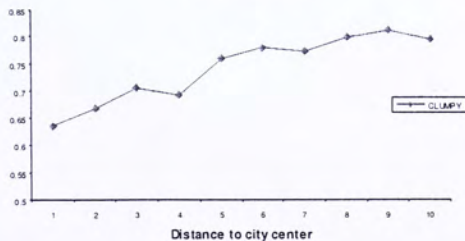
Area-weighted Mean Proximity Index



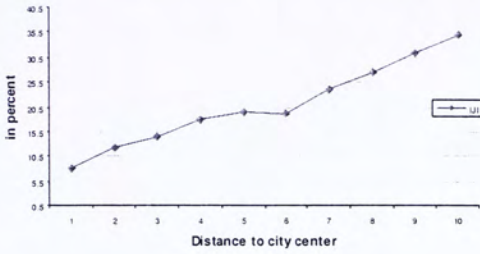
Area-weighted Mean Euclidean Nearest Neighbor Distance



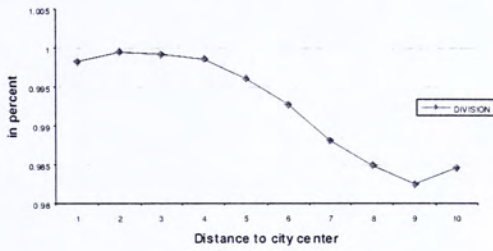
Clumpiness Index



Interspersion and Juxtaposition Index



Landscape Division Index



Effective Mesh Size

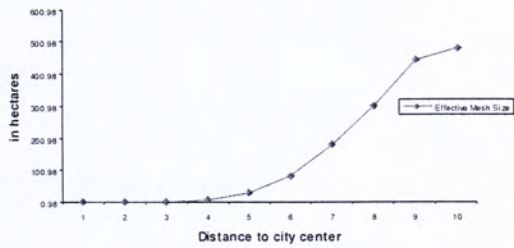


Figure A.23 Variability of class-metrics along buffer circles (Left) and buffer rings (Right) from city center of Nanjing.

CUHK Libraries



004270456